INEEL/EXT-02-00987
Rev. 1

# *INEEL Subregional Conceptual Model Report*

*Volume 1: Summary of Existing Knowledge of Natural and Anthropogenic Influences Governing Subsurface Contaminant Transport in the INEEL Subregion of the Eastern Snake River Plain*

*Brennon R. Orr*
*Aran T. Armstrong*
*David L. Bates*
*John M. Bukowski*
*Kent S. Sorenson*
*Douglas L. Whitmire*

*August 2002*

*Idaho National Engineering and Environmental Laboratory*
*Bechtel BWXT Idaho, LLC*

INEEL/EXT-02-00987
Rev. 1

# INEEL Subregional Conceptual Model Report

## Volume 1: Summary of Existing Knowledge of Natural and Anthropogenic Influences Governing Subsurface Contaminant Transport in the INEEL Subregion of the Eastern Snake River Plain

**Brennon R. Orr**
**Aran T. Armstrong**
**David L. Bates**
**John M. Bukowski**
**Kent S. Sorenson**
**Douglas L. Whitmire**

**August 2002**

**Idaho National Engineering and Environmental Laboratory**
**Idaho Falls, Idaho 83415**

**Prepared for the**
**U.S. Department of Energy**
**Assistant Secretary for Environmental Management**
**Under DOE Idaho Operations Office**
**Contract DE-AC07-99ID13727**

# EXECUTIVE SUMMARY

The National Research Council has defined a conceptual model as "an evolving hypothesis identifying the important features, processes, and events controlling fluid flow and contaminant transport of consequence at a specific field site in the context of a recognized problem." Presently, several subregional conceptual models are under development at the Idaho National Engineering and Environmental Laboratory (INEEL). Additionally, facility-specific conceptual models have been described as part of INEEL environmental restoration activities. Compilation of these models is required to develop a comprehensive conceptual model that can be used to strategically plan for future groundwater research activities at the INEEL.

Conceptual models of groundwater flow and contaminant transport at the INEEL include the description of the geologic framework, matrix hydraulic properties, and inflows and outflows. They also include definitions of the contaminant source term and contaminant transport mechanisms.

The geologic framework of the INEEL subregion is described by the geometry of the system, stratigraphic units within the system, and structural features that affect groundwater flow and contaminant transport. These elements define geohydrologic units that make up the Snake River Plain Aquifer (SRPA).

The United States Geological Survey (USGS) conceptual model encompasses approximately 1,920 $mi^2$ of the eastern Snake River Plain. The Waste Area Group (WAG)-10 model includes the USGS area and additional areas to the northeast and southeast. Both conceptual models are bounded to the northwest by the Pioneer Mountains, Lost River Range, and Lemhi Mountains. They are bounded to the southeast by groundwater flow paths determined from aquifer water-level contours. The upgradient extent of the USGS model is a water-level contour that includes the northeastern boundary of the INEEL. The WAG-10 model includes more of the Mud Lake area to utilize previous estimates of underflow into the subregion. Both conceptual models extend approximately 25 miles to the southwest of the INEEL, a distance sufficient to include known concentrations of contaminant tracers.

Several hypotheses have been developed concerning the effective thickness of the SRPA at the INEEL. The USGS model has defined the effective thickness from electrical resistivity and borehole data to be as much as 2,500 ft in the eastern part of the subregion and as much as 4,000 ft in the southwestern part. The WAG-10 model has developed two alternatives using aquifer-temperature and electrical-resistivity data. The "thick" aquifer interpretation utilizes colder temperature data and includes a north-trending zone in which the thickness exceeds 1,300 ft and with a maximum thickness of 1,700 ft. The "thin" aquifer interpretation minimizes aquifer thickness, with thickness ranging from 328 to 1,300 ft. Facility-specific models generally have focused efforts on the upper 250 ft of saturation.

Conceptual models have utilized a stratigraphic data set to define geohydrologic units within the INEEL subregion. This data set, compiled from geophysical logs and cores from boreholes, correlates the thick, complex stack of basalt flows across the subregion. Conceptual models generally concur that the upper geohydrologic unit consists of a section of highly fractured, multiple, thin basalt flows and sedimentary interbeds. Beneath this unit is an areally extensive, thick, unfractured basalt flow that rises above the water table southwest of the INEEL. The bottom unit consists of a thick section of slightly- to moderately-altered basalt.

Subregional conceptual models concur that structural features across the plain affect groundwater flow and contaminant transport. Structural uplift and subsidence has modified the orientation of geohydrologic units. Volcanic rift features, including vent corridors, locally affect the distribution of hydraulic properties of the aquifer.

Matrix hydraulic properties of the basalt and interbedded sediments of the eastern Snake River Plain include hydraulic conductivity (the measure of the capability of these rocks to transmit water) and the storage coefficient (the measure of the capability of these rocks to store water). The subregional and facility-specific conceptual models all note a large range in hydraulic conductivity from tests in the SRPA and vadose zone. The hydraulic conductivity estimates from aquifer tests in 114 aquifer wells at the INEEL ranged from 0.01 to 32,000 ft/day. A similar range was observed in wells completed in perched water bodies. The distribution of hydraulic conductivity in the INEEL subregion is not defined by any of the subregional or facility-specific conceptual models because of heterogeneities attributed to the complex, layered system of overlapping basalt flows and the occurrence of volcanic vent corridors that significantly affect hydraulic conductivity. Subregional estimates of the storage coefficient range from 5 to 20%. Facility-specific estimates, calculated using inverse numerical models of hydraulic and chemical information, range from 3 to 6%.

The configuration of subregional groundwater flow field depends on flows into and out of the subregion. These flows occur as underflow from regional and tributary basin systems, flow across the base of the aquifer, and recharge from infiltrating precipitation and streamflow.

Underflow into and out of the INEEL subregion is estimated indirectly in conceptual models from gradient and hydraulic property information. Underflow estimates into the subregion are within 5% of each other (1,225 and 1,298 $ft^3/s$). The USGS model estimates about 2,350 $ft^3/s$ of underflow out of the region, based on limited gradient and hydraulic-property information.

Conceptual models concur that small flows probably enter the SRPA flow system across the base of the aquifer. The USGS model estimates that approximately 44 $ft^3/s$ of flow may enter the aquifer throughout the subregion. The WAG-10 model infers from temperature data that flows may be larger in some areas.

Subregional and facility-specific estimates of recharge from areal precipitation are derived from tracer and other studies. The USGS conceptual model estimates that areal recharge from precipitation is 0.02 to 0.04 ft/year with a maximum recharge contribution of about 70 $ft^3/s$ over the entire subregion. The WAG-10 conceptual model uses similar estimates for areal recharge and suggests that direct precipitation on the plain locally recharges the aquifer to a limited degree, particularly when snow melts rapidly in the spring. The net effect of recharge from precipitation on contaminant transport is probably very small when compared to other sources of inflow and is a less important consideration than more concentrated sources such as streamflow infiltration.

Large volumes of water have been recharged historically to the SRPA in response to episodic runoff from the Big Lost River drainage basin. Recharge has occurred along the channel of the Big Lost River and in the INEEL spreading areas near sources of INEEL-derived contaminants. This source of large episodic recharge has locally affected hydrologic conditions in the vadose zone and aquifer. However, the effect of this recharge on contaminant transport is not well understood. The USGS tracer test conducted in the INEEL spreading areas in 1999 demonstrated that rapid, lateral flow can occur in the vadose zone in response to episodic recharge. Subregional and WAG-specific studies (in proximity to episodic effects of streamflow recharge) recognize that more information is required to adequately assess the effects of episodic recharge on flow and contaminant migration.

Subregional conceptual models concur on the magnitude of underflow into the SRPA from contributing mountain basins to the northwest. The USGS calculates that 361 $ft^3/s$ of underflow enters the aquifer from the Big Lost River basin, 226 $ft^3/s$ of underflow enters the aquifer from the Little Lost River basin, and 102 $ft^3/s$ of underflow enters the aquifer from the Birch Creek basin. These estimates are derived from mean annual basin yield calculations and streamflow data. The WAG-10 estimates incorporate an uncertainty of 25% into the USGS estimates.

The migration of contaminants within the vadose zone and SRPA is controlled by the source term and by mechanisms that enhance or impede transport. The migration of contaminants is defined by the distribution of those contaminants in water within the aquifer and vadose zone.

The source term includes a definition of the inventory of contaminants of concern and the mechanism for release. Contaminants have been released to the subsurface through injection wells, infiltration ponds, spills, and as waste materials buried at disposal sites. Little site-specific data regarding contaminant chemical forms and mechanisms of release have been incorporated into INEEL conceptual models.

Contaminant transport within the INEEL subregion is controlled by chemical speciation, adsorption, complexation, facilitated transport, and other chemical and physical processes. Few studies have been conducted that describe the specific contaminant-water-rock interactions that are known to occur in similar terrain. WAG specific studies, with a few exceptions, rely on generalized knowledge of chemical behavior. Little site-specific data regarding contaminant chemical forms or mechanisms of release have been incorporated into INEEL conceptual models.

These components of the INEEL subregional conceptual model, when integrated, describe the field of flow through the subregion. They also define the distribution of contaminants within the system. Additional information is required to adequately define key features of flow and contaminant transport. This information includes carefully designed research activities, deep-drilling programs, and well-posed numerical analyses within the context of the subregional conceptual model.

# Contents

# Figures

# Tables

# ACRONYMS

| | |
|---|---|
| AEC | Atomic Energy Commission |
| ANL-W | Argonne National Laboratory-West |
| ANPP | Aircraft Nuclear Propulsion Program |
| ARA | Auxiliary Reactor Area |
| ARD | anaerobic reductive dechlorination |
| BBWI | Bechtel BWXT Idaho, LLC |
| bls | below land surface |
| BORAX | Boiling Water Reactor Experiment |
| CEC | cation exchange capacity |
| CERCLA | Comprehensive Environmental Response, Compensation, and Liability Act |
| CFA | Central Facilities Area |
| COC | contaminant of concern |
| CP | Chemical Waste Pond |
| CWP | Cold Waste Pond |
| DOD | Department of Defense |
| DOE | Department of Energy |
| DOE-ID | Department of Energy Idaho Operations Office |
| EBR | Experimental Breeder Reactor |
| ECF | Expended Core Facility |
| EPA | Environmental Protection Agency |
| FFA/CO | Federal Facility Agreement and Consent Order |
| HDT | Historical Data Task |
| HWMA | Hazardous Waste Management Act |
| ICPP | Idaho Chemical Processing Plant |
| IET | Initial Engine Test |

| | |
|---|---|
| INEEL | Idaho National Engineering and Environmental Laboratory |
| INTEC | Idaho Nuclear Technology and Engineering Center |
| IRA | interim remedial action |
| ISB | in situ bioremediation |
| IWD | Industrial Waste Ditch |
| KAPL | Knolls Atomic Power Laboratory |
| LOFT | Loss-of-Fluid Test |
| LSIT | Large-Scale Infiltration Test |
| LUST | leaking underground storage tank |
| MCL | maximum contaminant level |
| MNA | monitored natural attenuation |
| NAT | neutron-probe access tube |
| NPTF | New Pump and Treat Facility |
| NRF | Nuclear Reactor Facility |
| NRTS | National Reactor Testing Station |
| OU | operable unit |
| PBF | Power Burst Facility |
| R&D | research and development |
| RASA | Regional Aquifer Systems Analysis |
| RCRA | Resource Conservation and Recovery Act |
| RD/RA | Remedial Design/Remedial Action |
| RFP | Rocky Flats Plant |
| RI | remedial investigation |
| RI/BRA | remedial investigation/baseline risk assessment |
| RI/FS | remedial investigation/feasibility study |
| ROD | Record of Decision |

| | |
|---|---|
| RWMC | Radioactive Waste Management Complex |
| SDA | Subsurface Disposal Area |
| SLP | Sewage Leach Pond |
| SMC | Specific Manufacturing Capabilities Facility |
| SNL | spent nuclear fuel |
| SPERT | Special Power Excursion Reactor Test |
| SRPA | Snake River Plain Aquifer |
| SWIFT | Sandia waste isolation flow and transport |
| TAN | Test Area North |
| TIMS | Thermal Ionization Mass Spectrometry |
| TRA | Test Reactor Area |
| TSF | Technical Support Facility |
| USGS | United States Geological Survey |
| VOC | volatile organic compound |
| WAG | waste area group |
| WRRTF | Water Reactor Research Treatment Facility |
| WWP | Warm Waste Pond |

# INEEL Subregional Conceptual Model Report

## Volume 1—Summary of Existing Knowledge of Natural and Anthropogenic Influences Governing Subsurface Contaminant Transport in the INEEL Subregion of the Eastern Snake River Plain (Draft)

## 1. INTRODUCTION

In 1949, the United States set aside 890 $mi^2$ of the eastern Snake River Plain to be developed as the National Reactor Testing Station (NRTS). The purpose of the NRTS was to provide an isolated location where prototype nuclear reactors could be designed, built, and tested. The NRTS later was renamed the Idaho National Engineering Laboratory (INEL). In January 1997, the U.S. Department of Energy (DOE) designated the INEL as the Idaho National Engineering and Environmental Laboratory (INEEL) to highlight Idaho's role in developing waste-cleanup and other environmental technologies (see Figure 1-1).

In December 1991, the DOE entered into a Federal Facilities Agreement and Consent Order (FFA/CO; DOE-ID 1991) with the Environmental Protection Agency (EPA) and the State of Idaho to implement the remediation of the INEEL. The goals of the agreement were to ensure that potential or actual releases of hazardous substances to the environment are thoroughly investigated and that appropriate response actions are taken to protect human health and the environment. To implement the agreement, the INEEL embarked on a decade-long, multi-million-dollar effort to systematically collect environmental data assessing the nature and extent of contamination resulting from past activities. In the FFA/CO, the INEEL is divided into 10 Waste Area Groups (WAGs), which are designations for decision units as defined in the Comprehensive Environmental Response, Compensation, and Liability Act (CERCLA; 42 USC § 9601 et seq.). With the exception of WAG 10, which is a site-wide designation, the WAGs are associated with individual facilities at the INEEL (see Figure 1-2).

Numerous subregional and facility-scale scientific studies have been conducted during the 50-year history of the INEEL to characterize its geologic and hydrologic setting and to evaluate the fate and transport of radioactive, inorganic, and organic chemical wastes disposed to the subsurface from INEEL activities as part of the FFA/CO. In 2001, the DOE initiated a water integration project at the INEEL to better coordinate operations, scientific research, and subsurface monitoring programs. The ultimate goal of the water integration project is to reduce risk to the public, workers, and the environment.

### 1.1 Purpose and Scope

A key objective of the DOE water-integration project at the INEEL is to coordinate development of a subregional conceptual model of groundwater flow and contaminant transport that is based on the best available understanding of geologic and hydrologic features. The first step in this process is to compile and summarize the current conceptual models of groundwater flow and contaminant transport at the INEEL that have been developed from extensive geohydrologic studies conducted during the last 50 years.

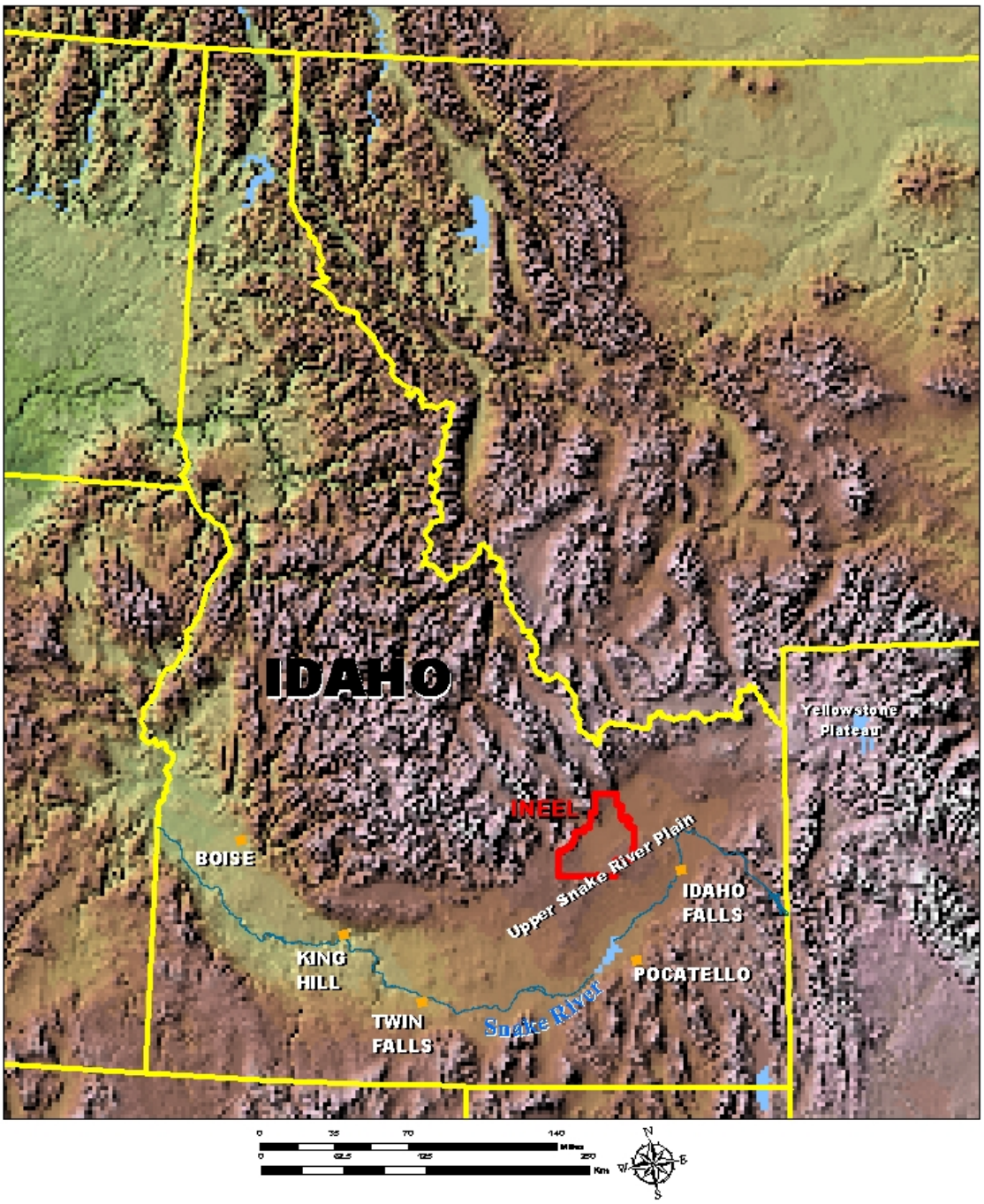


Figure 1-1. Location of the INEEL.

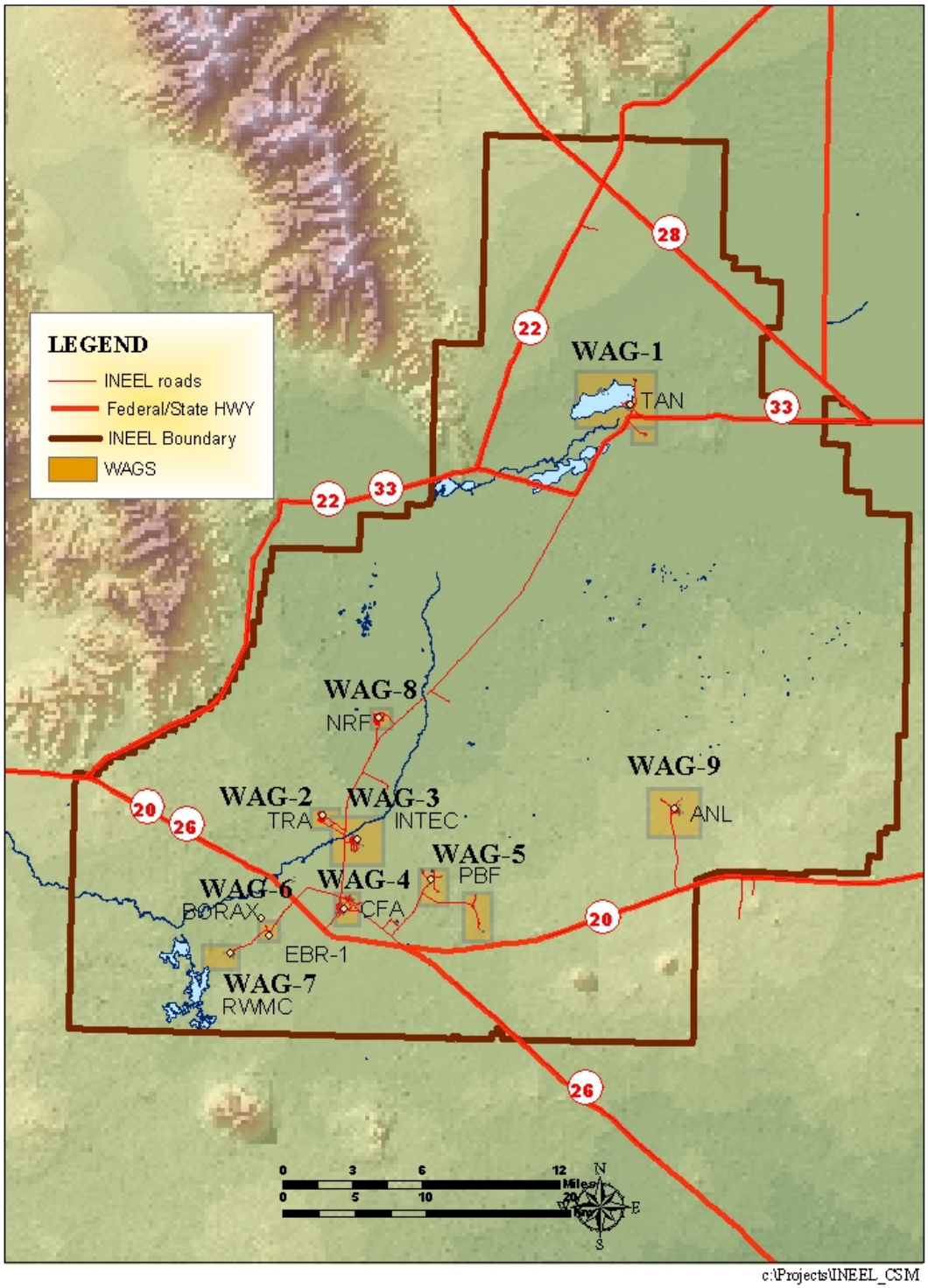


Figure 1-2. Location of facilities and designated waste area groups at the INEEL.

As part of this project, North Wind Environmental, Inc., under contract to the INEEL Contractor, Bechtel BWXT Idaho (BBWI), has compiled a summary of subregional and facility-specific geohydrologic investigations that have been conducted at the INEEL since its inception in the early 1950's. Subregional-scale investigations typically encompassed hundreds of square miles and included much of the INEEL; facility-scale investigations encompassed tens of square miles and focused on individual facilities at the INEEL.

This summary includes a description of the components of current conceptual models of flow and transport used in INEEL subregional and facility-specific geohydrologic investigations. The summary also presents a discussion of competing hypotheses and additional data requirements, as identified by those investigations.

## 1.2 Definition of a Conceptual Model

The National Research Council (2001) defined a conceptual model as "an evolving hypothesis identifying the important features, processes, and events controlling fluid flow and contaminant transport of consequence at a specific field site in the context of a recognized problem." Remson et al. (1971) state that the solution to a groundwater problem requires "knowledge of the system functioning and of the auxiliary conditions describing the system constraints." Remson et al. define the system functioning as a set of generally non-linear differential equations that mathematically describe the way that the system operates. The auxiliary conditions include the system geometry (system dimensions), matrix characteristics (capability of the system materials to store and transmit water), and boundary conditions. These boundary conditions describe what is happening at geologic or hydrologic boundaries. Boundaries may include head boundaries (e.g., aquifer interface with a lake), flow boundaries (underflow and vertical flow across the base of the aquifer), zero-flow boundaries (e.g., mountain-front), free-surface boundaries (interface between the water table and vadose zone, affected by changes in storage and by recharge from areal precipitation, streamflow, and wastewater infiltration), and symmetry boundaries (e.g., flow path). These conceptual model components define the flow field (distribution of head and flux). A complete conceptual model, consisting of a description of the geohydrologic framework of the system including the system geometry and matrix properties and the definition of flow boundaries and geohydrologic conditions that affect those boundaries, can be used to develop a well-posed set of mathematical equations that represent flow and/or transport of contaminants through the system.

The conceptual model evolves with improved understanding of the geologic and hydrologic features that control flow and contaminant transport. Each aspect of the conceptual model includes definition of competing hypotheses about those geologic and hydrologic features. As these competing hypotheses are identified, they can be tested to further refine the conceptual model.

Numerical analyses (numerical models) can be used to test the adequacy of the conceptual model to describe the flow system, to evaluate those aspects of the conceptual model that require refinement through additional data collection, and to test competing hypotheses. These numerical models are based on assumptions that may or may not be representative of the conceptual model. A numerical model that is based on a defensible conceptual model provides a means to integrate the conceptual model components.

A numerical model only can provide a predictive capability that is limited to the range and knowledge of system conditions and stresses that define the conceptual model. For example, a numerical model calibrated to moderate pumping withdrawals and water-level declines may not be able to adequately predict declines associated with extreme withdrawals.

A numerical model is limited by the purpose of the study. For example, components essential to a conceptual model of water supply will be different than components essential to a conceptual model of

contaminant transport. A common numerical simulator may not effectively integrate conceptual model components for different types of studies.

Conceptual models (and numerical models) generally are dependent on the scale of the system. Those components essential to an INEEL subregional conceptual model may be different than those components essential to a facility-scale model. For example, a subregional model may adequately describe groundwater flow by lumping the complex basalt stratigraphy into a few hydrogeologic units. The facility-scale model may require differentiation of individual flows or even parts of individual flows.

## 1.3 Geohydrologic Setting

The geohydrologic framework at the scale of the INEEL subregion and specific facilities is described within the context of the geology and hydrology of the eastern Snake River Plain. The geologic context has been shaped by the origin and structural development of the plain. The hydrologic context is controlled by the distribution of regional recharge, characteristics of regional groundwater flow, and discharge from the Snake River Plain Aquifer (SRPA).

### 1.3.1 Regional Geology

The eastern Snake River Plain (see Figure 1-3) represents a long and complex geologic and structural history. This history, briefly described by Hackett et al. (1986) and Whitehead (1992), has resulted in a thick section of fractured basalt flows that form the geohydrologic framework of the SRPA.

***1.3.1.1 Origin of the Eastern Snake River Plain.*** The geologic history of the eastern Snake River Plain began about 650 million years ago with a 300-million-year period of deposition of shallow marine, sedimentary rocks along an ancient continental margin (Hackett et al. 1986). Subsequent subduction of the oceanic plate beneath the North American continental plate compressed the continental crust, developing major thrust faults, uplifting the marine sedimentary rocks, and forming mountain ranges. These ranges are visible to the west of what now is the eastern Snake River Plain. During the next 300 million years, continued subduction resulted in melting of oceanic crustal material that was intruded to form the massive Idaho Batholith. Uplift of the batholith formed the granitic mountains of central Idaho. Later, subduction and melting resulted in extensive volcanism and deposition of the Challis Volcanics throughout much of central Idaho.

Approximately 17 million years ago, shifted crustal movement began to stretch the continental plate. These extensional forces created a broad band of crustal faulting that formed the Basin and Range structure, a sequence of subparallel uplifted mountain blocks and intervening basins that extends across much of the western United States.

Over the last 15 million years, the North American continental plate has drifted rapidly (approximately 3.5 cm/year) over a stationary convection plume or “hot spot” in the earth’s mantle (Hackett and Smith 1992). This movement over the plume-heated crustal material resulted in a progressive sequence of downwarping, faulting, and volcanism that extended from eastern Oregon to the Yellowstone Plateau (see Figure 1-1). Volcanism was characterized by eruptions of high-volume, bimodal rhyolite and basalt (Wood and Kienle 1990).

The direction of continental drift initially was to the northwest, forming the western Snake River Plain. The occurrence of basalts near King Hill (see Figure 1-1), with an estimated age of 6.2 million years (Armstrong et al. 1975), infers that the direction of plate movement has shifted to the southwest during the last 5 to 10 million years. Melted crustal material over the “hot spot” emplaced a series of presently buried rhyolitic calderas in a northeast progression (Wood and Kienle 1990). These calderas

were followed in the next 2 to 5 million years by abundant basaltic volcanism. The "hot spot" presently lies beneath the Yellowstone Plateau. This sequence formed the eastern Snake River Plain (see Figure 1-1), an arcuate structural basin in southeastern Idaho that is more than 170 miles long, 60 miles wide, and has downwarped several kilometers in places (Arnett and Smith 2001). This structural basin is filled with a thick complex of rhyolitic volcanic rocks and basaltic flows originating from numerous vents and fissures across the plain.

***1.3.1.2 Structure of the Eastern Snake River Plain.*** Faults are not well defined along the downwarped eastern Snake River Plain. However, seismic data indicate that large-displacement faults may bound the plain (Whitehead 1992). Sparlin et al. (1982) suggested that faults along the northern boundary of the plain may have a displacement of as much as 13,000 ft. Whitehead (1992) suggested that volcanic materials filling the downwarped plain may be as much as 16,000 ft thick.

Downwarping and volcanic activity probably resulted in differential subsidence throughout the eastern Snake River Plain. This subsidence resulted in a regionally distorted orientation of bedded basalt and differences in thickness of sedimentary units deposited on the developing plain during periods of volcanic quiescence.

Whitehead (1992) observed that "volcanic vents appear to be randomly scattered, but some are aligned along rift zones." These rift zones, trending northwest across the eastern Snake River Plain, "appear to be extensions of adjacent basin-and-range structures" (Kuntz 1978). Anderson et al. (1999) stated that vent corridors associated with these rift zones on the eastern Snake River Plain average about 1 to 2 miles in width and 5 to 15 miles in length. These vent corridors are characterized by aligned vents, dikes, and fissures.

### 1.3.2 Regional Hydrology

The SRPA, one of the most productive aquifers in the United States, underlies the eastern Snake River Plain (see Figure 1-3). This aquifer has been estimated by various researchers to contain from 80 to 200 million (some say as much as 1 billion) acre-ft of water. The aquifer provides a source of drinking water to more than 200,000 people and supplies irrigation water to a large, regional agricultural and aquacultural economy.

The SRPA predominantly consists of numerous, thin basalt flows with hydraulically connected interflow zones (Whitehead 1992). According to Whitehead, the aquifer is thickest in the central part of the plain and thins toward the margins. The basalt flows are commonly interbedded with thin, fine-grained alluvial and fluvial sedimentary units. Arnett and Smith (2001) note that the processes of basaltic volcanism following the Yellowstone hotspot resulted in small batches of basaltic magma, ensuring that individual basalt flows were relatively thin. The magma contained large volumes of open vesicles and was characterized by a thick, porous, and permeable basal rubble zone.

The aquifer is underlain in most areas by older basaltic and silicic volcanic rocks. These older rocks are characterized by reduced permeability that is attributed to secondary mineralization, thicker flows, and fewer interflow zones (Whitehead 1992). In the western part of the eastern Snake River Plain, the aquifer is underlain by extensive sedimentary units.

Recharge to the SRPA occurs from irrigation and river seepage, infiltration of areal precipitation, and tributary-basin underflow. Water in the aquifer flows generally to the southwest (see Figure 1-1). Ackerman (1995) estimated that the travel time through the aquifer is as much as 350 years.

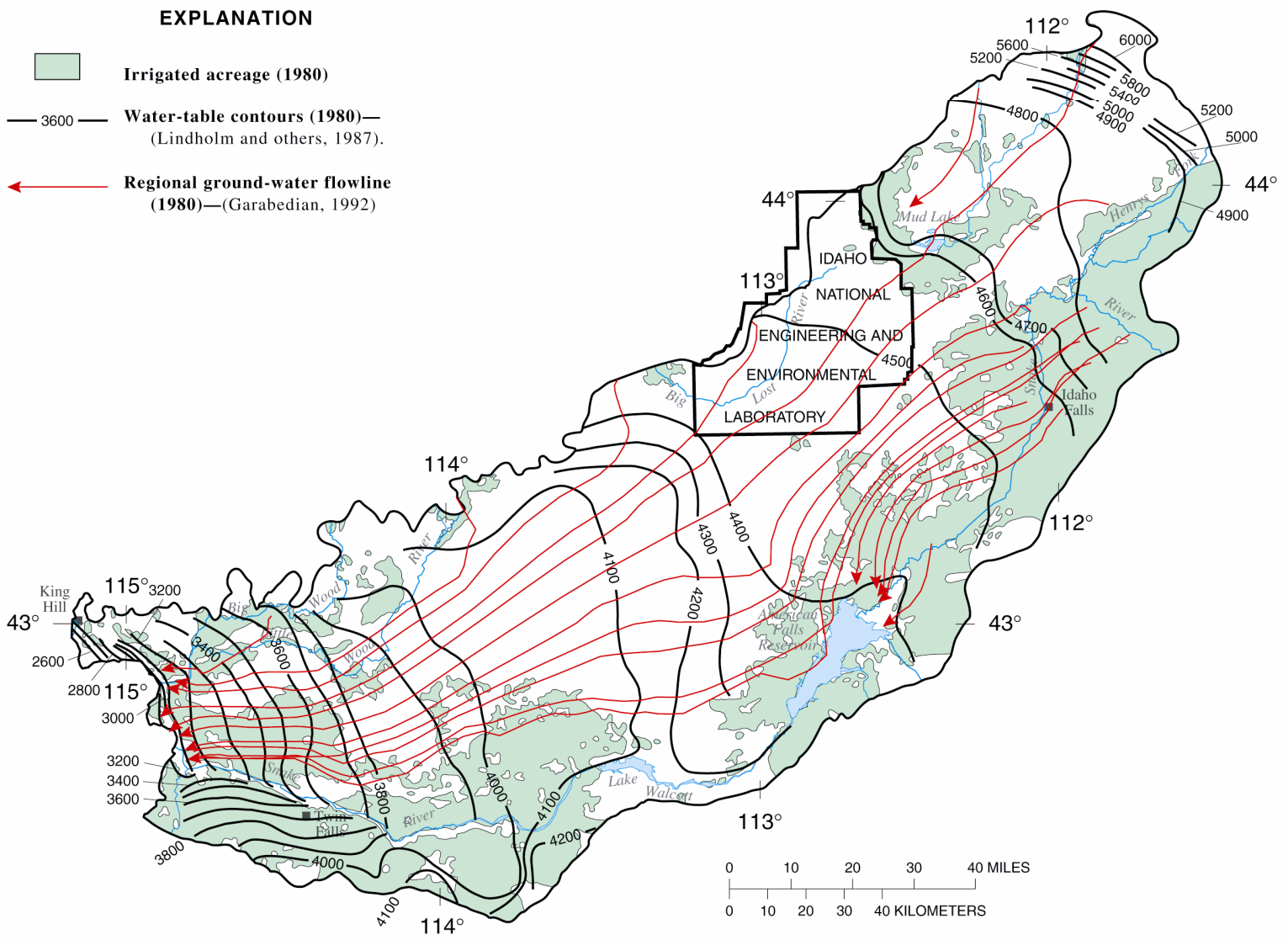


Figure 1-3. Extent of the SRPA (from Ackerman et al. in preparation).

Discharge from the SRPA predominantly occurs from large springs in the Thousand Springs area along the Snake River between Twin Falls and King Hill (see Figure 1-1). These springs include some of the nation's largest springs. Whitehead (1992) reported that these springs discharged 6,000 $ft^3/s$ of water to the river in 1980. Aquifer discharge also occurs from groundwater pumpage for irrigation, municipal, and domestic supply.

Groundwater in the eastern Snake River plain occurs in the deep-seated geothermal system and the overlying eastern SRPA. Geochemical and isotopic evidence suggests that groundwater in the aquifer is of local meteoric origin. Water in the underlying geothermal system has an estimated residence time of 17,000 years, while the overlying eastern SRPA has a residence time estimated at a maximum of 200 to 350 years. Solutes primarily enter aquifer water through dissolution of minerals contained in the aquifer matrix and secondarily through anthropogenic sources (Wood and Low 1988).

### 1.3.3 References Cited


Ackerman, D.J., 1995, *Analysis of Steady-State Flow and Advective Transport in the Eastern Snake River Plain Aquifer System*, Water-Resources Investigations Report 94-4257 (DOE/ID-22120), U.S. Geological Survey.

Anderson, S.R., Kuntz, M.A., and Davis, L.C., 1999, *Geologic Controls of Hydraulic Conductivity in the Snake River Plain Aquifer at and near the Idaho National Engineering and Environmental Laboratory*, Water-Resources Investigations Report 99-4033 (DOE/ID-22155), U.S. Geological Survey.

Armstrong, R.L., Leeman, W.P., and Malde, A.G., 1975, "K-Ar dating, Quaternary and Neogene volcanic rocks of the Snake River Plain," *Idaho: American Journal of Science,* Vol. 275, No. 3, p. 225-251.

Arnett, R.C., and Smith, R.P., 2001, *WAG 10 Groundwater Modeling Strategy and Conceptual Model: Idaho National Engineering and Environmental Laboratory Report*, INEEL/EXT-01-00768, Revision B.

Hackett, B., Pelton, J., and Brockway, C., 1986, *Geohydrologic Story of the Eastern Snake River Plain and the Idaho National Engineering Laboratory*, Idaho National Engineering and Environmental Laboratory, Booklet prepared for the U.S. Department of Energy.

Hackett, W.R., and Smith, R.P., 1992, "Quaternary volcanism, tectonics, and sedimentation in the Idaho National Engineering Laboratory area," ed. J. R. Wilson, *Field Guide to Geologic Excursions in Utah and Adjacent Areas of Nevada, Idaho, and Wyoming, Geological Society of America Rocky Mountain Section Guidebook*, Utah Geological Survey Miscellaneous Publication 92-3, pp. 1-18.

Kuntz, M. A., 1978, *Geology of the Arco-Big Southern Butte Area, Eastern Snake River Plain, and Potential Volcanic Hazards to the Radioactive Waste Management Complex and Other Waste Storage and Reactor Facilities at the Idaho National Engineering Laboratory,* U.S. Geological Survey Open File Report 78-691, U.S. Geological Survey.

National Research Council, 2001, "Conceptual models of flow and transport in the fractured vadose zone," *National Academy Press*, Washington, D.C.

Remson, I., Hornberger, G.M., and Molz, F.J., 1971, *Numerical methods in subsurface hydrology,* John Wiley and Sons, Inc.

Sparlin, M.A., Braile, L.W., and Smith, R.B., 1982, "Crustal Structure of the Eastern Snake River Plain Determined from Ray Trace Modeling of Seismic Refraction Data," *Journal of Geophysical Research*, Vol. 87, No. 4, p. 2,619-2,633.

Whitehead, R.L., 1992, *Geohydrologic framework of the Snake River Plain Regional Aquifer System*, Idaho and Eastern Oregon: U.S. Geological Survey Professional Paper 1408-B, U.S. Geological Survey.

Wood and Kienle, 1990, *Volcanoes of North America: United States and Canada,* Cambridge University Press.

Wood, W.W., and Low, W.H., 1988, *Solute Geochemistry of the Snake River Plain Regional Aquifer System*, Idaho and Eastern Oregon: U.S. Geological Survey Professional Paper 1408-D, U.S. Geological Survey.

# 2. SUBREGIONAL GEOHYDROLOGIC STUDIES

Numerous researchers have studied the geology and hydrology of parts of the eastern Snake River Plain that include the INEEL (see Figure 2-1). Some of these studies were conducted to assist in facility construction; others were conducted to monitor the movement of contaminants through the subsurface. Each of these studies represented an evolving understanding of subregional groundwater flow and contaminant transport. The following section describes key studies representing groundwater flow and contaminant transport at the INEEL. Subsequent sections will present and contrast key geologic and hydrologic components of the conceptual models that were developed in each of these studies.

## 2.1 Previous Subregional Studies

The DOE and its predecessor agencies, DOE Contractors, and the United States Geological Survey (USGS) have conducted geohydrologic studies since the late 1940's within the INEEL subregion to characterize groundwater flow and contaminant transport and to evaluate risk to human health and the environment. Other researchers, including State of Idaho agencies, other federal agencies, and Universities, have participated in studies at and near the INEEL in conjunction with regulatory, oversight, and research programs.

### 2.1.1 United States Geological Survey

The present USGS conceptual model of groundwater flow at the INEEL has evolved from a series of investigations that began in the late 1940's. These investigations included site characterization studies and studies that evaluated aspects of the fate and transport of contaminants in the subsurface. The USGS also has maintained long-term monitoring networks designed to collect water-quality and water-level data from numerous wells at the INEEL.

Beginning in 1948, the USGS conducted a series of geologic and hydrologic studies at the INEEL in conjunction with the construction, operation, and environmental safety of facilities. Most of this early work was summarized in a series of USGS Professional Papers (Nace et al. 1972, and Nace et al. 1975).

During the 1970's, the USGS conducted a subregional assessment of contaminant transport. This work included the continued development of conceptual models of flow and transport as part of numerical modeling work presented in a series of reports by Robertson (1974 and 1977). The work by Nace et al. and Robertson contributed greatly to the present understanding of the geohydrologic framework and of the distribution and transport of contaminants in groundwater.

In 1986, the USGS initiated a series of studies to develop a comprehensive conceptual model of groundwater flow at the INEEL. This series included subregional studies that described the basalt-sediment stratigraphy and geohydrologic framework of the SRPA at the INEEL (Anderson et al. 1996; Anderson et al. 1997; Anderson and Liszewski 1997; and Anderson et al. 1999), distribution of aquifer hydraulic properties (Ackerman 1991a, 1991b; Anderson et al. 1999), and episodic recharge from surface-water features (Bennett 1990). These studies drew heavily from the earlier work by Nace et al. and Robertson, and from regional work conducted as part of the USGS Regional Aquifer Systems Analysis (RASA). The body of work will be summarized in a report describing the conceptual model of flow in the INEEL subregion (Ackerman et al. in preparation).

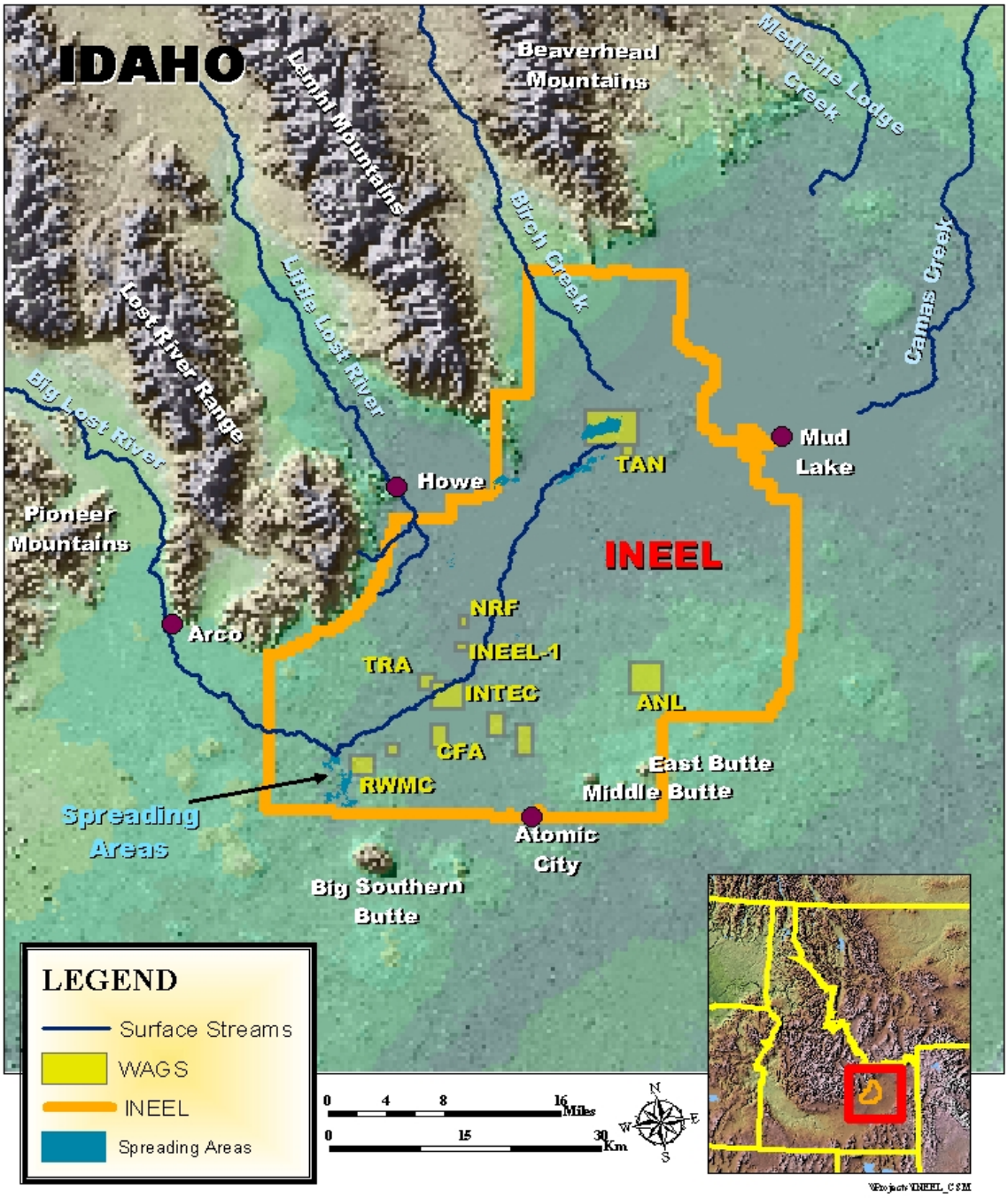


Figure 2-1. Location of the INEEL, INEEL facilities, and selected surface water features.

A USGS study that provided a better understanding of underflow into the INEEL subregion was conducted in the early 1990's. This study evaluated water-use alternatives in the Mud Lake area (see Figure 2-1) northeast of the INEEL (Spinazola 1994a; 1994b). This study incorporated parts of the northern INEEL downgradient from Mud Lake.

Several site-specific studies were conducted by the USGS to provide improved understanding of subregional groundwater flow. Beginning in 1998, the USGS initiated a study to better characterize the role of sedimentary interbeds in vadose-zone flow and contaminant transport. This study included a drilling component designed to develop techniques for recovery of relatively undisturbed, unconsolidated interbed samples. It also included a component to evaluate hydraulic characteristics of these interbeds (Perkins and Nimmo 2000). In 1999, the USGS conducted a tracer study (Nimmo et al. 2001) in the INEEL spreading areas (see Figure 2-1). This test demonstrated rapid lateral flow in the vadose zone over large distances. The USGS continues to use a deep drilling program designed to improve the understanding of subregional stratigraphic and structural features controlling groundwater flow.

A series of USGS studies evaluated geochemical data to improve the understanding of groundwater flow and contaminant transport in the INEEL subregion. One of these studies (Knobel et al. 1997) delineated natural geochemical reactions to determine the effect of rock/water interaction on groundwater chemistry at the INEEL. Another study (Carkeet et al. 2001; Swanson et al. 2002) evaluated the geochemistry of water from tributary mountain drainages that contribute recharge as underflow and surface flow to the eastern Snake River Plain. Busenberg et al. (1993, 1998, 2000, and 2001) used chlorofluorocarbon and isotopic data to evaluate recharge, geochemical interactions, and groundwater flow in the subregion. Cecil et al. (2000) used measured contaminant concentrations in groundwater as tracers to evaluate characteristics of flow, including regional-scale aquifer dispersivity. A series of reports described laboratory studies to evaluate the strontium-partitioning coefficient for interbeds and basalts (Liszewski et al. 1997; Liszewski et al. 1998; Colello et al. 1998; Pace et al. 1999; and Rosentreter et al. 1999).

### 2.1.2 INEEL Researchers

Since the early 1990's, INEEL researchers have conducted a subregional assessment of groundwater flow and contaminant transport to support environmental restoration activities at the INEEL and its facilities. This work, known as WAG 10 studies, was implemented through the FFA/CO and signed in 1991 by the DOE, the EPA, and the State of Idaho. This assessment, based in part on earlier USGS and other investigations, consisted of a sequence of numerical and other studies to evaluate groundwater flow in the subregion.

These INEEL studies included development of an Environmental Impact Statement numerical model (Arnett and Springer 1994) to simulate flow and transport in the south-central part of the INEEL.

McCarthy et al. (1995) constructed a regional WAG-10 numerical model. This model included the entire eastern Snake River Plain to examine flow at the INEEL while preserving regional influences.

A series of temperature studies has been conducted since the 1960's to examine heat flow and structural features (Blackwell 1989 and 1990; Blackwell and Steele 1992; Blackwell et al. 1992; Olmsted 1962; Smith et al. 2001; Brott et al. 1981; and Wood and Bennecke 1994). These studies provided information about the effective base of the SRPA and supported groundwater mass balance studies.

Smith et al. (2000) examined the implications of water temperature, water chemistry, and the regional geophysical setting in defining groundwater flow through the INEEL subregion. Smith (2001) evaluated the thickness of the SRPA at the INEEL to support WAG-10 numerical modeling efforts.

Arnett and Smith (2001) presented many of the components of the INEEL conceptual model of groundwater flow. These components integrated conceptual components derived from previous INEEL, USGS, and other geohydrologic studies. Work has continued since the release of the conceptual model report to refine the understanding of the geohydrologic framework and other components of the conceptual model.

A series of site-specific studies were conducted by INEEL researchers that provided further understanding of the characteristics of subregional groundwater flow. In 1979, a 10,365-ft deep test hole (see Figure 2-1) was drilled to evaluate possible geothermal resources beneath the INEEL. Information acquired from this test hole (Mann 1986) provided information about geohydrologic conditions in rocks underlying the SRPA.

The Integrated Large-Scale Pumping and Infiltration Tests (Wood and Norrell 1996) provided information about hydrologic properties of the vadose zone and SRPA near the Radioactive Waste Management Complex (RWMC) at the INEEL and examined the implications of vadose-zone flow in that part of the INEEL subregion. This study provided valuable information about the capability of the vadose zone to transport water and contaminants to the aquifer.

INEEL researchers evaluated water-rock interactions and their effects on transport of radionuclides (Johnson et al. 2000; Luo et al. 2000). This work also provided information about preferential flowpaths in the aquifer.

In 2000, INEEL researchers initiated the vadose-zone research park in conjunction with construction of new Idaho Nuclear Technology and Engineering Center (INTEC) wastewater disposal ponds 2 mi southwest of INTEC (see Figure 2-1). This park consists of a series of instrumented testholes installed prior to wastewater disposal to evaluate effects of wastewater infiltration on the vadose zone.

Additionally, researchers have conducted numerous facility-specific studies designed to evaluate contaminant transport at a smaller scale. Key facility-scale studies are presented in later sections of this summary. These studies also have provided information about subregional movement of water and contaminants.

### 2.1.3 Other Researchers

University and State of Idaho researchers have conducted studies that have provided information about subregional groundwater flow and contaminant transport. Frederick and Johnson (1996 and 1997) evaluated vertical characteristics of flow in the SRPA. Welhan and Wylie (1997) and Welhan and Reed (1997) examined the distribution of hydraulic properties of the aquifer.

## 2.2 INEEL Subregional Conceptual Models of Flow and Transport

Conceptual models of flow and transport within the INEEL subregion integrate the evolving understanding of the geologic framework and hydrologic conditions of the subregion. Two subregional conceptual models presently in preparation are the USGS conceptual model and the WAG-10 conceptual model.

### 2.2.1 Components of Subregional Conceptual Models of Saturated and Unsaturated Flow

Subregional researchers developed their conceptual understanding of flow based on their best understanding of the subregional geometry, distribution of matrix characteristics, and aquifer boundary conditions. The following sections summarize components of these concepts as presented in the USGS and WAG-10 subregional studies.

***2.2.1.1 Mathematical Representation of Subregional Groundwater Flow.*** Subregional studies typically assume that groundwater flow at the scale of the INEEL is best represented mathematically as flow through a porous media. Robertson (1974) assumed that subregional flow in the aquifer obeyed Darcy's law but stated that this assumption may not be completely accurate. Whitehead (1992) stated that, while hydraulic properties of basalt vary widely within a short distance, the effects of local heterogeneity may be minimized at a larger scale and that homogeneous conditions may be assumed.

***USGS—***The USGS conceptualizes subregional groundwater flow as occurring through an equivalent porous media with nonuniform properties (Ackerman et al. in preparation). Ackerman et al. states that this representation is considered appropriate for modeling subregional transport of conservative, nonsorbing contaminants. Flow is considered to be unconfined (Ackerman et al. in preparation) but the layered system is characterized by very small vertical to horizontal permeability

***WAG-10—***The WAG-10 conceptual model of subregional flow, similar to that of the USGS, represents flow in the subregion as occurring through a heterogeneous equivalent porous media.

***2.2.1.2 Geometry of the Subregion.*** The following sections review and contrast system dimensions and describe stratigraphic and structural controls of groundwater flow and contaminant transport as conceptualized in the USGS and WAG-10 subregional studies.

***Subregional System Dimensions—***The lateral dimensions of the various INEEL subregional studies differ because no distinct subregional hydrologic boundaries exist to the northeast, southwest, and southeast. Limited vertical stratigraphic data provide different conceptual models of the effective thickness of the SRPA.

***USGS—***The USGS subregional conceptual model encompasses 1,940 $mi^2$ of the eastern Snake River Plain (see Figure 2-2) and is intermediate in size between the regional flow system (10,800 $mi^2$; see Figure 1-3) and the INEEL facility-scale (less than about 10 $mi^2$; see Figure 1-2; Ackerman et al. in preparation). The subregion is smaller than the subregion defined by Robertson (2,600 $mi^2$, extending from the north INEEL boundary to approximately 25 mi south of the INEEL). The USGS subregional system is approximately 70 mi long and 30 mi across (see Figure 2-2), beginning at the 4,600-ft elevation groundwater contour to the northeast. The subregion is bounded to the southeast by a southwest-trending groundwater flow path along the eastern INEEL boundary and is bounded to the northwest by the mountains and tributary valleys of the Bitterroot, Lemhi, Lost River, and Pioneer mountain ranges. The subregion is bounded to the southwest approximately 25 mi downgradient from the southern boundary of the INEEL, at a distance sufficient to include known contaminant concentrations (chlorine-36) in groundwater. (Ackerman et al. in preparation).

Robertson's study assumed that the subregional thickness of the aquifer averaged 250 ft because of apparent layering effects. According to Robertson, "This upper layer appears to be somewhat separated from and more permeable than the lower zones" (Robertson 1974; Robertson et al. 1974).

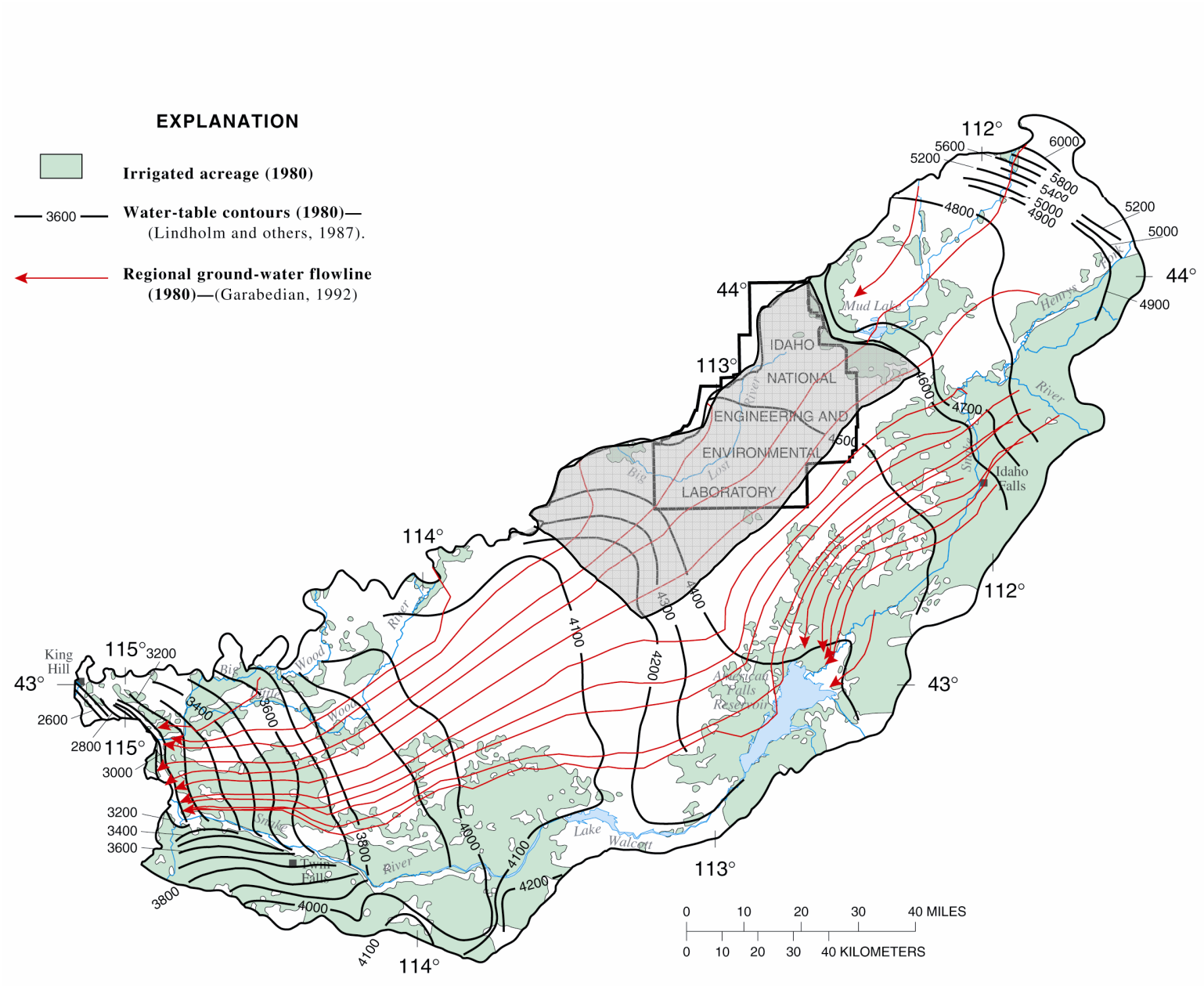


Figure 2-2. Extent of the USGS INEEL subregional conceptual model, eastern SRPA, Idaho (From Ackerman et al. in preparation).

The current USGS conceptual model groups the complex basalt stratigraphy of the eastern Snake River Plain into three hydrogeologic units (Unit 1, Unit 2, and Unit 3) based on common hydraulic properties (see Figure 2-3; Ackerman et al. in preparation). Unit 1 consists of many younger, thin, fractured basalt flows and interbedded sediments; unit 1 basalts are below the water table in the central part of the INEEL subregion and range in thickness from 0 to perhaps as much as 300 ft. Unit 2 underlies unit 1 and consists of younger, thick, dense basalt flows and interbedded sediments; unit 2 rises above the water table in the southwestern part of the INEEL subregion. Unit 3 consists of rocks of intermediate age that are slightly altered and interbedded with sediments. Unit 3 rocks are saturated throughout the INEEL subregion and represent the thickest part of the aquifer. Based on Whitehead's (1986) estimates from electrical resistivity and drillhole data, the base of Unit 3 may exceed 2,500 ft below the water table in the eastern part of the subregion and more than 4,000 ft in the southwestern part (Ackerman et al. in preparation).

WAG-10—***The WAG-10 conceptual model (see Figure 2-4) was extended beyond INEEL boundaries to "better accommodate regional effects and to ensure that groundwater movement beyond the INEEL boundaries can be included" (Arnett and Smith 2001). The WAG-10 conceptual model is bounded on the northwest by the mountains and tributary valleys of the Bitterroot, Lemhi, Lost River, and Pioneer Mountain Ranges. The southwest boundary corresponds to an equipotential line of the water table that is sufficiently distant from the INEEL. The northeast boundary overlaps a part of the USGS Mud Lake model area (Spinazola 1994) to permit use of fluxes calculated from Spinazola's numerical modeling study as underflow into the subregion. The southeastern boundary corresponds to a southwest trending flow line across which no flow is assumed.*** The OU 10-08 subregion includes about 3,000 $mi^2$ of the eastern Snake River Plain.

Smith (2001) used an aquifer temperature data set and an electrical resistivity data set in conjunction with limited deep testhole data to develop two interpretations of aquifer thickness (see Figure 2-5). The "thick" aquifer interpretation, based on colder temperatures, includes a north-trending zone exceeding 400 m in thickness (1,300 ft; Arnett and Smith 2001); the maximum thickness is 520 m (1,700 ft). The thin aquifer interpretation minimizes aquifer thickness, assuming that the aquifer gradually thickens toward the center of the plain from a thickness of 100 m (328 ft) or less along the northwest to a maximum of 400 m (1,300 ft).

The WAG-10 conceptual model uses hydrogeologic units similar to those of the USGS based on Anderson's stratigraphic data and interpretations. An upper fractured basalt is equivalent to the USGS unit 1. Composite layer 7 is equivalent to USGS unit 2. Composite layer 7 intersects the water table south of the INEEL. It is not perceived to be a flow barrier.

***Stratigraphic Controls on Groundwater Flow—***The vadose zone and SRPA in the INEEL subregion is comprised of at least 178 basalt-flow groups, 6 andesite-flow groups, 103 sedimentary interbeds, and at least 4 rhyolite domes (Anderson and Liszewski 1997). The small-scale stratigraphic features associated with individual basalt flows comprising this complex stratigraphic sequence affect the horizontal and vertical flow of water in the subregion.

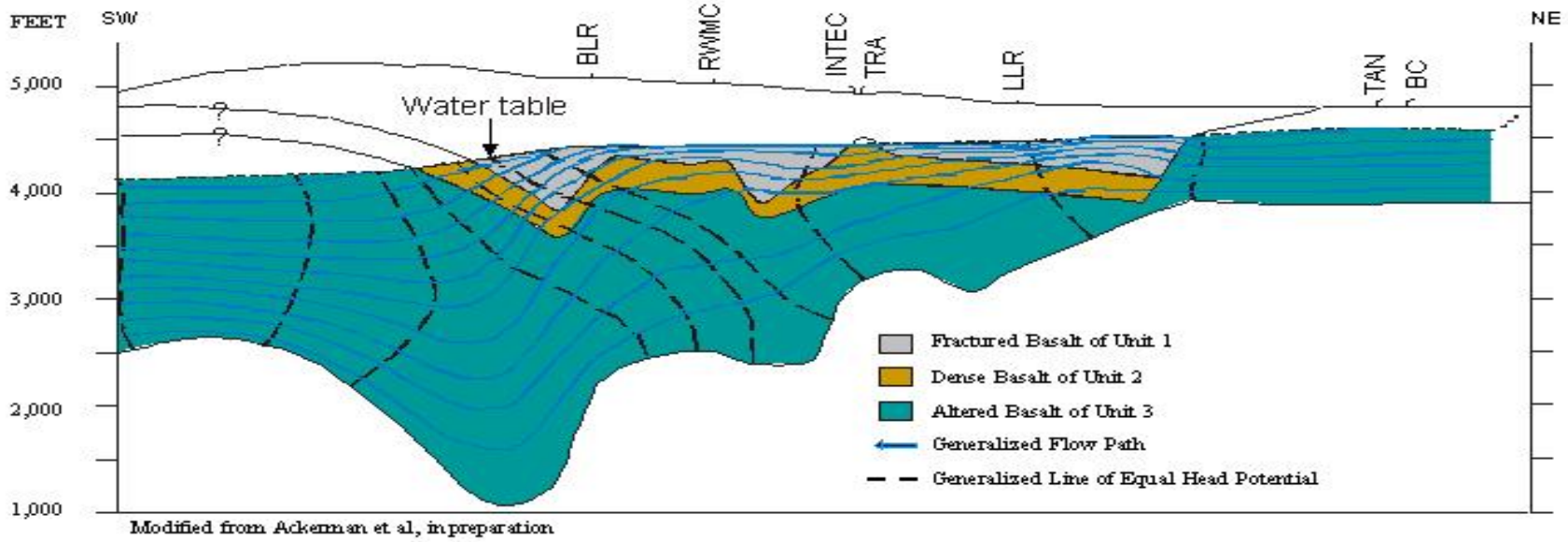


Figure 2-3. Geohydrologic units differentiated in the USGS INEEL subregional conceptual model from stratigraphic data (Modified from Ackerman et al, in preparation).

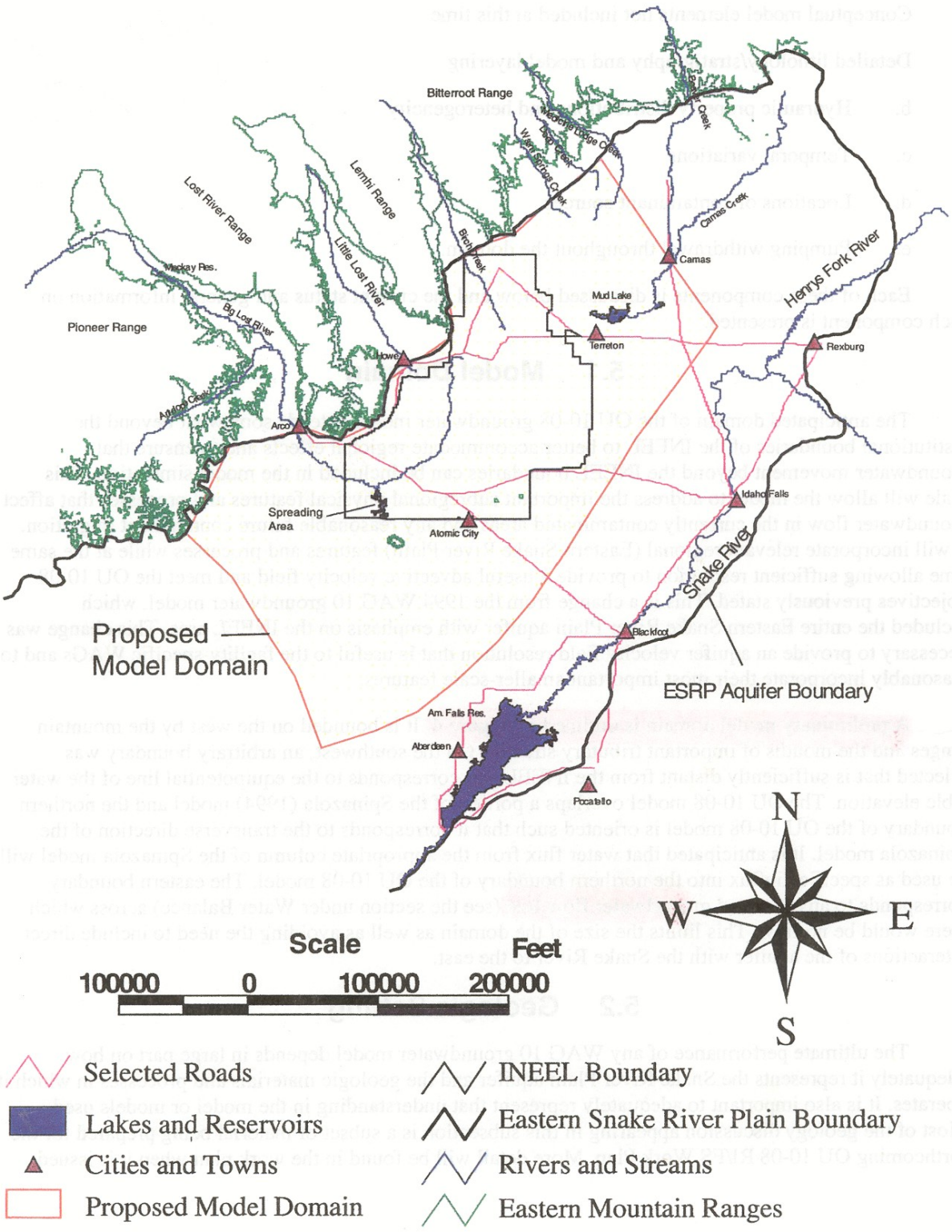


Figure 2-4. Extent of WAG-10 conceptual model of the INEEL subregion (from Arnett and Smith 2001).

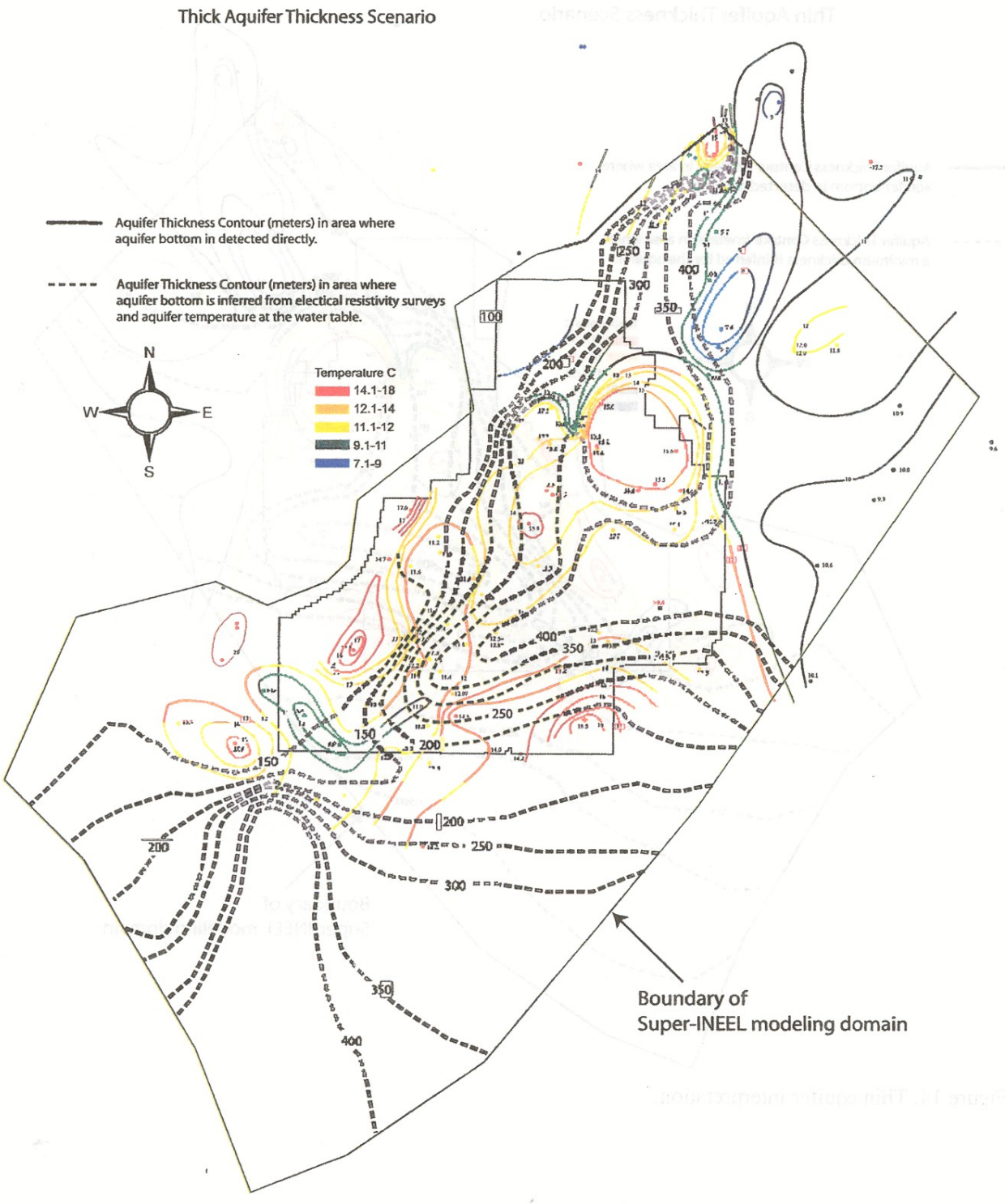


Figure 2-5. WAG 10 interpretations of aquifer thickness for the INEEL subregion (from Arnett and Smith 2001).

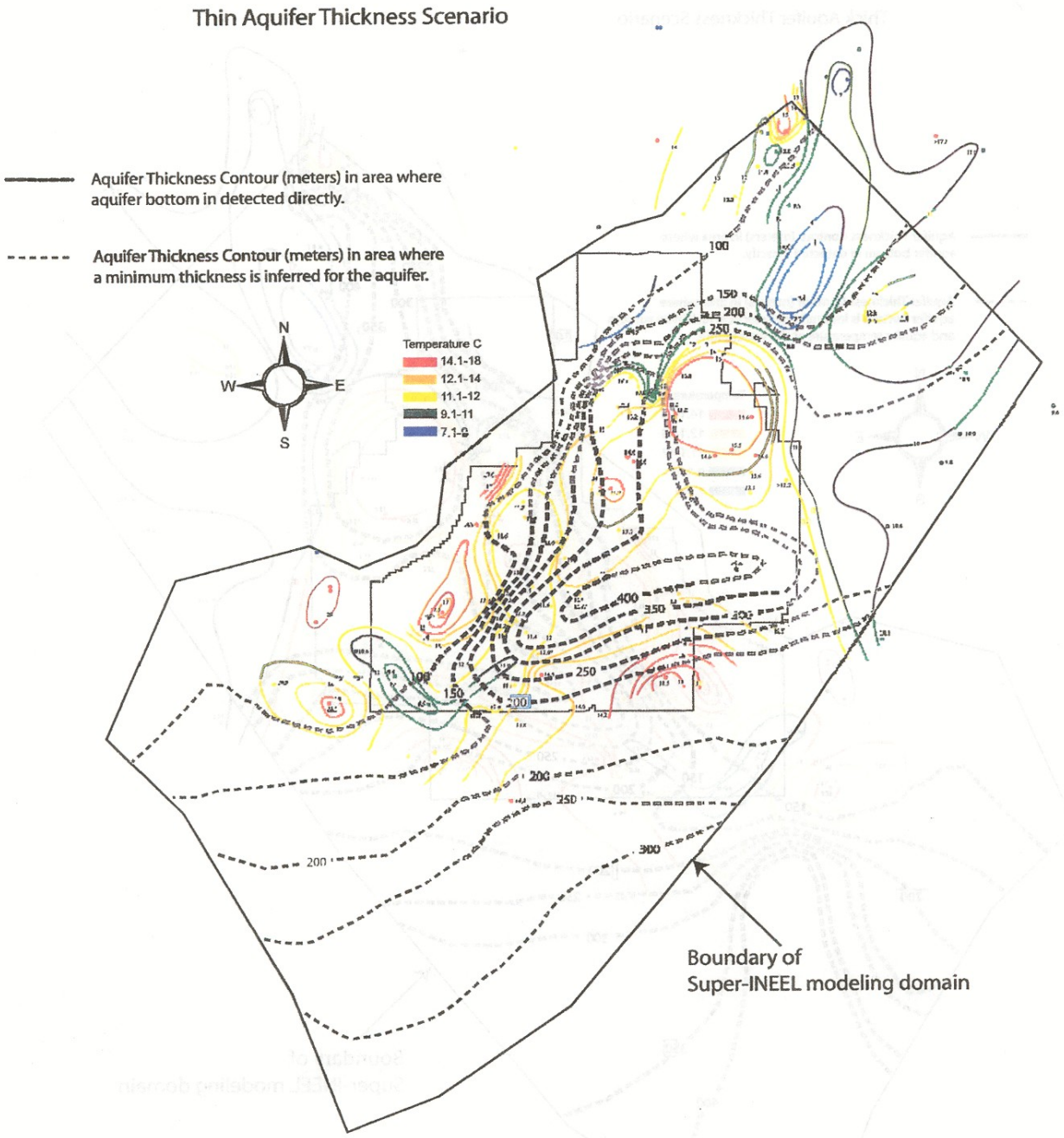


Figure 2-5. (continued).

***USGS—***Jones (1963) describes flow through basalts as occurring in very permeable sheets of flow breccia, scoria, and cinders. He notes that these sheets are of variable thickness and are underlain and overlain by dense basalt. Individual sheets may extend laterally for miles and even tens of miles, providing continuous conduits for flow. Tracer studies and sustained yields of wells substantiate that these sheets are connected vertically through fractures with other sheets, providing continuity throughout the aquifer system. Flow barriers occur where these sheets thin.

Robertson states that "most of the permeability of the basaltic portions of the aquifer can be attributed to large voids, fissures, crevices, and other macroscopic openings associated with the interflow zones," (Robertson et al. 1974).

Garabedian (1992) cites the work of Davis (1969), which states that the hydraulic conductivity associated with a single basalt flow is anisotropic, with the largest values in the direction of the flow and parallel to the orientation of rubble zones, lava tubes, and cooling fractures. Garabedian concludes that anisotropy associated with single flows is minimized at larger scales because the alignment of the numerous basalt flows in the plain is random.

According to Anderson et al. (1999), hydraulic conductivity is largest in thin pahoehoe flows and near-vent volcanic deposits. Hydraulic conductivity is smallest in flows and deposits cut by dikes.

The upper basalts (unit 1) of the SRPA within the INEEL subregion are characterized by tube-fed pahoehoe flows with numerous, very permeable interflow zones (Ackerman et al. in preparation). Lower basalts (unit 2) consist of thick tube-fed pahoehoe flows with dense flow interiors and few interflow zones (Ackerman et al., in preparation). The slightly to moderately altered basalts of intermediate age (unit 3) are characterized by reduced effective porosity (Ackerman et al. in preparation).

Increased percentages of sediments related to the coalescing depocenters of the Big Lost River, Little Lost River, Birch Creek, Camas Creek, and Mud Lake are correlated to changing hydraulic gradients across the INEEL (Ackerman et al. in preparation).

***WAG-10—***The stratigraphic framework of the WAG-10 conceptual model is built on subregional correlations by Anderson and Liszewski (1997). Sediment content associated with the Big Lost River trough may control local changes in hydraulic gradient.

WAG-10 stratigraphy includes the HI interbed, a widespread sedimentary unit overlying Anderson's I basalt flow group, because it is a key lithologic surface for the WAG 3 conceptual model (Arnett and Smith 2001). Arnett and Smith (2001) note that this interbed locally can affect groundwater flow.

***Structural Controls on Groundwater Flow—***The geology of the eastern Snake River Plain has been modified by regional structural deformation and the nature of volcanism on the plain. Movement of water and transport of contaminants through the vadose zone and the SRPA within the INEEL subregion is controlled by these large-scale structural features.

***Structural Deformation—***Differential uplift and subsidence in the INEEL subregion has been attributed, in part, to the cyclic emplacement of mafic materials and subsequent eruptive periods (Anderson et al. 1997). Older basalt flow groups were tilted, folded, and fractured repeatedly by this process of structural deformation (Anderson 1991).

Geologic features modified by structural deformation include rising or dipping units, possible fractured basalt flows, and abrupt lateral changes in ages and sediment content of stratigraphic intervals. These features, attributed to past differential subsidence and uplift, may affect groundwater flow and contaminant transport (Anderson and Liszewski 1997).

Anderson and Liszewski (1997) observe that "the locations of concealed stratigraphic and lithologic features attributed to areas of past differential subsidence and uplift at and near the CFA, TAN, and RWMC and past differential subsidence beneath the Big Lost River coincide with the locations of observed changes in hydraulic gradients of the water table…" According to Anderson and Liszewski (1997), "The coincidence of changes in hydraulic gradients and concealed stratigraphic and lithologic features attributed to past differential subsidence and uplift suggest that these features may affect the movement of water and waste in the aquifer at and near the INEL."

Ackerman et al. (in preparation) infer the structural rise of thick, small permeability basalts above the water table southwest of the INEEL subregion. They suggest that this rise may force groundwater to flow at an angle to the longitudinal orientation and maximum permeability of the interflow zones between basalt flows. This apparent feature corresponds to a steepening of the hydraulic gradient in that area because the permeability across the thickness of the basalt flows probably is much smaller than the longitudinal permeability.

Vertical fractures derived from differential subsidence and uplift may cut many basalt flows and interbeds in the subregion (Anderson 1991). Anderson notes that these fractures may provide channels for movement of water and contaminants through the unsaturated zone to the aquifer.

The distribution of hydraulic properties in the INEEL subregion is related, in part, to structural features such as sedimentary troughs (Ackerman et al. in preparation). Ackerman et al. (in preparation) suggest that the hydraulic gradient is controlled in part by the combined thickness of sedimentary interbeds, which originated in part from large-scale differential subsidence. Anderson and Liszewski (1997) note that hydraulic gradient changes are associated, in part, with changes in sediment content related to subsidence. Arnett and Smith (2001) state that the distribution and lithology of sedimentary interbeds within basalts exert a strong influence on flow in the vadose zone and in the aquifer in the INEEL subregion. According to Arnett and Smith, the thick section of lake sediments deposited in the Mud Lake area may impede groundwater flow, resulting in steeper hydraulic gradients. In contrast, the distribution and lithology of interbeds to the south may enhance flow through the central part of the INEEL.

Large changes in aquifer thickness throughout the subregion are attributed to tectonic subsidence and uplift that control the configuration of subregional hydrogeologic units (Ackerman et al. in preparation). Anderson (1997) suggests that differential uplift and subsidence controlled the apparent rates of basalt and sediment accumulation and stratigraphic section thicknesses. Anderson and Liszewski (1997) observe that reduced stratigraphic thickness mountainward of the Big Lost River can be attributed to differential subsidence. According to Anderson and Liszewski (1997), steeper hydraulic gradients are correlated to these reduced stratigraphic thickness that are attributed to differential subsidence. Arnett and Smith (2001) observe that strong subsidence in the north-central part of the INEEL resulted in a large, persistent, closed basin in which a thick sequence of lake sediments (as much as 100 m thick) have accumulated. Anderson and Liszewski (1997) also attribute increased sediment content near Test Area North (TAN) to subsidence.

The position of the Big Lost River has long been controlled by basalt flows (Arnett and Smith 2001). As a result, thicker composite accumulations of sedimentary interbeds along the present-day channel of the Big Lost River have been observed. Arnett and Smith (2001) note that numerous interbeds

occur beneath the present channel and become less numerous and decrease in thickness away from the channel.

***Volcanism—***The particular nature of volcanism on the eastern Snake River Plain is responsible for the resulting stratigraphy and present landforms, including a sequence of volcanic rift zones, plains-style volcanism (Knutson et al. 1990), large-scale distribution of Quaternary and Tertiary basalts and sediments, and silicic volcanic features.

Structural features related to the nature of volcanism on the eastern Snake River Plain may affect the movement of groundwater and contaminants. These features include volcanic rift zones and associated volcanic features.

Several volcanic rift zones occur within the INEEL subregion (Kuntz et al. 1992). These rift zones include the Arco-Big Southern Butte volcanic rift zone, Axial Volcanic rift zone, and the Lava Ridge rift zone (see Figure 2-6). Each of these rift zones is characterized by numerous fissures, dikes, and past volcanic eruptions.

Arnett and Smith (2001) observe that northwest-oriented major faults and rift zones perpendicular to the eastern Snake River Plain axis may locally influence the direction of groundwater flow, creating local anisotropy. Garabedian (1992) similarly notes that large-scale fractures in rift zones perpendicular to the axis of the eastern Snake River Plain may result in anisotropy of flow over broad areas.

Anderson et al. (1999) observe that the largest range of hydraulic conductivity occurs in volcanic rift zones with many aligned vents and fissures. According to Anderson et al. (1999), "the largest variety of rock types and the greatest range of hydraulic conductivity are in volcanic rift zones, which are characterized by numerous aligned volcanic vents and fissures related to underlying dikes. Volcanic features related to individual dike systems within these rift zones are approximated in the subsurface by narrow zones referred to as vent corridors. Vent corridors at and near the INEEL generally are perpendicular to groundwater flow and average about 1 to 2 × 5 to 15 mi. Forty-five vent corridors are inferred to be beneath the INEEL and adjacent areas" (see Figure 2-7).

The distribution of numerous volcanic features associated with vent corridors may affect the distribution of hydraulic properties (Anderson et al. 1999). Areas near volcanic vents may provide localized, preferential pathways for groundwater flow. Dikes may impede flow and reduce the hydraulic conductivity (Meyer and Souza 1995; Hughes et al. 1997). Anderson and Liszewski (1997) note that hydraulic gradient changes within the INEEL subregion are, in part, associated with a zone of numerous fissures, dikes, and past volcanic eruptions related to the Arco-Big Southern Butte volcanic rift zone.

Vent corridors at the INEEL typically are oriented at right angles to the subregional direction of groundwater flow. Heterogeneities in the distribution of hydraulic properties associated with these vent corridors may control local and subregional transport of contaminants. For example, the longitudinal dimension of a TCE plume at TAN is oriented approximately 90 degrees from the southwest direction of groundwater flow expected from water-level data and nearly parallel to the orientation of rift zone features (Hughes et al. 1997). Similarly, Kuntz et al. (2002) observes that low hydraulic conductivities and distortions in the distribution of strontium-90 concentrations in groundwater south of INTEC may be associated with a concealed vent corridor. At the subregional scale, Anderson et al. (1999) suggests that the hydraulic complexities associated with vent corridors may affect the dispersion of tritium and other contaminants in the aquifer.

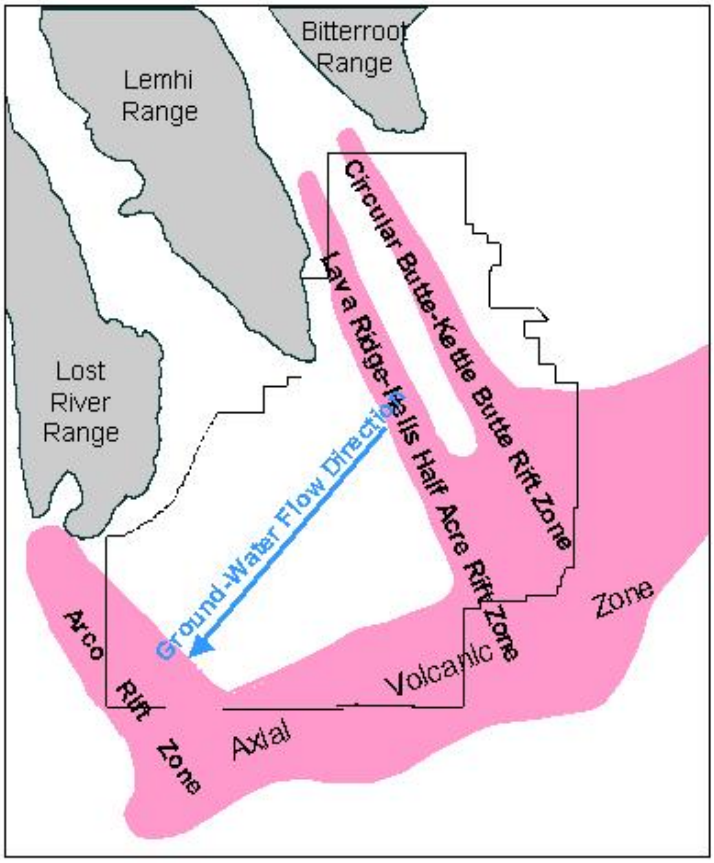


Figure 2-6. Location of volcanic rift zones in the INEEL subregion (adapted from Bartholomay et al. 2002).

Rhyolitic ash-flow tuffs underlie the Snake River Plain basalts at the INEEL at depths ranging from 2,200 to 3,800 ft bls (Anderson et al. 1999). These tuffs typically are altered hydrothermally, with fractures sealed by secondary mineralization (Garabedian 1992).

***2.2.1.3 Matrix Characteristics.*** Hydraulic characteristics of the rock matrix of the SRPA and vadose zone include hydraulic conductivity and the storage coefficient. This section will review and contrast the distribution of matrix characteristics as conceptualized in the USGS and WAG-10 subregional studies.

***Permeability—***Hydraulic conductivity is a measure of the capacity of a geologic medium to transmit water. The hydraulic conductivity distribution within basalts and interbedded sediments of the SRPA controls the configuration of the flow field and contaminant migration in the aquifer.

USGS—Geohydrologic data from the 10,365-ft deep test hole INEL-1 located southwest of the Nuclear Reactor Facility (NRF), indicate that the hydraulic conductivity of rocks below a depth of 1,500 ft is much smaller than that of basalts in the upper 200 to 800 ft. If these conditions persist over the INEEL, hydraulic conductivity of the deeper rocks may be two to five orders of magnitude less than the shallow basalts (Mann 1986).

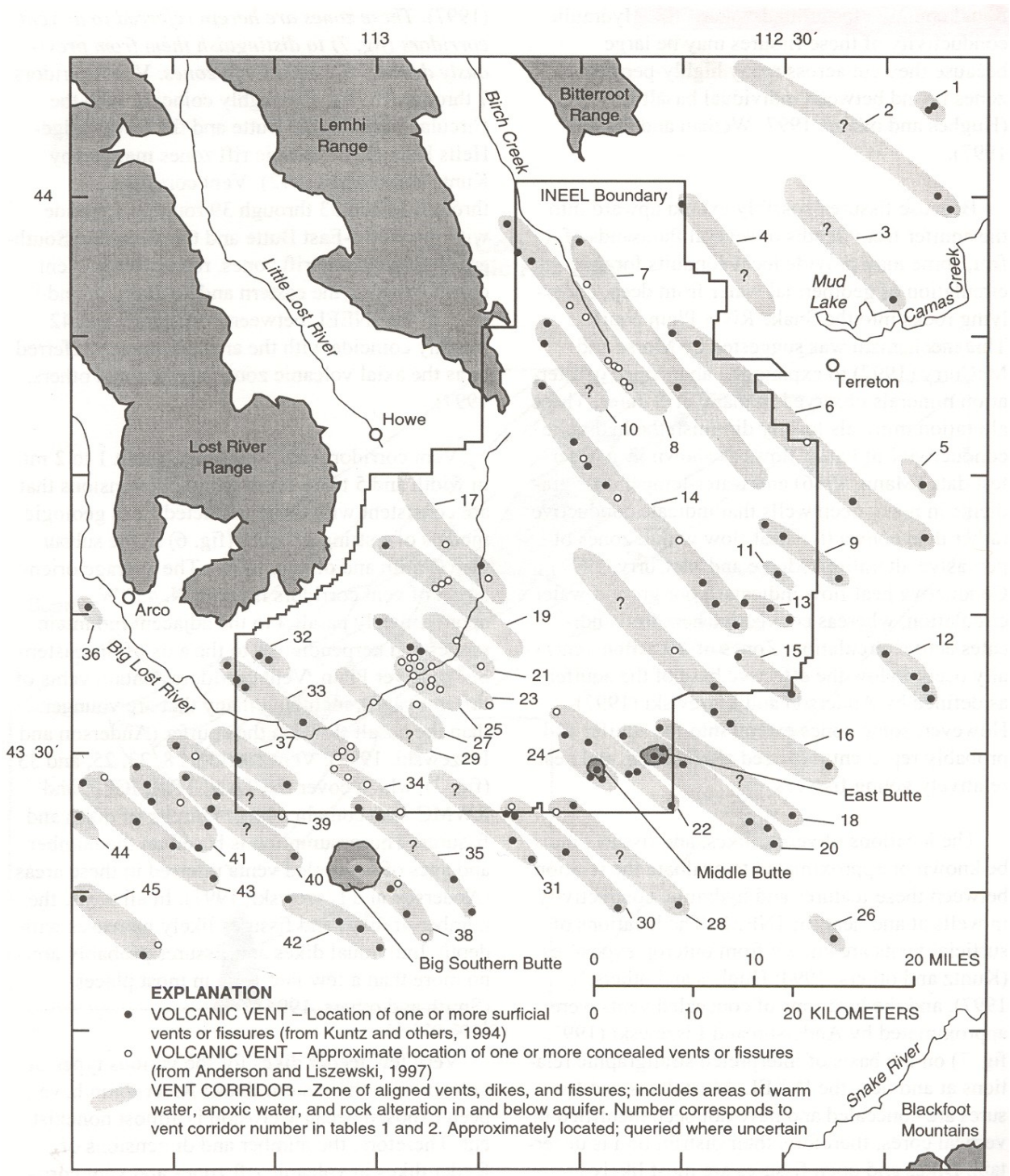


Figure 2-7. Location of vent corridors at the INEEL (from Anderson et al. 1999)

According to Anderson et al. (1999), the hydraulic conductivity of basalt and interbedded sediment that compose the SRPA at and near the INEEL ranges from about $1.0 \times 10^{-2}$ to $3.2 \times 10^{4}$ ft/d. Anderson et al. (1999) state that "this six-order of magnitude range of hydraulic conductivity was estimated from single-well tests in 114 wells, and is attributed mainly to the physical characteristics and distribution of basalt flows and dikes."

Anderson et al. (1999) note that "three broad categories of hydraulic conductivity corresponding to six general types of geologic controls can be inferred from the distribution of wells and vent corridors. Hydraulic conductivity of category 1…ranges from $1.0 \times 10^{2}$ to $3.2 \times 10^{4}$ ft/d, and corresponds to (1) the contacts, rubble zones, and cooling fractures of thin, tube-fed pahoehoe flows; and (2) the numerous voids present in shelly pahoehoe and slab pahoehoe flows; and bedded scoria, spatter, and ash near volcanic vents. Hydraulic conductivity of category 2 …ranges from $1.0 \times 10^{0}$ to $1.0 \times 10^{2}$ ft/d, and corresponds to (3) relatively thick, tube-fed pahoehoe flows that may be ponded in topographic depressions; and (4) thin, tube-fed pahoehoe flows cut by discontinuous dikes. Hydraulic conductivity of category 3…ranges from $1.0 \times 10^{-2}$ to $1.0 \times 10^{0}$ ft/d, and corresponds to (5) localized dike swarms; and (6) thick, tube-fed pahoehoe flows cut by discontinuous dikes."

Bulk hydraulic conductivity of the fractured basalt of unit 1 ranges from about 0.01 to 32,000 ft/d (Anderson et al. 1999). Estimates greater than 100 ft/d are principally associated with interflow zones of thin flows. Smaller estimates probably are associated with localized dikes or dike swarms. Ackerman et al. (in preparation) estimates that the bulk hydraulic conductivity for dense basalt of unit 2 at the INEEL ranges from about 0.01 to 800 ft/d. The average hydraulic conductivity of unit-3 basalts probably is about one order of magnitude smaller than that of younger basalts (Ackerman et al. in preparation).

WAG-10—***INEEL researchers concur with the large range of hydraulic conductivity.*** Distributions of hydraulic conductivity were not presented in the WAG-10 conceptual model (Smith and Arnett 2001). Average values at the subregional scale have not been estimated because of heterogeneity attributed to the complex stratigraphy of basalt and the effects of volcanic rift zones on hydraulic properties (even at the large scale) and because of the potential to assign misleading mean property values[1].

***Other Researchers—***According to Johnson and Frederick (1997), aquifer test results at INTEC support a conceptual model of an aquifer locally characterized by highly heterogeneous hydraulic properties that appears homogeneous when examined in a sufficiently large scale. Tests suggest that vertical hydraulic conductivity is substantially less than horizontal hydraulic conductivity (Johnson and Frederick 1997). These tests also indicate that the aquifer responds to stress as a leaky confined system, with contributions from above and beneath (Johnson and Frederick 1997).

Welhan and Reed (1997), in a study conducted by the Idaho Geological Survey and Idaho State University, analyzed the regional spatial correlation structure of bulk horizontal hydraulic conductivity in fractured basalt of the eastern Snake River Plain. They suggest that the spatial distribution of zones of large hydraulic conductivity may be controlled by the lateral dimensions, spatial distribution, and interconnection between highly permeable interflow zones.

***Storage—***The storage coefficient is the measure of the capability of an aquifer to store water. The storage coefficient of an unconfined aquifer is approximated by the effective porosity of the rocks that make up the aquifer. The effective porosity is the percentage of rock volume that consists of

---

1 ***Ron Arnett, written communication, 2002***

interconnected voids. The effective porosity of the SRPA includes open fractures, interconnected vesicles, and rubble-zone openings in basalt and intergranular openings in sedimentary interbeds.

***USGS—***Robertson (1974) assumed porosity to be 10% based on best available evidence. Laboratory determinations of total and effective porosity made from basalt cores at the INEEL ranged from 6 to 37% and 4 to 22%, respectively (Johnson 1965). In the current USGS subregional conceptual model, the effective porosity of fractured basalt is estimated to range from 5 to 25%. The porosity of dense basalt probably is at the lower end of this range (Ackerman et al., in preparation).

WAG-10—Distributions of effective porosity and storage coefficient were not presented in the WAG-10 conceptual model (Smith and Arnett 2001). Average values at the subregional scale have not been estimated because of heterogeneity even at the large scale and because of the potential to assign misleading mean property values (see footnote 1).

***Other Researchers—***Frederick and Johnson (1996) conducted packer tests in four wells near INTEC. Test data indicated that the basalts of the SRPA respond locally as a leaky confined aquifer with a composite storage coefficient of $7.0 \times 10^{-6}$ (Frederick and Johnson 1996).

***2.2.1.4 Subregional Boundary Conditions.*** Flow into and out of the INEEL subregion occurs as regional underflow, flow across the base of the aquifer, areal and episodic recharge to the water table, and tributary basin underflow. This section will review and contrast physical and hydrologic boundaries to the INEEL subregion as conceptualized in the USGS and WAG-10 subregional studies.

***Regional Underflow—***Regional groundwater flow within the eastern Snake River Plain passes through the INEEL subregion. No direct measurement can be made to quantify this flux. Estimates must be indirectly calculated from known head gradients and hydraulic properties of the SRPA at upgradient and downgradient boundaries to the subregion.

***USGS—***The USGS conceptual model calculates underflow across the northeast boundary (see Figure 2-2) to be 1,225 $ft^3/s$ (approximately 887,000 acre-ft/year; Ackerman et al., in preparation). This underflow estimate is based on published gradient data and transmissivity estimates. Underflow leaving the subregion across the southwest boundary is estimated to be 2,350 $ft^3/s$.

***WAG-10—***The WAG-10 conceptual model receives underflow from the northern part of the eastern Snake River Plain across its northeast boundary (Arnett and Smith 2001). This underflow is based on outflows estimated from a numerical modeling study (Spinazola 1994). Spinazola estimates underflow out of the Mud Lake subregion to be 938,000 acre-ft/year (1,298 $ft^3/s$), within about 5% of the USGS underflow estimate.

***Flow Across the Base of the Aquifer—***The SRPA is underlain by older basalts and rhyolitic rocks characterized by low permeability. Water may move from these deeper rocks into the aquifer or may move from the aquifer into the deeper rocks. Little information is available about the magnitude or direction of flow across this boundary.

***USGS—***The hydraulic head increased with depth across the estimated base of the aquifer in the INEL-1 test hole. If conditions observed in the INEL-1 test hole persist over the INEEL subregion, the deep, low-permeability rocks may contribute an upward component of flow to the SRPA (Mann 1986). Mann (1986) estimated a flow of only about 20 $ft^3/s$ across the INEEL. This rate of flow, if extended to the USGS INEEL subregion, would be about 44 $ft^3/s$ (Ackerman et al. in preparation). Because of the estimated small magnitude of flow across the base (up to three times less the amount attributed to areal

precipitation) the USGS assumes that flow across the base of the aquifer is zero (Ackerman et al. in preparation).

***WAG-10—***The WAG-10 conceptual model observes that the hydraulic conductivity at the base of the aquifer is greatly reduced compared to the overlying aquifer (Arnett and Smith 2001). This reduction in hydraulic properties probably restricts aquifer recharge from deeper rocks. A small upward flow probably occurs across the bottom of the aquifer. Locally, these flows may be larger as evidenced by higher temperatures (see footnote 1).

***Mountain Front—***The mountain-front boundary to the northwest of the INEEL subregion consists of the edges of the Pioneer Range, Lost River Range, and Lemhi Mountains (see Figure 2-1). Rocks of these mountains may contribute a small amount of underflow and surface-water runoff to the eastern Snake River Plain.

***USGS—***The USGS conceptual model assumes a constant flow across the northwest mountain-front boundary of 40 $ft^3/s$ (Ackerman et al. in preparation). This flow is included in the USGS subregional water balance as part of the tributary basin underflow (Ackerman et al. in preparation).

***WAG-10—***The WAG-10 conceptual model identifies a limited amount of recharge that may enter the aquifer as direct runoff from the mountain ranges (Arnett and Smith 2001). The WAG-10 model does not attempt to quantify this source of recharge.

***Flow Path Boundary—***Both the USGS and WAG-10 conceptual models employ a flow path to delineate the southeastern boundary of the INEEL subregion. The flow path permits subregional analysis without having to account for regional stresses from the Snake River and other parts of the eastern Snake River Plain.

***USGS—***Ackerman et al. (in preparation) arbitrarily chose a generalized flow path (see Figure 2-2) representing flow in three dimensions that was derived from Garabedian (1992) and Ackerman (1995) to represent the southeastern boundary of the USGS conceptual model. The selected flow line bounds all but the extreme southeastern part of the INEEL. No flow is assumed to cross that boundary.

***WAG-10—***The southeastern boundary of the WAG-10 conceptual model, similar to that of the USGS model, coincides with a regional groundwater flow line (see Figure 2-4). The selected flow line is east of the USGS flow line and bounds all of the INEEL. Because flow is parallel to the flow path, no flow is assumed to cross that boundary (Arnett and Smith 2001).

***Water-Table Boundary—***Subregional recharge at the water table includes diffuse areal recharge from precipitation and focused episodic recharge from infiltration of surface water. These sources of recharge must pass through the vadose zone, which ranges in thickness from about 200 to more than 900 ft in the subregion.

***Areal Recharge—***Precipitation in the form of snow and rain provides an average of 8 to 10 in. annually over the eastern Snake River Plain (Garabedian 1992). Most of this precipitation is returned to the atmosphere through evaporation and transpiration. A small amount of precipitation is recharged to the SRPA from infiltration.

USGS—***Mundorff et al. (1964) estimates that recharge from precipitation may vary from 0.02 ft/year in the central part of the eastern Snake River Plain to as much as 0.3 ft/year near Craters of the***

***Moon.*** Kjelstrom (1995) estimates an average recharge rate of 0.08 ft/year from a basin water-budget analysis.

Cecil et al. (1992) used environmental tracer data and neutron logging data to estimate net water infiltration rates through soils at the INEEL. Chlorine-36 and tritium concentrations and neutron logs in shallow boreholes indicated that net infiltration ranges from 0.36 to 1.1 cm/year. This range is equivalent to 2 to 5% of the annual precipitation. Busenberg (2001) suggests that areal recharge occurs both as continuous spatially distributed diffuse recharge resulting from widespread percolation through the entire unsaturated zone and occasional concentrated recharge resulting from short-term penetration of water along distinct pathways through the unsaturated zone.

Ackerman et al. (in preparation) uses 2 to 5% of precipitation, as determined by Cecil et al. (1992) to estimate a recharge rate of 0.02 to 0.04 ft/year. They estimated that recharge would be about 70 $ft^3/s$ over the entire subregion using the upper value of 0.04 ft/year. Ackerman et al. determined that the net effect of recharge from precipitation is probably very small when compared to other sources of inflow; it is a less important consideration than more concentrated sources such as streamflow infiltration.

***WAG-10—***Arnett and Smith (2001) state that direct precipitation on the plain locally recharges the aquifer to a limited degree, particularly when snow melts rapidly in the spring. The present WAG-10 conceptual model uses the Cecil et al. (1992) estimate of approximately 0.03 cm/year.

***Episodic Recharge from Streamflow—***Streamflow onto the eastern Snake River Plain quickly infiltrates, providing a source of focused, episodic recharge to the SRPA in the vicinity of surface-water features. These features include the channel of the Big Lost River and the INEEL spreading areas (see Figure 2-1), which are flood-control structures constructed in 1959 to prevent downstream flooding on the Big Lost River.

***USGS—***Bennett (1990) measured infiltration rates along the channel of the Big Lost River for a range of discharges. Infiltration rates ranged from 1 to as much as 28 $ft^3/s$ per mile. Bennett observes that aquifer water levels near the RWMC and north of the NRF were substantially affected by recharge from the Big Lost River.

Busenberg (2001) observes that occasional concentrated recharge may result from the short-term penetration of water along distinct pathways through the unsaturated zone that bypass the greater part of its volume. Busenberg cites avenues for rapid focused recharge along the channel of the Big Lost River, spreading areas, and at the Big and Little Lost River Sinks.

A tracer test conducted in the INEEL spreading areas (see Figure 2-1) demonstrated rapid lateral flow in the vadose zone as distant as 1 mi (Nimmo et al. 2001). Vertically, tracer water traveled from land surface to the aquifer in about 9 days. This test showed that concentrated recharge quickly reaches the aquifer and can move large distances laterally in the vadose zone.

The USGS conceptual model notes the temporal and spatial variability of episodic infiltration. The effect of episodic streamflow infiltration is considered to be much more significant to contaminant transport than areal recharge because it is concentrated near areas of known sources (Ackerman et al. in preparation). Ackerman et al. (in preparation) notes that the "lateral spreading of contaminants may be strongly influenced by these episodic recharge events and resulting temporal fluctuations in water-table gradients."

***WAG-10—***The WAG-10 conceptual model uses streamflow data to estimate mean channel infiltration rates for the Big Lost River (McCarthy et al. 1995). These estimates have not been adjusted for evapotranspiration.

***Tributary Basin Underflow—***Mountain basins tributary to the eastern Snake River Plain contribute both surface-water flow and underflow as recharge to the SRPA. The underflow component is not well known but has been indirectly estimated by researchers.

***USGS—***The USGS conceptual model estimates 361 $ft^3/s$ of underflow from the Big Lost River basin (see Figure 2-1) based on the difference between Kjelstrom's (1986) calculations of the mean annual basin yield and the Brennan et al. (2001) calculation of annual mean streamflow (Ackerman in preparation). The conceptual model estimates that underflows for the Little Lost River and Birch Creek are equivalent to the mean annual basin yields of 226 and 102 $ft^3/s$, respectively (Ackerman et al. in preparation), because streamflow out of both basins is very small. Tributary basin underflow includes a minor amount of recharge derived from mountain fronts.

***WAG-10—***The earlier WAG-10 model (McCarthy 1995) incorporated underflows estimated by Garabedian (1989). The present WAG-10 conceptual model incorporates an uncertainty of about 25% and estimates that the average underflows are 315 to 535 $ft^3/s$ for the Big Lost River Basin, 160 to 270 $ft^3/s$ for the Little Lost River, and 80 to 140 $ft^3/s$ for Birch Creek (Arnett and Smith 2001). The WAG-10 conceptual model also includes underflow estimates for Medicine Lodge Creek of 40 to 70 $ft^3/s$.

***Pumpage Withdrawals and Recharge from Wastewater Disposal—***Well pumpage furnishes all of the water used at the INEEL for industrial, public supply, and irrigation. Most of this water is returned to the subsurface through wastewater disposal facilities, including injection wells, infiltration ponds, and leach fields. Some irrigation pumpage occurs upgradient of the INEEL.

***USGS—***The USGS conceptual model estimates that net pumpage withdrawals in the INEEL subregion (pumpage minus wastewater disposal to the subsurface) total about 34 $ft^3/s$. This volume accounts for wastewater disposed to injection wells and infiltration ponds at the INEEL.

***WAG-10—***The WAG-10 subregion includes irrigated parts of the Mud Lake area (see Figure 2-4). Because of this, net pumpage withdrawals are larger than those estimated in the USGS conceptual model. However, pumping withdrawals throughout the domain are considered to be less critical than for a facility-scale model (Arnett and Smith 2001).

2.2.1.5 Hydraulics of Flow. The integration of components of the subregional conceptual models is defined by the distribution of hydraulic head, gradient, and direction of flow. Groundwater flow in the INEEL subregion takes place in the vadose zone and the SRPA.

***Snake River Plain Aquifer—***The INEEL subregion field of flow within the SRPA is a physical integration of all of the processes that are (or should be) represented by the elements of the conceptual model. This physical integration is defined by the horizontal and vertical distribution of head and gradient.

***Areal Distribution of Head and Gradient—***The subregional field of flow is defined by the areal distribution of hydraulic head and gradient. The distribution of hydraulic head is determined from water levels in wells.

***USGS—***Ackerman et al. (in preparation) states that "the regional and subregional direction of groundwater flow is from the northeast to the southwest (see Figure 2-8). Flow directions within the INEEL vary locally from southeast to southwest and fluctuate in response to episodic recharge from streamflow infiltration. Water-table gradients are greatest immediately upgradient of the northeastern boundary, 30 ft/mi, and southwest of the INEEL, 25 to 30 ft/mi. Beneath the INEEL, gradients are much smaller, 4 ft/mi, and precise definition of flow direction is difficult to determine."

***WAG-10—***Flow paths from hydraulic data infer that water in the SRPA flows generally to the southwest across the INEEL (Arnett and Smith 2001). However, groundwater chemistry data and hydraulic head distributions indicate a significant eastward component to groundwater flow. This concept is consistent with geologic evidence of a thinning aquifer to the west (Arnett and Smith 2001).

Rohe (2000) used a three-point comparison of heads in wells to examine the magnitude and direction of groundwater flow at different scales (see Figure 2-9). At larger scales, flow directions obtained using this three-point comparison converge on the generally southwest direction of groundwater flow across the INEEL subregion. At local scales (within a three-point area of less than 7 $mi^2$), flow directions are characterized by an increasingly wide divergence in orientation. This divergence at the local scale may reflect hydrologic heterogeneities attributed by some researchers (Anderson et al. 1999; Hughes et al. 1997) to features associated with concealed vent corridors. Rohe used rose diagrams to compare flow directions with time for specific three-point areas (see Figure 2-10). He observes that local variations in flow direction with time may be attributed to episodic recharge in the Big Lost River.

***Vertical Distribution of Head and Gradient—***The vertical distribution of head within the SRPA defines the potential for vertical flow and deep circulation of water and contaminants. Vertical head data in the INEEL subregion are limited.

***USGS***—If conditions identified in the drilling and testing phases of the INEL-1 test hole persist over most of the INEEL, water that is recharged locally to the SRPA does not circulate to depths of more than 1,000 to 2,000 ft (Mann 1986). The present USGS conceptual model suggests that water in the upper part of the aquifer generally moves horizontally at the INEEL and that vertical flow is impeded by the horizontal and subhorizontal layering of basalt (Ackerman et al., in preparation).

***WAG-10***—The vertical distribution of head varies across the INEEL subregion. The gradient generally is upward in the deepest parts of the aquifer (see footnote 1).

***Flow velocity—***Estimates of flow velocity have been made by various researchers from tracer-test and hydraulic data. Estimates for the USGS and WAG-10 conceptual models are summarized in the following sections.

***USGS***—Early tracer tests, using contaminants disposed to the injection well at INTEC, inferred that flow velocities were relatively high, ranging from 24 to 141 ft/d near INTEC (Jones 1963). Jones ascertained that groundwater flow within the basalts is preferential, moving primarily as sheet flow in sheets of breccia, fractures, and scoria that may laterally extend for miles. Flow velocities estimated from tracer studies were only indirectly related to gradient and no inferences regarding velocity could be drawn from gradient data, which suggests that these velocities are apparent velocities within a sheet and do not represent the average velocity.

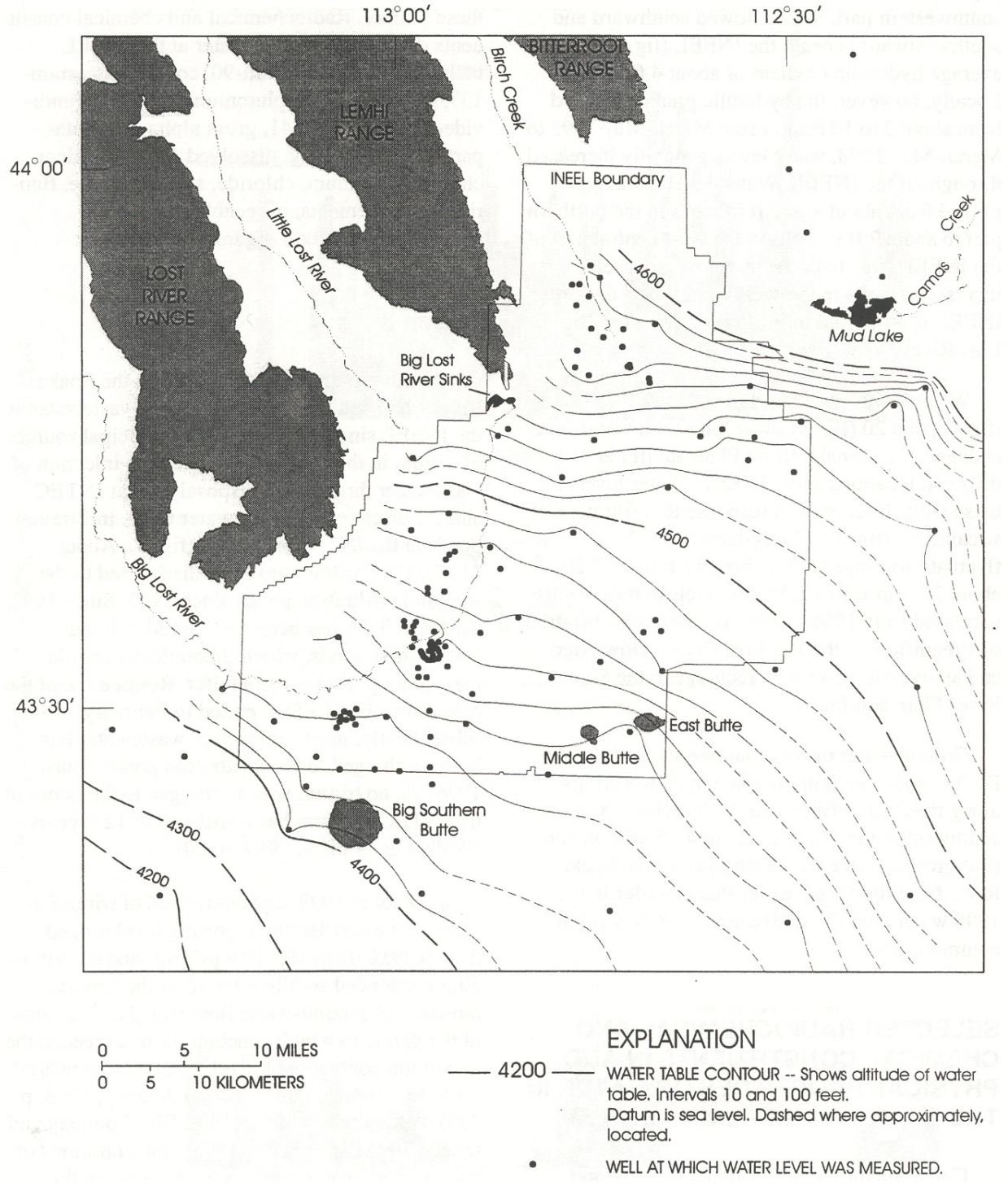


Figure 2-8. Altitude of the water table in the SRPA in the vicinity of the INEEL, 1998 (from Bartholomay et al. 2000).

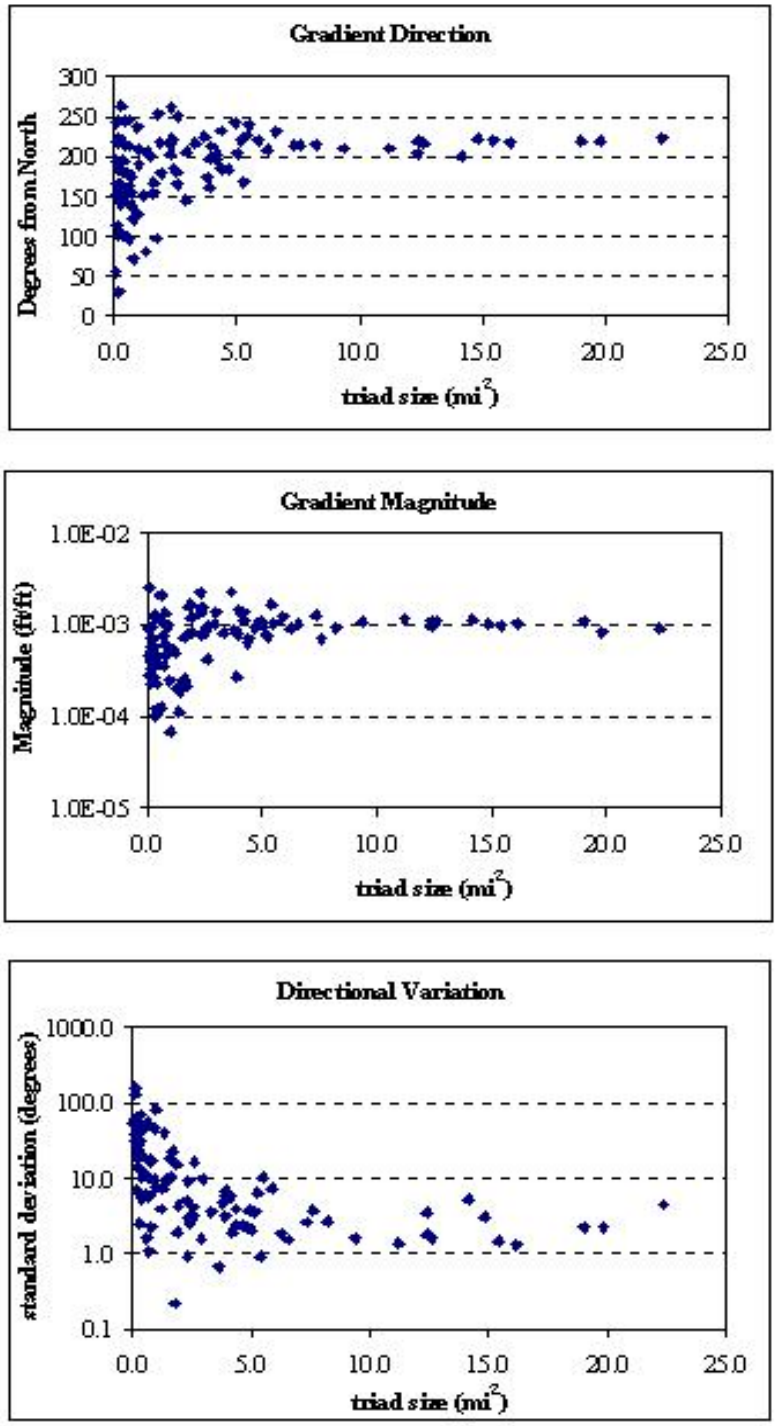


Figure 2-9. Comparison of the direction and magnitude of flow gradients in the SRPA at different scales (Michael Rohe, 2002, written communication).

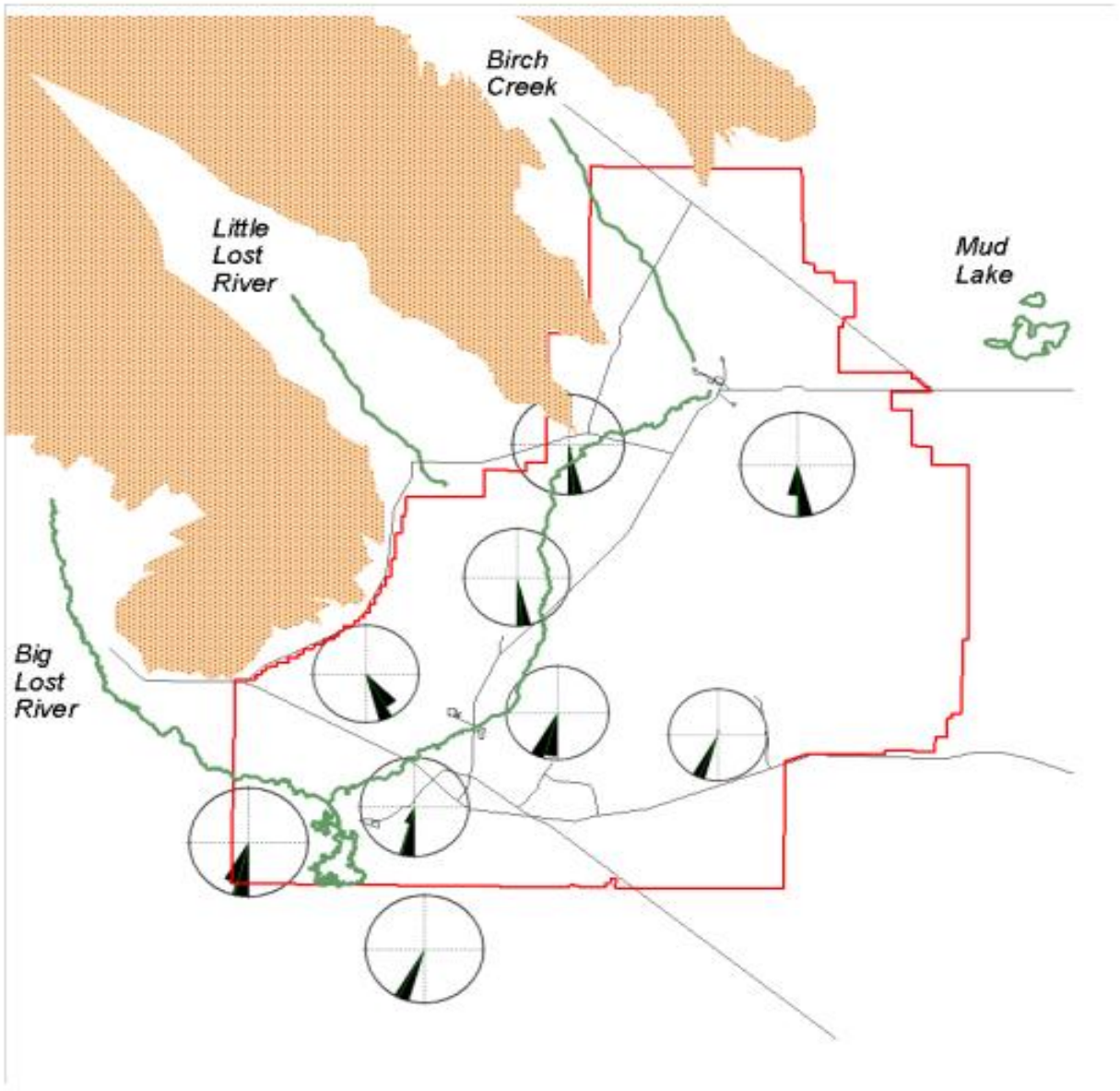


Figure 2-10. Comparison of the temporal variation of groundwater flow directions in the SRPA (Michael Rohe, 2002, written communication).

Ackerman et al. (in preparation) observes that long-term contaminant monitoring indicates Unit 1 flow velocities range from 5 to 20 ft/d. They note that "the use of contaminant first arrivals to define flow velocities probably reflects preferential flow along the many interflow zones of the thin, fractured basalt flows comprising the uppermost unit of the aquifer."

***WAG-10—***Variations of uranium isotope ratios in groundwater indicate that preferential flow paths originate from the Birch Creek and Little Lost River drainage basins (Luo et al. 2000). Johnson et al. (2000) used strontium isotope ratios to postulate preferential flow paths that channel water originating from the Little Lost River and Birch Creek valleys across the INEEL.

***Vadose Zone—***Subregionally, the vadose zone ranges from less than 200 to more than 900 ft thick. Diffuse areal recharge, focused episodic recharge, and INEEL-derived contaminants disposed at and near the land surface through wastewater infiltration ponds and shallow burial sites must pass through the vadose zone to reach the SRPA.

***Distribution and Movement of Water in the Vadose Zone—***Water moves as unsaturated and saturated flow in the vadose zone beneath the eastern Snake River Plain. Unsaturated flow takes place in response to diffuse areal recharge and rapid, vertical flow in fractures. Saturated flow takes place locally beneath areas of focused recharge (Big Lost River channel, INEEL spreading areas, infiltration ponds). Unsaturated flow is largely vertical while saturated flow is both vertical and horizontal.

***USGS—***The USGS has monitored water levels and contaminant concentrations in perched-water bodies that have formed in the 400-ft thick vadose zone beneath wastewater infiltration ponds at the Test Reactor Area (TRA) and INTEC (Cecil et al. 1991). At the TRA, perched-water bodies have included an area of saturated basalt and sedimentary interbeds as large as 1 × ½ mi. These perched-water bodies occur in association with thick sedimentary interbeds in the upper several hundred ft of the vadose zone (Orr 1999). Beneath these interbeds, water moves in the vadose zone as unsaturated flow.

The USGS identified four lithologic features that control the formation of perched groundwater zones at the INEEL (Cecil et al. 1991). These features included (1) contrasts in vertical hydraulic conductivity between basalt flows and sedimentary interbeds, (2) reduced vertical hydraulic conductivity in interflow baked zones, (3) reduced vertical hydraulic conductivity in dense unfractured basalt, and (4) reduced vertical hydraulic conductivity from sedimentary and chemical filling of fractures in basalt. Several of these features were identified at INTEC from geophysical logs.

At the TRA, water originating from infiltration ponds moves rapidly through surficial sediments, primarily as vertical, unsaturated, and saturated intergranular flow. Recharge enters underlying basalts, moving rapidly as vertical macropore flow in fractures and laterally through interflow rubble zones. Fractures may or may not be completely filled. Recharge continues downward entering heterogeneous, layered, sedimentary interbeds and moving through the saturated and unsaturated intergranular flow through an anisotropic porous medium. Beneath the interbeds, water moves rapidly downward to the aquifer as unsaturated macropore flow in fractures (Orr 1999).

Perched water also has been observed in proximity to surface-water features including the Big Lost River and the INEEL spreading areas. Repetitive neutron logging studies near the Big Lost River and the spreading areas demonstrated increasing moisture content in response to surface-water flows.

At the RWMC, zones of increased moisture content have been detected at or above sedimentary interbeds. Some researchers have long postulated that the source of water was from the INEEL spreading

areas. Other researchers attributed the presence of moist zones could be attributed to local flooding and recharge occurring at the RWMC.

During a 1999 tracer test (Nimmo et al. 2001), conducted by the USGS during a period of streamflow diversion to the INEEL spreading area, the chemical tracer moved downward beneath spreading areas through the 600-ft-thick vadose zone within 9 days, demonstrating the potential for rapid vertical transport (about 70 ft/d). The tracer also was detected in vadose-zone wells nearly 1 mi distant. First detections indicated that the horizontal flow rate may exceed 46 ft/d and that perched water beneath the RWMC is derived in part from lateral flow from the spreading areas. The test indicated that nonisotropic, horizontal spreading of focused recharge can occur over distances of a few kilometers through laterally extensive, nearly saturated, interconnected rubble zones (Nimmo et al. 2001). Nimmo et al. suggest that this flow may enhance contaminant transport vertically and horizontally (also exposing contaminants to a larger volume of sedimentary material and enhancing sorbing potential for non-conservative contaminants).

The tracer test conducted by the USGS at the INEEL spreading areas in 1999 demonstrated that saturated flow occurs within the vadose zone in response to flows into the spreading areas. Tracer detections in water from wells completed above the B-C interbed adjacent to the spreading areas, within the Subsurface Disposal Area of the RWMC and at the Large-Scale Infiltration Test (LSIT) 1 mi east of the spreading areas, demonstrated that rapid lateral flow occurs in response to spreading-area flows.

***WAG-10—***The LSIT was conducted in 1994 to investigate the bulk hydrologic properties of basalts in the vadose zone (Wood and Norrell 1996). This test concluded, based on tracer data, changes in moisture content, and detailed stratigraphic information that water movement was controlled predominantly by fractured, rubble and breccia zones (Wood and Norrell 1996). The test noted that lateral flow was apparent in vadose-zone basalts directly beneath the infiltration basin. Lateral flow was not observed beyond the basin extent except at the surface of the B-C sedimentary interbed where it was controlled by the topography of the interbed. These data indicated that the interbed serves as a barrier to vertical flow and contaminant transport. The test indicated that fractures in the upper vesicular zone of a basalt flow were more actively involved in water transmission than were those fractures located in the dense flow interiors.

A vadose zone research park was initiated in 2000 in conjunction with construction of new INTEC percolation ponds. This research park, consisting of instrumented boreholes and wells adjacent to the new ponds, will provide researchers with a better understanding of the moving of water as unsaturated and saturated flow in the vadose zone.

### 2.2.2 Water-Rock Geochemical Interactions

The chemical nature of water in the SRPA is in part dependent on chemical interactions with the basalts and sediments in the aquifer. Geochemical data provide an understanding about the transport of contaminants. These data also provide an independent assessment of the flow field.

Olmsted (1962) characterized groundwater at the INEEL into several chemical compositions. The first, derived from mountainous carbonate drainages to the west, is enriched in calcium, magnesium, and bicarbonate and occurs over much of the western part of the INEEL (Busenberg et al. 2001). The second, derived from the area northeast of the INEEL, is characterized by increased occurrence of rhyolitic and andesitic rocks and is enriched in calcium, magnesium, and bicarbonate, but with a larger equivalent fraction of sodium, potassium, fluoride, silica, and chloride. This water composition is typical of much of the eastern part of the INEEL. A third composition, characterized by increased concentrations of nitrate

and chloride and decreased concentrations of bicarbonate, is derived from recharge of irrigation water and wastewater at the INEEL.

### 2.2.3 Subregional Contaminant Transport

Small concentrations of selected contaminants that have been disposed to the subsurface at INEEL facilities have been detected over broad areas. At the subregional scale, these small concentrations serve primarily to provide long-term groundwater tracer test information. This section will briefly summarize these contaminant source terms and their subregional distribution in groundwater. The WAG-10 conceptual model restricts itself to an analysis of flow. More detailed discussion will be developed in facility-scale presentations.

***2.2.3.1 Contaminant Source Term.*** At the subregional scale, small concentrations of contaminants in groundwater provide information about the conceptual model of groundwater flow. Contaminants that have been used as subregional tracers include tritium, iodine-129, and chlorine-36.

About 32,000 Ci of tritium have been disposed to the subsurface at the TRA and INTEC since 1952. At the TRA, wastewater containing tritium has been disposed to wastewater infiltration ponds. At INTEC, wastewater containing tritium was disposed to an injection well until 1984; subsequent disposal was to wastewater infiltration ponds.

An estimated 1.52 Ci of iodine-129 have been disposed to the subsurface at INTEC to the injection well and infiltration ponds. Small concentrations of chlorine-36 also have been disposed to the subsurface.

***2.2.3.2 Contaminant Transport Mechanisms.*** The distribution of small concentrations of selected contaminants at the subregional scale is dependent on the capability of those contaminants to persist in the flow system. The ion exchange and sorption capacity of geologic materials affects the persistence of dissolved constituents in groundwater moving through those materials. Those contaminants that are more reactive to the processes of sorption and ion exchange are less likely to be detected at any distance from the source.

Contaminants moving within basalt will be less likely to be affected by ion exchange because the ion-exchange capacity of basalt is relatively small (Nace 1975). However, the presence of clays enhances ion exchange. Montmorillonite, the most abundant clay mineral associated with the rocks of the eastern Snake River Plain at the INEEL, is one of the more efficient ion-exchange minerals (Nace 1975).

Tritium, because it composes part of the water molecule, is nonreactive and provides a measure of advective flow. Detectable concentrations over a large area of the INEEL are attributed to the conservative nature of this radionuclide and to the large quantities disposed to the subsurface since 1952. Much smaller quantities of chlorine-36 and iodine-129 were disposed to the aquifer. These relatively conservative contaminants persist and are detectable at very small concentrations in groundwater.

The WAG-10 conceptual model does not directly include transport. However, important elements of transport include source strength, release rates, and processes of sorption and decay. The conceptual model's most important elements are the average linear pore velocity and direction, as interpreted from the geometry, hydraulic parameters, effective porosity, geochemistry, and temperature (see footnote 1).

#### *2.2.3.3 Subregional Distribution of Selected Contaminants in the SRPA*

The subregional distribution of contaminants in the aquifer provides information about velocity of flow and the distribution of the flow field. The disposal of tritium, iodine-129, and chlorine-36 to an injection well and infiltration ponds has resulted in small, detectable concentrations of these radionuclides over a large area.

***Tritium—***Small, detectable concentrations of tritium have been measured in wells downgradient from INTEC and TRA. In 1985, tritium concentrations at the instrument detection limit of 0.5 pCi/mL were measured at the south boundary of the INEEL (Pittman et al. 1988). The area of the INEEL in which tritium concentrations in groundwater exceeded the instrument detection limit was estimated to exceed 50 $mi^2$. By 1998, this area and measured concentrations had decreased (Bartholomay et al. 2000; see Figure 2-11). Decreases are attributed to radioactive decay and decreases in disposal of tritium to the subsurface.

Researchers have long noted that the dimensions of the tritium plume are not what would be expected in a uniform system of groundwater flow through an isotropic, homogeneous medium. Robertson (1974) observes that the extended lateral dimension of the tritium plume implies considerable lateral dispersion within the aquifer. Robertson et al. (1974) infer that this large lateral dimension may be derived in part from the coalescing plumes originating from TRA and INTEC and from the effects of episodic recharge along the Big Lost River. Ackerman et al. (in preparation) note that the spatial and temporal variability suggest that the hydraulic complexities associated with vent corridors also may affect the dispersion of contaminants.

***Iodine-129 and Chlorine-36—***Small concentrations of iodine-129, one to two orders of magnitude greater than the calculated background concentration, and chlorine-36, were detected in wells 15 and 16 mi hydraulically downgradient from the INTEC disposal well (Mann and Beasley, 1994; Cecil et al. 2000). A minimum velocity was estimated from iodine-129 data to be about 6 ft/d. Comparison of concentrations at different depths indicated that iodine-129 is not distributed uniformly with depth (Mann and Beasley, 1994). A horizontal flow velocity was estimated from chlorine-36 data to be about 10 ft/d (Cecil et al. 2000). The chlorine-36 data inferred that preferential flow may occur within the heterogeneous, layered basalt aquifer.

## 2.3 Numerical Analyses

Several subregional numerical analyses have been developed to test subregional conceptual models. This section briefly describes those numerical analyses.

### 2.3.1 USGS

***2.3.1.1 Robertson, 1974.*** Digital modeling techniques were applied to the analysis of contaminant transport. The model indicated that transverse hydraulic dispersion had a significant influence on the migration of contaminants.

2.3.1.2 ***Goode and Konikow, 1990—***Transient flow conditions were applied to Robertson's (1974) numerical model. These conditions permitted use of larger dispersivities than those derived by Robertson, with the longitudinal dispersivity larger than the transverse dispersivity. However, Goode and Konikow determined that incorporation of transient flow did not significantly improve the understanding of those processes that control transport of contaminants.

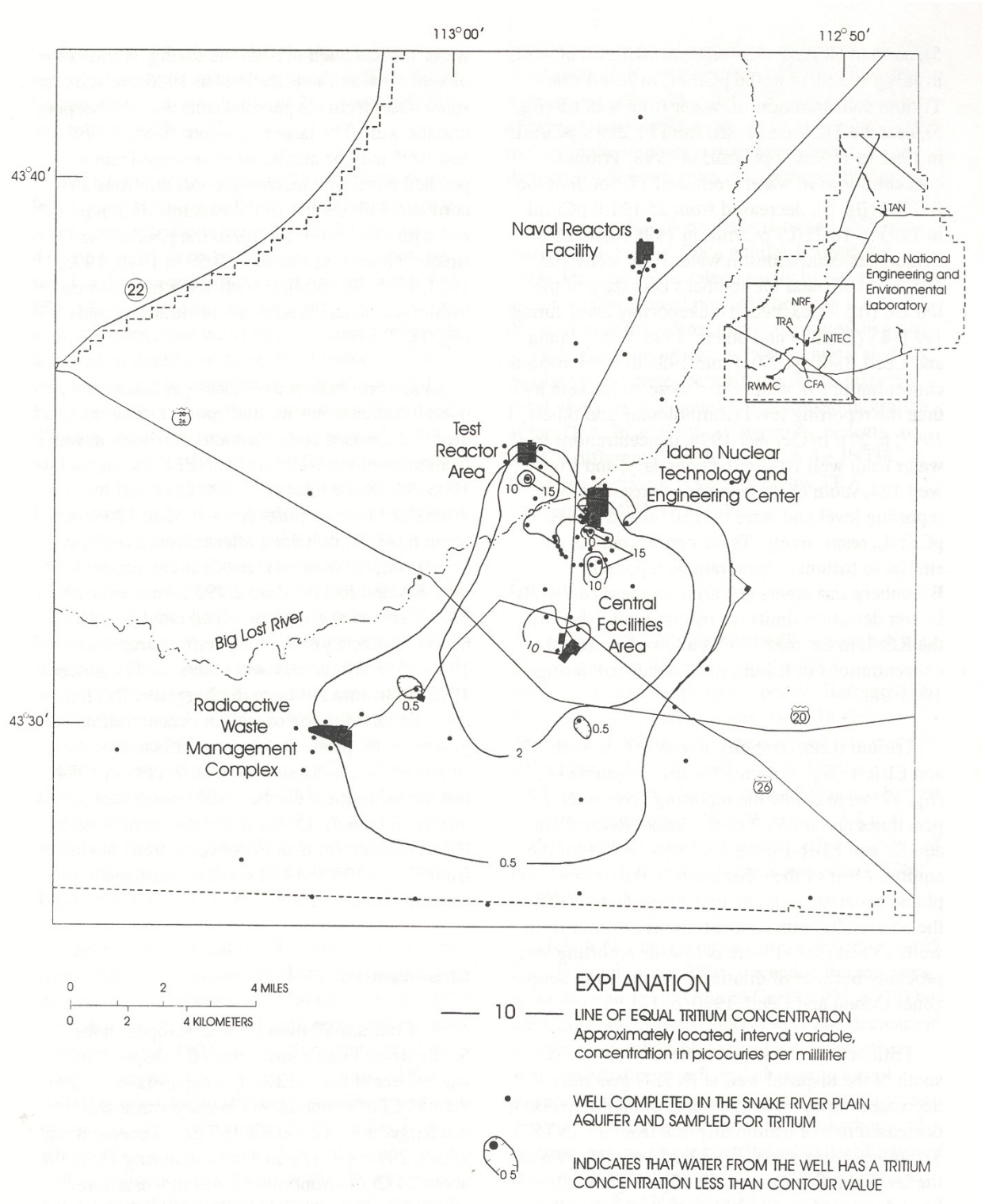


Figure 2-11. Tritium concentrations in water from the SRPA at the INEEL, 1998 (from Bartholomay et al. 2000).

***2.3.1.3 Ackerman et al. (in preparation)—***The USGS presently is completing a sequence of steady-state, transient, and solute transport models of the INEEL subregion. These models are based on the USGS conceptual model (Ackerman et al. in preparation). Simulations are evaluating the role of episodic flow, structural features, and stratigraphic features in the configuration of the flow field and contaminant transport.

### 2.3.2 WAG-10

***2.3.2.1 Arnett and Springer, 1994.*** This numerical model was developed to support the INEEL Environmental Impact Statement. The model simulated groundwater flow across the INEEL and contaminant transport in the south-central part of the INEEL. The flow model was two dimensional with variable grid spacing. The contaminant transport model consisted of a separate submodel domain that focused on areas of contamination.

***2.3.2.2 McCarthy et al. 1995.*** The model developed for WAG 10 simulated groundwater flow near the INEEL while preserving regional influences. This model simulated flow over the same region as Garabedian's regional model. TheWAG-10 model, while integrating regional and subregional scales, did not provide adequate resolution to support individual waste area groups.

## 2.4 Summary of Competing Hypotheses and Additional Data Requirements

Competing hypotheses have been developed to explain the distribution and movement of contaminants within the INEEL subregion. These competing hypotheses generally are developed because data and understanding are limited. The following section briefly summarizes competing hypotheses and data requirements as identified by conceptual models and numerical analyses.

### 2.4.1 Orientation and Distribution of Geohydrologic Units

The USGS hypothesizes the rise of geohydrologic unit 2 above the water table south of the INEEL. The orientation of unit 2 would force water in the aquifer to move across the unit in the direction of presumed minimal permeability. This hypothesis infers the downward movement and deeper circulation of water and contaminants in that area. The true orientation, extent, and hydraulic properties of unit 2 south of the INEEL are not well defined because of limited testhole data and the large depths required to drill new coreholes. This hypothesis is non-unique and is only one of several hypotheses that may explain steepening hydraulic gradients.

### 2.4.2 Effect of the Combined Thickness of Sedimentary Interbeds on the Flow Field

The USGS conceptual model hypothesizes that increased sediment percentages within the Big Lost Trough affect the hydraulic gradient, rate of flow, and contaminant transport.

### 2.4.3 Thickness and Effective Base of the Aquifer

Several competing hypotheses are based on estimates of the thickness and the effective base of the SRPA. The WAG-10 conceptual model hypothesizes a "thick" (greater than 1,300 ft in places) and a "thin" aquifer based on two interpretations of temperature and electrical resistivity data. The USGS conceptual model hypothesizes a much thicker aquifer (exceeding 4,000 ft in places) based on electrical resistivity and borehole data. All three models rely heavily on indirect information that may have significant errors in interpretation. While these models vary greatly, little is understood about importance

of aquifer thickness on contaminant transport at the INEEL. Additional temperature and water-chemistry data are needed near Argonne National Laboratory West and Atomic City to define the aquifer base in those areas. Calibrated temperature logs are needed from all new wells. Stratigraphic, temperature, and chemistry data are needed from an additional well in the area of inferred uplift and thinning aquifer hypothesized near well USGS-22.

### 2.4.4 Flow Across the Base of the Aquifer

The potential for flow across the base of the aquifer is not well known. The USGS conceptual model minimizes flow and assumes that it essentially does not exist. According to Mann (1986) "geologic and hydraulic information is inadequate…to define the magnitude of this inflow (from underlying rocks) and the effective base of the aquifer at all but a few locations at the INEL and on the Snake River Plain."

### 2.4.5 Preferential vs. Nonpreferential Flow

Geochemical data (uranium and strontium isotope ratios) infer that subregional preferential flow paths may exist that would facilitate selective rapid transport of contaminants downgradient. In contrast, limited head data and the random orientation of basalt flows and interflow zones and the large degree of interconnection between interflow zones have been interpreted to suggest that water and contaminants move non-preferentially at the subregional scale.

### 2.4.6 Deep Circulation

The potential for preferential flow along interflow zones implies large horizontal to vertical anisotropy that may restrict the downward movement of water and contaminants across the uppermost unit of the aquifer beneath the INEEL. Based on this hypothesis, contaminants will tend to remain shallow in the system. Vertical contaminant profiling data are insufficient to verify or negate this hypothesis. Few data are available to evaluate how head gradients and flow directions vary with depth. Information is needed about hydraulic and geochemical properties of the HI interbed and its importance in restricting vertical mixing.

### 2.4.7 Enhanced Dispersion of Contaminants Resulting from the Spatial and Temporal Variability of Streamflow Infiltration

Episodic streamflow infiltration is considered to be much more significant to contaminant transport than is recharge from areal precipitation. Ackerman et al. (in preparation) states that "lateral spreading of contaminants may be strongly influenced by these episodic recharge events and resulting temporal fluctuations in water-table gradients." This hypothesis is of increased interest because of the location of contaminant sources in proximity to surface-water features.

### 2.4.8 Characterization of Low-permeability Zones

Distribution of contaminants in water from the SRPA near TAN, INTEC, and RWMC has been explained by the presence of low-permeability zones. Additional data are needed to improve the definition of these zones.

### 2.4.9 The Effect of Vent Corridors on the Flow Field

Vent corridors are largely inferred from the orientation of existing vents. Little information is available to define the effect of these features on the field of groundwater flow.

### 2.4.10 References Cited


Ackerman, D.J., Anderson, S.R., Davis, L.C., Orr, B.R., Rattray, G.W., and Rousseau, J.P., in preparation, "A Conceptual Model of Flow in the Snake River Plain Aquifer at and Near the Idaho National Engineering and Environmental Laboratory with Implications for Contaminant Transport," U.S. Geological Survey Water-Resources Investigations Report (TBD).

Anderson, S.R., Kuntz, M.A., and Davis, L.C., 1999, *Geologic Controls of Hydraulic Conductivity in the Snake River Plain Aquifer at and near the Idaho National Engineering and Environmental Laboratory, Idaho*, U.S. Geological Survey Water-Resources Investigations Report 99-4033, U.S. Geological Survey.

Anderson, S.R., Liszewski, M.J., and Cecil, L.D., 1997, *Geologic Ages and Accumulation Rates of Basalt-flow Groups and Sedimentary Interbeds in Selected Wells at the Idaho National Engineering Laboratory, Idaho,* U.S. Geological Survey Water-Resources Investigations Report 97-4010 U.S. Geological Survey.

Anderson, S.R., and Liszewski, M.J., 1997, *Stratigraphy of the Unsaturated Zone and the Snake River Plain Aquifer at and near the Idaho National Engineering Laboratory, Idaho*, U.S. Geological Survey Water-Resources Investigations Report 97-4183, U.S. Geological Survey.

Arnett, R.C., and Smith, R.P., 2001, *WAG 10 Groundwater Modeling Strategy and Conceptual Model*, INEEL/EXT-01-00768, Bechtel BWXT Idaho, LLC, Idaho National Engineering and Environmental Laboratory.

Bartholomay, R.C., Tucker, B.J., Davis, L.C., and Greene, M.R., 2000, *Hydrologic Conditions and Distribution of Selected Constituents in Water, Snake River Plain Aquifer, Idaho National Engineering and Environmental Laboratory, Idaho, 1996 through 1998*, U.S. Geological Survey Water-Resources Investigations Report 00-4192, U.S. Geological Survey.

Bartholomay, R.C., Davis, L.C., and Link, P.K., 2002, "Introduction to the Hydrogeology of the Eastern Snake River Plain," Link, P.K. and Muele, L.L., eds., Geology, Hydrogeology, and Environmental Remediation, Idaho National Engineering and Environmental Laboratory, Eastern Snake River Plain, Idaho, Boulder, Colorado*, Geological Society of America,* Special Paper 353.

Bennett, C.M., 1990, *Streamflow Losses and Groundwater Level Changes along the Big Lost River at the Idaho National Engineering Laboratory, Idaho*, U.S. Geological Survey Water-Resources Investigations Report 90-4067, U.S. Geological Survey.

Blackwell, D.D., 1989, "Regional Implications of Heat Flow of the Snake River Plain, Northwestern United States," *Tectonophysics*, v.164, p.323-343.

Blackwell, D.D., 1990, *Temperatures and Heat Flow in INEL-GT1 and WO-2 Boreholes, Snake River Plain, Idaho*, EG&G Informal Report, EGG-NPR-10690, Idaho National Engineering and Environmental Laboratory, EG&G Idaho, Idaho Falls, Idaho.

Blackwell, D.D., and Steele, J.L., 1992, "Geothermal Map of North America: DNAG Continent-Scale Map-006," *Geological Society of America*, Decade of North American Geology series.

Blackwell, D.D., Kelley, S., and Steele, 1992, *Heat Flow Modeling of the Snake River Plain*, EG&G Informal Report, EGG-NPR-10790, Idaho National Engineering and Environmental Laboratory, EG&G, Idaho, Idaho Falls, Idaho.

Brott, C.A., D.D. Blackwell, and J.P. Ziagos, 1981, "Thermal and Tectonic Implications of Heat Flow in the Eastern Snake River Plain, Idaho," *Journal of Geophysical Research*, v. 86, p. 11,709-11,734.

Busenberg, E., Weeks, E.P., Plummer, L.N., and Bartholomay, R.C., 1993, *Age Dating Groundwater by Use of Chlorofluorocarbons ($CCl_3F$ and $CCl_2F_2$), and Distribution of Chlorofluorocarbons in the Unsaturated Zone, Snake River Plain Aquifer, Idaho National Engineering Laboratory, Idaho*, U.S. Geological Survey Water-Resources Investigations Report 93-4054 (DOE/ID-22107), U.S. Geological Survey.

Busenberg, E., Plummer, L.N., Bartholomay, R.C., and Wayland, J.E., 1998, *Chlorofluorocarbons, Sulfur Hexafluoride, and Dissolved Permanent Gases in Groundwater from Selected Sites in and near the Idaho National Engineering Laboratory, Idaho*, 1994-97: U.S. Geological Survey Open-File Report 98-274 (DOE/ID-22151), U.S. Geological Survey.

Busenberg, E., Plummer, L.N., Doughten, M.W., Widman, P.K., and Bartholomay, R.C., 2000, *Chemical, Isotopic, and Gas Compositions of Ground and Surface Waters from Selected Sites in and near the Idaho National Engineering Laboratory, Idaho*, 1994-97: U.S. Geological Survey Open-File Report 00-81 (DOE/ID-22164), U.S. Geological Survey.

Busenberg, E., Plummer, L.N., and Bartholomay, R.C., 2001, *Estimated Age and Source of the Young Fraction of Groundwater at the Idaho National Engineering and Environmental Laboratory*, U.S. Geological Survey Water-Resources Investigations Report 01-4265 (DOE/ID-22177), U.S. Geological Survey.

Carkeet, Colleen, Rosentreter, J.J., Bartholomay, R.C., and Knobel, L.L., 2001, *Geochemistry of the Big Lost River Drainage Basin, Idaho*, U.S. Geological Survey Water-Resources Investigations Report 01-4031 (DOE/ID-22174), U.S. Geological Survey.

Cecil, L.D., Welhan, J.A., Green, J.R., Frape, S.K., and Sudicky, E.R., 2000, "Use of Chlorine-36 to Determine Regional-Scale Aquifer Dispersivity, Eastern *Snake River Plain Aquifer*, Idaho/USA," *Nuclear Instruments and Methods in Physics Research*, B 172 (2000), p. 679-687.

Cecil, L.D., Pittman, J.R., Beasley, T.M., Michel, R.L., Kubik, R.L., Sharma, P., Fehn, U., and Gove, H.E., 1992, *Water Infiltration Rates in the Unsaturated Zone at the Idaho National Engineering Laboratory Estimated from Chlorine-36 and Tritium Profiles, and Neutron Logging*, Proceedings of the 7th International Symposium on Water-Rock Interaction, July 13-18, 1992, Yousifk, Kharaka, and Ann S. Maest, editors, p. 709-714.

Frederick, D.B., and Johnson, G.S., 1996, "Estimation of Hydraulic Properties and Development of a Layered Conceptual Model for the *Snake River Plain Aquifer* at the Idaho National Engineering Laboratory, Idaho," *State of Idaho INEL Oversight Program and Idaho Water Resources Research Institute Research and Technical Completion Report*.

Frederick, D.B., and Johnson, G.S., 1997, *Depth and Temporal Variations in Water Quality of the Snake River Plain Aquifer in Well USGS-59 near the Idaho Chemical Processing Plant at the Idaho National Engineering and Environmental Laboratory*, Idaho Water Resources Research Institute Research Technical Note 97-1.

Garabedian, S.P., 1992, *Hydrology and Digital Simulation of the Regional Aquifer System, Eastern Snake River Plain, Idaho*, U.S. Geological Survey Professional Paper 1408-F, U.S. Geological Survey.

Goode, D.J., and Konikow, L.F., 1990, "Reevaluation of Large-Scale Dispersivities for a Waste Chloride Plume—Effects of Transient Flow," Presented at the International Conference on Calibration and Reliability in Groundwater Modeling, *International Association of Hydrological Sciences*, September 6-9, 1990, The Hague, The Netherlands.

Hughes, S.S., Casper, J.L., and Geist, D.J., 1997, "Potential Influence of Volcanic Constructs on Hydrogeology Beneath Test Area North, Idaho National Engineering and Environmental Laboratory, Idaho," *Proceedings, 32nd Symposium, Engineering, Geology, and Geotechnical Engineering*.

Johnson, A.I., 1965, *Determination of Hydrologic and Physical Properties of Volcanic Rocks by Laboratory Methods*, ed. D.N. Wadia, D.N., Commemorative volume, Mining and Metallurgical Institute of India, p. 50-63 and 78.

Johnson, Roback, McLing, Bullen, DePaolo, Doughty, Hunt, Smith, Cecil, and Murrell, 2000, "Groundwater 'Fast Paths' in the Snake River Plain Aquifer—Radiogenic Isotope Ratios as Natural Groundwater Tracers," *Geology*, October 2000, v. 28, no. 10, p. 871-874.

Jones, P.A., 1963, "The Velocity of Groundwater Flow in Basalt Aquifers of the Snake River Plain, Idaho," Extract of Publication No. 64, *International Association of Scientific Hydrology*, Berkeley, p. 225-234.

Knobel, L.L., Bartholomay, R.C., and Orr, B.R., 1997, *Preliminary Delineation of Natural Geochemical Reactions, Snake River Plain Aquifer System, Idaho National Engineering Laboratory and Vicinity, Idaho*: U.S. Geological Survey Water-Resources Investigations Report 97-4093 (DOE/ID-22139), U.S. Geological Survey.

Kuntz, M.A., Covington, H.R., and Schorr, L.J., 1992, "An Overview of Basaltic Volcanism of the Eastern Snake River Plain, Idaho," eds. Link, P.K., Kuntz, M.A., and Platt, L.B., *Regional Geology of Eastern Idaho and Western Wyoming: Geological Society of America,* Memoir 179, p. 227-267.

Kuntz, M.A., Anderson, S.R., Champron, D.E., Lanphere, M.A., and Grunwald, D.J., 2002, "Tension Cracks, Eruptive Features, Dikes, and Faults Related to Late Pleotocene-Holocene Basaltic Volcanism and Implementation for the Distribution of Hydraulic Conductivity in the Eastern Snake River Plain, Idaho," Link, P.K. and Muele, L.L., eds., Geology, Hydrogeology, and Environmental Remediation, Idaho National Engineering and Environmental Laboratory, Eastern Snake River Plain, Idaho, *Geological Society of America*, Special Paper 353.

Luo, S., Ku, T., Roback, R., Murrell, M., and McLing, T.L., 2000, "In-situ Radionuclide Transport and Preferential Groundwater Flows at the INEEL (Idaho)," Decay-series disequilibrium studies, *Geochimica et Cosmochimica Acta*, Vol. 64, No. 5, p. 867-881.

Mann, L.J., and Beasley, T.M., 1994, *Iodine-129 in the Snake River Plain Aquifer at and near the Idaho National Engineering Laboratory, Idaho, 1990-91*, U.S. Geological Survey Water-Resources Investigations Report 94-4053, U.S. Geological Survey.

McCarthy, J.M., Arnett, R.C., Newpauer, R.M., Rohe, M.J., and Smith, C., 1995, *Development of a Regional Groundwater Flow Model for the Area of the Idaho National Engineering Laboratory, Eastern Snake River Plain Aquifer*, INEL-95/0169, Idaho National Engineering and Environmental Laboratory, Lockheed Martin Idaho Technologies Company, Idaho Falls, Idaho.

Nace, R.L., Deutsch, Morris, and Voegeli, P.T., 1972, *Physical environment of the National Reactor Testing Station, Idaho – A Summary*, edited by Subitsky, Seymore, U.S. Geological Survey Professional Paper 725-A, U.S. Geological Survey.

Nace, R.L., Voegeli, P.T., Jones, J.R., and Deutsch, Morris, 1975, *Generalized Geologic Framework of the National Reactor Testing Station, Idaho*, edited by Subitsky, Seymore, U.S. Geological Survey Professional Paper 725-B, U.S. Geological Survey.

Nimmo, J. R., K. S. Perkins, P. A. Rose, J. P. Rousseau, B. R. Orr, B. V. Twining, and S. R. Anderson, 2001, "2001 Kilometer-Scale Rapid Flow in a Fractured-Basalt Unsaturated Zone at the Idaho National Engineering and Environmental Laboratory," *2001 Conference Proceedings, March 26–28, 2001, Toronto*, ed. B. H. Kueper, K. S. Novakowski, and D. A. Reynolds.

Olmsted, F.H., 1962, *Chemical and Physical Character of Groundwater in the National Reactor Testing Station, Idaho*, IDO-22043-USGS, U.S. Geological Survey.

Pittman, J.R., Jensen, R.G., and Fischer, P.R., 1988, *Hydrologic Conditions at the Idaho National Engineering Laboratory, 1982 to 1985*, U.S. Geological Survey Water-Resources Investigations Report 89-4008 (DOE/ID-22078), U.S. Geological Survey.

Robertson, J. B., R. Schoen, and J. T. Barraclough, 1974, *The Influence of Liquid Waste Disposal on the Geochemistry of Water at the National Reactor Testing Station, Idaho, 1952-1970,* U.S. Geological Survey Open-File Report (IDO-22053).

Robertson, J.B., 1974, *Digital Modeling of Radioactive and Chemical Waste Transport in the Snake River Plain Aquifer at the National Reactor Testing Station, Idaho – 1952-1970*, U.S. Geological Survey Open-File Report (IDO-22054), U.S. Geological Survey.

Robertson, J.B., 1977, *Numerical modeling of subsurface radioactive solute transport from waste-seepage ponds at Idaho National Engineering Laboratory*, U.S. Geological Survey Open-File Report 76-717 (IDO-22057), U.S. Geological Survey.

Rohe, M.J., November 2000, *Application of a Geometric Technique for Estimating Local-Scale Hydraulic Gradients from Aquifer Water Level Data*, Geological Society of America Annual Meeting and Exposition Abstracts, Reno, Nevada.

Smith, R.P., Blackwell, D.D., McLing, T.L., 2001, "Temperature Distribution in the *Snake River Plain Aquifer* Beneath the Idaho National Engineering and Environmental Laboratory (INEEL) -- Implications for Aquifer Flow and Geothermal Input," *Geological Society of America Abstracts with Programs*, v.33, no.6, p. A-107.

Smith, R.P., 2001, "Aquifer Thickness Assessment for Use in OU 10-09-8 Groundwater Modeling Activities," (TBD), Bechtel BWXT Idaho, LLC, Idaho National Engineering and Environmental Laboratory, Idaho Falls, Idaho.

Spinazola, J.M., 1994, *Geohydrology and Simulation of Flow and Water Levels in the Aquifer System in the Mud Lake Area of the Eastern Snake River Plain, Eastern Idaho*, U.S. Geological Survey Water-Resources Investigations Report 93-4227, U.S. Geological Survey.

Swanson, S.A., Rosentreter, J.J., Bartholomay, R.C., and Knobel, L.L., 2002, *Geochemistry of the Little Lost River Drainage Basin, Idaho*, U.S. Geological Survey Water-Resources Investigations Report 02-4120 (DOE/ID-22179), U.S. Geological Survey.

Welhan, J.A., and Reed, M.F., 1997, "Geostatistical Analysis of Regional Hydraulic Conductivity Variations in the *Snake River Plain Aquifer*, Eastern Idaho," *GSA Bulletin*, July 1997, no. 7; p. 855-868.

Welhan, J.A., and Wylie, A.H., 1997, "Stochastic Modeling of Hydraulic Conductivity in the *Snake River Plain Aquifer*—2. Evaluation of Lithologic Controls at the Core and Borehole Scales," *Proceeding on the Symposium on Engineering Geology and Geotechnical Engineering*, 32d, Boise, Idaho, March 26-28, 1997, p. 93-107.

Wood, S.H. and Bennecke, W., 1994, "Vertical Variation in Groundwater Chemistry Inferred from Fluid Specific-Conductance Well Logging of the *Snake River Plain Aquifer*, Idaho National Engineering Laboratory, Southeastern Idaho," *Proceedings of the 30th Symposium on Engineering Geology and Geotechnical Engineering*, p.267-283.

Wood, T.R., and Norrell, G.T., 1996, *Integrated Large-Scale Aquifer Pumping and Infiltration Tests, Groundwater Pathways: Summary Report*, INEL-96/0256, Rev. 0, Idaho National Engineering and Environmental Laboratory, Lockheed Martin Idaho Technologies Company, Idaho Falls, Idaho.

# 3. FACILITY-SCALE GEOHYDROLOGIC STUDIES

Many facility-scale geohydrologic studies have been conducted at the INEEL in conjunction with characterization and remediation activities. These studies have provided information needed to develop facility-scale conceptual models of flow and transport. They also have provided valuable information about components of the subregional conceptual models. Subsequent subsections summarize the conceptual models of flow and transport developed at each WAG.

## 3.1 Waste Area Group 1

WAG-1 is the designation for the collection of CERCLA operable units (OUs) associated with the TAN facility, which is located in the northwestern section of the INEEL (see Figure 3-1). Several sub-areas at TAN include the Technical Support Facility (TSF), the Initial Engine Test Facility (IET), the Loss of Fluid Test Facility (LOFT), the Specific Manufacturing Capabilities Facility (SMC), and the Water Reactor Research Test Facility (WRRTF). The TSF consists primarily of facilities designed for handling, examination, storage, and research and development of spent nuclear fuel. The IET is the location of the former Aircraft Nuclear Propulsion Program (ANPP), which served to develop and test nuclear jet engines in the 1950s and 1960s. The LOFT and SMC are contiguous facilities located west of TSF, and include old buildings from the decommissioned ANPP. The LOFT is a decommissioned facility where nuclear reactor safety tests were conducted. The SMC is an active facility that manufactures components for a U.S. Department of Defense (DOD) non-nuclear weapons system. The WRRTF is located in the southeastern corner of the WAG-1 boundary and consists of two buildings that house several non-nuclear tests—mostly for simulating and testing water systems used in reactors. Potential sources for contamination at these facilities include injection wells, settling ponds and lagoons, tanks, spills, solid waste disposal sites, and burn pits.

During routine sampling of water supply wells in 1987, trichloroethylene (TCE) was detected in the groundwater at TAN. Subsequent investigations delineated an extensive aqueous TCE plume at the facility. It was determined that injection of liquid and sludge wastes (both organic and radioactive) into well TSF-05 was the most probable source of TCE in the nearly 2-mi long plume (Kaminsky et al. 1994; Figure 3-2). In addition to TCE, six other contaminants of concern (COCs) were identified: (1) tetrachloroethylene (PCE); (2) 1,2-dichloroethylene (DCE); (3) strontium-90 (Sr-90); (4) tritium (H-3); (5) cesium-137 (Cs-137); and (6) uranium-234 (U-234).

### 3.1.1 Summary of WAG-1 Site Conceptual Model

A characterization program was initiated after detection of TCE in groundwater at TAN to determine the extent of groundwater contamination. The first comprehensive approach at developing a conceptual model for TAN was the *Remedial Investigation Final Report with Addenda for the Test Area North Groundwater OU 1-07B at the INEL* (Kaminsky et al. 1994). The *Test Area North Site Conceptual Model and Proposed Hydrogeological Studies OU 1-07B* describes the development of the original conceptual model for WAG-1 (Sorenson, et al. 1996). That effort identified data gaps in the initial conceptual model that required further field studies and numerical modeling. Subsequent documents were produced that summarized the additional work and provided updates to the conceptual model in light of the new data gathering (Bukowski and Sorenson 1998a; Bukowski et al. 1998; and Wymore et al. 2000). The purpose of this section is to provide a summary of the WAG-1 conceptual model using information contained in the documents referenced above.

***3.1.1.1 Geologic Framework.*** The geologic framework at TAN, including the geometry, geologic features, and stratigraphic character of the basalt flows and sedimentary units, controls flow and contaminant transport in the vadose zone and aquifer. This section describes the size, shape, and composition of the area included in the WAG-1 conceptual model.

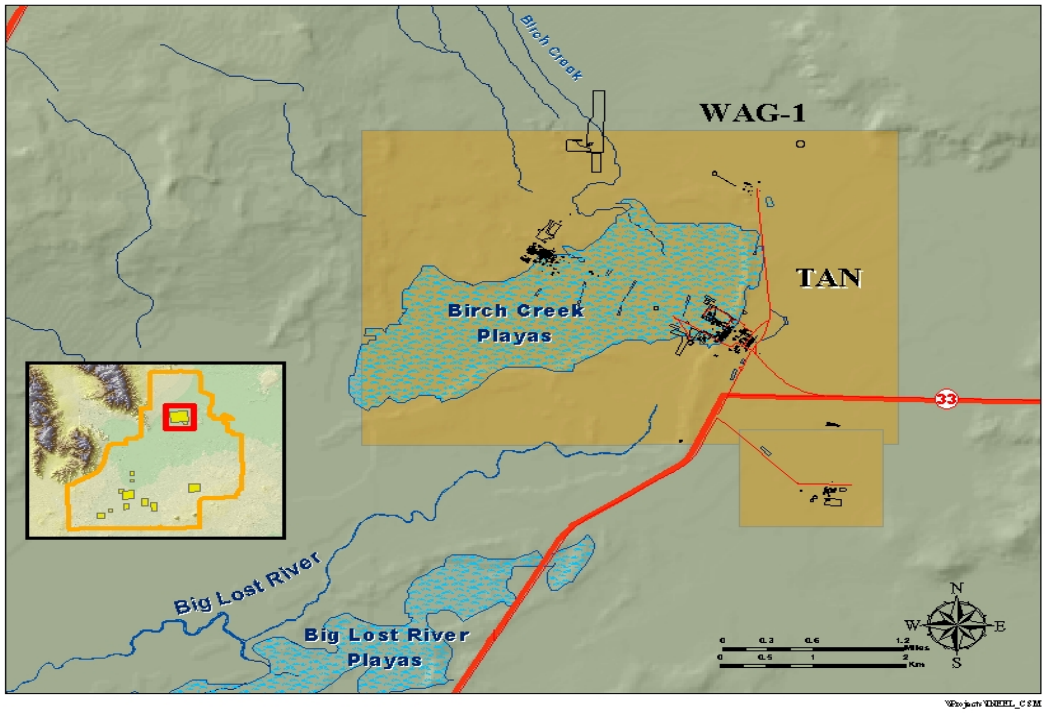


Figure 3-1. WAG 1 is associated with the TAN facility in the northwestern portion of the INEEL.

***3.1.1.2 Geologic Framework—***The vadose zone at TAN is approximately 200 to 230 ft thick. The SRPA at TAN is estimated to be about 600 ft thick, although the upper 200 to 300 ft appears to be hydraulically isolated from deeper zones due to the presence of a low hydraulic conductivity zone (i.e., sedimentary interbed) discussed in the next section.

***Geology—***The stratigraphy at TAN consists of thin pahoehoe basalt flows intercalated with sedimentary interbeds that accumulated between the basalt flows during periods of eruptive hiatus. This basalt/sediment stack is mantled with surficial sediments ranging from 5 to 75 ft in thickness throughout TAN that have accumulated during the last 900,000 years of eruptive quiescence.

TAN is located between two volcanic rift zones that cross the eastern Snake River Plain. The Circular Butte-Kettle Butte Rift Zone lies to the north of TAN, and the Lava Ridge-Hell's Half Acre Rift Zone lies to the southwest. The presence of the rift zone to the southwest of TAN may help explain the peculiar groundwater flow direction observed at TAN, which is discussed in the next section.

Two studies of the stratigraphy at TAN were conducted by the USGS. The first study was conducted by Lanphere et al. in 1994. In this study, 21 individual basalt flows were identified in four coreholes to a depth of 1,100 ft at TAN using petrography, age determinations, and paleomagnetic properties of the core samples for correlation. In addition, Lanphere et al. (1994) used K-Ar and paleomagnetic analyses of core samples and basalt outcrop at Circular Butte to delineate 21 subsurface basalt flows at TAN.

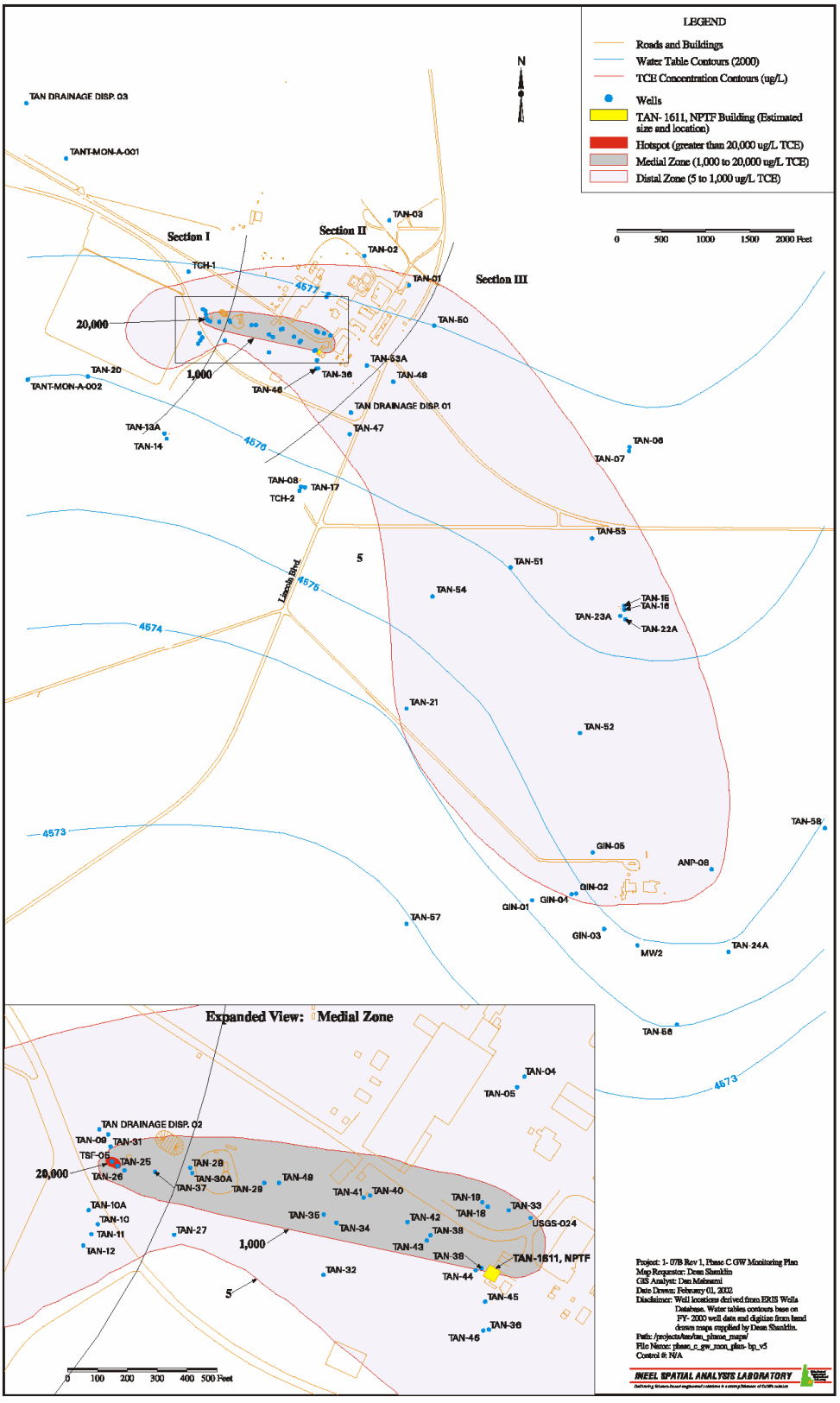


Figure 3-2. TAN TCE Plume Map based on 1996 data.

A second study of TAN stratigraphy was conducted by Anderson and Bowers (1995). A cross sectional diagram from this work is presented in Figure 3-3. This study utilized the core data from Lanphere et al. (1994) as the basis for making correlations among 53 additional wells at TAN. The natural gamma logs (which are sensitive to the small differences in potassium content and natural-gamma emissions of basalt flows from different source areas or eruptive episodes) of these wells were used to correlate the stratigraphic units in the coreholes. A total of 22 individual basalt flows were identified in the upper 500 ft of the subsurface at TAN. In addition, several sedimentary interbeds were also identified. In all, basalt flows account for 90% and sedimentary interbeds account for 10% of the upper 500 ft of the subsurface at TAN. The individual basalt flows were assigned to ten groups based on similar age, paleomagnetic properties, and natural gamma emissions. These groups were assigned alphabetic designations beginning with LM and continuing through R based on age and position. They were named to reflect their older age with respect to flow groups A through L from the southern portion of the INEEL.

A total of five to ten sedimentary units are interbedded with the basalt flow groups. Two of these were identified as major interbeds and were designated as the PQ and QR interbeds based on their position in the basalt flow group stack. The PQ interbed occurs at approximately 200 bls in the vicinity of TSF-05 and occurs in only 36 of the 60 wells that penetrate to a depth where it may be expected (Sorenson 2000). The average thickness of the PQ interbed (where encountered) is 6.1 ft. The interbed appears to dip at about $0.5^{o}$, striking at $10^{o}$ east of south; so while it is present above the water table upgradient from TSF-05, it dips below the water table downgradient. Therefore, the PQ interbed may cause locally confining or semi-confining conditions in the aquifer at TAN, and may also act as a barrier to contaminant flow or provide sorption sites for contaminants.

The QR interbed occurs at approximately 400 ft bls in the vicinity of TSF-05 and is apparently laterally continuous. The assumption of lateral continuity is based on the fact that the interbed is present in all 29 wells that penetrate to a depth where it may be expected (Sorenson 2000). The average thickness of the QR interbed is 17 ft, which is almost three times that of the PQ interbed thickness. The QR interbed exhibits the more gentle dip of $0.15^{o}$, and has a strike of about $12^{o}$ west of south. Analyses of chemical and pumping data from wells completed above and below the QR interbed strongly suggest that the interbed may serve as a barrier to vertical groundwater flow and associated contaminant transport. That is, TCE concentrations below the interbed are several magnitudes lower than concentrations above the interbed. Further, TAN-18, which is completed below the interbed, shows no response to pumping in nearby wells completed above the interbed.

Lanphere et al. (1994) used K-Ar dating to estimate a difference in age of approximately 600,000 years between the Q and R basalt flow groups straddling the interbed. These measurements indicate a significant hiatus of volcanic activity during which material comprising the interbed that is consistent with the observed continuity of the interbed could be deposited. The bottom boundary provided by the QR interbed limits the contaminated thickness of the aquifer to approximately 200 ft near TSF-05, and about 250 ft near the down-gradient extent of the TCE plume.

***3.1.1.3 Matrix Characteristics.*** This section discusses the primary properties of the aquifer matrix that control groundwater flow through the system at TAN.

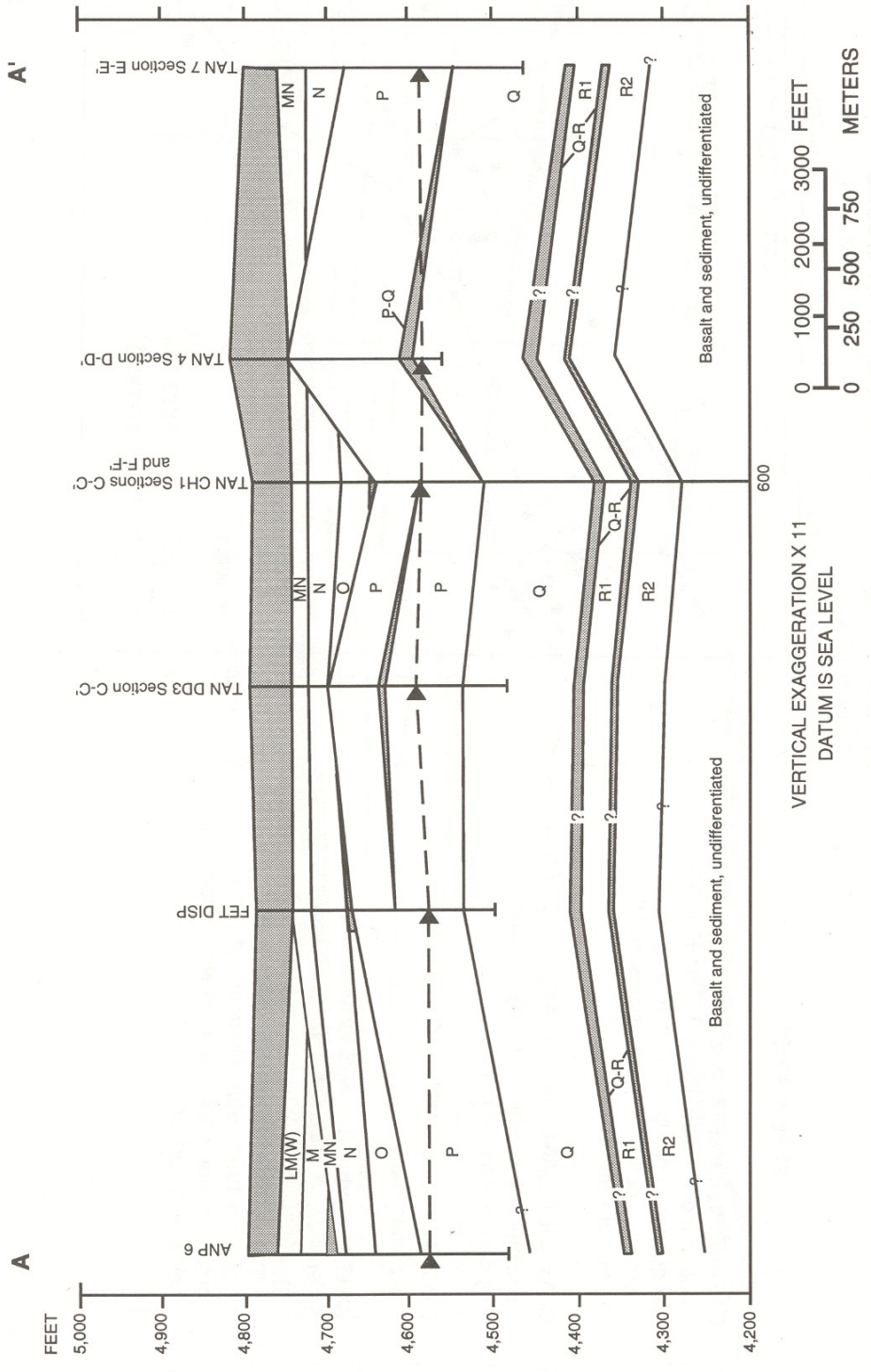


Figure 3-3. Stratigraphy of the WAG 1 site (Anderson and Bowers 1995).

***Permeability—***Permeability is the inherent ability of a medium to transmit a fluid. In general, this ability is a function of the shape and size of void spaces in the material and the viscosity of the fluid that is flowing through the material. When water is the fluid under consideration, this fluid transmission ability is termed hydraulic conductivity. Transmissivity is the rate at which groundwater flows under a unit hydraulic gradient through a unit width and the entire thickness of an aquifer. Transmissivity is calculated by multiplying hydraulic conductivity by aquifer thickness. At TAN, most studies have produced estimates of transmissivity rather than hydraulic conductivity. This report will maintain consistency with the previous studies.

Transmissivity at TAN has been estimated using a variety of techniques. Ackerman (1991) utilized data from 183 aquifer tests throughout the INEEL, which included nine wells in the TAN vicinity (all are within 1.5 mi of TSF-05). The arithmetic mean of the transmissivities for the entire INEEL data set was approximately 93,000 $ft^2$/day, while the mode was about 60,000 $ft^2$/day. Analysis of data from wells in the TAN vicinity showed lower than average transmissivity, the highest of which was 31,000 $ft^2$/day. Kaminsky et al. (1994) utilized slug test data to determine the transmissivity distribution at TAN. Transmissivity estimates from these slug tests range from as little as 5 $ft^2$/day to as much as 7,310 $ft^2$/day. These estimates are even lower than Ackerman's estimates for TAN area wells. This is probably due to the use of slug tests, which sample a much smaller portion of the aquifer than pumping tests. Further, specific capacities of selected wells were used in transmissivity estimations ranging from 1,755 $ft^2$/day to 6975 $ft^2$/day (Sorenson et al. 1996). The results of additional single- and multiple-well pumping tests were summarized in Bukowski and Sorenson (1998b) and Bukowski et al. (1998). These results showed transmissivities ranging from about 1,000 $ft^2$/day to 500,000 $ft^2$/day. The high end of the range revealed that the transmissivity at TAN is not uniformly below the INEEL average.

Figure 3-4, adapted from Martian (1999) shows the calibrated hydraulic conductivity distribution at TAN for numerical modeling obtained through kriging and trending the transmissivity data for 22 wells in the area. In spite of the fact that this distribution did not include the results from Bukowski et al. (1998), those data were consistent with the distribution in Figure 3-4. Inspection of the available transmissivity data for TAN shows a distinct increasing trend in the direction of contaminant transport from TSF-05. The trend may be partially attributable to the performance of the pumping tests primarily in partially penetrating wells near TSF-05; however, transmissivity estimates from a pumping test in TAN-37, a fully penetrating well not impacted by the sludge injected into TSF-05, are also much lower than those from down-gradient wells (Bukowski et al. 1998). A second potentially important observation is that all transmissivity estimates from wells south of the TCE plume are very low relative to the rest of the area (Sorenson et al. 1996; Martian 1999). While it is acknowledged that data from the five wells (TAN-20, TAN-13A, TAN-14, TAN-8, and TAN-21) are hardly sufficient to demonstrate conclusively that a low transmissivity "boundary" may be contributing to the deviation of groundwater flow in the upper portion of the plume from the regional gradient, they are consistent with that hypothesis.

***Porosity—***Effective porosity of the SRPA beneath TAN has not been directly measured. Rather, it has been estimated through model calibration to the tritium plume and through inverse modeling of pumping and tracer test results. On the plume scale, the effective porosity was estimated at about 3%. This value is approximately half of what has been estimated during a similar, large-scale characterization effort at the INEEL (Rodriguez et al. 1997). This lower effective porosity is most likely due to the relatively older age of the TAN basalt flows, which typically have lower effective porosities (Whitehead 1992). The inverse modeling approach has produced estimates ranging from 0.5 to 2.1% in all cases with the exception of an 8.5% value for two wells separated by only 20 ft (Bukowski et al. 1998).

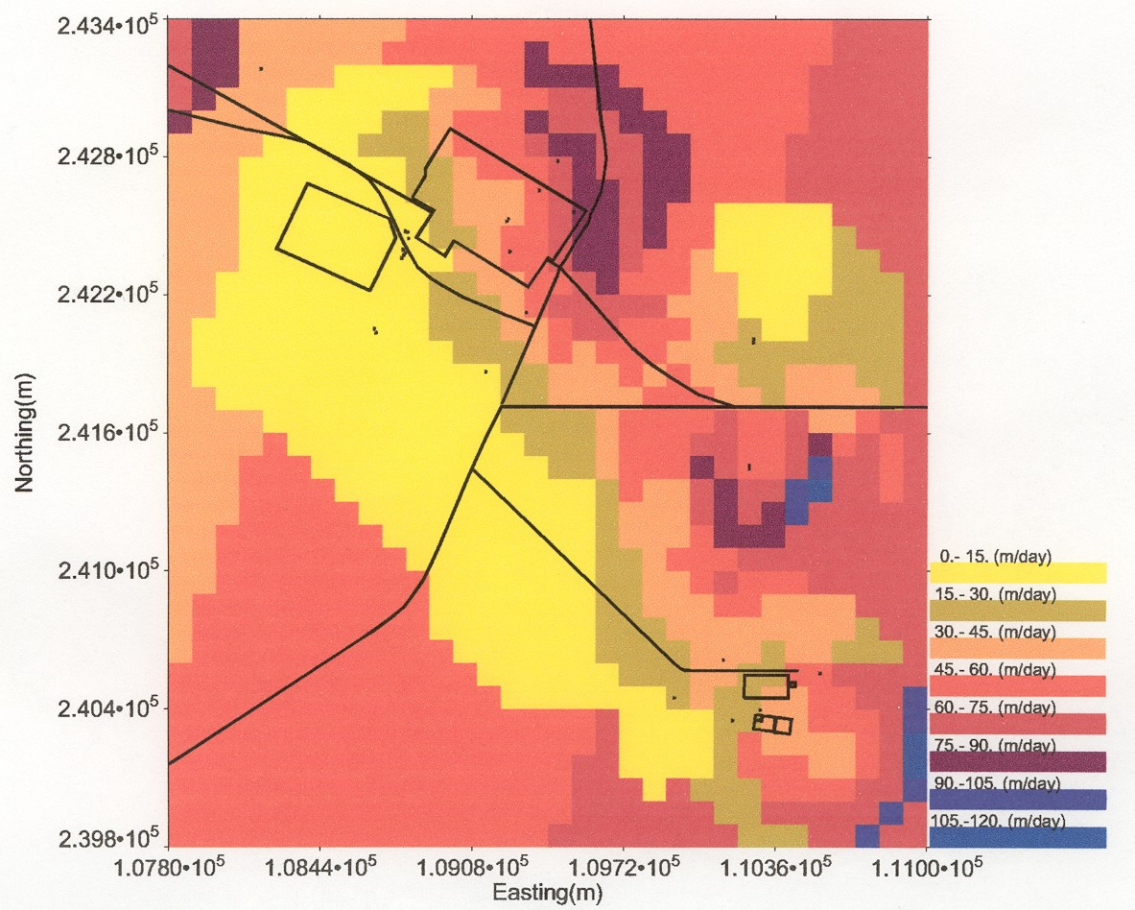


Figure 3-4. Hydraulic conductivity distribution at TAN obtained through kriging and trending of transmissivity data from 22 wells (Martian 1999).

Injection of sludge wastes into TSF-05 may have significantly reduced the effective porosity of the aquifer in the vicinity of the injection well. As mentioned above, the effective porosity of the unaffected aquifer at TAN has been estimated at about 1 to 3% (Martian 1999; Bukowski et al. 1998). The effective porosity in the immediate vicinity of TSF-05 was estimated at about 0.05% based on tracer test data analysis (Bukowski and Sorenson 1998a). The sludge injection apparently produced significant reductions in effective porosity to a radial distance of about 100 ft from TSF-05 (Sorenson 2000). Figure 3-5 shows the extent of the low effective porosity zone as estimated using tracer test data and analysis of elevated gamma activity.

***3.1.1.4 Recharge/Discharge Sources.*** This section presents the available knowledge of sources and sinks of water in the eastern SRPA in the WAG-1 vicinity. This discussion includes both natural and anthropogenic sources.

Natural Recharge/Discharge Sources—***The principal source of recharge to the SRPA near TAN is from regional underflow. Figure 2-8 indicates that much of the underflow is derived from the Mud Lake area to the northeast. Some recharge may occur from tributary basin underflow. These basins include drainages along the flanks of the Beaverhead Mountains and Birch Creek drainage. However, the effect of these recharge contributions on hydrologic conditions at TAN is not well understood.***

***Some recharge may be derived from infiltration of water along the channel of Birch Creek and diversions to the northwest of***

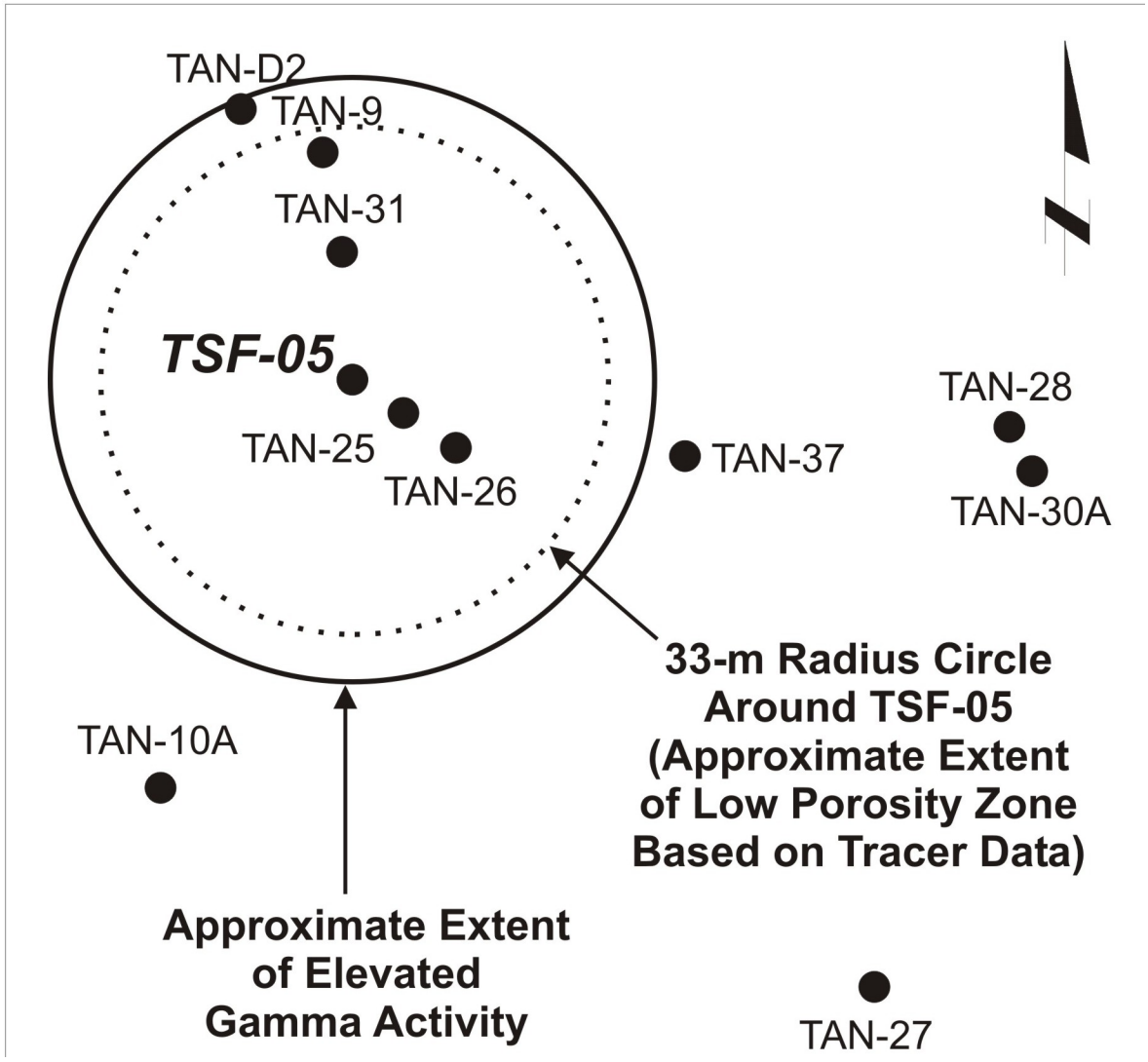


Figure 3-5. Extent of the low effective porosity zone as estimated using tracer test data and analysis of elevated gamma activity (Sorenson 2000).

TAN. The quantity of water available for recharge is small compared to regional underflow. Recharge from direct precipitation provides a source of local recharge to the SRPA. Again, the amount of recharge derived from direct precipitation is small compared to regional underflow. Cyclical changes in water levels appear to be linked to wet and dry periods and to seasonal effects of melting snow and groundwater pumpage for irrigation. These changes range from 2 to 4 ft.

***Artificial Recharge/Discharge Sources—***A significant source of artificial recharge at TAN until 1972 was the TSF-05 injection well, which was drilled in 1953. TSF-05 was drilled to 305 ft in depth, and was completed with 12-in. perforated casing with a gravel pack filling the annulus between the casing and the 20-in. borehole. This well was designed for the disposal of liquid wastes and concentrated evaporator sludges generated during the operations of the various TAN facilities. The composition of the disposed liquids included organic, inorganic, and low-level radioactive wastewaters (Kaminsky et al. 1994). Wastes were disposed in TSF-05 for almost 20 years, after which wastewaters were routed to a disposal pond. The amounts of wastes disposed during the operations of TSF-05 are discussed in a subsequent section.

Another injection well (TAN-53A) was drilled in the WAG-1 vicinity. The purpose of this well is to serve as an injection point for the effluent of the New Pump and Treat Facility (NPTF). The NPTF is the selected remedy for restoration of the medial zone of the TAN TCE plume. Thus, water entering the aquifer at this well is free of contamination.

Another artificial recharge source at TAN is the TSF-07 disposal pond. This pond is unlined and has accepted wastewater since its construction in 1972. At present time, the disposal pond only accepts sanitary wastewater. However, contaminated water has been released in the past. Data presented in the TAN Site Conceptual Model (Sorenson et al. 1996) indicate that discharge rates to the pond ranged from 100,000 to 1,000,000 gal per month during the early to middle 1990s. Water placed in the disposal pond either evaporated or infiltrated through the pond bottom. Between 1972 and 1985, approximately 0.039 Ci of Sr-90 were discharged to the disposal pond. Perched water has been observed at the basalt-sediment interface beneath the pond and was sampled in 1990 and 1991. Sr-90 was detected in these samples in the range of 1.0 to 136.0 pCi/L (Medina 1993). The probably source of the observed perched water is the TSF-07 disposal pond.

Two production wells are in use at TAN, TAN-01 and TAN-02. The pumps in these production wells were cycled on alternately every 6 to 24 hours at a rates of about 1,000 gal/min. through the 1990s. Only TAN-02 is currently in use as a water supply well for TAN. In addition, the NPTF includes a set of three extraction wells that will be operated alone or in combination at rates of up 120 gal/min.

***3.1.1.5 Hydraulics.*** The regional hydraulic gradient in the TAN area has been estimated using water levels from 49 wells (Kaminsky et al. 1994). The gradient was determined to be approximately 3.5 ft/mi, with groundwater flowing to the south-southeast (see Figure 3-6). Similar results based on additional water level information were reported by Bukowski and Wells (1999). The additional information included several new wells near the up-gradient portion of the plume, which was consistent with the eastward flow direction in that area as indicated by the shape of the TCE plume.

The SRPA water table at TAN is relatively flat with a local gradient of about 1 ft/mi (Kaminsky et al. 1994). The inferred direction of subregional groundwater flow in the vicinity of TAN is to the southwest (see Figure 2-8; Kaminsky et al. 1994). Water-level data from wells at TAN indicated that the local direction of groundwater flow is to the southeast. The local change in flow direction is reflected in the generally east and southeast orientation of the TCE plume. Hughes et al. (1997) postulate that the plume orientation is parallel to the general orientation of volcanic rift zones. This feature may indicate the local effect of vent corridors and associated structures on the configuration of the groundwater flow field and contaminant transport near TAN.

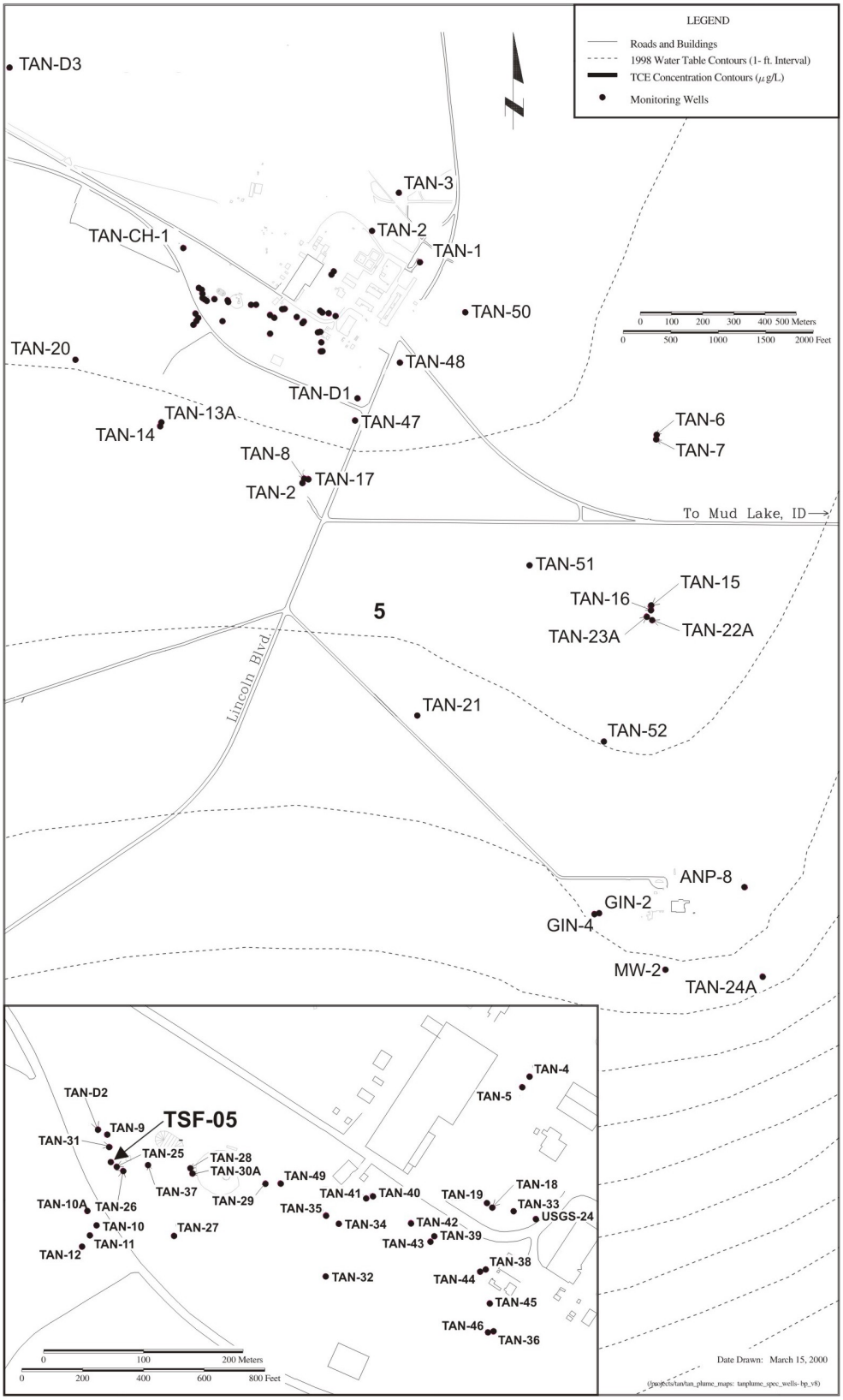


Figure 3-6. Water level elevations for the WAG 1 area.

As implied above, the groundwater flow direction deviates sharply from the regional direction in the up-gradient portion of the TAN TCE plume. Several hypotheses have been proposed to explain this aberrant behavior. Groundwater flow direction seems to be governed by at least four features: (1) the regional southerly gradient, (2) pumping at the TAN production wells, (3) recharge from the TSF-07 disposal pond, and (4) a general area of low hydraulic conductivity south of TSF-05.

Kaminsky et al. (1994) proposed that the pumping of the water supply wells (TAN-1 and TAN-2) at TAN, which are located to the northeast of the TCE plume, acts to pull groundwater to the east from the regional flow direction. This magnitude of pumping has an effect on water levels in the surrounding aquifer. During pumping of these wells, a typical drawdown of 2.9 in. has been observed at a distance of 1,000 ft (Sorenson et al. 1996). This results in a substantial radius of influence, which may change groundwater flow direction in the aquifer surrounding these wells.

Due to the cyclic pumping schedule of the production wells and the lack substantial drawdown near TSF-05, this explanation alone is not enough to account for the observed change in groundwater flow direction. Drawdown in the TCE source area (i.e., at wells TAN-D2, TSF-05, TAN-25, TAN-26, TAN-27, TAN-28, TAN-30A, and TAN-49) during pumping of the production wells was measurable, but never exceeded a tenth of an inch. Another objection to the production wells being the only influence on pulling groundwater flow away from the source area involves the cyclic nature of pumping at the TAN production wells. During non-pumping cycles, groundwater direction should be restored to the regional southerly trend in the absence of the production well influence. Thus, the TCE plume should have a southerly component in flow direction as well as an easterly flow due to the influence of the natural gradient during non-pumping cycles. Instead, the shape of the TCE plume indicates that there is essentially no southerly component of flow in the up-gradient zone as seen in Figure 3-2.

Another factor that may affect the local gradient and groundwater flow direction is the operation of the TSF-07 disposal pond. Calculations based on simplifying assumptions have been performed that indicate a mound on the order of 2.4 in. may form at the water table due to the infiltration of wastewater from the disposal pond (Kaminsky et al. 1994). This results in a 50% increase in the local hydraulic gradient, which would then cause radial flow away from the effective area of the pond's influence on the aquifer (i.e., footprint). In the vicinity of TSF-05, this radial flow would be towards the east. Thus, groundwater would be pushed to the east in the vicinity of the TSF-07 footprint, and would subsequently take on a southerly component outside of the area of disposal pond influence.

Image well theory (Lohman 1972) was applied to pumping test data near TSF-05 (Bukowski and Sorenson 1998). In matching type curves to the time-drawdown data, late-time drawdown at several wells was overestimated. A possible cause of this overestimation is the presence of a recharge boundary. Image well analysis indicated that a recharge boundary lies in a position consistent with the location of the TSF-07 disposal pond.

In order to match the shape of the tritium and TCE plumes at TAN, Martian (1999) found it necessary to include recharge mounding from the pond in his numerical model. Also included in the model was a lower permeability zone south of TSF-05. As discussed previously, there is a systematic decrease in aquifer transmissivity to the south of TSF-05 that may be associated with the Lava Ridge-Hell's Half Acre volcanic rift zone. The recharge and the localized low-permeability zone appeared to be necessary to achieve eastward movement of groundwater at TAN.

***3.1.1.6 Groundwater Chemistry.*** Groundwater at TAN is enriched in calcium and bicarbonate. The chemical composition of groundwater at TAN reflects the clastic and carbonate rocks of source areas to the north and northwest.

***3.1.1.7 Contaminant Transport.*** Information about the distribution of contaminants in SRPA water at TAN has been used to develop the present understanding about those factors that facilitate or restrict contaminant transport in the subsurface (Kaminsky et al. 1994; Sorenson et al. 1996; Martian 1999). The following sections describe the contaminant inventory, extent of contamination, and mechanisms of contaminant release and transport at TAN.

***Source Term—***At WAG-1, the contaminant source term is described in the TAN Remedial Investigation Report (Kaminsky et al. 1994). The source term includes the types and amounts of contaminants believed to have been released to the subsurface. The TSF-05 injection well is the primary source of subsurface contamination at WAG-1 (Kaminsky et al. 1994). Sorenson et al. (1996) also implicated the TSF-07 disposal pond for some radionuclide contamination reaching the aquifer. In the case of the former, the release mechanism is simply injection of contaminants directly into the aquifer, along with long-term dissolution of nonaqueous contaminants and sorption/desorption of radionuclides. The release is complicated by the presence of injected sludge, which appears to trap even aqueous contaminants such as tritium for long periods of time (Sorenson et al. 1996; Sorenson 2000). For the latter, downward migration of water pumped to the pond through the vadose zone and a perched water body have allowed contaminants to reach groundwater. The sections that follow summarize the contaminant source investigations that were conducted on six waste sites considered to be potential contributors to groundwater contamination.

***TSF-05 Injection Well (TAN-330/TSF-05)—***The TSF-05 injection well was drilled in 1953 to a depth of 310 ft to dispose of liquid effluent generated from the ANPP. Discharges to TSF-05 have included organic sludge, treated sanitary sewage, process wastewaters, and low-level radioactive waste streams. Historical records provide little definitive information on the types and volumes of organic wastes disposed via the injection well; however, TCE is identified as the primary COC. It is estimated that from as little as 350 gal to as much as 25,670 gal of TCE were disposed in the well during its period of operation.

***TSF Disposal Pond (TAN-736/TSF-07)—***The TSF disposal pond is an unlined, diked area encompassing approximately 35 acres. The TSF-07 disposal pond, constructed in 1971, has historically received wastewater containing low-level radioactive waste, and continues to receive cold process water and treated sewage effluent under a wastewater Land Application Permit. Between 1972 and 1985, approximately 0.039 Ci of Sr-90 were disposed to the pond (Kaminsky et al. 1994).

***TSF Clarifier Pits—***The three TSF clarifier pits east of TAN-604 are rectangular concrete settling basins that have a total capacity of 3,158 gal (Kaminsky et al. 1994). They are located east of TAN-604. A flow with relatively low suspended solids exited the clarifiers and ultimately entered the TSF-05 Injection Well (until 1972) or the TSF-07 Disposal Pond (after 1972).

The pits were used for settling contaminated wastewater from the maintenance and paint shops at TAN-604 from 1957 to 1985. The suspected contaminants may have included an unknown volume of chemicals from cleaners, paint thinners, and paint strippers. The pits contain approximately 7.5 to 11 in. of cohesive sludge at the bottom with 1 to 2 in. of settled wastewater on top. Sludge samples from May 1988 and June 1989 contained acetone, methylene chloride, methyl ethyl ketone, toluene, and xylene. The TSF-11 clarifier pits were also connected to the TAN sewer plant, which is connected to the TSF-05 Injection Well and TSF-07 Disposal Pond. However, the quantity of painting and cleaning chemicals that could have actually reached the injection well or the disposal pond cannot be estimated. Large amounts of these chemicals would have been lost to bacterial degradation in the pipes and sewer plant, to volatilization in the trickling filter at the sewer plant, or in the pits themselves.

***IET Injection Well TAN-332 (IET-06)—***The IET injection well was drilled to a depth of 329 ft to dispose of effluent generated at IET (Kaminsky et al. 1994). The well is located at IET, north of TSF. Although little information is available that describes the well, it is assumed that the well received process wastewater and probably sanitary sewage, as a minimum. These process wastewaters may have included acidic ion exchange regenerants, waste diesel fuels and boiler blowdown from boilers, small amounts of engine coolant or fuels from the nuclear engine tests, and possibly wastes from a photo lab.

***WRRTF Injection Well (WRRTF-05)—***The WRRTF injection well commenced operation in 1957 and was subsequently abandoned in 1984. The well is located south of WRRTF and is thought to have received cooling water effluent, sanitary waste, and materials from laboratories and process drains. Evidence also suggests that hydrazine from facility operations was disposed in the well. The WRRTF injection well is currently grouted and inaccessible for sampling.

***TSF Intermediate-Level Waste Disposal System (TSF-09)—***This radioactive liquid water system collected, processed, and provided interim storage capacity for all intermediate-level radioactive liquid waste generated at TSF (Kaminsky et al. 1994). Drains and sumps located in areas with a high potential for contamination were piped to a waste transfer facility where radioactive waste was collected in one of three underground (10,000 gal) stainless-steel collection tanks (V-1, V-2, or V-3). From 1955 to 1972, liquid waste from the collection tanks was concentrated by an evaporator and the concentrate was transferred to long-term storage tanks. The condensate from the evaporator was then sent to the TSF-05 injection well.

In the late 1950s and early 1960s the evaporator concentrate in the bottom of the storage tanks was pumped out and sent to the injection well. It is possible that the majority of the sludge taken from the injection well during a sampling event in 1990 came from these tanks, but there is no information to confirm this assumption. In 1972, the process was modified so that the original evaporator downstream of the V-1, V-2, and V-3 tanks was removed and a new evaporator installed in the storage tank area.

When filled to capacity (~20 tons), the semi-solid radioactive waste was solidified by evaporation and the container was transferred to RWMC for disposal. Distillate from the evaporator flowed to the condenser and then to a condensate storage tank. The condensate was passed through a fabrication ion-exchange column for further removal of radioactive ions. Effluent from the ion exchanger was combined with other TSF low-level radioactive liquid waste before being discharged into the TSF disposal pond.

The TSF intermediate-level waste disposal system was designed to receive and treat waste that was too radioactively contaminated to be discharged to the TSF disposal pond. Any hazardous waste chemicals reaching this system were incidental to the processing of radioactive materials. The system potentially received corrosive materials from decontamination activities. In some instances, heavy metals (particularly mercury) were received during extensive usage periods in the late 1950s and early 1960s. Also, small quantities of potassium chromate were used in decontamination solutions from 1970 to 1974.

From the 1960s to 1975, the majority of radioactive material discharged to this system was eventually disposed at RWMC. The lesser amounts of radioactivity that were discharged in the condensate to either the TSF disposal pond or TSF-05 injection well were included in the quantities discussed earlier.

***Extent of Contamination—***Disposal of wastewater to injection wells and infiltration ponds at TAN has resulted in detectable concentrations of organic and radioactive contaminants in groundwater. The following sections describe the distribution of selected contaminants in water from the vadose zone and SRPA at TAN.

***Perched Water Contamination—***Contamination in the vadose zone and perched water bodies at TAN is attributed to the TSF-07 disposal pond where water pumped to the pond has migrated through the vadose zone and perched water body to reach the aquifer. These waters include treated sewage consisting of process water and wastes from rest rooms, sinks and showers. The effluent is pumped into the infiltration pond via the TAN-655 lift station and the TAN-623 Sewage Treatment Plant. The process wastewater consists of steam condensate, water and demineralizer discharges, cooling water, and air scrubber discharges among others. The water is transported directly to the lift station where it is mixed with the treated sewage wastewater before being pumped to the infiltration pond.

A perched water body has been known to exist at the sediment-basalt interface beneath the TSF-07 Disposal Pond. Samples of the perched water collected in 1990 and 1991 detected Sr-90 in the range of 1.0 to 136.0 pCi/L (Medina 1993). The data sets resulting from these sampling efforts indicate that Sr-90 from the pond has percolated through the surficial sediments to basalt and presents a strong argument that it has impacted the aquifer. The presence of Sr-90 in aquifer wells nearest the disposal pond, and an apparent local source of aquifer recharge evidenced by a local easterly gradient shift, provide corroborating evidence that TSF-07 was at least a minor source of groundwater contamination to the aquifer.

***SRPA Contamination—***Groundwater monitoring data indicate that the SRPA underlying TAN is contaminated with VOCs (TCE, PCE, cis-DCE, and trans-DCE) and radionuclides (H-3, Sr-90, and Cs-137). Widespread concentrations above background have also been documented for chloride, nitrate, sulfate, and alkalinity (Wymore et al. 2000). The TCE plume presented in Figure 3-3 effectively envelops the areas of the aquifer impacted by these contaminants. (The PCE, H-3, chloride, and sulfate plumes extend axially downgradient near WRRTF similar to that of the TCE plume, while the cis-DCE, trans-DCE, Sr-90, nitrate, and alkalinity plumes are localized around the hotspot at the TSF.) Total dissolved solids, sulfate, sodium, and coliform have also been detected in the aquifer based on groundwater monitoring conducted in accordance with the Wastewater Land Application Permit.

***Mechanisms that Affect Containment Fate and Transport at TAN—***The primary release mechanisms of contaminants to that portion of the SRPA underlying TAN include direct aquifer injection and associated long-term dissolution of nonaqueous contaminants and sorption/desorption of radionuclides. The release is complicated by the presence of injected organic sludge, which appears to trap even aqueous contaminants such as tritium for long periods of time (Sorenson et al. 1996; Sorenson et al. 2000). Advective flow is the predominant contaminant transport mechanism.

Strong evidence points to the TSF-07 disposal pond as a source of Sr-90. Sr-90 from the pond has percolated through the surficial sediments and may be a source of aquifer contamination. Relatively high levels of Sr-90 observed in wells TAN-10A, TAN-27, and TAN-D2 (which are all screened in the top 50 ft of the aquifer) but not in well TAN-11 (which is in the vicinity of these wells but is screened 100 ft deep in the aquifer) is consistent with a surface source of contamination.

Organic sludge in the formation surrounding TSF-05 represents the residual source that continues to contaminate groundwater at TAN (Kaminsky et al. 1994). The association of gamma-emitters in the sludge provides a means for using existing wells to estimate the residual source distribution. Downhole natural gamma and gamma spectroscopy logs were performed to establish the distribution of these radionuclides and use them as indicators of sludge distribution (Bukowski and Sorenson 1998b). The gamma logging data show that the radioactivity extended as far as 115 ft northwest of TSF-05. The depths of the elevated gamma activity correlated with high porosity zones in all wells near TSF-05 based on seismic tomography data. These observations indicate that the layered geological structure resulted in preferential, sub-horizontal flow paths for the sludge to migrate away from the injection well. The geometry of the contaminant plume is characterized as a very large, relatively low concentration fringe that surrounds and emanates from a much smaller, high concentration core. Within the core is a very

small residual source area that continued to contaminate fresh (upgradient) groundwater flowing through the hotspot prior to the beginning of remediation activities in 1996. The downgradient, dissolved phase portion of the TCE plume proceeds in an east-southeast direction from the TSF-05 source area and is nearly 2 mi in length. Natural attenuation of the distal dissolved phase portion of the plume has recently been documented to be occurring (Sorenson et al. 2000; DOE-ID 2001).

In particular, the distribution of TCE at TAN exemplifies the fringe and core hypothesis for the anatomy of chlorinated solvent plumes (Cherry 1996). A small high-concentration core is surrounded by a much larger, low concentration fringe (see Figure 3-2 and 3-7). The residual source area surrounding TSF-05, which serves to contaminate fresh groundwater flowing through from upgradient, has historical concentrations in excess of 10 mg/L, but only for a distance of approximately 50 ft downgradient. The residual source of contamination is believed to be composed primarily of the sludge that was injected into the well. Some of the sludge may have TCE concentrations as high as 3%. The core defined by the 1 mg/L isopleth in the figure extends approximately 1,500 ft downgradient of TSF-05 and is estimated to be about 300 ft wide. The low concentration fringe, in contrast, extends more than 1.4 mi beyond the core and is about 0.93 mi wide. The spatial scales of the residual source area, the core, and the fringe dictate the hydrogeologic scales that must be considered in the conceptual model for contaminant transport at TAN.

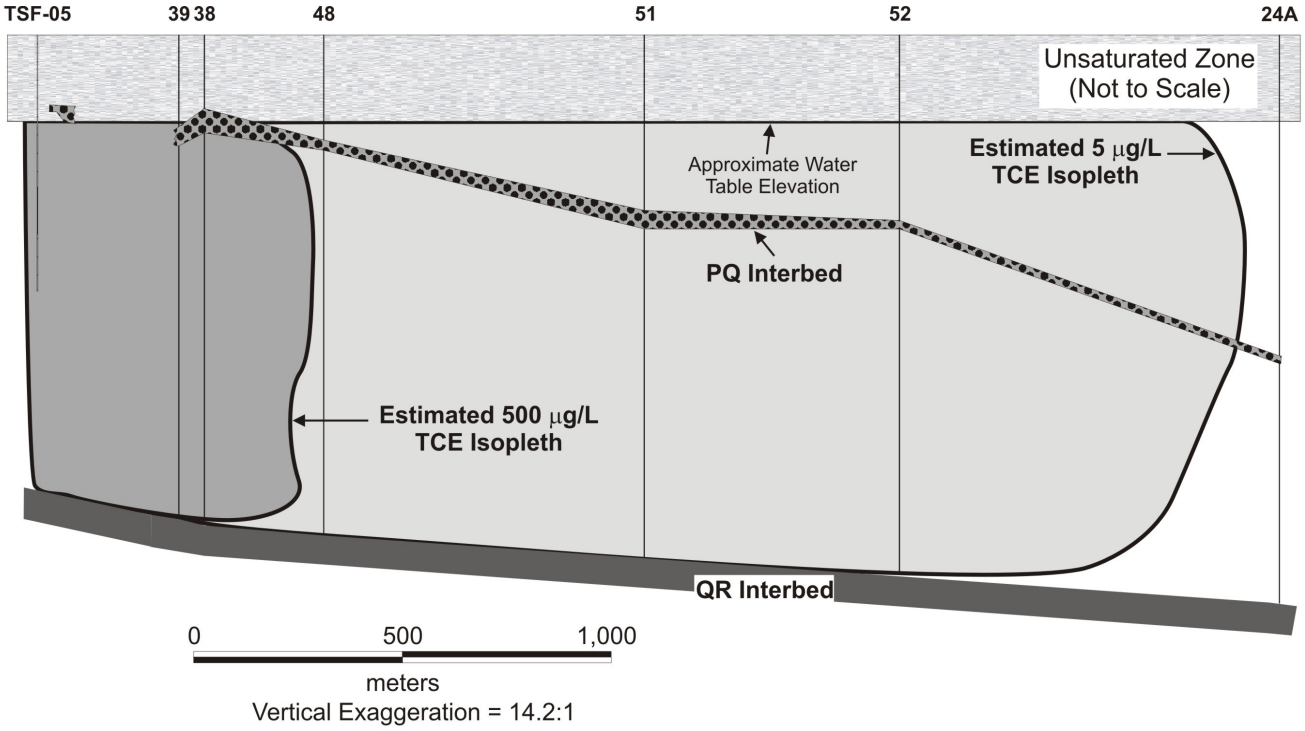


Figure 3-7. Conceptual model cross-section at the scale of the TCE plume fringe.

The TSF-05 contamination TAN is currently impacted by ongoing remediation activities that are focused on three plume zones (i.e., the hot spot, medial zone, and distal zone). The "hot spot" zone is the area immediately surrounding the TSF-05 injection well where TCE concentrations historically exceeded 20,000 parts per billion (ppb); the "medial zone" encompasses the areas where TCE concentrations have occurred between 1,000 and 20,000 ppb; and the "distal zone" is the portion of the plume where TCE concentrations are in the range of 5 to1,000 ppb. The selected remediation strategy for the TSF-05 "hot spot" is in situ bioremediation (ISB), which involves injecting sodium lactate as an electron donor amendment into the contaminant source area to stimulate indigenous bacteria to dechlorinate contaminants in the groundwater. The downgradient, dissolved phase portion of the medial zone of the plume is being treated through air-stripping technology with the recently constructed NPTF. The distal zone remedial strategy is monitored natural attenuation (MNA), which allows for the natural reduction of volume, toxicity, and mobility of contaminants without human intervention. Ongoing groundwater remediation activities at TAN result in a dynamic conceptual model of the contaminant distribution, fate, and transport.

All of the contaminants originate from the TSF-05 injection well with the exception of some Sr-90 from the TSF-07 disposal pond. These contaminants are associated with, and to some degree trapped in, the sludge that remains around the injection well (Kaminsky et al. 1994; Sorenson 2000). Within this residual source area, the small effective porosity (0.05 to 0.1%) is attributed to the sludge. Further downgradient, the effective porosity increases to a range of 1 to 3% based on inverse modeling of transient pumping response and contaminant distributions.

Radionuclides with long half-lives, including Cs-137, U-234, and a few other very low concentration radionuclides present at TAN, appear to sorb very strongly to the basalt and perhaps to the sludge around TSF-05. The only well in which these radionuclides have been detected in groundwater above drinking water standards is TSF-05 (Sorenson et al. 1996). As mentioned earlier, gamma spectroscopy has indicated that minor detectable concentrations of Cs-137 and Co-60 are present approximately 115 ft from TSF-05. Tritium, on the other hand, is not sorbed at all and is detected in nearly the same area as is TCE. Because of this, tritium makes a good conservative tracer for groundwater movement when its radioactive decay is taken into account. Sr-90 is intermediate between H-3 and the long-lived radionuclides in terms of sorption. Historically, Sr-90 has been detected as far downgradient from TSF-05 as USGS-24, but in the last several years, concentrations above the drinking water standard of 8 pCi/L have been confined to within about 600 ft of TSF-05 (Wymore et al. 2000). Because the distribution of long-lived radionuclides is so limited at TAN, and because the risk driver for WAG-1 is TCE, no effort has been made to determine actual sorption coefficients.

In the case of Sr-90, another mechanism that may affect transport is substitution into the crystal structure of calcite. While this mechanism has not been studied extensively at TAN, an ongoing research project at the INEEL, funded by the Environmental Management Science Program, is looking to induct the process as a potential remediation strategy for Sr-90. During enhanced ISB in the residual source area at TAN, it was noted that Sr-90 increased significantly in wells near TSF-05 along with calcium and magnesium, but that all of these cations quickly returned to baseline levels based on downgradient monitoring well data (Sorenson et al. 2000). The significance of this mechanism is not currently well understood.

The processes affecting fate of the chlorinated ethene compounds at TAN are quite different from those for the radionuclides. Sorption is not believed to be significant for these compounds based on experiments with TCE and basalt (Ingram et al. 1998). Biological degradation, however, impacts these contaminants significantly. Prior to the start of remediation activities, it was found that the organic material in the sludge had stimulated a process known as reductive dechlorination within about 250 ft of TSF-05 (Sorenson et al. 2000). This process allows chlorinated ethenes to be sequentially dechlorinated

to ethene when the process goes to completion (Freedman and Gossett, 1989); however, it was only observed to proceed as far as dichloroethene in the field. Based on the success of laboratory studies, a field evaluation to further stimulate this process was conducted and successful transformation of TCE to ethene was achieved in the field. This process has now been incorporated into the long-term remediation of the site (DOE-ID 2001).

Downgradient of the residual source area, insufficient carbon was present to drive reductive dechlorination and the system is quite oxygenated. In spite of this, it was found that concentrations of TCE were decreasing relative to those of PCE and tritium in the plume (Sorenson et al. 2000). This rate of decrease was quantified as a pseudo-first order process yielding a half-life for TCE between 9 and 22 years, depending on the assumptions used. It was hypothesized that aerobic cometabolism of TCE is occurring in the plume in spite of the oligotrophic conditions of the aquifer. Several factors were identified that corroborate this hypothesis, including laboratory studies demonstrating that bacteria capable of the process are present in the plume, the dissolved oxygen distribution, and the relative behavior of TCE and PCE (DOE-ID 2000). Based on these findings, monitored natural attenuation was incorporated into the long-term remediation strategy for the dissolved contaminant plume (DOE-ID 2001).

### 3.1.2 Numerical Analyses Performed to Date

Numerical analyses have been conducted to support remedial investigations at TAN as described in the following reports:

- **Kamininsky et al. 1994, TAN Groundwater RI/FS Contaminant Fate and Transport Modeling**

  The primary focus of the numerical simulations was to obtain future groundwater concentrations in the years 2024, 2040, and 2094 to support the Baseline Risk Assessment for the TAN groundwater OU. Groundwater modeling of the contaminants cis-1,2-DCE, trans-1,2-DCE, TCE, tritium, and Sr-90 conservatively assumed a constant fixed mass source in the TSF-05 injection well equal to sampling results obtained in 1992. The scope of the modeling study included base-case predictions of flow and contaminant movement. In addition, the sensitivity of predicted contaminant migration to the parameters used to implement the conceptual model was obtained. The sensitivity analysis was provided to illustrate the possible range of various predicted measures of contaminant transport given the uncertainty in the input estimates of physical properties describing the flow and transport domain. The simulations were found to be relatively insensitive to dispersivity. The sensitivity study showed that the primary parameter determining the fate of COC in the TAN groundwater system was the fixed source concentration assumed at the TSF-05 injection well.

- **Bukowski and Sorenson 1998a, Preliminary Numerical Modeling of TAN Hotspot**

  A numerical model of the area surrounding the TAN hotspot was developed to assist in characterizing the aquifer in the vicinity of TSF-05. The objective of the modeling was to provide data for use in the design of remedial activities, treatability studies, and other hydrogeologic studies. The model was intended to satisfy previously identified data gaps including the influence of pumping wells, horizontal heterogeneity, and vertical heterogeneity.

The Sandia waste isolation flow and transport (SWIFT) computer code was used to create a six-layer, three-dimensional, heterogeneous numerical model of the aquifer in the vicinity of well TSF-05. In order to obtain a reliable numerical tool for decision making, it was necessary to calibrate the model to reflect actual site conditions. Inverse modeling of three pumping tests has been use to perform the calibration. The three pumping tests included the first 2 hours of the continuous operations test conducted in April 1996, which included the pumping of TSF-05 only, the TAN-31 pumping test conducted in 1995, and the TAN-25 pumping test conducted in 1996. The calibration parameters for this model included porosity (which varies spatially) and the three-dimensional distribution of both horizontal and vertical hydraulic conductivity.

Inverse modeling of three different aquifer tests in the vicinity of TSF-05 was conducted in order to calibrate the hydraulic conductivity distribution and porosity within the model. Each aquifer test produced a conductivity distribution that provided a fit to the observed data, meeting the calibration target. For purposes of predictive modeling, it is desirable to have a single distribution that adequately captures all available data. The distribution obtained from the TAN-25 test inverse modeling was the best of the three at simulating all aquifer tests; however, it was not satisfactory at reproducing the results observed in the TAN-31 test. One explanation for this is that the aquifer responds differently to stress depending on where the stress is located because of the network of interflow zones and fractures. Another factor that plays a significant role is the non-unique nature of inverse modeling. While it might be possible with time to find a distribution that reconciles the results of the two tests, it is not practical. For this reason, both the TAN-25 hydraulic conductivity distribution and the TAN-31 distribution were retained for predictive modeling.

- **Martian 1999, Numerical Modeling Support of the Natural Attenuation Field Evaluation**

The modeling objective was to assess the mechanisms of natural attenuation (dispersion, sorption, and biodegradation). The petroleum engineering/geothermal simulator TETRAD was used to develop a numerical model for supporting the MNA remedial alternative. Tritium disposal and aquifer concentration records were used to calibrate model dispersivity and porosity. Because no TCE disposal history exists, the TCE source term was calibrated to current TCE concentrations by separating the TCE source term into two parts representing an initial and residual rate. This was performed to simulate the operational period of the well (initial rate) and the continuing source of TCE to the aquifer from dissolution, desorption, and diffusion of TCE from the sludge surround the TSF-05 injection well.

The TCE calibration revealed that the overall extent of the TCE plume could be matched either with our without including first-order degradation of TCE depending on the magnitude of the source term used. Without TCE degradation, a much larger residual source was required to achieve the observed TCE plume extent, resulting in high predicted concentrations of TCE in the upgradient portion of the dissolved plume.

When TCE degradation was included, however, a large initial source was used with a much smaller residual source to achieve the overall plume extent. A case with a TCE degradation half-life of 11 years provided a much better match to the observed TCE distribution within the plume than the case with no TCE degradation.

Sensitivity studies for both the tritium transport and TCE source term calibration were performed. The tritium transport calibration was most sensitive to the volume of water co-

injected with the waste in the TSF-05 injection well. The TCE source term calibration was most sensitive to the distribution of the initial source term. Both calibrated TCE simulations suggest that the TCE plume near TSF is receding or reaching a steady-state condition while the plume near WRRTF will continue to grow and concentrations will increase slowly over the next few decades.

A series of predictive simulations were also performed with the calibrated model to quantify the portion of the current TCE plume that must undergo remediation in order to meet the MCL after 100 years of advection, dispersion, and degradation. The results of these simulations indicate that advection and dispersion alone would only act as a remedial option for portions of the plume less than approximately 50 ug/L. However, if the half-life of TCE in the aerobic portion of the plume is 20 years or less, natural attenuation is a viable alternative for remediating the entire dissolved-phase portion of the TCE plume. As described above, a half-life for TCE of 11 years provided a good fit to the observed data.

- **Arnett 2002, TAN OU 1-07B ISB Groundwater Model Development and Initial Performance Simulation**

  Distribution of the electron donor was observed during ISB field evaluation phase to be a critical parameter for effectively implementing ISB at the OU 1-07B hot spot. Virtually all locations that received an adequate supply of the electron donor showed complete dechlorination of chloroethenes to ethane. Electron donor distribution using chemical oxygen demand (COD) as a surrogate was therefore selected as a single parameter that could be numerically modeled for various injection scenarios to predict the resulting extent of anaerobic reductive dechlorination (ARD) in the aquifer.

  The purpose of this modeling effort was to develop a groundwater model capable of adequately simulating the transport and distribution of injected electron donor within the OU 1-07B hotspot and to apply the model to assist in the design of an optimum injection strategy. The overall hotspot remediation strategy is to distribute the electron donor throughout the residual source area. The model was used to test two injection scenarios to assist in determining the most cost-effective remediation strategy. The scenario evaluation suggests that injecting a more dilute, almost double volume lactate solution would result in a donor distribution similar to that resulting from higher lactate concentrations in previous injections. Injection into two widely separate wells provides a better distribution of the electron donor across the hotspot than injection into well TSF-05 alone.

- **Whitmire and Bates 2002, NPTF Performance Simulation**

  A groundwater flow model was constructed to assess the effectiveness of the NPTF in capturing the medial zone of a TCE groundwater plume at the INEEL TAN facility. The groundwater flow model was constructed using the MODFLOW 1996 code in the DOD groundwater modeling system environment. Several simulations were run, including steady-state ambient and steady-state pumping flow field scenarios.

  Groundwater altitude data, representative of long-term local trends and hydraulic conductivity information, were used to determine parameters of the ambient and pumping flow field simulations. Observations of the drawdown in wells surrounding the extraction wells during several pre-startup test pumping scenarios were compared with model drawdown predictions to calibrate the flow model and to evaluate the size of the

groundwater capture zones induced by the pumping wells. The magnitude and distribution of hydraulic conductivity was adjusted until simulated and observed heads adequately matched.

Particle tracking was performed using the GMS/MODPATH package for a variety of scenarios including single and multiple pumping wells. The model will be used as a tool to estimate the size of groundwater capture zones during the operation of the pump-and-treat system. The model can further be used for system optimization to evaluate the potential effectiveness of future extraction/injection scenarios without the need to actually conduct pumping tests.

### 3.1.3 Summary of Key Conceptual Model Elements

- The transmissivity of the aquifer in the vicinity of TAN appears to be lower than much of the INEEL, mostly ranging from a few hundred or less to about 31,000 $ft^2$/day. Values as high as 500,000 $ft^2$/day have been measured, however, indicating that transmissivity is not uniformly less than the INEEL average.

- The regional hydraulic gradient is southerly and relatively flat at about 0.0002 ft/ft. Near TSF, however, an easterly gradient has been measured consistent with initial eastward migration of the contaminant plume. East of TSF, flow turns toward the south, consistent with the regional gradient.

- At least four factors have been identified that may contribute to the flow direction near TSF, but the relative significance of each has not been determined. They are: the regional, southerly gradient; the influence of the production wells, TAN-1 and TAN-2; recharge from the TSF-07 disposal pond; and a potential low permeability zone to the south of TSF.

- Two sedimentary interbeds appear to be very important for WAG-1. The QR interbed appears to be laterally continuous, isolating the upper 200 to 300 ft of the aquifer from the deeper aquifer. The PQ interbed is discontinuous, but has large enough continuous areas to cause locally confining conditions, and possibly impact contaminant transport.

- The effective porosity based on several analyses appears to be in the range of 1 to 3% in most of the area, but has been substantially reduced in the vicinity of TSF-05 due to the injected sludge.

- The groundwater velocity appears to increase from about 0.16 ft/day near TSF-05 to about 0.5 ft/day for most of the area.

- Dispersivity values on the order of 10 ft have been sufficient to match observed contaminant distributions.

- The primary source of contamination is the TSF-05 injection well. The sludge still remaining in the vicinity of the well acts as an ongoing, secondary source of contamination.

- Sorption has severely limited the transport of all radionuclides except tritium, which has the shortest half-life and is present only in concentrations below the drinking water standard.

- Anaerobic biodegradation is an important process impacting the fate of volatile organic compounds near TSF-05, but the downgradient aquifer is quite aerobic. TCE degradation appears to be occurring even in the aerobic aquifer, and has been attributed to a cometabolic process, but further work is needed to demonstrate the occurrence of the process directly.

### 3.1.4 References


Ackerman, D.J. 1991. Transmissivity of the Snake River Plain Aquifer at the Idaho National Engineering Laboratory, Idaho. U.S. Geological Survey Water-Resource Investigations Report 91-4058.

Anderson, S.R. and B. Bowers. 1995. Stratigraphy of the Unsaturated Zone and Uppermost Part of the Snake River Plain Aquifer at Test Area North, Idaho National Engineering Laboratory, Idaho. U.S. Geological Survey Water-Resources Investigations Report 95-4130.

Arnett, R, 2002, Test Area North Operable Unit 1-07B In Situ Bioremediation Groundwater Model Development and Initial Performance Simulation, INEEL/EXT-02-00560, Idaho National Engineering and Environmental Laboratory, Idaho Falls, Idaho.

Bukowski, J.M. and K.S. Sorenson. 1998a. Site Conceptual Model: 1996 Activities, Data Analysis, and Interpretation – Test Area North Operable Unit 1-07B. Prepared for the U.S. Department of Energy Idaho Operations Office, INEL/EXT-97-00556.

Bukowski, J.M. and K.S. Sorenson. 1998b. Well Characterization and Evaluation Report Supporting Functional and Operational Requirements for the New Pump and Treat Facility at Test Area North Operable Unit 1-07B. Prepared for the U.S. Department of Energy Idaho Operations Office, INEEL/EXT-97-01356.

Bukowski, J.M. and R.P Wells. 1999. Fiscal Year 1998 Groundwater Monitoring Annual Report Test Area North Operable Unit 1-07B. Prepared for the U.S. Department of Energy Idaho Operations Office, INEEL/EXT-99-00011.

Bukowski, J.M., H. Bullock, and E.R. Neher. 1998. Site Conceptual Model: 1997 Activities, Data Analysis, and Interpretation for Test Area North, Operable Unit 1-07B. Prepared for the U.S. Department of Energy Idaho Operations Office, INEEL/EXT-98-00575.

Cherry, J.A. 1996. "Conceptual Models for Chlorinated Solvent Plumes and Their Relevance for Intrinsic Remediation." In: Symposium on Natural Attenuation of Chlorinated Organics in Ground Water, pp. 29-30. Office of Research and Development, U.S. Environmental Protection Agency, Washington, DC, EPA/540/R-96/509.

DOE-ID, 2000, *Field Demonstration Report, Test Area North Final Groundwater Remediation,* Operable *Unit 1-07B*), DOE/ID-10718, 2000.

DOE-ID, 2001, *Record of Decision Amendment. Technical Support Facility Injection Well (TSF-05) and Surrounding Groundwater Contamination (TSF-23) and Miscellaneous No Action Sites, Final Remedial Action Idaho national Engineering and Environmental Laboratory, Idaho Falls, Idaho),* DOE/ID-10139 Amendment, 2001.

Freedman, D.L., and J.M. Gossett. 1989. "Biological Reductive Dechlorination of Tetrachloroethylene and Trichloroethylene to Ethylene Under Methanogenic Conditions." Applied Environmental Microbiology. 55:2144-2151.

Ingram, J.C., G.S. Groenewold, M.M. Cortez, D.L. Bates, M.O. McCurry, S.C. Ringwald, and J.E. Pemberton. 1998. "Surface Chemistry of Basalt and Related Minerals." In: Proceedings of

the 46th American Society for Mass Spectrometry Conference, pp. 1167. May 31-June 4, Orlando, Florida.

Kaminsky, J., K.N. Keck, A.L. Schafer-Perini, C.F. Hersley, R.P. Smith, G.J. Stormberg, and A.H. Wylie. 1994. Remedial Investigation Final Report with Addenda for the Test Area North Groundwater Operable Unit 1-07B at the Idaho National Engineering Laboratory. Prepared for the U.S. Department of Energy, EGG-ER-10643.

Lanphere, M.A., M.A. Kuntz, and D.E. Champion. 1994. Petrography, Age, and Paleomagnetism of Basaltic Lava Flows in Coreholes at Test Area North (TAN), Idaho National Engineering Laboratory. U.S. Geological Survey Open-File Report 94-686.

Lohman, S. W., 1972, Ground-water Hydraulics, Professional Paper 708, U.S. Geological Survey.

Martian, P., 1999, Numerical Modeling Support of the Natural Attenuation Field Evaluation for Trichloroethene at Test Area North, Operable Unit 1-07B, Idaho National Engineering and Environmental Laboratory, INEEL/EXT-97-01284, Rev. 1, Idaho National Engineering and Environmental Laboratory, Prepared for the U.S. Department of Energy Idaho Operations Office, Idaho Falls, Idaho.

Medina, S.M. 1993. Evaluation of Historical and Analytical Data on the TAN TSF-07 Disposal Pond. Prepared for the U.S. Department of Energy Idaho Operations Office, EGG-ERD-10422.

Rodriguez, R. R, A.L. Shafer, J. M. McCarthy, P. Martian, C. E. Burns, D. E. Raunig, N. A.. Burch, and R. L. Vanhorn, 1997, *Comprehensive RI/FS for the ICPP OU 3-13 at the INEEL RI/BRA Report*, DOE-ID-10534, Revision 0.

Schafer-Perini, A.L., 1993, Test Area North Groundwater Remedial Investigation/Feasibility Study Contaminant Fate and Transport Modeling Results, ER WAG1-21, Idaho National Engineering and Environmental Laboratory, EG&G Idaho, Inc., Idaho Falls, Idaho.

Sorenson, K. S., 2000. Intrinsic and Enhanced In Situ Biodegradation of Trichloroethene in a Deep, Fractured Basalt Aquifer. Ph.D. Dissertation, University of Idaho.

Sorenson, K. S., L. N. Peterson, R. E. Hinchee, and R. L. Ely, 2000. "An Evaluation of Aerobic Trichloroethene Attenuation Using First-Order Rate Estimation." Bioremediation Journal, 4(4):337-357.

Sorenson, K.S. and P. Schwind, 1996, Preliminary Numerical Modeling Results for the TAN Hotspot, J.D. Dustin Letter Report, 25:01:081-96, Parsons Engineering Science, Inc., Idaho Falls, Idaho.

Sorenson, K.S., A.H. Wylie, and T.R. Wood. 1996. Test Area North Site Conceptual Model and Proposed Hydrogeologic Studies Operable Unit 1-07B. Prepared for the U.S. Department of Energy Idaho Operations Office, INEL-96/0105.

Sorenson, K.S., J.P. Martin, H. Bullock, 2000, Field Evaluation Report of Enhanced In Situ Bioremediation, Test Area North, Operable Unit 1-07B, INEEL/EXT-2000-00258, Rev. 0.

Whitehead, R.L. 1992. Geohydrologic Framework of the Snake River Plain Regional Aquifer System, Idaho and Eastern Oregon, 32 pp. U.S. Geological Survey Professional Paper 1408-B.

Whitmire, D.L. and D.L. Bates, 2002, "Summary of Development and Calibration of a Steady-State Groundwater Flow Model Used to Determine the Capture Efficiency of the New Pump and Treat System at Test Area North, Operable Unit 1-07B (Draft)," INEEL/EXT-02-00661, Rev. B, Idaho National Engineering and Environmental Laboratory, North Wind Environmental Inc., Idaho Falls, Idaho.

Wymore, R. A., J. M. Bukowski, K. S. Sorenson, Jr., 2000, *Site Conceptual Model: 1998 and 1999 Activities, Data Analysis, and Interpretation for Test Area North Operable Unit 1-07B*, INEEL/EXT-2000-00188, Revision 0.

## 3.2 Waste Area Group 2

WAG 2 is the designation for the collection of 13 CERCLA OUs associated with the TRA. The TRA, built in the 1950s, is located in the south-central portion of the INEEL in the relatively flat-lying Big Lost River flood plain (see Figure 3-8). The primary mission for TRA has been to house high neutron flux nuclear reactors, and to test the effects of radiation on materials, fuels, and equipment. Currently, the only active reactor at TRA is the Advanced Test Reactor (ATR; 1967-present). In the past, TRA has housed the Materials Test Reactor (MTR; 1952-1970) and the Engineering Test Reactor (ETR; 1957-1982).

The purpose of this section is to provide a summary of the conceptual model for groundwater flow and contaminant transport at WAG 2. No original hydrogeologic interpretations are presented in this section. Rather, only the technical components that contribute to the development of the site conceptual model are presented. In addition, an index of all known WAG 2 hydrogeologic investigations is provided. The conceptual model is discussed in general terms in Section 3.2.2, followed by detailed discussions of hydrologic information in subsequent sections. Factors affecting contaminant transport are presented in Section 3.2.2.7, which, although it is not an exhaustive discussion of contaminant transport, presents several of the key factors currently under investigation. A history and comparison of the numerical models developed for WAG 2 is presented in Section 3.2.3. Finally, a brief discussion of ongoing conceptual model competing hypotheses is found in Section 3.2.4.

### 3.2.1 Background

Past and current research activities at TRA have produced chemical and radioactive wastes that underwent extraction and treatment, but still contained low levels of radioactivity and chemical solutions that required disposal. Liquid wastes were initially segregated into two streams. One waste stream was composed of sanitary waste and the other contained a mixture of low-level radioactive and chemical wastes. Subsequent segregation of wastes has taken place over the years. In the past, these wastes were disposed at various locations at TRA including the disposal well, the Warm Waste Pond (WWP), the Cold Waste Pond (CWP), the Chemical Waste Pond (CP), the Sewage Leach Pond (SLP), and the Retention Basin. Several releases of hazardous and radiological constituents have been associated with miscellaneous spills and leaking underground storage tanks (LUSTs).

In 1991, TRA facilities were designated as WAG 2 under the FFA/CO. This agreement established the procedural framework and schedule for CERCLA, RCRA, and Hazardous Waste Management Act (HWMA) response actions. The 1991 FFA/CO designated TRA into 13 OUs to be addressed through the CERCLA process. A total of 51 potential release sites comprise the 13 action OUs and one “no action” OU, and include a waste-water injection well, wastewater structures and settling ponds, LUSTs, rubble piles, cooling towers, french drains, and numerous spills. Contaminants of potential concern (COPCs) at TRA include petroleum products, acids, bases, polychlorinated biphenyls (PCBs), heavy metals, and radionuclides.

Numerous geohydrologic studies have been conducted in conjunction with remediation activities at TRA. Other studies have been conducted as part of the sitewide characterization of flow and transport. These studies have provided understanding of the elements of the conceptual model at TRA.

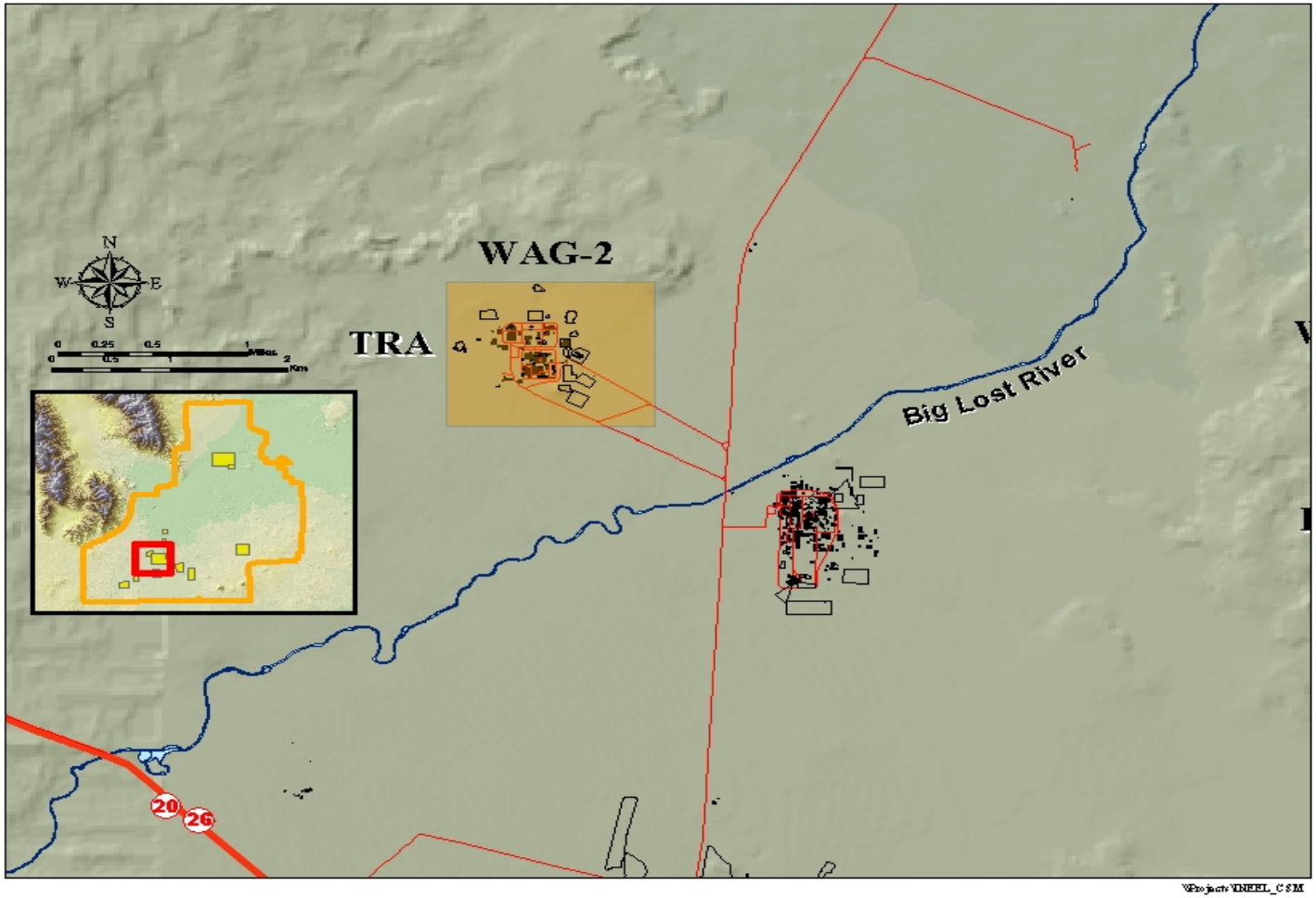


Figure 3-8. Location of TRA.

The Department of Energy-Idaho Operations Office (DOE-ID) conducted a comprehensive Remedial Investigation/Feasibility Study (RI/FS) in accordance with the FFA/CO (Burns et al. 1997). The purpose of the remedial investigation was to merge all previous WAG 2 investigations and thoroughly investigate sites not yet assessed in order to provide an accurate evaluation of the overall risk posed by WAG 2. The objectives of the RI/FS included identification and resolution of remaining data gaps, determination of nature and extent of contamination, determination of site-specific transport properties through review of past activities and additional field studies, determination of current and future cumulative and comprehensive risk to human health and the environment, develop and evaluate candidate remediation technologies, and develop and evaluate appropriate remedial alternatives based on the nine CERCLA criteria. The first four objectives were addressed in the RI/Baseline Risk Assessment (BRA) sections of the RI/FS, while the latter two were addressed in the feasibility study sections of the RI/FS (Burns et al. 1997).

### 3.2.2 Summary of the Present WAG-2 Conceptual Site Model

The present conceptual model of groundwater flow and transport at TRA is based on years of study—culminating in the RI/FS (Burns et al. 1997). In general, the geohydrologic framework at TRA is comprised of a complex intermingling of pahoehoe basalt flows and sedimentary deposits. Several sources of contamination exist at TRA, including a wastewater injection well, several disposal ponds, various spills, leaking pipes, and storage tanks. The following sections summarize the components of the conceptual model, including the geologic framework, matrix characteristics, sources of recharge and discharge, the hydraulics of the resultant flow field, chemistry of groundwater, and contaminant transport.

***3.2.2.1 Geologic Framework.*** The basalts and sediments that comprise the thick vadose zone and SRPA beneath TRA provide the geologic framework within which water and contaminants move in the subsurface. This geologic framework is defined by its geometry, stratigraphy, and structure.

***System Geometry—***TRA is located about 8 mi east of the Lost River Range promontory. The land surface at TRA is gently sloped to the southwest and is relatively flat, with elevations ranging from 4,945 ft on top of a rubble pile in the CWP to 4,908 ft at the bottom of the CP. The area within the double security fence at TRA is about 1,700 by 1,900 ft (approximately 70 acres). However, features pertinent to contaminant transport at TRA lie outside of this boundary. These features include the NSA, the WWP, the CWP, the CP, the SLP, and the SRPA. In total, the area of concern in regards to contamination associated with TRA encompasses approximately 100 acres.

The vadose zone at TRA is approximately 450 ft thick. The effective thickness of the SRPA, in the context of contamination migrating at TRA, is assumed to be approximately 250 ft thick.

This section will describe the physical dimensions of the area of interest around the TRA. Within the vadose zone, this area of interest includes the volume of basalt and sediments containing perched groundwater. In the SRPA, the area of interest includes known distributions of contaminants in groundwater.

Geology—TRA is located on the thick deposits of alluvial gravels associated with the relatively flat floodplain of the Big Lost River. This floodplain overlies the eastern Snake River basalt plain (Greeley 1982), formed by eruption of basalts from low shield volcanoes and vents. Overlapping flows and intercalated sedimentary deposits produced the complex stratigraphy underlying TRA.

Geologic features adjacent to TRA include a series of volcanic rift zones, rhyolite domes, and other eruptive features (Anderson 1991). The Arco volcanic rift zone extends southeast across the southwestern part of the INEEL. The axial volcanic rift zone extends southwest across the southeastern part of the

INEEL. The Lava Ridge volcanic rift zone extends southeast across the northern part of the INEEL. A series of rhyolite domes occur to the south. The AEC Butte is an eruptive feature in the TRA vicinity that was the source for an areally extensive, thick basalt unit. Due to the flat-lying character of the basalts and associated sedimentary units, it is concluded that no tectonic activity occurred in the immediate vicinity of TRA.

***3.2.2.2 Stratigraphy/Lithology.*** The stratigraphy at WAG 2 consists of a complex stack of pahoehoe basalt flows intercalated with sedimentary deposits above a rhyolitic basement. The upper portion of the basalt-sediment stack is capped with a thick section of surficial alluvial/fluvial deposits.

The manner in which fluids move through the vadose zone and aquifer is controlled by the nature of the media that comprise the vadose zone and aquifer. The purpose of this section is to discuss the stratigraphy and lithology of the unsaturated zone and aquifer beneath the TRA facility.

***Surficial Alluvium—***The surficial alluvial deposits are unconsolidated coarse-grained sediments laid down by the fluvial action of the nearby Big Lost River. These deposits (chiefly, sands and gravels) rest atop an undulating, massive basalt flow group; hence, the thickness of these deposits varies throughout the WAG 2 area. The lower portion of the surficial deposits appears consists of finer grained sediments that apparently collected in depressions in the basalt flows. In general, the thickness ranges from about 32 ft in the northwest section of the site to about 55 ft to the south of TRA, with a mean thickness of 49 ft (Anderson 1991).

***Basalt Flows—***Beneath the surficial alluvium at TRA lies a thick sequence of basalt flows and sedimentary interbeds. The basalt stratigraphy at TRA has been determined by thorough evaluation of cores and cuttings, and by correlation of geophysical logs from over 70 wells completed in the eastern SRPA (see Figure 3-9). A total of 17 basalt flow groups were identified, along with at least 8 sedimentary interbeds. These flow groups were designated BC through I, based on relative age. The basalt flows increase in thickness and decrease in hydraulic conductivity with depth. This decrease can be partially attributed to decreased interflow rubble zones and to mineralization within fractures and other porous regions of the flows.

The uppermost collection of basalt flow groups is about 160 ft thick, where the basalt flows are interrupted by a 50-ft thick sedimentary interbed, which acts as a barrier to groundwater flow and is discussed further in the next section. Another significant sedimentary interbed is encountered in well USGS-65 at about 500 ft bls and may play a large part in explaining the anomalously high chromium concentrations. The sequence of basalt flows and sedimentary deposits continues to 2,000 to 3,000 ft bls.

***Sedimentary Interbeds—***As stated earlier in this chapter, at least eight sedimentary interbeds have been identified at TRA. However, this discussion will focus on delineating those that have the greatest effect on contaminant transport at the facility. The only sedimentary interbed that has a significant presence and impact on movement of fluids in the subsurface occurs above the DE-4 basalt flow group at an approximate depth of 140 to 200 ft. The thickness of the sedimentary interbed is approximately 60 ft. This interbed has been encountered in 14 of 17 wells that were drilled in the area.

***3.2.2.3 Matrix Characteristics.*** The hydraulic properties of surficial sediments, basalts, and sedimentary interbeds at the TRA control the distribution of flow and contaminants in the vadose zone and SRPA. These properties (i.e., transmissivity and storage coefficient) define the capability of saturated and unsaturated rocks to transmit and store water.

***Vadose Zone—***The vadose zone is approximately 450 ft thick at TRA. Hydraulic properties of the thick, surficial sediments, sedimentary interbeds, and basalt flows of the vadose zone have been determined from aquifer-test data and laboratory analyses.

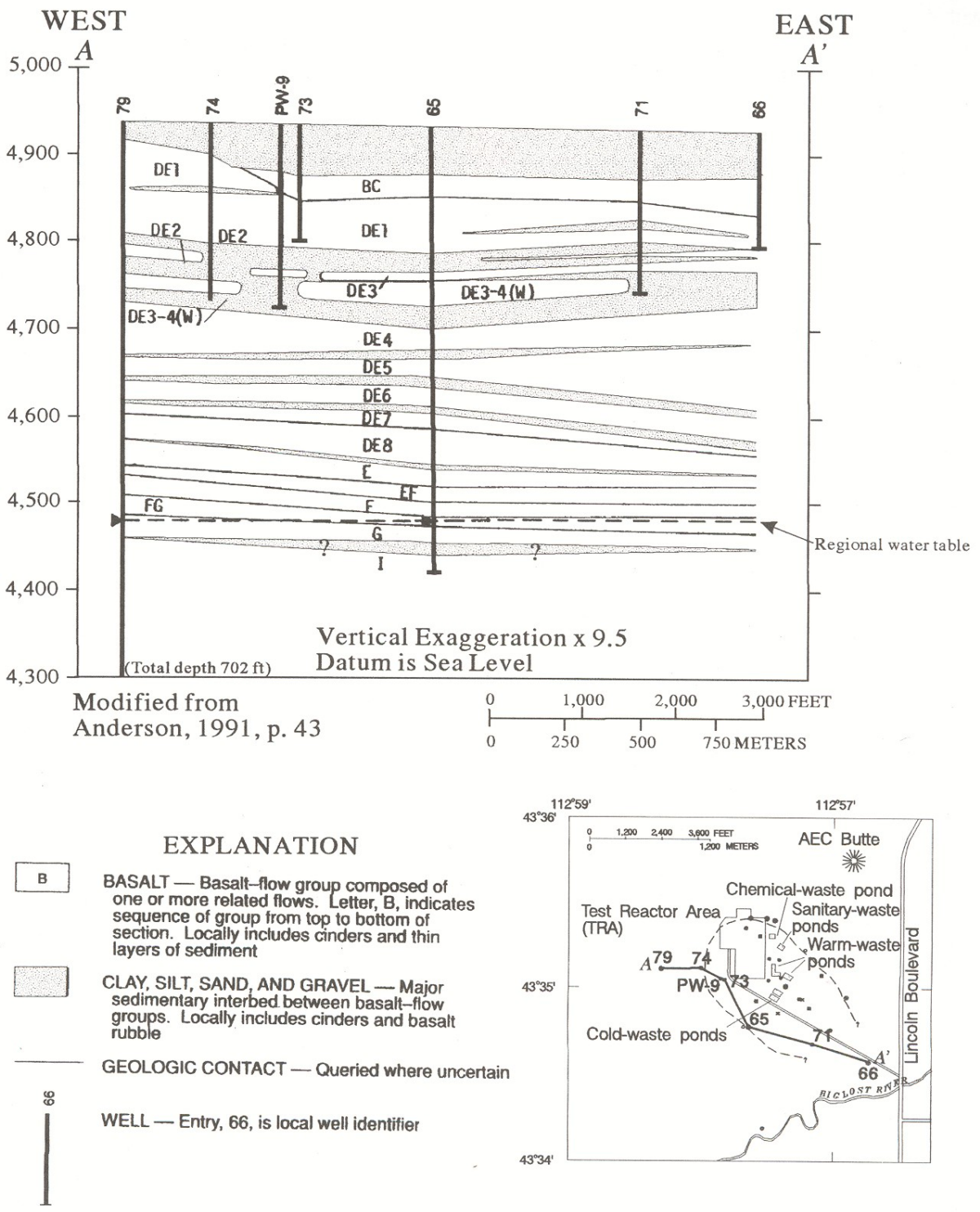


Figure 3-9. Stratigraphy of the vadose zone and upper SRPA at TRA (from Orr 1999).

***Surficial Sediments—***The upper portion of the unsaturated zone at WAG 2 consists primarily of coarse-grained fluvial deposits laid down by the Big Lost River. A total of 65 surficial alluvial samples were analyzed for grain size distribution. The mean percent weight of gravel fraction (>4.75 mm in diameter) was 49.2%, the sand fraction (0.075-4.74 mm in diameter) was 42.3%, and silt-clay fraction (0.005-0.074 mm in diameter) was 8.51%. The thickness of these deposits ranges from about 32 to 55 ft. The deposits are thickest to the south of TRA, and are thinner in the northwest. Finer-grained deposits collected in basalt depressions at the base of the alluvium. The alluvial gravels underlying TRA are very permeable, and the ability to store and transmit surface water to the subsurface within TRA is influenced by anthropogenic features such as buildings and tanks, roads, impermeable liners, and ditches. These features may serve to amplify infiltration rates by locally concentrating runoff and reducing evaporation. The total porosity for these sediments ranged from 15 to 45.4% and gravimetric water contents ranged from 2.1 to 32.6%. Hydraulic conductivity measurements ranged from $1.28 \times 10^{-5}$ ft/day to 59.5 ft/day (Doornbos et al. 1991). Robertson (1977) reported values of hydraulic conductivity ranging from 0.13 to 1,340 ft/day.

***Vadose Zone Interbed Sediments—***Core samples were collected from the basalt-interbed sequence at 140 to 200 ft bls at TRA (Doornbos et al. 1991). Grain size analysis of 28 core samples indicated a mean bulk clay content of 21.36%, a mean silt content of 38.6%, a sand content of 37.7%, and a gravel content of 0.9%. Clay content ranged from 2.2 to 55.6%, silt content ranged from 5.8 to 69.2%, sand content ranged from 0.9 to 87.5%, and gravel ranged from 0 to 10.1%. Total porosities for these sediments ranged from 20.4 to 54.8%. Laboratory-measured hydraulic conductivity measurements ranged from $4.82 \times 10^{-5}$ to 3.97 ft/day. Field-scale hydraulic conductivity measurements ranged from $5.18 \times 10^{-3}$ to 17.3 ft/day.

Bartholomay et al. (1989) tabulated the bulk mineralogy of interbed sediments from areas throughout the INEEL. In this report, a total of 105 samples were examined and determinations of bulk percentage of clay-sized fractions were made. Clay content ranged from 0 to 70%, with a median of about 25%. A total of 60 samples from interbeds exceeding 100 ft in depth were also examined. The bulk clay content for these samples averaged 20 and 50% very fine to fine-grained sand. Based on this grain-size analysis, hydraulic conductivity values ranging from $6.7 \times 10^{-4}$ to 40 ft/day were estimated (Todd 1980). Laboratory measurements of hydraulic conductivity for RWMC interbed sediments ranged from $3 \times 10^{-5}$ to 20 ft/day (McElroy and Hubbell 1990). Given the large percentage of fine-grained sediments in the interbeds, the range given by McElroy and Hubbell (1990) is probably the most accurate for the thick section of interbed sediments at TRA. Laboratory determinations of effective porosity of 11 interbed sediment core samples ranged from 34.2 to 51.4% (McElroy and Hubbell 1990).

***Vadose Zone Basalt Flows—***The basalt flows, comprising the majority of the vadose zone and the upper portions of the SRPA beneath TRA, make up a complex system of fractured and massive basalt flows with large ranges of hydraulic properties. The basalt-flow permeabilities are controlled by widely varying lithology within a particular flow (fractures, interflow rubble and pyroclastic zones, weathered zones, vesicularity, and massive zones). The vadose zone (and upper aquifer) permeabilities are controlled by the spatially changing lithologic characteristics for a given basalt flow and by the extent of basalt flows and interbeds.

Hydraulic conductivity of vadose zone basalt flows was initially approximated by Robertson (1977) at 10 ft/day. Since then, several single well pumping tests have been performed in the TRA area in order to determine hydraulic conductivity for these basalt units. Hydraulic conductivity estimates for wells completed in the BC flow group in the TRA vicinity ranged from about 5 to 790 ft/day, with a median of 24 ft/day (Ackerman 1991b). Aquifer tests in two wells (69 and 62) completed in the DE1 flow group were also performed. A value of 0.11 ft/day was estimated for well 69, while 88 ft/day was estimated for well 62 (Ackerman 1991b).

***SRPA—***Transmissivity for the SRPA beneath TRA is estimated at about $2.1 \times 10^6$ $ft^2$/day (Walton 1958). Assuming an effective thickness of the aquifer in the TRA area of 250 ft, the hydraulic conductivity is about 8,550 ft/day.

The effective porosity of the basalts is a measure of the interconnected pore spaces consisting of interflow rubble zones, fractures, and interconnected vesicles. The effective porosity of basalts at the INEEL as estimated by previous researchers ranges from as little as 0.05 to 23%, with 10% being the most accepted value (Robertson et al. 1974; Bishop 1991; Knutson et al. 1990; Garabedian 1992; and Ackerman 1995a).

***3.2.2.4 Recharge/Discharge Sources.*** Natural recharge to the SRPA at the TRA occurs from regional underflow, episodic infiltration of stream flow, and local precipitation. Artificial recharge occurs from disposal of TRA wastewater, application of lawn irrigation, and accidental leaks. Discharge from the aquifer at the TRA takes place as pumpage withdrawals.

Underflow in the SRPA—***Water in the SRPA that passed beneath TRA from the northeast is assumed to be consistent with WAG-10 underflow estimates from the transmissivity and hydraulic gradient. No estimates of underflow are given in the RI/FS (Burns et al. 1997).***

***Episodic Recharge—***Periodic flows in the channel of the Big Lost River southeast of TRA are associated with years of increased snowpack in the mountainous drainage areas to the west. Much of this water infiltrates along the stream channel. The volume of this source of episodic recharge can be significant during wet years. The channel of the Big Lost River is about 4,500 ft from the southeast corner of the TRA fenceline, and about 4,100 ft from the southeast corner of the 1964 cell of the WWP.

Perched water has been observed in the vadose zone adjacent to the Big Lost River during episodic flow. The extent and volume of these perched-water zones are not well known. However, during periods of flow, water levels in perched-zone wells (USGS-62 and USGS-71) near TRA rise abruptly (Robertson et al. 1974). Water table elevations in these wells were observed to rise and fall sharply in short time frames (a total of 7 months) with fluctuations exceeding 10 ft in both the rising and falling water table elevation scenarios (Barraclough et al. 1967). These fluctuations were attributed to recharge from unusually high flows in the Big Lost River. Tritium concentrations in USGS-62 did not decrease significantly in this timeframe, as would be expected if a large slug of water with no added tritium entered the perched water zone. Thus, recharge from the Big Lost River may cause perched water levels to rise (Barraclough et al. 1967).

***Recharge from Wastewater Disposal—***Liquid wastes have been generated at TRA during scientific and engineering research since 1952. The wastewater streams have always been separated into two types: sanitary and non-sanitary. The sanitary sewage has always been disposed to dedicated sewage lagoons. Non-sanitary waste streams are products of the following: cooling tower blowdown, drains from reactors and fuel storage cells, wash water from vent scrubbers, drains from laboratories, drains from hot cells, drains from the heat exchanger building, and drains from the process water building. Disposal systems for non-sanitary liquid waste streams include the WWP, the CWP, the CP, and the TRA disposal well. The amounts of wastewaters disposed in each of the locations mentioned above are listed in Table 3-1.

Table 3-1. Known or estimated amounts of wastewaters disposed at the TRA from 1952-1994 (modified from Orr, 1999).

| Year | WWP | CWP | CP | SLP | TRA Disposal Well | USGS-53 |
|---|---|---|---|---|---|---|
| 1952 | 0.67 | 0 | 0 | 1.32 | 0 | 0 |
| 1953 | 2.01 | 0 | 0 | 1.32 | 0 | 0 |
| 1954 | 12.7 | 0 | 0 | 1.32 | 0 | 0 |
| 1955 | 13.1 | 0 | 0 | 1.32 | 0 | 0 |
| 1956 | 12.57 | 0 | 0 | 1.32 | 0 | 0 |
| 1957 | 13.77 | 0 | 0 | 1.32 | 0 | 0 |
| 1958 | 33.29 | 0 | 0 | 1.32 | 0 | 0 |
| 1959 | 26.74 | 0 | 0 | 1.32 | 0 | 0 |
| 1960 | 29.55 | 0 | 0 | 1.32 | 0 | 1.19 |
| 1961 | 31.42 | 0 | 0 | 1.32 | 0 | 7.12 |
| 1962 | 37.83 | 0 | 5.6 | 1.32 | 0 | 0.59 |
| 1963 | 27.01 | 0 | 5.6 | 1.32 | 0 | 2.97 |
| 1964 | 22.99 | 0 | 5.6 | 1.32 | 0 | 5.34 |
| 1965 | 19.39 | 0 | 5.6 | 1.32 | 12.03 | 0 |
| 1966 | 17.51 | 0 | 5.6 | 1.32 | 12.03 | 0 |
| 1967 | 24.2 | 0 | 5.6 | 1.32 | 12.03 | 0 |
| 1968 | 25.13 | 0 | 5.6 | 1.32 | 12.97 | 0 |
| 1969 | 35.56 | 0 | 5.6 | 1.32 | 20.05 | 0 |
| 1970 | 37.57 | 0 | 5.6 | 1.32 | 26.60 | 0 |
| 1971 | 29.28 | 0 | 6.13 | 1.24 | 18.18 | 0 |
| 1972 | 29.01 | 0 | 9.73 | 1.37 | 17.25 | 0 |
| 1973 | 35.96 | 0 | 4.2 | 1.25 | 27.94 | 0 |
| 1974 | 32.89 | 0 | 4.19 | 1.1 | 49.87 | 0 |
| 1975 | 29.41 | 0 | 3.45 | 1 | 45.86 | 0 |
| 1976 | 29.41 | 0 | 3.54 | 1.1 | 61.10 | 0 |
| 1977 | 19.65 | 0 | 2.89 | 1.24 | 51.07 | 0 |
| 1978 | 16.71 | 0 | 2.79 | 1.26 | 36.23 | 0 |
| 1979 | 9.76 | 0 | 2.34 | 1.17 | 35.16 | 0 |
| 1980 | 7.89 | 0 | 1.56 | 1.09 | 44.52 | 0 |
| 1981 | 7.35 | 0 | 1.26 | 0.77 | 32.62 | 0 |
| 1982 | 6.86 | 26.52 | 1.19 | 0.68 | 4.95 | 0 |
| 1983 | 3.54 | 32.14 | 0.89 | 0.82 | 0 | 0 |

| Year | WWP | CWP | CP | SLP | TRA Disposal Well | USGS-53 |
|---|---|---|---|---|---|---|
| 1984 | 2.14 | 33.24 | 0.78 | 0.81 | 0 | 0 |
| 1985 | 2.74 | 29.73 | 0.8 | 0.96 | 0 | 0 |
| 1986 | 3.34 | 36.43 | 0.86 | 1.13 | 0 | 0 |
| 1987 | 2.53 | 23.85 | 0.73 | 0.91 | 0 | 0 |
| 1988 | 2.45 | 30 | 0.56 | 0.99 | 0 | 0 |
| 1989 | 2.58 | 39.3 | 1.03 | 1.09 | 0 | 0 |
| 1990 | 2.5 | 34 | 1 | 1.15 | 0 | 0 |
| 1991 | 3.49 | 25.57 | 1.15 | 1.75 | 0 | 0 |
| 1992 | 3.1 | 19.17 | 1.14 | 1.68 | 0 | 0 |
| 1993 | 1.94 | 33.42 | 0.86 | 1.81 | 0 | 0 |
| 1994 | 0 | 28.57 | 0.81 | 4.46 | 0 | 0 |
| **Total Waste Water Disposed** | **707.54** | **391.94** | **104.28** | **55.91** | **520.45** | **17.21** |
| **Annual Average** | **16.85** | **30.15** | **3.16** | **1.30** | **28.91** | **3.44** |

(discharge in units of cubic feet × $10^6$)

***TRA Disposal Well—***The TRA disposal well is located in the southeast corner of the facility. The disposal well was drilled to a depth of 1,271 ft and was perforated at three intervals: 512 to 697 ft bls, 930 to 1,070 ft bls, and 1,182 to 1,267 ft bls (Morris et al. 1965). During perforation of the 930 to 1,070 ft interval, the casing was severed at a depth of 1005 ft. The well began accepting wastewater in November of 1964. Fluid discharge to the well averaged 216 million gal per year, with a total estimate of about 3,900 million gal injected into the well (Hull 1989). The well was taken out of service in 1982 and capped. The former TRA disposal well is now used to monitor water levels and water quality of the SRPA beneath TRA.

***Well USGS-53—***USGS-53 is located in the southeast corner of TRA, near the WWP. This well is completed at 90 ft bls in the deep-perched water zone. Morris (1964) reports that this well was used for wastewater disposal from November 1960 to January 1962, from June 1963 to August 1963, and from November 1963 to September 1964. Based on an estimated injection rate of $1.48 \times 10^5$ gal/day, the total volume of wastewater injected into this well is calculated to be about $2.2 \times 10^8$ gal.

***Warm Waste Pond—***The WWP at TRA is an unlined infiltration structure that was designed to accept radioactive liquid wastes. However, for a period of 10 years (1952 to 1962) all non-sanitary wastewaters were disposed in the WWP, after which wastewater from the demineralization plant was rerouted to the CP. By 1964, only radioactive wastewaters were accepted at the WWP (Hull 1989). The WWP originally consisted of one cell that had bottom dimensions of 150 × 250 ft, 2:1 side slopes, and a depth of 15 ft. Decreasing infiltration capacity of the original cell from the buildup of chemical precipitates and algae led to the excavation of second and third disposal cells. The second cell was excavated in 1957 and had bottom dimensions of 125 × 230 ft, 2:1 side slopes, and a depth of 15 ft. The

third cell was excavated in 1964 and had bottom dimensions of 250 × 400 ft, 2:1 side slopes, and a depth of 6 ft. The total capacity of all three cells is about 2.1 million $ft^3$ (Hull 1989). Until 1979, an average of 24 million $ft^3$/year of wastewater was disposed of in the WWP, after which, the annual average dropped to about 4 million $ft^3$. The WWP was decommissioned in 1993 and radioactive wastewater was diverted to lined evaporation ponds.

***Retention Basin—***The Retention Basin was designed to hold radioactive effluent for a sufficient time to allow for the natural decay of short-lived radionuclides (Doornbos 1991). A secondary purpose for the basin was to serve as a holding area for cooling water from the reactor should it have been necessary to quickly drain it. The basin is a concrete structure 130 × 43 ft with a depth of 20 ft. The basin is divided into two chambers, each designed to hold 360,000 gal. The basin has been known to leak since the early 1970s, although is not known when the leak began (Hull 1989). The leakage rate is also unknown, but is estimated to be greater than 30 gal/min.

***Cold Waste Pond—***The CWP is located about 350 ft south of the WWP, and became operational in 1982 as an alternative disposal system to the injection well. The pond is unlined and is comprised of two cells, each 150 × 400 ft. The pond is used to dispose of cooling water from blowdown during reactor operations. During 12 years of operation (1982 through 1994), an average of 30 million $ft^3$/year of wastewater was disposed to the CWP (Orr 1999).

***Chemical Waste Pond—***The CP has been in operations since 1962. This unlined disposal unit is 170 × 170 ft and has 1:1 side slopes. This pond is used to dispose of water from ion exchange columns and water softeners. During the years 1962 through 1994, an average of 3.2 million $ft^3$ of wastewater was disposed to the CP (Orr 1999).

***Sewage Leach Ponds—***The SLPs were constructed to accept all sanitary wastewaters generated at TRA. The southern cell, constructed in 1950, is unlined and is approximately 185 × 45 ft. The northern cell, constructed in 1965, is also unlined and is approximately 185 × 30 ft. Through 1994, a total of 56 million $ft^3$ of wastewater was disposed to these cells, for an average of about 1.3 million $ft^3$/year (Orr 1999). These cells were replaced with lined units in 1995.

***Recharge from Precipitation—***Infiltration of local precipitation may augment recharge to perched water bodies. Long-term average precipitation at the INEEL is 8.7 in./year. Although pan evaporation losses greatly exceed average precipitation, water from snowmelt or heavy rains may infiltrate to a depth where it cannot be evaporated, particularly where runoff is focused by pavement and drainage ditches. Miller et al. (1990) estimates net recharge from precipitation to range from 1 to 4 in./year with a best estimate to be 1.6 in./per year. Assuming a net infiltration rate of 1.6 in./year and the area available for recharge at TRA to be approximately 3.2 million $ft^2$, approximately 3 million gal of water may be available for recharge annually from local precipitation.

***Aquifer Discharge to Production Wells—***Three production wells are in use at TRA. These wells are located in the northeast corner of the facility. From 1971 to 1990, an annual average of about 870 million gal of groundwater was pumped from TRA production wells (Doornbos et al. 1991).

***3.2.2.5 Hydraulics.*** The hydraulics of flow and transport at the TRA are defined by the integration of conceptual model components. System hydraulics include characterization of flow and transport in the vadose zone and within the SRPA.

***SRPA—***The SRPA is assumed to respond regionally as an unconfined aquifer. However, due to the layered character of the basalts and interbed sediments, groundwater flow may be locally confined or

partially confined. The flow field within the aquifer is defined by the hydraulic gradient, direction of flow, and flow velocity.

***Gradient and Flow Direction—***INEEL-wide water-level data collected during 1998 indicated the general direction of groundwater flow across the INEEL was toward the south and southwest at an average gradient of about 4 ft/mi (Bartholomay et al. 1997). Groundwater flow direction in the vicinity of TRA is consistent with regional trends. The gradient in the vicinity of TRA is less, averaging 1.9 ft/mi (Doornbos et al. 1991).

***Flow Rate (Horizontal)—***Groundwater flow velocity at TRA has been calculated using Darcy's law. Based on an average transmissivity of $2.2 \times 10^6$ gpd/ft, an aquifer effective thickness of 250 ft, an effective porosity of 10%, and a hydraulic gradient of 1.9 ft/mi, the average groundwater flow velocity at TRA was approximated to be 4.3 ft/day (Doornbos et al. 1991). Horizontal groundwater flow rates in the SRPA have been estimated to range from 0.3 to 7.6 m/day (1 to 25 ft/day) (Kaminsky et al. 1994; Robertson et al. 1974).

***Vadose Zone—***The vadose zone beneath TRA is approximately 450 ft thick. Water from surface or shallow subsurface recharge moves vertically through the vadose zone as unsaturated flow in fractured basalts without vertical permeability contrasts, and vertically and horizontally as saturated flow within perched water bodies.

***Perched Groundwater—***Perched water bodies form when the downward movement of infiltrating water is impeded by horizons of relatively low vertical hydraulic conductivity. Two perched water bodies have been identified at TRA. The primary source of the perched water at TRA is the historical discharge of wastewater to the various disposal ponds at the facility (i.e., WWP, CWP, CP, SLP, and Retention Basin). The upper perched water zone occurs in the immediate vicinity of the ponds and Retention Basin at the contact between the surficial sediments and the underlying basalt flows of the BC group at about 50 ft bls. The deep perched water zone that exists at about 150 bls is attributed to the disposal of wastewater to infiltration ponds and the reduced vertical hydraulic conductivity of a collection of interbed sediments and basalt flows encountered at that depth. In 1991, the altitude of the perched water table surface ranged from 4,706 to 4,861 ft above Mean Sea Level (MSL), the depth ranged from about 59 to 214 ft bls, and the deep perched water body covered an estimated 6,000 × 3,000 ft area (Doornbos et al. 1991). The maximum saturated thickness was about 150 ft. Given a porosity of 10%, the volume of deep perched water was calculated to be about $1.4 \times 10^8$ $ft^3$ in March 1991.

***3.2.2.6 Groundwater Chemistry.*** The composition of the groundwater beneath TRA is a result of the natural geochemical interactions between the aquifer matrix and the additions of chemically dissimilar disposal waters. Groundwater at TRA has been classified as calcium-bicarbonate type, which is indicative of recharge from the clastic and carbonate sedimentary rocks to the north and northwest (Robertson et al. 1974). Regions of increased specific conductance in groundwater beneath TRA have been identified and are attributed to the addition of sodium, chloride, nitrate, and sulfate to the SRPA from wastewater disposal practices at TRA. The primary sources of these salts are ion exchange columns and water softeners (Hull 1989).

***3.2.2.7 Contaminant Transport.*** Radioactive and chemical contaminants have been released to the subsurface at TRA since the early 1950's. Migration of these contaminants depends on the source, transport through the vadose zone, and transport through the aquifer. Migration of these contaminants has resulted in detectable concentrations in the aquifer and in perched groundwater bodies. The following sections briefly describe the contaminant source term, transport mechanisms, and distribution of contaminants in the subsurface.

***Source Term—***Radioactive and chemical contaminants have been contained in wastewater disposed at the TRA. In the past, contaminants have entered the vadose zone and SRPA at the TRA through several unlined percolation ponds, disposal wells, and various spills and leaks. This section will describe the source term inventory, release mechanisms, and release rates.

Contaminants released to the subsurface since the early 1950's have included radionuclides, inorganic chemicals, and organic chemicals. However, the primary COCs at TRA are hexavalent chromium ($Cr^{6+}$) and tritium ($^{H-3}$) due to the fact that these contaminants were the only ones found to exceed any Federal Primary Drinking Water Standard (Doornbos et al. 1991). Other radionuclides and chemicals disposed of at TRA include strontium-90 (Sr-90), cesium-137 (Cs-137), cobalt-60 (Co-60), Cr-51, sodium (Na), chloride (Cl), and sulfate ($SO_4^{2-}$).

During 1952 through 1993, about 10,500 Ci of tritium, 93 Ci of Sr-90, and 138 Ci of Cs-137 were disposed to the WWP. Approximately 2,390 Ci of Cr-51 were disposed to the WWP during 1979 through 1998. Approximately 442 Ci of Co-60 was disposed to the WWP during 1952 through 1988. During 1952 to 1964, approximately 24,000 lb of $Cr^{6+}$ was disposed to the WWP. Subsequently, an estimated 31,000 lb of $Cr^{6+}$ was injected into the SRPA during 1965 through 1972, when the use of chromates as a corrosion inhibitor was discontinued (Hull 1989). In addition, inorganic chemicals were disposed to TRA ponds. Approximately 173,000 lb of sodium was disposed to the CP during 1996 through 1998. Approximately 3,600 lb of chloride was discharged into the CWP at the TRA during 1996 through 1998. Approximately 833,000 lb of sulfate was discharged to the CP and CWP at the TRA during 1996 through 1998.

Contaminant migration is controlled, in part, by the point and mechanism of release. Contaminant release in the vadose zone delays the arrival of contaminants at the water table. More reactive contaminants may be temporarily or permanently attached to sites within the vadose zone. Methods of introduction of contaminants in to the vadose zone and aquifer at TRA include unlined disposal ponds, disposal wells, and various accidental leaks and spills. The amount of water released at each of these sites is described in previous sections and is listed in Table 3-2.

***Extent of Contamination and Contaminant Inventory—***Contaminant concentrations have been monitored in water from perched groundwater bodies and in the SRPA. Subsequent sections describe the distribution, extent, and inventory of selected contaminants in water from the vadose zone and the aquifer beneath the TRA. A network of monitoring wells was utilized to analyze water from the shallow and deep perched water zones beneath the TRA and the underlying SRPA. Samples from these wells were analyzed for the constituents in the following sections in order to delineate the extent of perched and groundwater contamination at the TRA (Bartholomay and Tucker 2000).

***Tritium (H-3)—***Samples from nine wells completed the shallow perched zone at TRA were all below reporting limits in 1998. During the same year, samples from wells completed in the deep perched water zone range from below reporting limits to as much as 116 +/- 4 pCi/L (Bartholomay and Tucker 2000). The distribution of tritium in the deep perched water zone in 1998 is illustrated in Figure 3-10 (Bartholomay and Tucker 2000, p 12). Factors affecting the distribution of H-3 in perched water at TRA include proximity to radioactive waste disposal ponds, depth of water below the ponds, variable tritium disposal rates, radioactive decay of tritium, and dilution effects of the CP and Big Lost River recharge.

Groundwater in the SRPA has also been impacted by tritium disposal at TRA. Figure 3-11 (Bartholomay et al. 2000) depicts the distribution of tritium in the SRPA beneath the TRA. This map is based on groundwater data collected in 1998 (Bartholomay et al. 2000).

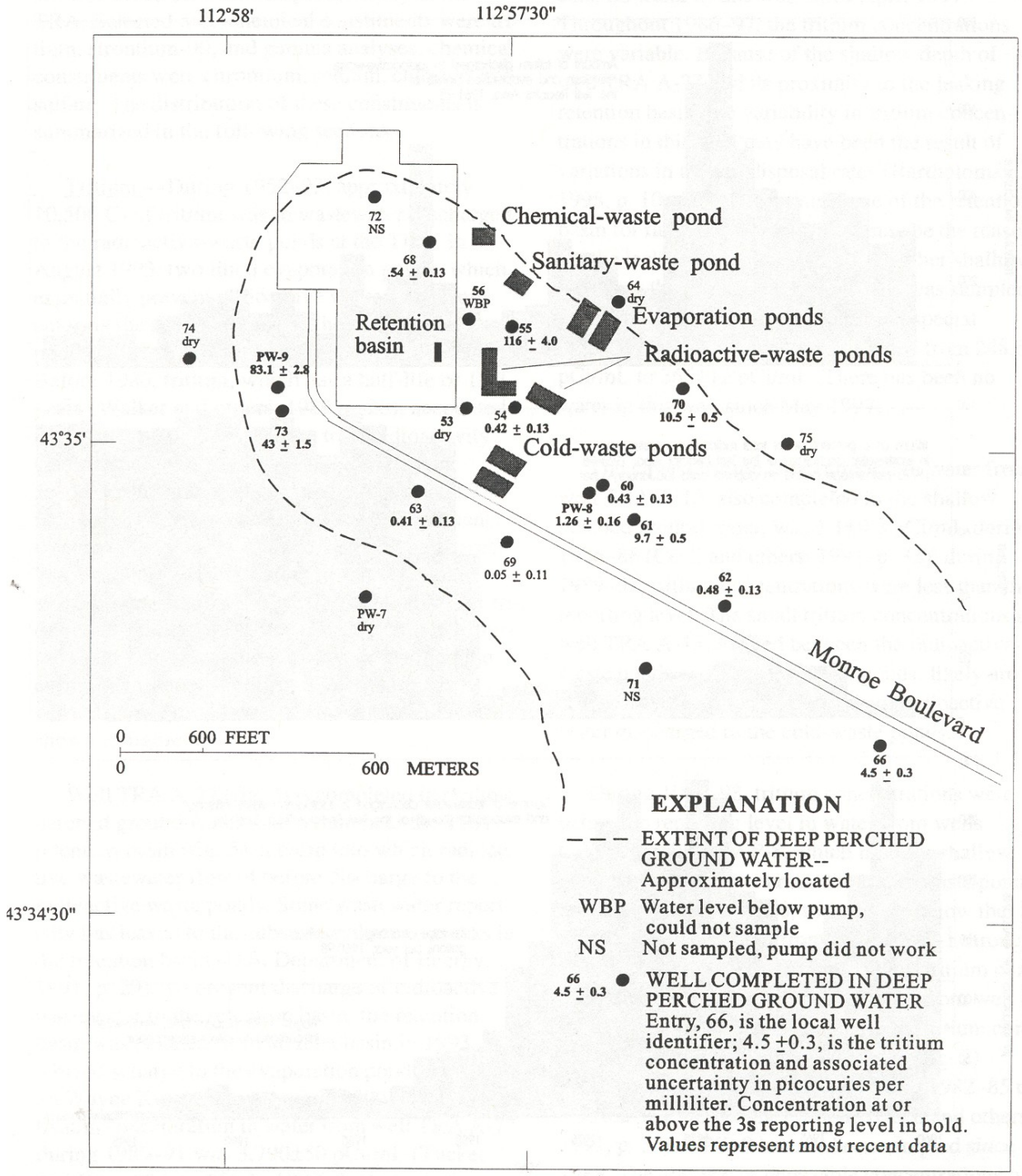


Figure 3-10. Tritium concentrations in the deep perched water zone at TRA, 1998 (from Bartholomay and Tucker 2000).

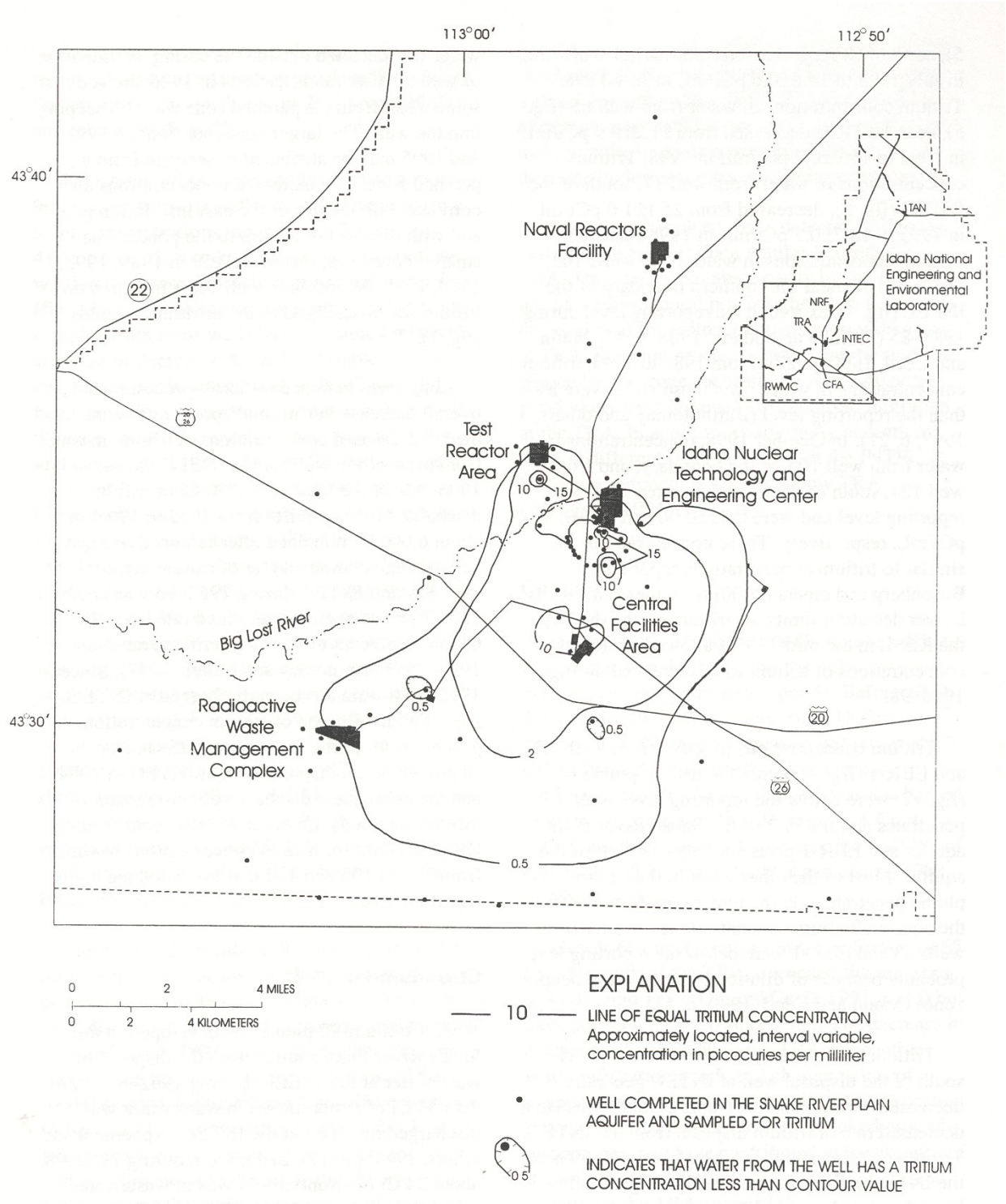


Figure 3-11. Tritium concentrations in water in the SRPA, 1998 (from Bartholomay et al. 2000).

***Strontium-90 (Sr-90)—***Concentrations of Sr-90 were variable in wells completed in the deep perched zone in 1998 with values ranging from below reporting limits to as much as 59 +/-2 pCi/L (Bartholomay and Tucker 2000). The distribution of Sr-90 in the deep perched water at the TRA is depicted in Figure 3-12 (Bartholomay et al. 2000).

Sr-90 is not present above reporting limits in the SRPA at the TRA (Bartholomay et al. 2000). The absence of an Sr-90 plume at TRA can be attributed to the fact that Sr-90 was only discharged at the surface in disposal ponds and was sorbed onto sediments in the vadose zone and therefore could not reach the SRPA.

***Cesium-137 (Cs-137)—***Only one well (TRA A-77) completed in the shallow perched zone yielded concentrations exceeding the reporting limit for Cs-137 during 1996 through 1998 (Bartholomay and Tucker 2000). The values ranged from 1,200 +/-110 pCi/L in 1997 to 42,300 +/-1,800 pCi/L in 1996. Reduced disposal rates and the sorption of Cs-137 to soil particles are the most probable causes of the general lack of detections of Cs-137 in perched water at the TRA.

No Cs-137 was detected in the SRPA at TRA in 1996 through 1998 (Bartholomay et al. 2000).

***Chromium-51 (Cr-51)—***Cr-51 was not detected in any perched water wells at the TRA during 1996 through 1998 (Bartholomay and Tucker 2000). The absence of Cr-51 in the perched water at TRA is most likely due to the decreased disposal rates and the relatively short half-life of Cr-51 (27.7 days).

No Cr-51 was detected in the SRPA at TRA in 1996 through 1998 (Bartholomay et al. 2000).

***Cobalt-60 (Co-60)—***During 1996 through 1998, Co-60 was detected above reporting limits in only two wells at the TRA (Bartholomay and Tucker 2000). Concentrations in TRA A-77 ranged from 7,700 +/-260 pCi/L in October 1996 to 13,900 +/-500 pCi/L in April 1996. Co-60 was measured at 220 +/-30 pCi/L in USGS-56 in April 1997. The limited presence of Co-60 in the perched water at the TRA is most likely due to proximity to the former leaking Retention Basin and the presence of a large amount of suspended sediment in the water samples collected (Bartholomay and Tucker 2000).

No Co-60 was detected in the SRPA at TRA in 1996 through 1998 (Bartholomay et al. 2000).

***Hexavalent Chromium ($Cr^{6+}$)—***In 1998, $Cr^{6+}$ was detected in deep perched water wells at concentrations ranging from less than 14 to 98 μg/L (Bartholomay and Tucker 2000). The distribution of $Cr^{6+}$ in the deep perched water at the TRA is depicted in Figure 3-13 (Bartholomay and Tucker 2000).

Only one sample collected during 1996 through 1998 was above the MCL of 100 μg/L for total Cr (Bartholomay et al. 2000). The concentration in USGS-65 (located to the south of the TRA) was reported at 168 μg/L. Other samples contained less than 14 to as much as 26 μg/L during October 1998.

***Sodium—***Sodium concentrations ranged from 7.6 to 20 mg/L in the shallow perched water at the TRA during 1996 through 1998 (Bartholomay and Tucker 2000). Samples from the deep perched water zone ranged from 6.1 to 1,000 mg/L in sodium concentration during the same time period.

Sodium was detected above background at only one well completed in the SRPA at the TRA (Bartholomay et al. 2000). The concentration of sodium in the MTR Test well was reported at 42 mg/L in 1998.

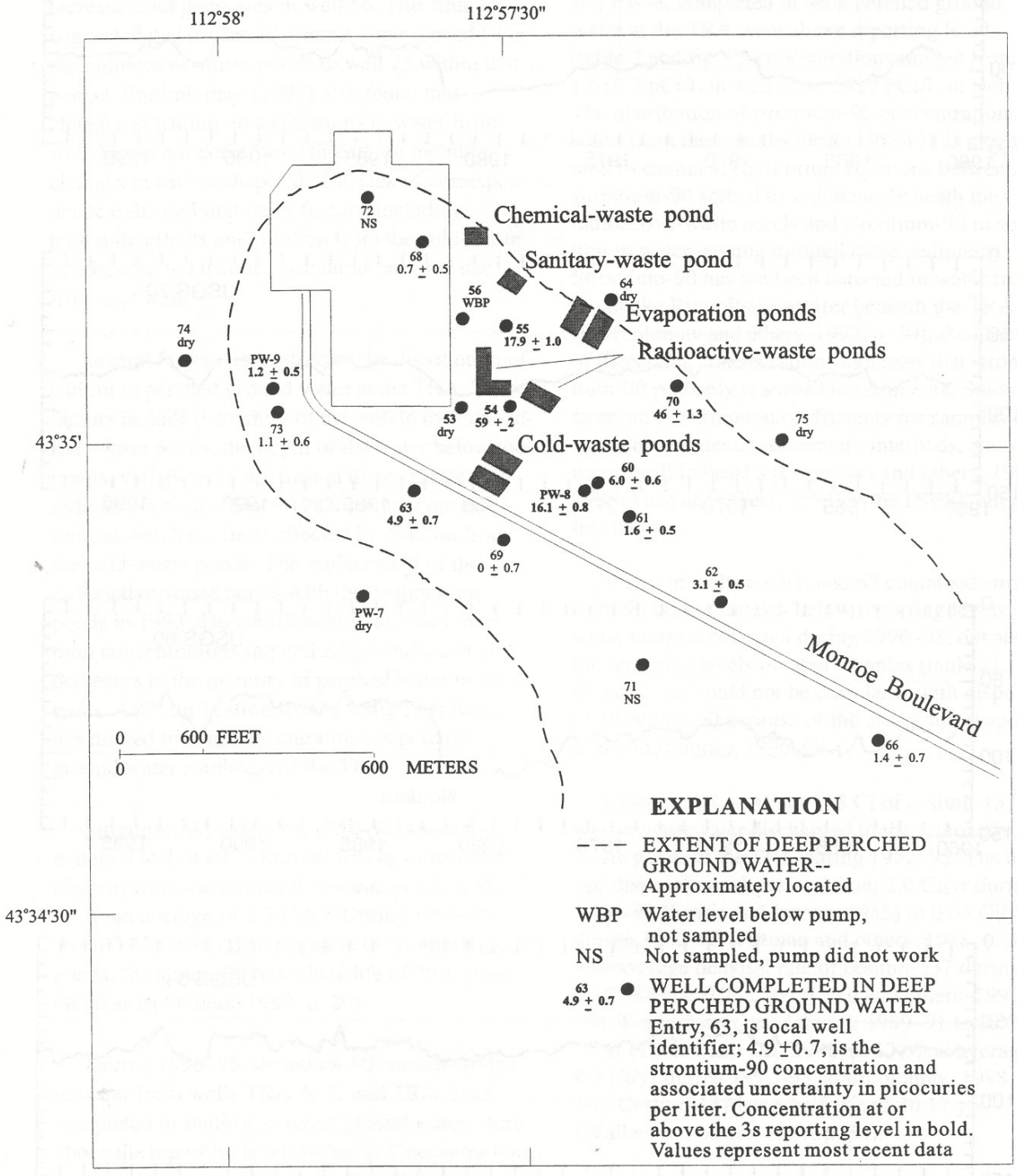


Figure 3-12. Strontium-90 concentrations in the deep perched water zone at TRA, 1998 (from Bartholomay and Tucker 2000).

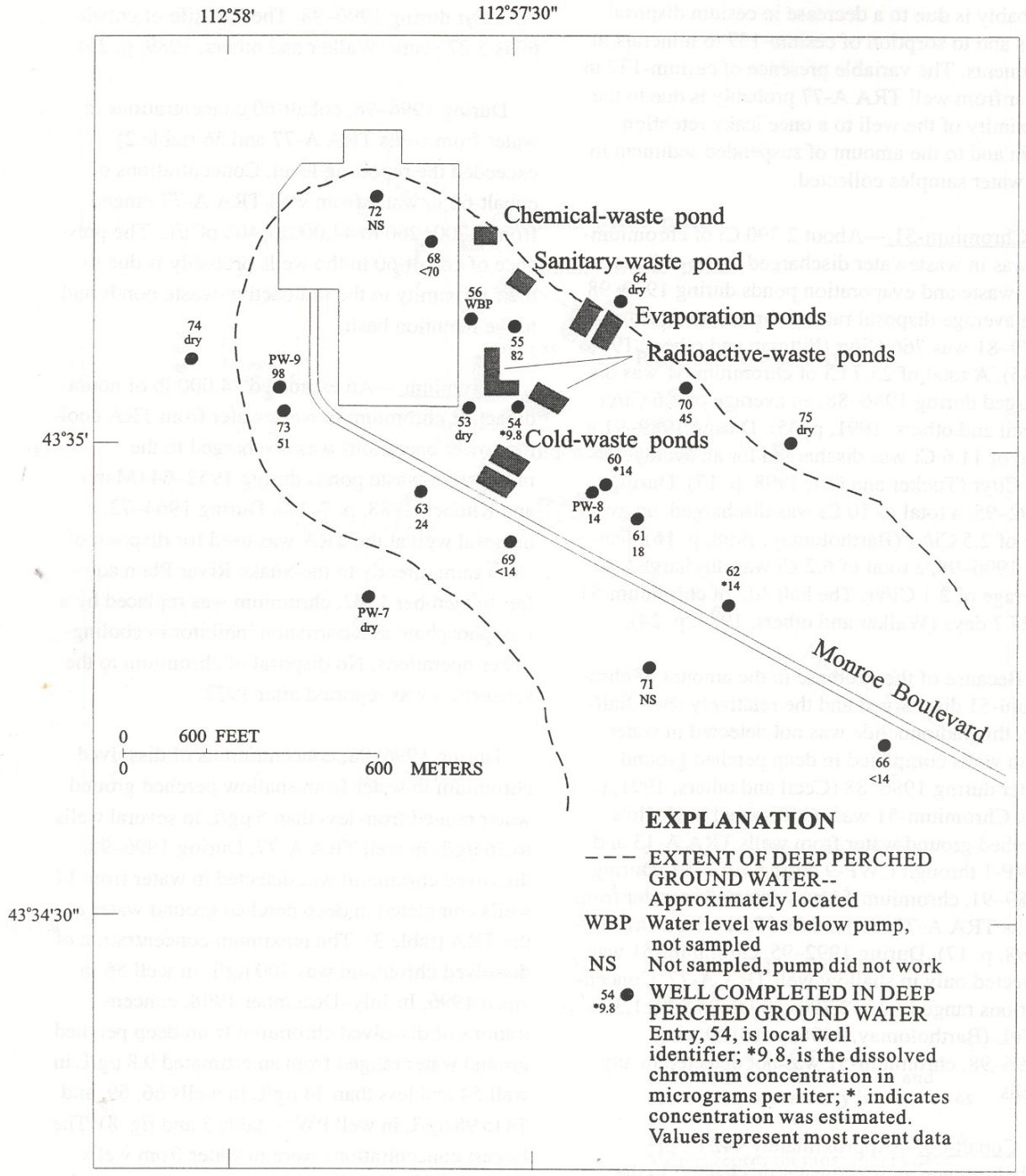


Figure 3-13. Chromium concentrations in the deep perched water zone at TRA, 1998 (Bartholomay and Tucker 2000).

***Chloride—***Chloride concentrations ranged from 9.3 to 27 mg/L in the shallow perched water at the TRA during 1996 through 1998 (Bartholomay and Tucker 2000). Samples from the deep perched water zone ranged from 3.1 to 43 mg/L in sodium concentrations during the same time period.

Chloride in USGS-65 was reported at 18 mg/L, while all other samples from wells completed in the SRPA at the TRA were below 15 mg/L in chloride concentration.

***Sulfate—***A maximum of 340 mg/L of sulfate was reported for the shallow perched water zone at TRA (Bartholomay and Tucker 2000). Concentrations of sulfate in wells completed in the deep perched water zone at the TRA ranged from 92 to 276 mg/L in 1998. The distribution of dissolved sulfate in the deep perched water zone at the TRA is depicted in Figure 3-14 (Bartholomay and Tucker 2000).

Water collected in 1998 from two wells completed in the SRPA at the TRA contained dissolved sulfate above background levels. The values were reported at 54 mg/L for MTR Test and 147 mg/L for USGS-65 (Bartholomay et al. 2000).

***Transport Mechanisms—***Those mechanisms considered to be important for the transport of contaminants in the vadose zone at TRA include radioactive decay, sorption, rate of infiltration from different sources of recharge, and effective porosity. Mechanisms that control transport in the aquifer include radioactive decay, sorption, groundwater dispersivity, effective porosity, and the velocity of flow.

Transport of contaminants from spills that were contained in surficial sediments is facilitated by water for release to the deeper subsurface from those soils. Water may originate from facility irrigation, piping losses, and shallow infiltration from percolation ponds.

### 3.2.3 Numerical Analyses Performed to Date at TRA

***3.2.3.1 Robertson (1977).*** Robertson (1977) modeled contaminant transport from surface source areas to the SRPA beneath the TRA. The purpose of the model was to gain a better understanding of contaminant distribution beneath the TRA disposal ponds, including a better quantitative understanding of hydraulic and chemical controls on movement of contaminants in the subsurface. The model was used to estimate future migration of contaminants in the subsurface and evaluate the potential effects on the SRPA. The model concluded that the only contaminant reaching the SRPA was tritium. The general result of the model was that only contaminants with low sorbing potential and relatively long half-lives would reach the SRPA. Non-radioactive chemicals (e.g., sodium, and chloride) were predicted to reach the aquifer, which is also consistent with what was observed in the aquifer at that time. The model predicted that, other than tritium, no other radioactive contaminants should reach the aquifer in the future.

***3.2.3.2 Burns et al. (1997).*** GWSCREEN was used to assess the effect on groundwater from release of selected contaminants at the TRA for use in the BRA (Burns et al. 1997). The results of the GWSCREEN run indicate that contaminants present in the soil at the TRA pose no threat the to the SRPA.

Orr (1999). ***Orr (1999) developed a transient numerical simulation of flow through the perched water system at the TRA and to refine the estimates of the hydraulic properties that control the presence and movement of water through these zones. The model utilized a block-centered approach with 4 layers, each representing areas of distinct hydraulic properties (i.e., basalt and interbed units) in the vadose zone beneath the TRA. The model calibration results were in adequate agreement with the observed hydrologic conditions at the site. A simulation was run in the model to evaluate the effect of the cessation of recharge in 1994. The simulation indicated that all layers would drain in 4 years in the absence of recharge.***

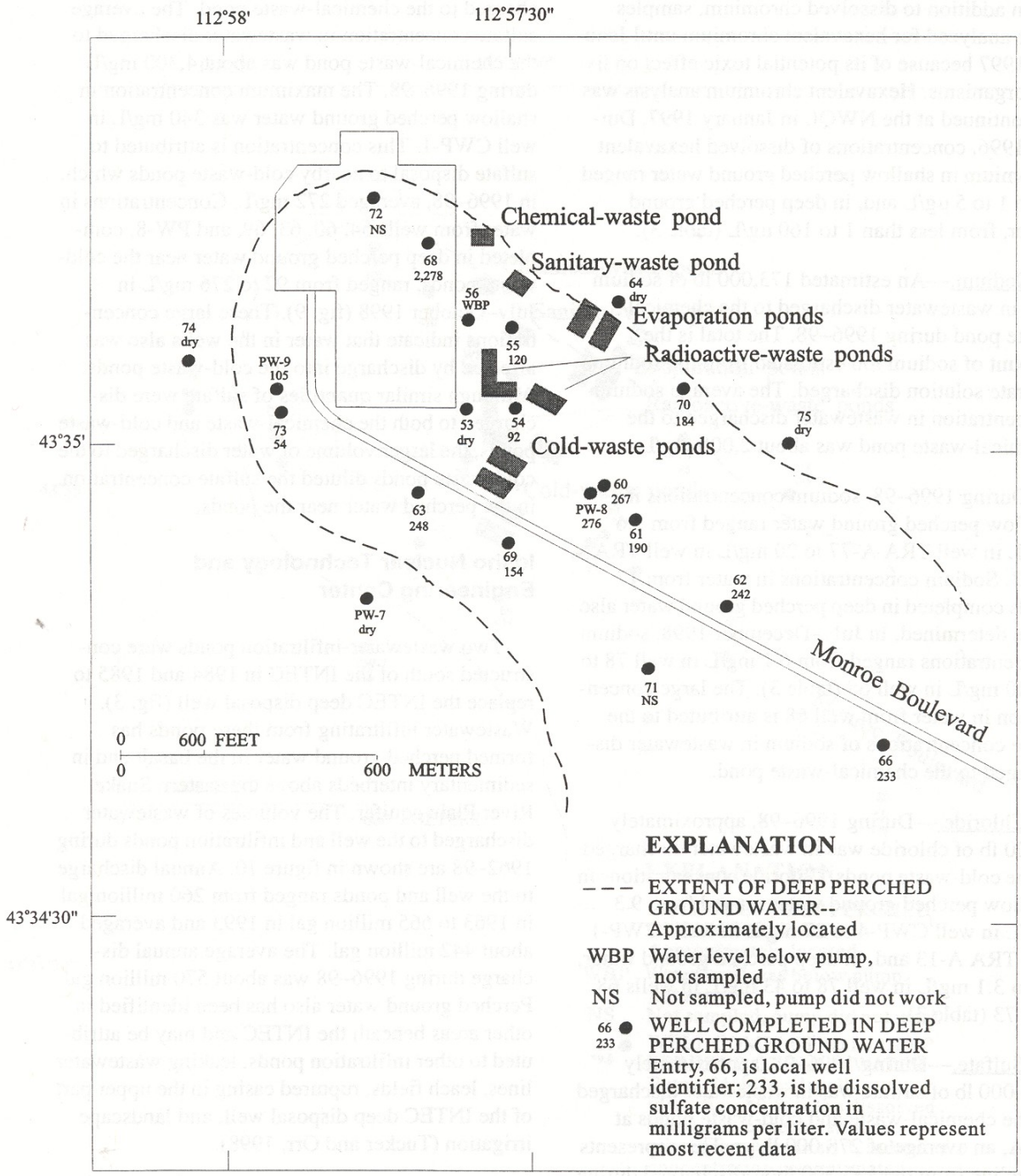


Figure 3-14. Sulfate concentrations in the deep perched water zone at TRA, 1998 (Bartholomay and Tucker 2000).

### 3.2.4 Summary of Competing Hypotheses and Additional Data Requirements

***3.2.4.1 Vertical Distribution of Contaminants in SRPA.*** Most aquifer wells at the TRA are completed in the upper portion of the SRPA. The vertical distribution of contaminants at depth in the aquifer is not well understood. Deeper wells in the SRPA at TRA are needed in order to better evaluate the vertical distribution of contaminants in the aquifer.

***3.2.4.2 Big Lost River Influence.*** Perched water has been observed in the vadose zone adjacent to the Big Lost River during episodic flow. The extent and volume of these perched-water zones are not well known. Thus, more work needs to be performed in order to better our understanding of the influence of flux from the Big Lost River on the perched water system at the TRA.

### 3.2.5 References Cited


Ackerman, D. J., 1991a, *Transmissivity of the Snake River Plain Aquifer at the Idaho National Engineering Laboratory*, U.S. Geological Survey Water-Resources Investigations Report 91-4058, U.S. Geological Survey.

Ackerman, D.J., 1991b, Transmissivity of perched aquifers at the Idaho National Engineering Laboratory, Idaho: U.S. Geological Survey Water-Resources Investigations Report 91-4114 (-22099).

Ackerman, D.J., 1995, *Analysis of Steady-State Flow and Advective Transport in the Eastern Snake River Plain Aquifer System, Idaho*, U.S. Geological Survey Water-Resources Investigations Report 94-4257 (DOE/ID-22120), U.S. Geological Survey.

Anderson, S. R., 1991, Stratigraphy of the Unsaturated Zone and Uppermost Part of the Snake River Plain Aquifer at the Idaho Chemical Processing Plant and Test Reactor Area, Idaho National Engineering Laboratory, Idaho, USGS Water-Resources Investigations Report 91-4010 (DOE-ID-22095), U.S. Geological Survey.

Barraclough, J. T. et al., 1967, Hydrology of the National Reactor Testing Station, Idaho, 1966, U.S. Geological Survey Open-File Report, Waste Disposal and Processing TID-4500, IDO-22049, U.S. Geological Survey.

Bartholomay, R. C., and Tucker, B. J., 2000, *Distribution of Selected Radiochemical and Chemical Constituents in Perched Ground Water, Idaho National Engineering and Environmental Laboratory, Idaho, 1996-98*, U.S. Geological Survey Water-Resources Investigations Report 00-4222 (-22168), U.S. Geological Survey.

Bartholomay, R. C., Tucker, B. J., Ackerman, D. J., and Liszewski, M. J., 1997, *Hydrologic Conditions and Distribution of Selected Radiochemical and Chemical Constituents in Water, Snake River Plain Aquifer, Idaho National Engineering Laboratory, Idaho, 1992 through 1995*; U.S. Geological Survey Water-Resources Investigations Report 97-4086 (-22137), U.S. Geological Survey.

Bartholomay, R. C., Tucker, B. J., Davis, L. C., and Greene, M. R., 2000, *Hydrologic Conditions and Distribution of Selected Constituents in Water, Snake River Plain Aquifer, Idaho National Engineering and Environmental Laboratory, Idaho, 1996 through 1998*, U.S. Geological Survey Water-Resources Investigations Report 00-4192 (-22167), U.S. Geological Survey.

Bartholomay, R.C., Knobel, L.L., and Davis, L.C., 1989, Mineralogy and grain size of surficial sediment from the Big Lost River drainage and vicinity, with chemical and physical characteristics of geologic materials from selected sites at the Idaho National Engineering Laboratory, Idaho, U.S. Geological Survey Open-File Report 89-384 (DOE/ID-22081).

Bishop, C. W., August 1991, *Abbreviated Sampling and Analysis Plan Test Reactor Area Perched Water Zone Testing to Determine Aquifer Properties*, EGG-WM-9718, Idaho National Engineering and Environmental Laboratory, EG&G, Idaho, Idaho Falls, Idaho.

Burns, D.E., Davis, K.M., Flynn, S.C., Keck, J.F., Hampton, N.L., Owen, A.H., Van Horn, R.L., 1997, Comprehensive Remedial Investigation/Feasibility Study for the Test Reactor Area Operable Unit 2-13 at the Idaho National Engineering and Environmental Laboratory, Lockheed Idaho Technologies Company, DOE/ID-10531, revision 0, February.

Doornbos, M. H., et al., August 1991, *Environmental Characterization Report for the Test Reactor Area, Volumes I and II*, EGG-WM-9690, Rev. 0, Idaho National Engineering and Environmental Laboratory, EG&G Idaho, Idaho Falls, Idaho.

Garabedian, S.P., 1992, *Hydrology and Digital Simulation of the Regional Aquifer System, Eastern Snake River Plain, Idaho*, U.S. Geological Survey Professional Paper 1408-F, U.S. Geological Survey.

Greeley, R., 1982, "The Style and Basaltic Volcanism in the Eastern Snake River Plain, Idaho," *Cenozoic Geology of Idaho*, ed. B. Bonnichsen and R. M. Breckenridge, Idaho Bureau of Mines and Geology, Bulletin 26.

Hull, L. C., October 1989, *Conceptual Model and Description of the Affected Environment for the TRA Warm Waste Pond (Waste Management Unit TRA-03)*, EG&G Idaho, Inc., Informal Report EGG-ER-8644, Idaho National Engineering and Environmental Laboratory, EG&G Idaho, Idaho Falls, Idaho.

Kaminsky, J.F., Keck, K.N., Schafer-Perini, A.L., Hersley, C.F., Smith, R.P., Stormberg, F.J., and Wylie, A.H., 1994, *Remedial Investigation Final Report with Addenda for the Test Area North Groundwater Operable Unit 1-07B at the Idaho National Engineering Laboratory, Volume 1*, Idaho Falls, Idaho, EG&G Idaho, Inc. Report EGG-ER-10643, variously paged [available from U.S. Department of Energy, Idaho Operations Office, 785 DOE Place, Idaho Falls, ID 83401-1562].

Knutson, C. F., et al., 1990, *FY 89 Report: RWMC Vadose Zone Basalt Characterization*, Prepared for the U.S. Department of Energy Idaho Operations Office, Informal Report EGG-WM-8949, Idaho National Engineering and Environmental Laboratory, EG&G Idaho, Idaho Falls, Idaho.

McElroy, D., and Hubbell, J., 1990, *Hydrologic and Physical Properties of Sediments at the Radioactive Waste Management Complex, Idaho National Engineering Laboratory*, EG&G Idaho, Inc., Informal Report EGG-BG-9147, Idaho National Engineering and Environmental Laboratory.

Miller, S. M., Hammel, J.E., and. Hall, L. F., 1990, *Characterization of Soil Cover and Estimation of Water Infiltration at Central Facilities Area II, Idaho National Engineering Laboratory*, Research Technical Completion Report for Contract C85-110544, University of Idaho.

Morris, D. A., et al., 1964, *Hydrology of Subsurface Waste Disposal, National Reactor Testing Station, Idaho, Annual Progress Report*, IDO-22046-USGS, U.S. Geological Survey.

Morris, D. A., J. T. Barraclough, G. H. Chase, W. E. Teasdale, and R. G. Jensen, 1965, *Hydrology of Subsurface Waste Disposal, National Reactor Testing Station, Idaho, Annual Progress Report, 1964*, U.S. Geological Survey, IDO-22047-USG, U.S. Geological Survey.

Orr, B. R., 1999, *A Transient Numerical Simulation of Perched Ground-Water Flow at the Test Reactor Area, Idaho National Engineering and Environmental Laboratory, Idaho, 1952-94*, U.S. Geological Survey Water-Resources Investigations Report 99-4277, U.S. Geological Survey.

Robertson, J. B., 1977, *Numerical Modeling of Subsurface Radioactive Solute Transport from Waste-Seepage Ponds at the Idaho National Engineering Laboratory*, U.S. Geological Survey Open-File Report 76-717, IDO-22057, U.S. Geological Survey.

Robertson, J.B., Schoen, R., and Barraclough, J.T., 1974, *The influence of liquid waste disposal on the geochemistry of water at the National Reactor Testing Station, Idaho*, U.S. Geological Survey Open-File Report, IDO-22053, U.S. Geological Survey.

Todd, D. K., 1960, *Groundwater Hydrology*, 2nd ed., John Wiley & Sons.

Walton, W. C., 1958, *Analysis of Aquifer Tests at the National Reactor Testing Station, Idaho, 1949-1957*, U.S. Geological Survey, IDO-22034, U.S. Geological Survey.

## 3.3 Waste Area Group 3

Waste Area Group 3 is the designation for the collection of CERCLA OUs associated with the INTEC. INTEC is located in the south-central part of the INEEL on the relatively flat floodplain adjacent to the Big Lost River (see Figure 3-15).

INTEC facilities were constructed in the early 1950's, primarily to reprocess spent nuclear fuel rods and to stabilize high-level liquid wastes through calcinization. Presently, the INTEC mission is to safely store spent nuclear fuel and prepare it for shipment to an offsite repository, to develop technology to safely treat high-level and liquid radioactive waste that resulted from past spent-fuel reprocessing activities, and to remediate past environmental releases.

This chapter summarizes the current conceptual model of groundwater flow and contaminant transport at WAG 3. It also serves as an index to previous investigations and sources of WAG 3 hydrologic information. This section does not present any original hydrogeologic work, but simply summarizes technical elements that contribute to the conceptual model. The conceptual model is discussed in general terms in Section 3.3.2, followed by detailed discussions of hydrologic information in subsequent sections. Factors affecting contaminant transport are presented in Section 3.3.2.6. Although it does not include an exhaustive discussion of contaminant transport, Section 3.3.2.6 presents several of the key factors currently under investigation. A history and comparison of the numerical models developed for WAG 3 is presented in Section 3.3.3. Finally, a brief discussion of ongoing conceptual model competing hypotheses is found in Section 3.3.4.

### 3.3.1 Background

Numerous geohydrologic studies have been conducted in conjunction with remediation activities at INTEC. Other studies have been conducted as part of the sitewide characterization of flow and transport. These studies have provided an understanding of the elements of the conceptual model at INTEC.

In 1991, INTEC facilities were designated as WAG 3 under the FFA/CO (DOE-ID 1991). This agreement established the procedural framework and schedule for CERCLA, Resource Conservation and Recovery (RCRA), and HWMA response actions. The 1991 FFA/CO designated INTEC (then known as the Idaho Chemical Processing Plant [ICPP]) into two OUs. OU 3-13 included all INTEC areas with the exception of the Tank Farm, which was designated as OU 3-14. OU 3-13 was investigated to identify the potential contaminant releases and exposure pathways to the environment from individual sites as well as the accumulated effects of related sites. The OU 3-13 RI/FS (DOE-ID 1997b) identified a total of 99 release sites, of which 46 were demonstrated to have a potential risk to human health or the environment. These 46 sites were divided into seven groups based on similar media, COCs, accessibility, or geographic proximity.

The INTEC RI/BRA was completed in 1997 to determine comprehensive risks posed by past releases at WAG 3 (DOE-ID 1997a). The INTEC Feasibility Study also was completed in 1997 to determine and evaluate feasible remedial alternatives (DOE-ID 1997b) and identify any additional information that was needed. Review of the Feasibility Study by the National Remedy Review Board resulted in preparation of a Feasibility Study supplement, which was completed in 1998 (DOE-ID 1998).

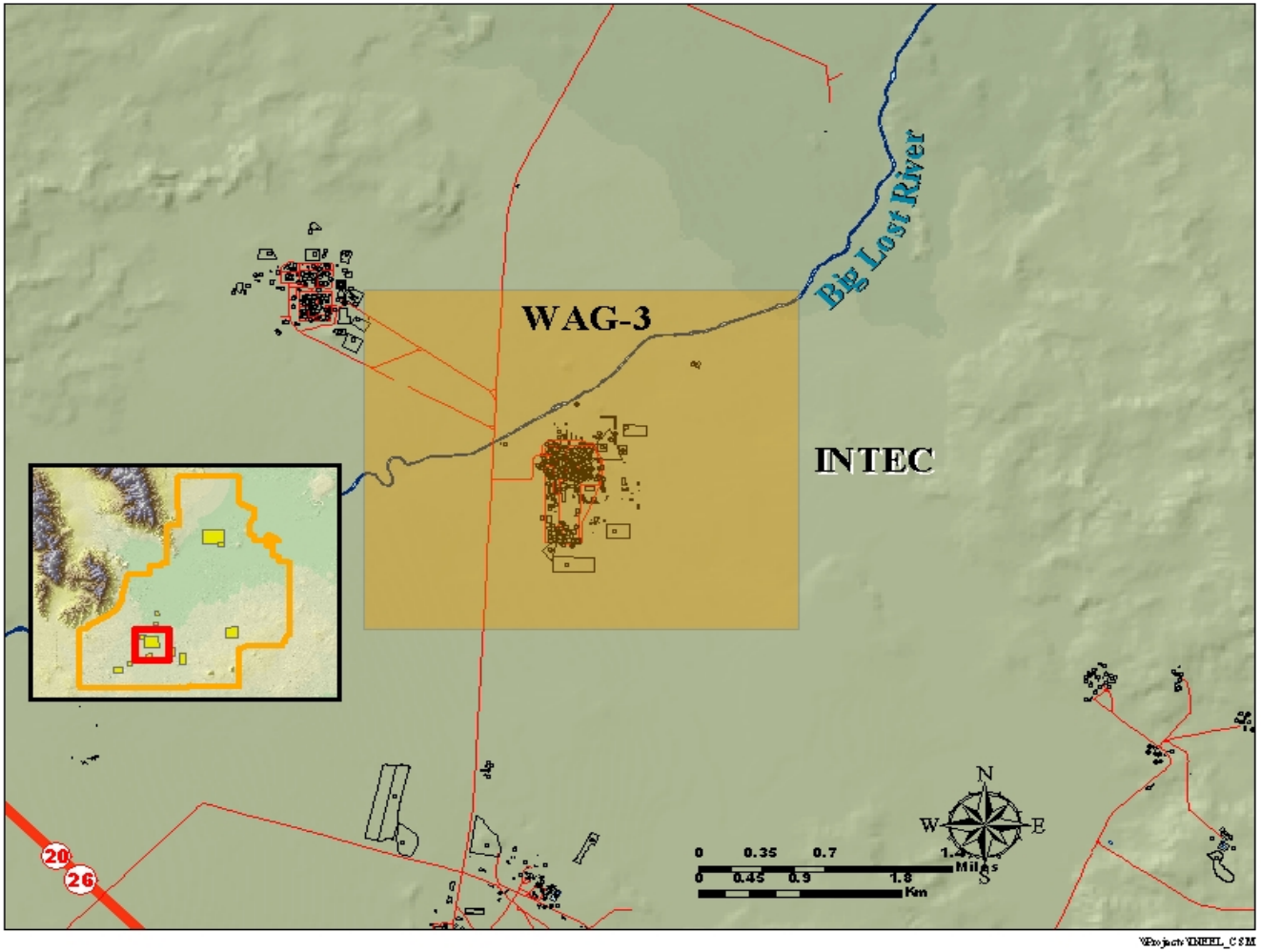


Figure 3-15. Location of the INTEC and WAG 3.

The OU 3-13 Record of Decision (ROD), which was signed in 1999 (DOE-ID, 1999), presents the selected remedial actions for the seven groups identified in the RI/BRA and specifically provides for Group 4 perched water monitoring to assess the perched water drain-out and contaminant flux into the SRPA (DOE-ID 1999). A monitoring system and installation plan (DOE-ID, 2000a) was developed to describe work elements required to implement the selected remedies presented in the ROD. In turn, a field sampling plan (DOE-ID, 2000b), a tracer test plan (DOE-ID, 2000c), and a long-term monitoring plan (DOE-ID, 2000d) were developed to implement the monitoring system and installation plan. Data collected as a result of those plans through October 15, 2001 are presented in the *Phase I Monitoring Well and Tracer Study Report for Operable Unit 3-13, Group 4, Perched Water* (DOE-ID 2002a).

The USGS has conducted studies at INTEC to characterize flow and contaminant transport through the vadose zone and the aquifer. Anderson (1991) correlated basalt flow groups and sedimentary interbeds in the vadose zone and SRPA beneath INTEC. This study provided a basis for description of the geohydrologic framework at INTEC. Cecil et al. (1991) examined the formation of perched groundwater zones and perching mechanisms in the vadose zone at INTEC and other sites. Ackerman (1991a and 1991b) evaluated hydraulic properties of basalts in the SRPA and perched groundwater zones in wells located at INTEC and other sites. Mann and Beasley (1994) evaluated the distribution of iodine-129 in groundwater as a result of disposal to a deep injection well at INTEC.

Additionally, the USGS has maintained a long-term network of wells to monitor water-level changes and the distribution of radioactive and chemical constituents in groundwater. Contaminant distribution and water-level data from aquifer wells at and near INTEC are included in a series of hydrologic conditions reports (Pittman et al. 1988; Orr and Cecil 1991; Bartholomay et al. 1995; Bartholomay et al. 1997; and Bartholomay et al. 2000). A parallel series of reports describe conditions in perched groundwater zones at INTEC and other sites (Cecil et al. 1991; Tucker and Orr 1998; and Bartholomay and Tucker 2000). A report by Bennett (1990) describing infiltration losses on the Big Lost River provides information about episodic recharge near INTEC.

Other researchers have conducted studies at INTEC to evaluate aspects of flow and transport in the SRPA. Morin et al. (1993) used geophysical logging techniques to evaluate the vertical dimension of groundwater flow at INTEC. Frederick and Johnson (1996) used water-level data from packer tests in four INTEC wells to estimate hydraulic properties and to develop a layered conceptual model of the SRPA. Frederick and Johnson (1997) examined the vertical and temporal water-chemistry profiles in a well near INTEC to evaluate geochemical data variations in a stratified system.

### 3.3.2 Summary of the Present WAG-3 Conceptual Site Model

The current conceptual model of groundwater flow and contaminant transport at INTEC is based on the understanding that the geohydrologic framework consists of a highly complex sequence of layered basalt and sediment units (DOE-ID 1997a). Key features of the conceptual model include the thick, complex systems of layered basalts and sedimentary units in the vadose zone; areally extensive recharge from infiltration ponds and point source recharge from features such as steam vents; the location of the Big Lost River directly northwest of INTEC; occurrence of perched groundwater beneath several INTEC facilities; distributed and point contaminant sources at the surface, in perched water, and in the aquifer; and proximity of INTEC to the TRA. The following sections summarize the components of the conceptual model including the geologic framework, matrix characteristics, sources of recharge and discharge, the hydraulics of the resultant flow field, chemistry of groundwater, and contaminant transport.

***3.3.2.1 Geologic Framework.*** The basalts and sediments that comprise the thick vadose zone and SRPA beneath INTEC provide the geologic framework within which water and contaminants move in the subsurface. This geologic framework is defined by its geometry, stratigraphy, and structure.

***System Geometry—***INTEC is located about 10 mi east of the Lost River Mountain Range. Local features pertinent to contaminant transport at INTEC, which include INTEC and associated facilities, the Big Lost River, and TRA (see Figure 3-15) are located within an area of a few square miles. INTEC encompasses 200 acres and extends approximately 3,600 ft from north to south, and 2,000 ft from east to west. The channel of the Big Lost River runs to the northeast directly adjacent to the northwest corner of the INTEC fence. The TRA lies approximately 1 mi to the northwest.

Known distributions of contaminants in the vadose zone at INTEC are restricted to the areas immediately adjacent to the INTEC fences. The area of interest within the vadose zone (see Figure 3-15) extends from INTEC about 6,600 ft from east to west and 9,800 ft from north to south (DOE-ID 1997a).

The known distribution of contaminants in the SRPA encompasses a much larger area (see Figure 2-11). The tritium plume above a detection limit of 5 pCi/mL, attributed in part to disposal of radioactive wastewater at INTEC, has been estimated to exceed 50 $mi^2$ in the past. Because of the extent of contamination, the area of interest in the aquifer extends almost 2 mi north of INTEC, 7 mi south of the INEEL boundary, 4 mi east of INTEC, and almost 16 mi west of the RWMC (DOE-ID 1997a).

The combined thickness of the alluvial gravels, basalts, and sedimentary interbeds comprising the vadose zone beneath INTEC is approximately 450 ft. Within the SRPA at INTEC, the region of interest predominantly includes perhaps 100 ft of layered basalt flows, an intervening interbed of unknown extent, and a deeper basalt flow group that may exceed a thickness of several hundred feet in places (DOE-ID 1997a).

***Geology—***INTEC is located on the thick deposits of alluvial gravels associated with the relatively flat floodplain of the Big Lost River. This floodplain overlies the eastern Snake River basalt plain, formed by eruption of basalts from low shield volcanoes and vents. Overlapping flows produced the complex stratigraphy underlying INTEC.

Geologic features adjacent to INTEC include a series of volcanic rift zones, rhyolite domes, and other eruptive features (Anderson 1991). The Arco volcanic rift zone extends southeast across the southwestern part of the INEEL. The axial volcanic rift zone extends southwest across the southeastern part of the INEEL. The Lava Ridge volcanic rift zone extends southeast across the northern part of the INEEL. A series of rhyolite domes occur to the south. The AEC Butte is an eruptive feature about 2 mi northwest of INTEC that was the source for an areally extensive, thick basalt unit.

***Stratigraphy/Lithology—***The vadose zone and SRPA beneath INTEC (see Figure 3-16) consist of a thick layer of surficial alluvium underlain by a sequence of interbedded basalt flows and sedimentary interbeds (Mann, 1986). Older basaltic and rhyolitic rocks occur at depth.

***Surficial Alluvium—***Surficial alluvium at INTEC consists largely of fluvially deposited gravels. The gravels are medium to fine-grained and cover the underlying basalts with an average thickness of 45 ft (DOE-ID 2002a). Much of the gravels at INTEC have been reworked, particularly in the vicinity of the Tank Farm Complex, where gravels were removed during construction activities and later by remedial activities.

***Basalt Flows—***A thick sequence of basalt flows and sedimentary interbeds lies beneath the gravels at INTEC. Borehole INEL-1, drilled to a depth of 10,365 ft about 4.5 mi north of INTEC, encountered 2,000 ft of this sequence. The basalt stratigraphy beneath INTEC has been described through physical characterization of cores and cuttings and by geophysical logging from over 70 wells completed in the SRPA (Anderson 1991; see Figure 3-16).

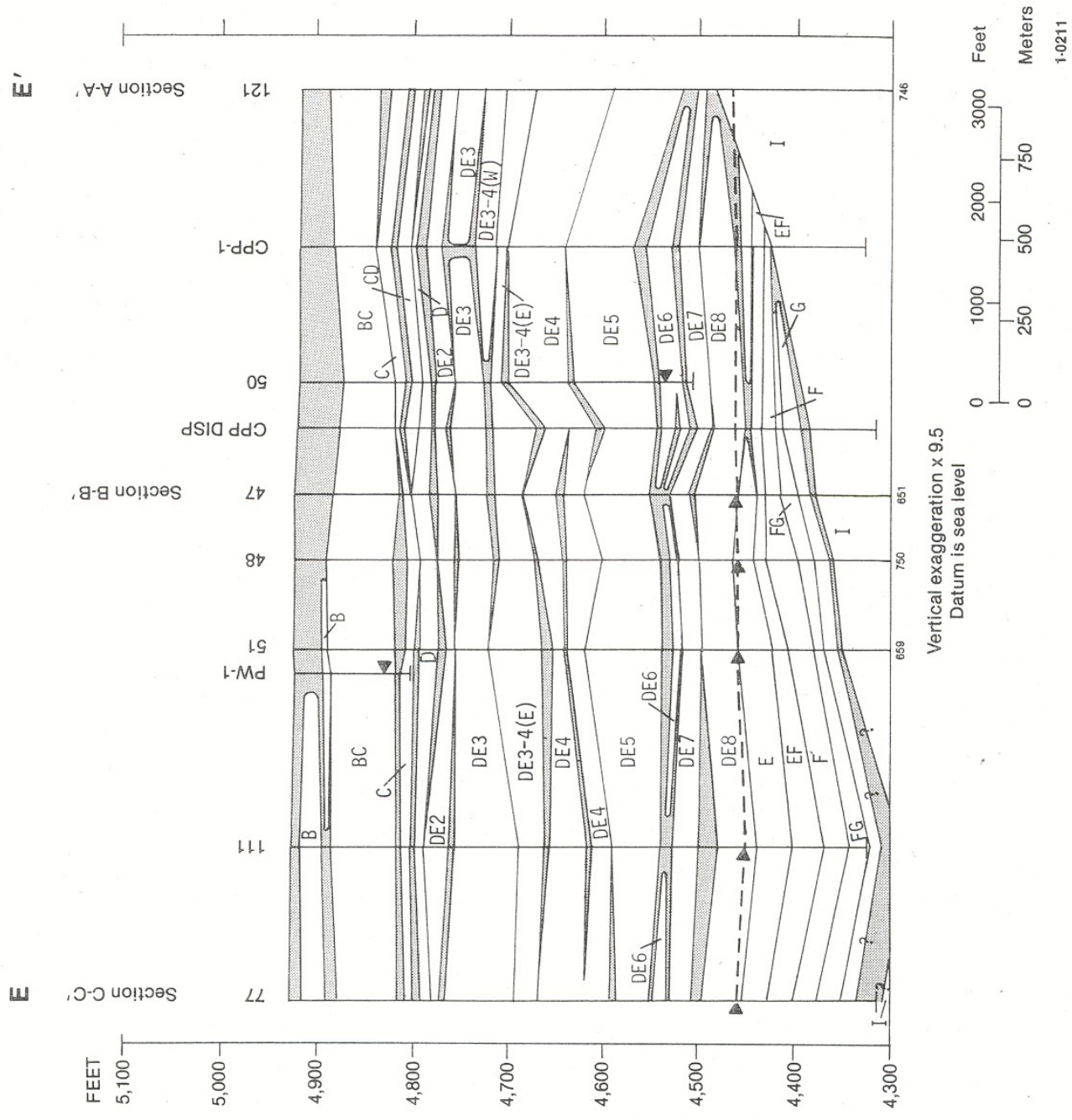


Figure 3-16. Stratigraphy of basalt flow groups and sedimentary interbeds at INTEC (from Anderson 1991).

Anderson (1991) describes five composite stratigraphic units in the vadose zone beneath INTEC. These units include at least 14 basalt flow groups consisting of thin to thick basalt flows and related sedimentary interbeds. Anderson identifies two composite stratigraphic units within the upper part of the SRPA at INTEC. The upper unit consists of at least six flow groups composed of thin, discontinuous basalt flows that are underlain by a widespread sedimentary interbed. The lower unit consists of flow group I. This unit is composed predominantly of thick basalt flows and minimal sediment.

The basalt flows beneath INTEC are characterized as overlapping lobes of basalt intermixed with larger basalt flows of relatively uniform thickness (DOE-ID 1997a). Changes in flow thickness frequently are attributed to changes in basalt flow characteristics or proximity to the flow margins. Basalt flow characteristics, including the presence of pyroclastic deposits on or within a flow or increased flow vesicularity, may enhance the effects of erosion. These characteristics can vary both laterally and vertically within an individual flow, and the same flow can exhibit weathered, vesicular, fractured, and massive textures in different locations and depths.

Stratigraphic correlation of flows across the site has been accomplished by geophysical methods; however it is difficult due to similarities between flows. Numerous flows appear as irregular and discontinuous lobes which overlap more continuous flows (see Figure 3-16; DOE-ID 1999).

The basalt flows increase in thickness and decrease in hydraulic conductivity with depth. This decrease can be partially attributed to decreased interflow rubble zones and to mineralization within fractures and other porous regions of the flows.

At INTEC, the part of the SRPA considered to be of interest by the WAG-3 RI/BRA (DOE-ID 1997a) includes the upper composite stratigraphic unit (identified in the report as the H flow group and includes Anderson's [1991] E through H flow groups), the HI interbed, and upper sections of the lower composite stratigraphic unit (identified as the I flow group). The effective thickness was established to include the total penetration of the deep injection well, assuming that most mixing of contaminants will take place in that interval (DOE-ID 1997a). The combined thickness of these units of interest in the aquifer is estimated to be approximately 250 ft. Underlying basalts, although part of the SRPA, are considered in the WAG-3 conceptual model to lie beneath the area of interest in terms of contaminant transport.

***Sedimentary Interbeds—***Multiple sedimentary interbeds have been identified among the basalt flows at INTEC. These interbeds were deposited during long periods of volcanic quiescence. With several exceptions, they are not areally continuous and consist of sands and silts with some clay, probably of eolian and fluvial origin. Most individual sedimentary interbeds typically are from 1 to 5 ft thick. Interbed morphology appears to be controlled by the topography of the underlying basalt and by the length and nature of the local erosional and depositional environment between successive eruptive events.

In the vadose zone, significant accumulations of sedimentary interbeds are associated with upper basalt flows designated by Anderson (1991) as the C through the DE2 basalt flow groups. These sediments appear to be a thick sequence of sands overlain and underlain by silts and clays. Significant accumulations of interbeds also are associated with deeper vadose zone basalts designated by Anderson (1991) as the DE6 through DE8 basalt flow groups. The sediments associated with these deeper basalt flow groups generally consist of fluvial gravels, silts, and clays.

A sedimentary interbed (HI interbed) occurs in most wells near INTEC at the base of the upper composite stratigraphic unit. This widely distributed interbed is considered in the WAG-3 conceptual model to be a dominant stratigraphic feature in the aquifer (DOE-ID 1997a) and is believed to hydraulically separate the upper and lower stratigraphic units in the aquifer (Arnett and Smith 2001).

Sedimentary interbeds associated with the lower composite stratigraphic unit (I flow group) are minimal, ranging from 0 to 3% of the total thickness (Anderson 1991).

***3.3.2.2 Matrix Characteristics.*** Unsaturated and saturated hydraulic conductivity and effective porosity of sediments and basalts control the storage and movement of water through the vadose zone and the SRPA beneath INTEC. These hydraulic properties are derived from the lithologic and stratigraphic character of the eastern Snake River Plain.

***Vadose Zone—***The vadose zone is approximately 450 ft thick at INTEC (see Figure 3-16). Hydraulic properties of the thick, surficial sediments, sedimentary interbeds, and basalt flows of the vadose zone have been determined from aquifer test data and laboratory analyses.

***Surficial Sediments—***The alluvial gravels underlying INTEC are very permeable, and the ability to store and transmit surface water to the subsurface within INTEC is influenced by anthropogenic features such as buildings and tanks, roads, impermeable liners, and ditches. These features may serve to amplify infiltration rates by locally concentrating runoff and reducing evaporation. The gravels near the Big Lost River have been are observed to contain perched water zones during and shortly after episodic flows of sufficient magnitude to laterally transmit water.

***Vadose-Zone Interbed Sediments—***Hydraulic properties of vadose-zone interbed sediments determined from aquifer tests and laboratory analyses include saturated hydraulic conductivity, moisture content, and porosity. Hydraulic conductivity was determined from aquifer tests conducted in sedimentary interbeds in six INTEC perched-water wells, which ranged from 0.11 to 5.1 ft per day (DOE-ID 1997a). Saturated hydraulic conductivities determined from laboratory analyses of interbed sediments in the vadose zone beneath INTEC ranged from $1.5 \times 10^{-4}$ to 6.2 ft per day (DOE-ID 1997a).

Laboratory initial moisture content of five INTEC core samples ranged from 12.7 to 33.2% by volume (DOE-ID 1997a). Calculated porosity ranged from 33.6 to 61%.

***Vadose-Zone Basalt Flows—***The basalt flows, comprising the majority of the vadose zone and the upper portions of the SRPA beneath INTEC, make up a complex system of fractured and massive basalt flows with large ranges of hydraulic properties. The basalt-flow permeabilities are controlled by widely varying lithology within a particular flow (i.e., fractures, interflow rubble and pyroclastic zones, weathered zones, vesicularity, and massive zones). The vadose zone (and upper aquifer) permeabilities are controlled by the spatially changing lithologic characteristics of individual basalt flows and by the extent of basalt flows and interbeds.

Hydraulic conductivities measured in saturated basalt flows associated with perched groundwater bodies in the unsaturated zone (in perched zones) beneath INTEC range from 0.57 to 9.6 ft per day, and average 4.3 ft per day (n = 6). These values were determined by pumping/recovery drawdown test methods (DOE-ID 1997a) and were within the range of 0.014 to 790 ft per day estimated by Ackerman (1991b) from 43 tests in 22 wells at TRA and INTEC.

The INTEC conceptual model assumes that fracture network dominates vadose-zone flow and that the system can be treated as an anisotropic, "single-porosity" media, neglecting the matrix permeability (DOE-ID 1997a). The ratio of horizontal to vertical permeability is estimated to be 300 to 1. The effective porosity of the fractured basalt is estimated to be 5%.

***SRPA—***Transmissivity estimates of the SRPA from INTEC well data ranges from 10 to 760,000 $ft^2$ per day (DOE-ID 1997a; Ackerman 1991a). This five-order of magnitude difference locally impacts the

groundwater flow direction and contaminant distribution in the vicinity of INTEC (DOE-ID, 1997a). Hydraulic conductivity estimates, made by dividing the transmissivity by the saturated thickness of the open interval of the well, ranged from 0.1 to 10,000 ft per day with an average of about 1,300 ft per day. Values above the HI interbed probably are much larger. The aquifer transmissivity decreases with depth because of thicker flows beneath the HI interbed and because of mineralization along/within fractures and interflow zones. In places, the HI interbed may cause confined or semi-confined conditions in the SRPA below it. However, this probably is not an issue beneath INTEC where the HI interbed is relatively thin.

The effective porosity of the basalts is a measure of the interconnected pore spaces consisting of interflow rubble zones, fractures, and interconnected vesicles. The effective porosity of basalts at INTEC has been estimated by previous researchers to be 10%. Inverse modeling techniques and contaminant distribution data were used to estimate an effective porosity of 6%.

***3.3.2.3 Recharge/Discharge Sources.*** Sources of water in the subsurface beneath INTEC include underflow within the SRPA, episodic flows in the Big Lost River, disposal of wastewater to the deep injection well and percolation ponds, leakage from piping, and precipitation. Aquifer discharge at INTEC occurs as pumpage from production wells.

***Underflow in the SRPA—***Water in the SRPA that passed beneath INTEC from the northeast is assumed to be consistent with WAG-10 underflow estimates from transmissivity and hydraulic gradient. No estimates of underflow are given in the RI/BRA (DOE-ID, 1997a, Appendix F).

***Episodic Recharge—***Periodic flows in the channel of the Big Lost River adjacent to INTEC are associated with years of increased snowpack in the mountainous drainage areas to the west. Much of this water infiltrates along the stream channel. The volume of this source of episodic recharge can be significant during wet years (DOE-ID 1997a).

Perched water has been observed in the vadose zone adjacent to the Big Lost River during episodic flow. The extent and volume of these perched-water zones are not well known. However, during periods of flow, water levels in perched-zone wells near INTEC rise abruptly (DOE-ID 1997a).

***Recharge from Wastewater Disposal—***Wastewater has been disposed at INTEC using an injection well and infiltration ponds. Additionally, water has been released to the shallow subsurface through stream condensate disposal and by leakage from system piping.

***Injection Wells—***The ICPP injection well was used during 1952 through 1984 to discharge water containing low-level radioactive and chemical wastes directly to the SRPA (Bartholomay et al. 2000). This injection well was drilled to a depth of 597 ft and cased with 16-in. carbon steel casing. The well casing was perforated from 412 to 452 ft and from 490 to 593 ft. The average annual discharge during 1952 through 1984 was approximately 363 million gal for an average of about 1 million gal per day. In the late 1960's and early 1970's, failure of the ICPP injection well resulted in discharge of wastewater directly to the vadose zone at a reported depth of 226 ft (DOE-ID 1997a).

***Recharge from Surface and Shallow Subsurface Wastewater Disposal—***Table 3-2 (modified from DOE-ID 1997a, Table 2-7) summarizes the estimated volume of surface or near-surface recharge available from various sources at INTEC. These sources include service wastewater percolation ponds, sewage treatment ponds, leakage from water systems, irrigation, and disposal of steam condensate.

Table 3-2. Estimated volume of recharge from wastewater disposal and leakage at INTEC.

| Source | Northern part of INTEC Volume (gal/yr) | Northern part of INTEC Percent | Entire Facility Volume (gal/yr) | Entire Facility Percent |
|---|---|---|---|---|
| Service wastewater | None | 0 | 690,000,000 | 95.8 |
| Sewage treatment ponds | 15,000,000 | 58 | 15,000,000 | 2.1 |
| Water system leaks | 3,980,000 | 16 | 3,980,000 | 0.6 |
| Landscape irrigation | 1,568,000 | 6 | 1,568,000 | 0.2 |
| Precipitation infiltration | 3,800,000 | 15 | 8,000,000 | 1.1 |
| Steam condensate | 1,300,000 | 5 | 1,700,000 | 0.2 |
| CPP-603 Basins | None | 0 | 49,275 | <0.1 |
| **Total** | 25,648,000 | 100 | 720,297,275 | 100 |

The largest surficial source of recharge from wastewater disposal at INTEC is from disposal to the two service waste percolation ponds located immediately to the south of the facility. An average of approximately 690 million gal per year of service wastewater has been discharged to these percolation ponds since their construction in 1984. An additional 15 million gal per year are discharged into the infiltration galleries of the new sewage treatment plant in the northeastern corner of the facility.

Identification of perched groundwater bodies beneath INTEC, with no known source of recharge, led to a water inventory study (Richards 1994). This study was performed to determine whether water was leaking from the plant's water supply and wastewater systems in sufficient quantities to support these perched water bodies. The study determined that leakage from the fire water system and the potable water system historically provided nearly 4 million gal per year of recharge. These leaks have been repaired, but the potential exists that other unknown leaks may be present in the 14 mi of piping. Assuming a 5% error in metering, an annual undetected leakage volume of as much as 38.4 million gal could occur.

Landscape watering systems in the northern part of the INTEC irrigate approximately 1.5 acres of lawn. Approximately 2.35 million gal are used annually to water INTEC lawns. Of this, a net volume of approximately 1.57 million gal is available for infiltration and recharge.

The discharge of steam condensate from facility heating may provide another source of recharge to the subsurface. The average annual volume of steam condensate discharged to the ground is estimated to be 1.7 million gal. A total of 1.3 million gal are discharged where the condensate could contribute recharge to perched water beneath the northern part of INTEC.

In addition, precipitation at INTEC is channeled into a system of ditches and runoff infiltration ponds. This source provides an estimated 8 million gal per year for recharge to the shallow subsurface.

***Recharge from Precipitation—***Infiltration of local precipitation may augment recharge to perched water bodies. Long-term average precipitation at the INEEL is 8.7 in. per year. Although pan evaporation losses greatly exceed average precipitation, water from snowmelt or heavy rains may infiltrate to a depth

where it cannot be evaporated, particularly where runoff is focused by pavement and drainage ditches. Miller et al. (1990) estimated net recharge from precipitation to range from 1 to 4 in. per year with a best estimate to be 1.6 in. per year. Assuming a net infiltration rate of 1.6 in. per year and the area available for recharge at INTEC to be approximately 184 acres, approximately 8 million gal of water may be available for recharge from local precipitation.

***Discharge from the SRPA to INTEC Groundwater Pumpage—***The INTEC uses an average of approximately 2.1 million gal of water per day or 767 million gal per year (DOE-ID 1997a). Much of this water is recharged through facility disposal systems. Water is supplied from two raw-water wells and two potable-water wells located in the northern part of the facility. This water is carried through about 14 mi of piping from the primary water systems at the INTEC, including the raw-water, fire-water, treated (softened) water, demineralized water, steam-condensate, landscape-watering, potable-water, service-waste (industrial wastewater), and sanitary waste systems.

***3.3.2.4 Hydraulics.*** The character of subsurface flow at INTEC is defined by the integration of components of the WAG-3 conceptual model. Saturated flow occurs in the SRPA. Saturated and unsaturated flow occurs in the vadose zone.

***Snake River Plain Aquifer—***Flow within the SRPA is believed to be unconfined. However, because of the layered character of the basalts and interbeds, flow locally may be confined or partially confined (DOE-ID 1997a). The flow field within the aquifer is defined by the hydraulic gradient, direction of flow, and flow velocity.

***Gradient and Flow Direction—***INEEL-wide water-level data collected during 1998 indicated the general direction of groundwater flow across the INEEL was toward the south and southwest at an average gradient of about 4 ft/mi (see Figure 2-8 in Chapter 2; Bartholomay et al. 2000). The gradient in the vicinity of INTEC is less, averaging 1.2 ft/mi (DOE-ID 1997a).

Locally, the direction of groundwater flow may vary due to the variability of the hydraulic characteristics of the aquifer within a small area (DOE-ID 1997a). A region of relatively small transmissivity directly to the south of the INTEC locally affects the direction of flow as well as distribution of contaminants (DOE-ID 1997a). Recharge from episodic flow in the Big Lost River has been demonstrated to modify the direction of flow (DOE-ID 1997a). Pumpage from INTEC supply wells also can locally affect the direction of flow (DOE-ID 1997a).

***Flow Rate (Horizontal)—***Groundwater flow velocities between INTEC and downgradient wells were calculated using iodine-129 data, which were estimated to range from 5 to 20 ft per day with an average of 10 ft per day (Robertson et al. 1974). Iodine-129 first-arrival data provided an estimate of about 6 ft per day (Mann and Beasley 1994). Horizontal groundwater flow rates in the SRPA have been estimated to range from 0.3 to 7.6 m/day (1 to 25 ft/day; Kaminsky et al. 1994; Robertson et al., 1974).

***Vadose Zone—***The vadose zone beneath INTEC is approximately 450 ft thick. Water from surface or shallow subsurface recharge moves vertically through the vadose zone as unsaturated flow in fractured basalts without vertical permeability contrasts, and vertically and horizontally as saturated flow within perched water bodies.

***Unsaturated Flow—***Little information is available about unsaturated flow in the vadose zone at INTEC. Comparison of neutron moisture logs in a well located near the two service-waste ponds indicated that moisture content increased beneath those ponds when disposal began in 1984 (Cecil et al. 1991). Increased moisture content has been observed in unsaturated parts of the vadose zone (Cecil et al.

1991). Moisture content in 15 interbed samples from nine vadose-zone coreholes ranged from 12.7 to 56.8% by volume (DOE-ID 1997a).

Rapid lateral flow has been observed in the vadose zone in response to recharge. The 1999 tracer test at the INEEL spreading areas demonstrated that water can move laterally in the vadose zone for significant distances (Nimmo et al. 2001). Water-level changes in a perched zone well near the Big Lost River west of INTEC were used to estimate a lateral flow velocity as large as 3 ft per hour (DOE-ID 1997a).

***Perched Groundwater—***Perched groundwater zones have been identified in the vadose zone beneath sources of surface and shallow subsurface recharge in the northern part and southern part of INTEC. Several discontinuous zones of perched water have formed as a result of site operations and natural recharge sources at the interface between the surface alluvium and the shallowest basalt flow, in upper basalts, and in deeper basalts.

Perched groundwater has been detected in the upper basalts beneath the sewage treatment pond and beneath the Tank Farm in the northern part of INTEC, near building CPP-603, and beneath the percolation ponds south of INTEC (DOE-ID 2002). Upper perched groundwater zones occur at depths from 100 to 140 ft. The upper perched water zones are fragmented, rather than continuous, zones of saturation that occur above the CD and D interbeds and the in the DE3 interbed. Water-level and water-chemistry data indicate that upper perched groundwater zones beneath the north and south parts of INTEC are separated and chemically different (DOE-ID 2002b). The actual extent of these perched water bodies is not well defined and the connections between the perched water bodies are not well understood (DOE-ID 2002).

Multiple water sources may provide recharge to the upper perched water body in the northern part of INTEC. These sources may include recharge from the Big Lost River, the wastewater treatment lagoons, and operational water distribution system releases. A tracer study was begun in 2001 to differentiate the contributions of these possible recharge sources.

Perched water has been identified beneath two areas of southern INTEC. A small perched water body has been identified in the vicinity of building CPP-603, and a larger perched water body has developed from the discharge of wastewater to the percolation ponds.

Deeper perched groundwater zones occur in basalts at depths ranging from 320 to 420 ft. The extent of deep perched water is not well defined. Seven wells in the northern part of INTEC and two wells in the southern part monitor deep perched groundwater (DOE-ID 2002a). The lower zones are formed because of decreased permeability associated with sedimentary interbeds at depths ranging from 383 to 426 ft (DOE-ID 2002a, 5-22).

Water levels in the lower perched groundwater zone have been monitored since the early 1960s in USGS-50. The water level in this well has been fairly consistent, ranging between 287 and 382 ft, except for a period in the late 1960s and 1970s when the water level rose approximately 90 ft in response to casing collapse in the ICPP injection well (DOE-ID 2002a). During this period, wastewater was discharged directly to the vadose zone at a reported depth of 226 ft (Fromm et al. 1994). Discharge of wastewater directly into the vadose zone resulted in a possible source of contamination of the deep perched groundwater zone.

***3.3.2.5 Groundwater Chemistry.*** Water from the SRPA in the southern half of the INEEL typically is enriched in calcium, magnesium, and bicarbonate (Knobel et al. 1997). Aquifer water

underlying INTEC is similar in composition. The background concentrations of sodium, chloride, sulfate, and nitrate are 10, 15, 10 to 40, and 5 mg/L, respectively (Robertson et al. 1974). Wastewater disposed to the injection well and percolation ponds has increased the concentrations of these and other ions in groundwater downgradient from INTEC (Bartholomay et al. 2000).

Perched groundwater bodies have formed in response to wastewater disposal at INTEC. Wastewater originates from the SRPA, but chemical processes at INTEC modify the water chemistry. The chemistry of water in perched groundwater bodies is chemically different depending on the location and source (see Figure 3-17; DOE-ID 2000b).

***3.3.2.6 Contaminant Transport.*** Radioactive, inorganic, and organic chemical contaminants were contained in wastewater disposed to the subsurface at INTEC through routine wastewater disposal practices and through spills and leakage. Migration of these contaminants has resulted in detectable concentrations in the aquifer and in perched groundwater bodies. The following sections briefly describe the contaminant source term, transport mechanisms, and distribution of contaminants in the subsurface.

***Source Term—***Radioactive, inorganic chemical, and organic chemical contaminants derived from INTEC operations have been disposed to injection wells and French drains, percolation ponds, pits, and leach fields. Contaminants also have been introduced to the subsurface through spills and piping leakage at the Tank Farm and other sites. Principal sources of contamination at the INTEC have been derived from historical waste disposal to the deep disposal well, leakage from the concrete holding tanks in building CPP-603, and accidental releases to the environment (DOE-ID 1997a). Wastewater currently is discharged to two percolation ponds and sewage treatment ponds. Based on pond-sediment characterization data and the chemistry of the waste streams to these disposal points, these two sources do not contribute significantly to the inventory of contaminants. However, water movement from these ponds may affect the migration of contaminants in other areas of the INTEC. The source term is defined by the contaminant inventory, method of release, and rate of release.

***Contaminant Inventory—***Contaminants released to the subsurface since the early 1950's have included radionuclides, inorganic chemicals, and organic chemicals. Table 3-3, modified from Table 5-42 of Appendix F, INTEC Remedial Investigation report (DOE-ID 1997a), summarizes the total mass or activity of contaminants of potential concern and the point of disposal.

***Release Mechanisms—***Contaminant migration is controlled, in part, by the point and mechanism of release. Contaminant release in the vadose zone delays the arrival of contaminants at the water table. More reactive contaminants may be temporarily or permanently attached to sites within the vadose zone.

- **ICPP Injection Well, CPP-23**

  Since 1952, INTEC processes have generated large volumes of plant-cooling wastewater and condensate that contained small quantities of radioactive and inorganic contaminants (DOE-ID 1997a). The ICPP injection well was used to dispose these low-level radioactive and chemical wastes to the SRPA during 1952 through 1984.

  The ICPP injection well was drilled in 1950 to a total depth of 597 ft (24-in. borehole), cased with 16-in. carbon steel casing, and gravel packed. Casing was perforated from a depth of 412 to 452 ft and from 490 to 593 ft. During 1967 and 1968, the injection well collapsed at a depth of 226 ft. In 1970, the injection well was redrilled and a new liner was installed. During this time, wastewater was disposed to well USGS-50.

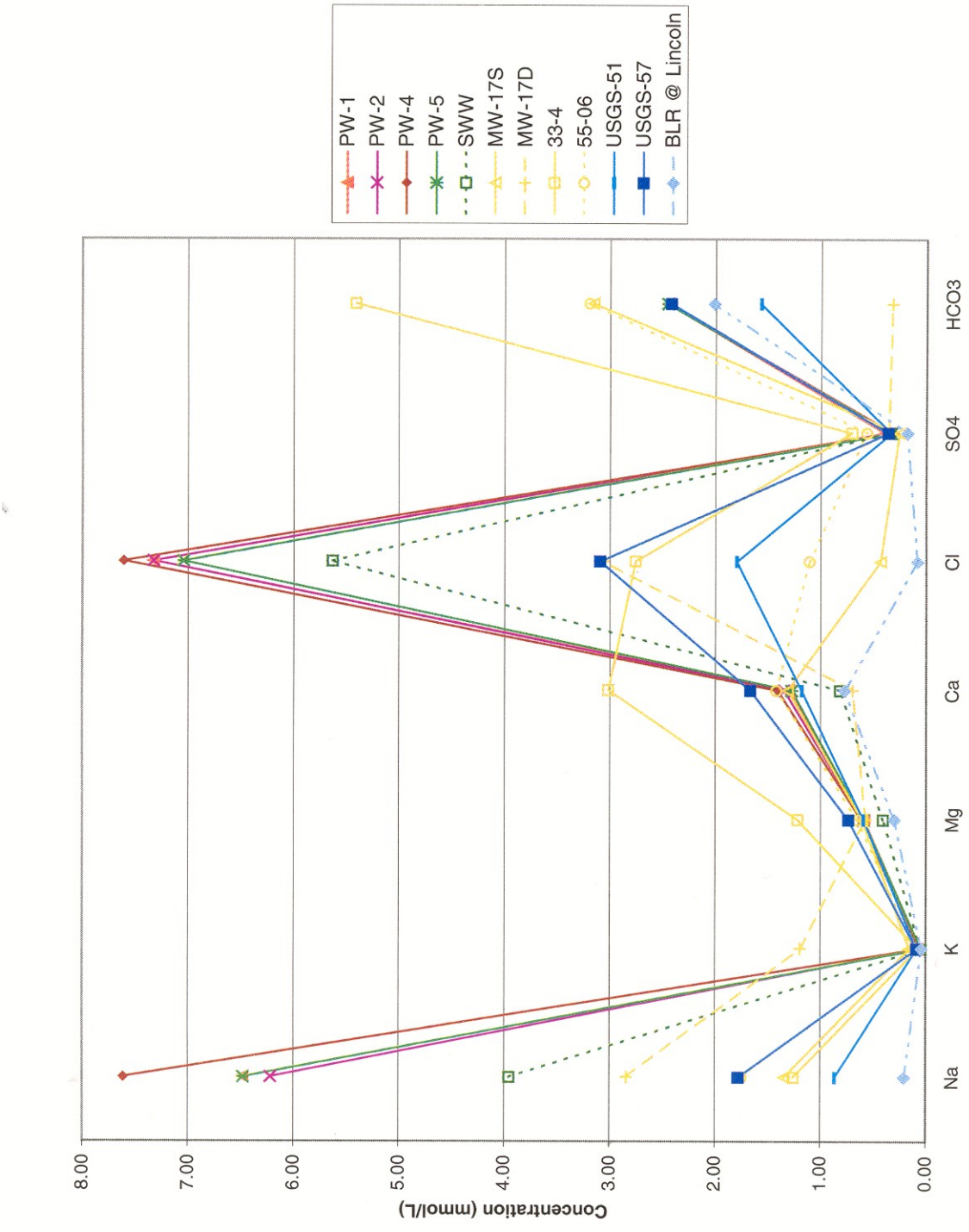


Figure 3-17. Schoeller diagram of water quality for perched water, service wastewater, the SRPA, and the Big Lost River (from DOE-ID 2002b).

Table 3-3. Summary of total mass or activity for COCs and contamination sources at INTEC.

| Contaminant of Potential Concern | Units | Known Release | | Service Waste | | Soil Contamination | Total |
|---|---|---|---|---|---|---|---|
| | | Tank Farm | Other | Injection Well | Percolation Ponds | | |
| Arsenic | Kg | 0 | 0 | 0 | 0 | 457 | 457 |
| Chromium | Kg | 16.0 | 0 | 0 | 0 | 120 | 136 |
| Mercury | Kg | 28.1 | 0 | 400 | 0 | 596 | 1,024 |
| Americium-241 | Ci | 110 | 0 | 0.123 | 0 | 0.905 | 111 |
| Cobalt-60 | Ci | 68.4 | 0 | 1.24 | 0.0112 | 106 | 176 |
| Cesium-137 | Ci | 26,800 | 309 | 25.8 | 0.534 | 2,680 | 29,815 |
| Tritium | Ci | 18.5 | 378 | 20,100 | 999 | 0 | 21,496 |
| Iodine-129 | Ci | 0.00705 | 0 | 1.39 | 0.0820 | 0.0389 | 1.52 |
| Neptunium-237 | Ci | 0.216 | 0 | 1.07 | 0 | 0.133 | 1.42 |
| Total Plutonium | Ci | 1,180 | 0 | 0.822 | 0.0692 | 10.2 | 1,191 |
| Strontium-90 | Ci | 18,000 | 309 | 24.3 | 0.295 | 1,110 | 19,444 |
| Technetium-99 | Ci | 2.58 | 0 | 0 | 0 | 0.106 | 2.69 |
| Total Uranium | Ci | 0.747 | 0 | 0.269 | 0.0701 | 0.940 | 2.03 |

The CPP-23 injection well released wastewater and contaminants directly to the SRPA (DOE-ID 1997a). The injection well also released wastewater and contaminants to the vadose zone during periods of casing collapse (DOE-ID 1997a). Some of the contaminant inventory introduced to the vadose zone has been released slowly to the aquifer through vertical saturated and unsaturated flow.

Most of the tritium disposed at INTEC was released from the injection well directly to the aquifer or deeper parts of the vadose zone (20,100 Ci). A total of 400 kg of mercury was disposed from the injection well. Only a small percentage of strontium-90 and cesium-137 was disposed directly to the aquifer from the injection well. A total of 1.39 Ci of iodine-129 and 1.07 Ci of neptunium-237 were disposed.

- **CPP-603 Basins**

  The CPP-603 fuel storage basins have been operational since 1952. These basins store spent fuel assemblies prior to processing of the assemblies. The basins consist of three reinforced-concrete, unlined fuel-storage basins connected by a transfer channel.

  Leakage from the fuel storage basins has been estimated to be from 500 to 700 L per day (DOE-ID 1997a). The principle contaminant in tank leakage water is cesium-137.

- **Tank Farm**

  Leakage and spills from the Tank Farm distribution system have released contaminants to the surficial sediments. Known Tank Farm leakage accounts for most of the INTEC releases of cesium-137 (26,800 Ci), strontium-90 (18,000 Ci), total plutonium (1,180 Ci), americium-241 (110 Ci) and technetium-99 (2.58 Ci), and much of the release of cobalt-60 (68.4 Ci;). These activities are not corrected for radioactive decay.

- **Soil Contamination**

  Spills and leakage have resulted in contaminated-soil sites at INTEC. Contaminants at these sites include arsenic (457 kg), chromium (120 kg), and mercury (596 kg). Significant radionuclides include cesium-137 (2,680 Ci), strontium-90 (1,110 Ci), and cobalt-60 (106 Ci).

- **Percolation Ponds**

  The service waste ponds were constructed in 1984 to replace the CPP injection well for disposal of service wastewater. These ponds were designed to allow infiltration of water to the subsurface.

  Tritium was the predominant constituent disposed to the service waste ponds. A total of about 1,000 Ci were disposed from 1984 to the present.

***Extent of Contamination—***Contaminant concentrations have been monitored in perched groundwater bodies (Bartholomay and Tucker 2000) and in the SRPA. Subsequent sections describe the distribution and extent of selected contaminants in the vadose zone and in the aquifer.

***Vadose Zone—***Water from wells completed in upper perched-water bodies in the northern part of INTEC contains large gross-alpha and gross-beta activities. Activities in the upper perched water body are attributed primarily to strontium-90 and technetium-99. Tritium and technetium-99 concentrations increase from the upper to deeper perched zones; strontium-90 concentrations decrease. Upper perched water in the northern part of INTEC contains nitrate concentrations above the maximum contaminant level.

Two perched water bodies have been identified in the southern part of INTEC. One perched water body attributed to leakage from CPP-603 contains tritium, technetium-99, strontium-90, and uranium-234. Water from several wells completed in perched-water bodies beneath the percolation ponds contained strontium-90 above the MCL of 8 pCi per liter. Inorganic constituents in both perched-water bodies include chloride, nitrate, manganese, and iron.

Deeper perched zones at INTEC are monitored in four wells. Water from these wells contains concentrations of tritium, strontium-90, and technetium-99. Only tritium has exceeded the maximum contaminant level.

### *SRPA*

- **Tritium**

  Tritium activities attributed to wastewater disposal at INTEC and TRA have been detected in water from the SRPA above the instrument detection limit of 0.5 picoCi/L over a large area of the INEEL. In 1985, this area exceeded 50 $mi^2$ and had reached the southern boundary of the INEEL (Pittman et al. 1988). Tritium activities exceeded the maximum contaminant level of 20 picoCi/mL in wells located more than 3 mi downgradient from INTEC. Since 1985, the area containing water exceeding the instrument detection limit has decreased. Within the area, tritium activities also have decreased. In 1998, activities, attributed primarily to disposal from INTEC and TRA, were less than the maximum contaminant level (Bartholomay et al. 2000). Activity decreases are attributed to radioactive decay and reduction in disposal of wastewater containing tritium.

- **Strontium-90**

  Strontium-90 has been detected in water from the SRPA directly downgradient from INTEC. In 1985, the estimated area of the strontium-90 plum was about 2 $mi^2$ (Pittman et al. 1988). Slight decreases in the area of the strontium-90 plume and concentrations in water from wells are attributed to changes in wastewater disposal and radioactive decay. Since 1989, strontium-90 concentrations have remained relatively constant.

- **Iodine-129**

  Aquifer water samples were collected during 1977, 1981, 1986, and 1990 through 1991 for iodine-129 analyses at INTEC (Mann and Beasley 1994). During 1990-91, samples were collected from 50 aquifer wells. Concentrations ranged from 0.0000006±0.0000002 to 3.82±0.19 picoCi/L. The average concentration in water from 18 wells was 0.81±0.19 picoCi/L compared to 1.3±0.26 picoCi/L in 1986. Mann et al. (1988) reported a similar decrease between the 1981 and 1986 sampling events. Decreases in the I-129 concentration in groundwater at the ICPP are attributed to decrease in disposal, a change from the disposal well to the percolation ponds, and dilution by infiltration of stream flow from the Big Lost River.

  During the WAG 3 Remedial Investigation, I-129 concentrations in wells USGS-67, LF2-12, and LF3-08 were 1±0.3 pCi/L, 1.2±0.3 pCi/L, and 0.9±0.3 picoCi/L, respectively. Two of these wells are located several miles downgradient from the INTEC.

- **Technetium-99**

  Technetium-99 was detected in water from 32 of the 44 wells sampled during the WAG-3 Remedial Investigation. The largest concentrations of Tc-99 were detected in the north central portion of the ICPP in water from wells MW-18, USGS-47, and USGS-52. Concentrations were 448±4, 235±3, and 174±2 picoCi/L, respectively. The technetium-99 plume extends to the southwest of the ICPP and includes wells USGS-123, USGS-57, and

USGS-39. The maximum Tc-99 concentration outside the ICPP security perimeter fence is 49 pCi/L in well USGS-123.

- **Cesium-137**

  Cesium-137 has been detected in several wells in response to disposal to the injection well. No cesium-137 concentrations have been detected in recent years (Bartholomay et al. 2000).

- **Actinides**

  Plutonium isotopes were detected in water samples through 1987 in several wells near INTEC. These detections were attributed to disposal to the injection well. Americium-241, a decay daughter of plutonium-241, was detected as recently as 1995 in several wells near INTEC. Since then, plutonium isotopes and americium-241 have remained less than the reporting level (Bartholomay et al. 2000).

***Mechanisms that Affect the Fate and Transport of Contaminants in Groundwater at TRA—***Those mechanisms considered to be important for the transport of contaminants in the vadose zone at INTEC include radioactive decay, sorption, rate of infiltration from different sources of recharge, and effective porosity[1]. Mechanisms that control transport in the aquifer include radioactive decay, sorption, groundwater dispersivity, effective porosity, and the velocity of flow.

Transport of contaminants from spills that were contained in surficial sediments is facilitated by water for release to the deeper subsurface from those soils. Water may originate from landscape irrigation, piping losses, and shallow infiltration from percolation ponds (DOE-ID 1997a). The dye tracer test presently underway (DOE-ID 2001) is designed to improve understanding of the distribution and source of water in the vadose zone.

Effective porosity estimates have been made from inverse modeling of contaminant distributions (tritium and iodine-129). These estimates are dependent on the assumed thickness of the aquifer and vertical mixing of the contaminant throughout the aquifer thickness.

### 3.3.3 Numerical Analyses Performed to Date at INTEC

Numerical simulations of water and contaminant transport in both the vadose zone and aquifer beneath INTEC have been conducted to support the OU 3-13 RI/FS (DOE-ID 1997a, Book 2). Both models are discussed in the following sections.

***3.3.3.1 Vadose-Zone Model.*** The vadose zone model parameterized four interbed units (the Upper-1, Upper-2, middle, and lower units) based on the geospatial distribution of the interbeds in existing boreholes. The conceptual model used to parameterize the hydrologic budget of the vadose zone included allowances for precipitation, fire water losses, lawn irrigation, injection of water at ICPP-603, infiltration at the sewage treatment plant, infiltration of percolation pond water, and steady state infiltration from the Big Lost River. The model was calibrated to water levels measured in perched water wells. The transport portion of the model was calibrated to observed concentrations of chloride and tritium (conservative tracers).

---

[1] ***Pete Martian, oral communication, 8/2/02***

***3.3.3.2 Aquifer Model.*** The aquifer model domain was substantially larger than the domain selected for the vadose zone numerical simulations. As a result, it was necessary to add recharge to the aquifer model in all locations except the overlap portion of the two domains. Infiltration from the Big Lost River was estimated (and parameterized) as the average linear surface water flow loss between the river's diversion (near the RWMC) to the Lincoln Boulevard bridge (near INTEC) for the uppermost reach of the river inside the aquifer domain. Flow losses between the Lincoln Boulevard bridge and the Big Lost River playas were used to simulate infiltration in the lower reach of the Big Lost River including in the aquifer domain. Pumping discharge from wells CPP-02 and CPP-04 also was included in the aquifer model. Boundary conditions for the aquifer simulations were imported from the WAG 10 groundwater flow model.

In addition, primary COCs at TRA were included in the aquifer simulations because of the potential that the two plumes (TRA and INTEC) could commingle and affect cumulative risk calculations at receptor points. Like the vadose zone transport model, the transport portion of the aquifer model was calibrated to both dissolved chloride and tritium concentrations in water beneath the site.

The two models (vadose zone and aquifer) were considered adequate to represent hydraulic conditions and the transport of contaminants beneath INTEC during 1950-95. Model-calibrated distribution coefficients ($K_d$s) were used for the numerical simulations and were considered uniform in each medium (i.e., basalt and interbed). While the distribution of materials with different sorption characteristics is believed to be highly complex in the subsurface beneath INTEC, the parameterized homogeneous distribution of $K_d$s in soil and basalt were determined to be adequate to reproduce observed contaminant concentrations.

### 3.3.4 Summary of Competing Hypotheses and Additional Data Requirements

Geohydrologic research associated with WAG-3 remediation activities has identified areas of research needed to better understand contaminant transport in the subsurface at INTEC. The following list is a partial listing of these research areas and competing hypotheses.

***3.3.4.1 Local Sources of Recharge.*** Percolation ponds, piping leakage, landscape irrigation water, and the Big Lost River provide sources for formation of water-perched groundwater bodies and for contaminant transport. The present dye tracer test (DOE-ID 2001c) is designed to improve the understanding of the distribution of these local sources of water.

***3.3.4.2 Source Term.*** The input estimates of available process water and contaminant mass are uncertain. Estimates also are uncertain of those physical properties that have a primary influence on flow and contaminant transport domain.

***3.3.4.3 Well Completions.*** Inadequate well completions may facilitate vertical movement of contaminants by creating additional subsurface flow routes.

***3.3.4.4 Treatment of Sedimentary Interbeds in the Unsaturated Zone.*** Previous numerical analyses lumped the 14 interbeds in the vadose zone beneath INTEC into three units. This lumping may result in an overestimation of the effect of interbeds on lateral flow.

***3.3.4.5 Preferential Flow in the Vadose Zone.*** The rate of vertical flow through the unsaturated zone at INTEC is not well known. Vertical velocities may be underestimated by lumping of interbeds in previous analyses and disregarding the possibility for preferential flow.

***3.3.4.6 HI Sedimentary Interbed.*** Little is known about the effect of the HI interbed in separating upper and lower flow systems and contaminant transport.

***3.3.4.7 Storage Coefficient.*** A storage coefficient of 6% was used in WAG-3 analyses. Subsequent analyses using a thicker aquifer (based on Dick Smith's temperature data) resulted in a storage coefficient of 3%.

***3.3.4.8 Effective Thickness of the Aquifer.*** In terms of contaminant transport, the effective thickness of the SRPA has been estimated to be 250 ft. Information is needed about the actual thickness, anisotropy, and the vertical distribution of contaminants in the aquifer at INTEC.

***3.3.4.9 Injection Well.*** Contaminants are assumed to have been uniformly injected across the perforated interval of the injection well. However, this assumption probably has not been accurate. The HI interbed and basalt interflow zones and casing plugging and collapse may have resulted in differential injection of wastewater.

### 3.3.5 References Cited


Ackerman, D.J., 1991a, *Transmissivity of the Snake River Plain Aquifer at the Idaho National Engineering Laboratory, Idaho*, U.S. Geological Survey Water-Resources Investigations Report 91-4058 (-22097), U.S. Geological Survey.

Ackerman, D.J., 1991b, *Transmissivity of Perched Aquifers at the Idaho National Engineering Laboratory, Idaho*, U.S. Geological Survey Water-Resources Investigations Report 91-4114 (-22099), U.S. Geological Survey.

Anderson, S. R., 1991, *Stratigraphy of the Unsaturated Zone and Uppermost Part of the Snake River Plain Aquifer at the Idaho Chemical Processing Plant and Test Reactor Area, Idaho National Engineering Laboratory, Idaho*, USGS Water-Resources Investigations Report 91-4010 (-22095), U.S. Geological Survey.

Arnett, R.C., and Smith, R.P., 2001, *WAG 10 Groundwater Modeling Strategy and Conceptual Model*, INEEL/EXT-01-00768, Bechtel BWXT Idaho, LLC, Idaho National Engineering and Environmental Laboratory, Idaho Falls, Idaho.

Bartholomay, R. C., Orr, B. R., Liszewski, M. J., and Jensen, R.G., 1995, *Hydrologic Conditions and Distribution of Selected Radiochemical and Chemical Constituents in Water, Snake River Plain Aquifer, Idaho National Engineering Laboratory, Idaho, 1989 through 1991*, U.S. Geological Survey Water-Resources Investigations Report 97-4175 (-22123), U.S. Geological Survey.

Bartholomay, R. C., Tucker, B. J., Ackerman, D. J., and Liszewski, M. J., 1997, *Hydrologic Conditions and Distribution of Selected Radiochemical and Chemical Constituents in Water, Snake River Plain Aquifer, Idaho National Engineering Laboratory, Idaho, 1992 through 1995*, U.S. Geological Survey Water-Resources Investigations Report 97-4086 (-22137), U.S. Geological Survey.

Bartholomay, R. C., and Tucker, B. J., 2000, *Distribution of Selected Radiochemical and Chemical Constituents in Perched Ground Water, Idaho National Engineering and Environmental*

*Laboratory, Idaho, 1996-98*, U.S. Geological Survey Water-Resources Investigations Report 00-4222 (-22168), U.S. Geological Survey.

Bartholomay, R. C., Tucker, B. J., Davis, L. C., and Greene, M. R., 2000, *Hydrologic Conditions and Distribution of Selected Constituents in Water, Snake River Plain Aquifer, Idaho National Engineering and Environmental Laboratory, Idaho, 1996 through 1998*; U.S. Geological Survey Water-Resources Investigations Report 00-4192 (-22167), U.S. Geological Survey.

Bennett, C. M., 1990, S*treamflow Losses and Groundwater Level Changes along the Big Lost River at the INEL, Idaho*, U.S. Geological Survey Water-Resources Investigation Report 86-4204, -22091. U.S. Geological Survey.

Cecil, L. D., Orr, B.R., Norton, T., and Anderson, S.R., 1991, *Formation of Perched Ground-Water Zones and Concentrations of Selected Chemical Constituents in Water, Idaho National Engineering Laboratory, Idaho, 1986–88*, U.S. Geological Survey Water-Resources Investigations Report 91-4166, -22100, U.S. Geological Survey.

DOE-ID, 1991, *Federal Facility Agreement and Consent Order for the Idaho National Engineering Laboratory*, U.S. Department of Energy Idaho Operations Office, U.S. Environmental Protection AgencyRegion 10, State of Idaho Department of Health and Welfare.

DOE-ID, November 1997a, *Comprehensive RI/FS for the Idaho Chemical Processing Plant OU 3-13 at the INEEL-Part A, RI/BRA Report Final*, DOE/ID-10534, U.S. Department of Energy Idaho Operations Office, Idaho Falls, Idaho.

DOE-ID, November 1997b, *Comprehensive RI/FS for the Idaho Chemical Processing Plant OU 3-13 at the INEEL-Part B, FS Report Final*, DOE/ID-10572, U.S. Department of Energy Idaho Operations Office, Idaho Falls, Idaho.

DOE-ID, 1998, *Comprehensive RI/FS for the Idaho Chemical Processing Plant OU 3-13 at the INEEL—Part B, FS Supplement Report*, Revision 2, U.S. Department of Energy Idaho Operations Office, DOE-ID-10619, October.

DOE-ID, October 1999, *Final Record of Decision Idaho Nuclear Technology and Engineering Center, Operable Unit 3-13*, U.S. Department of Energy Idaho Operations Office, DOE/ID-10660, Revision 0, U.S. Department of Energy Idaho Operations Office, Idaho Falls, Idaho.

DOE-ID, 2000a, *Monitoring system and Installation Plan for Operable Unit 3-13, Group 5, Snake River Plain Aquifer*, DOE-ID-10782, U.S. Department of Energy, Idaho Operations Office, Idaho Falls, Idaho.

DOE-ID, 2000b, *Field sampling plan for Operable Unit 3-13, Group 4 perched water well installation*, DOE/ID-10745, U.S. Department of Energy Idaho Operations Office, Idaho Falls, Idaho, September.

DOE-ID, 2000c, *Tracer test plan for Operable Unit 3-13 Group 4, perched water*, DOE/ID-10762, U.S. Department of Energy Idaho Operations Office, Idaho Falls, Idaho, September.

DOE-ID 2000d, *Long-term monitoring plan for Operable Unit 3-13, Group 4 perched water*, DOE/ID-10746, U.S. Department of Energy, Idaho Operations Office, September.

DOE-ID, April 2002a, *Phase I Monitoring Well and Tracer Study Report for Operable Unit 3-13, Group 4, Perched Water*, DOE/ID-10967, U.S. Department of Energy Idaho Operations Office, Idaho Falls, Idaho.

DOE-ID, 2002b, *ICDF Complex groundwater monitoring plan*, U.S. Department of Energy Idaho Operations Office, -10955, May.

Frederick, D.B., and Johnson, G.S., 1996, *Estimation of Hydraulic Properties and Development of a Layered Conceptual Model for the Snake River Plain Aquifer at the Idaho National Engineering Laboratory, Idaho,* Idaho Water Resources Research Institute Research Technical Completion Report.

Frederick, D.B., and Johnson, G.S., 1997, *Depth and Temporal Variations in Water Quality of the Snake River Plain Aquifer in Well USGS-59 near the Idaho National Engineering Laboratory*, Idaho Water Resources Research Institute Research Technical Note 97-1.

Fromm, J., Welhan, J., Curry, M., and Hackett, W., 1994, "Idaho Chemical Processing Plant (ICPP) injection well – Operations history and hydrochemical inventory of the waste stream, Hydrogeology, waste disposal, science, and politics," *Proceedings of the 30th Symposium on Engineering Geology and Geotechnical Engineering*.

Kaminsky, J. F. et al., 1994, *Remedial Investigation Final Report with Addendum for Test Area North Groundwater Operable Unit 1-07B at the Idaho National Engineering Laboratory*, EGG-ER-10643.

Knobel, L.L., Bartholomay, R.C., and Orr, B.R., 1997, *Preliminary Delineation of Natural Geochemical Reactions, Snake River Plain Aquifer System, Idaho National Engineering Laboratory and vicinity, Idaho*, U.S. Geological Survey Water-Resources Investigations Report 97-4093 (DOE/ID-22130), U.S. Geological Survey.

Mann, L. J., 1986, *Hydraulic Properties of Rock Units and Chemical Quality of Water for INEL-1; A 10,365-foot Deep Test Hole Drilled at the Idaho National Engineering Laboratory, Idaho*, U.S. Geological Survey Water-Resources Investigations Report 86-4020, IDO-22070, U.S. Geological Survey.

Mann, L.J., Chew, E.W., Morton, J.S., and Randolph, R.B., 1988, *Iodine-129 in the Snake River Plain Aquifer at the Idaho National Engineering Laboratory, Idaho*, U.S. Geological Survey Water-Resources Investigations Report 88-4165, U.S. Geological Survey.

Mann, L.J., and Beasley, T.M., 1994, *Iodine-129 in the Snake River Plain Aquifer at and near the Idaho National Engineering Laboratory, 1990-91*, U.S. Geological Survey Water-Resources Investigations Report 94-4053, U.S. Geological Survey.

Miller, S. M., Hammel, J.E., and. Hall, L. F., 1990, *Characterization of Soil Cover and Estimation of Water Infiltration at Central Facilities Area II, Idaho National Engineering Laboratory*, Research Technical Completion Report for Contract C85-110544, University of Idaho.

Morin, R.H., Barrash, Warren, Paillet, F.L., and Taylor, T.A., 1993, *Geophysical logging studies in the Snake River Plain aquifer at the Idaho National Engineering Laboratory—wells 44, 45, and 46*, U.S. Geological Survey Water-Resources Investigations Report 92-4184.

Nimmo, J.R., Perkins, K.S., Rose, P.E., Rousseau, J.P., Orr, B.R., Twining, B.V., and Anderson, S.R., 2001, *Kilometer-scale rapid flow in a fractured-basalt unsaturated zone at he Idaho National Engineering and Environmental Laboratory*, Fractured Rock 2001 Conference Proceedings, March 26-28, 2001, Toronto, Novakowski, K.S., and Reynolds, D.A., eds.

Orr, B. R. and L. D. Cecil, 1991, *Hydrologic Conditions and Distribution of Selected Chemical Constituents in Water, Snake River Plain Aquifer, Idaho National Engineering Laboratory, Idaho, 1986 to 1988*, U.S. Geological Survey Water-Resources Investigations Report 91-4047 (-22096), U.S. Geological Survey.

Pittman, J.R., Jensen, R.G., and Fischer, P.R., 1988, *Hydrologic Conditions at the Idaho National Engineering Laboratory, 1982 to 1985*, U.S. Geological Survey Water-Resources Investigations Report 89-4008, U.S. Geological Survey.

Richards, B. T., January 1994, *ICPP Water Inventory Study*, WINCO-1181-1184.

Robertson, J.B., Schoen, R., and Barraclough, J.T., 1974, *The Influence of Liquid Waste Disposal on the Geochemistry of Water at the National Reactor Testing Station, Idaho*, U.S. Geological Survey Open-File Report, IDO-22053, U.S. Geological Survey.

Thomas, T. R., 1988, *Modeling Hypothetical Groundwater Transport of Nitrates, Chromium, and Cadmium at the Idaho Chemical Processing Plant*, WINCO-1060.

Tucker, B. J., and Orr, B. R., 1998, *Distribution of Selected Radiochemical and Chemical Constituents in Perched Ground Water, Idaho National Engineering Laboratory, Idaho, 1989-91*; U.S. Geological Survey Water-Resources Investigations Report 98-4028 (-22144), U.S. Geological Survey.

Wood, T. R., D. Bates, C. W. Bishop, G. L. Heath, L. C. Hull, R. M. Lehman. S. O. Magnuson, E. D. Mattson, J. M. McCarthy, I. Porro, P. D. Ritter, M. Roddy, J. B. Sisson, R. P. Smith, August 2000, *Deficiencies in vadose zone understanding at the Idaho National Engineering and Environmental Laboratory*, INEEL/ EXT-99-00984, Idaho National Engineering and Environmental Laboratory, Bechtel BWXT Idaho, LLC, Idaho Falls, Idaho.

# 3.4 Waste Area Group 4

## 3.4.1 Background

Waste Area Group 4 is the designation for the collection of CERCLA OUs associated with the Central Facilities Area (CFA). CFA is located in the south-central part of the INEEL about 1½ mi south of INTEC and almost 3 mi south of the TRA (see Figure 3-18).

The original CFA mission was testing of U.S. Navy gunnery. Military housing and test support facilities were built at CFA during the 1940s. As the mission of the INEEL evolved over time, the facilities at CFA were modified to provide crafts support, laboratory space, and a variety of services including medical, fire, and food services.

A detailed conceptual model has not been developed for WAG 4. Because the potential risks associated with past WAG 4 activities were considered relatively low, there has not been a large effort to characterize the hydrologic system or to monitor potential contaminant transport pathways. What site-specific information is available was developed in support of the WAG 4 RI/FS (Burgess et al. 2000) and is summarized in this chapter for convenience. This section does not present any original hydrogeologic work, but simply summarizes technical elements that contribute to the conceptual model.

## 3.4.2 Summary of the Present WAG-4 Conceptual Site Model

### *3.4.2.1 Geologic Framework*

***System Geometry—***The WAG 4 facilities cover an area roughly 2 mi in diameter. The Big Lost River bed is approximately 1.5 mi northwest of CFA at its nearest pint. Groundwater (i.e., SRPA) is approximately 480 ft bls.

***Geology—***As with other INEEL sites, WAG 4 geology is comprised of a complex layering of basalt flows and thin sedimentary deposits. Each basalt flow group is comprised of numerous basalt lava flows that erupted from nearby vents. As described in previous chapters, each flow is typically composed of a basalt zone of highly permeable rubble; a lower vesicular zone; a dense, massive and jointed central zone; and upper vesicular zone; and a cap of slabby lava crust. Interbed sediments consist of fine-grained eolian and alluvial clays, silts, sands, and some gravels.

***Stratigraphy/Lithology—***Lithologic information is available from only a few wells in the WAG 4 area. Over a dozen sedimentary deposits have been encountered, but a stratigraphic correlation has not been developed. In general, the interbeds are thin and discontinuous and described as sand, silt, and clay. The saturated zone is approximately 480 ft bls. Several cross sections presented in the RI/FS are included here for convenience. Stratigraphic cross sections in the CFA area (adapted from Burgess et al. 2000) are shown in Figures 3-19 through 3-21.

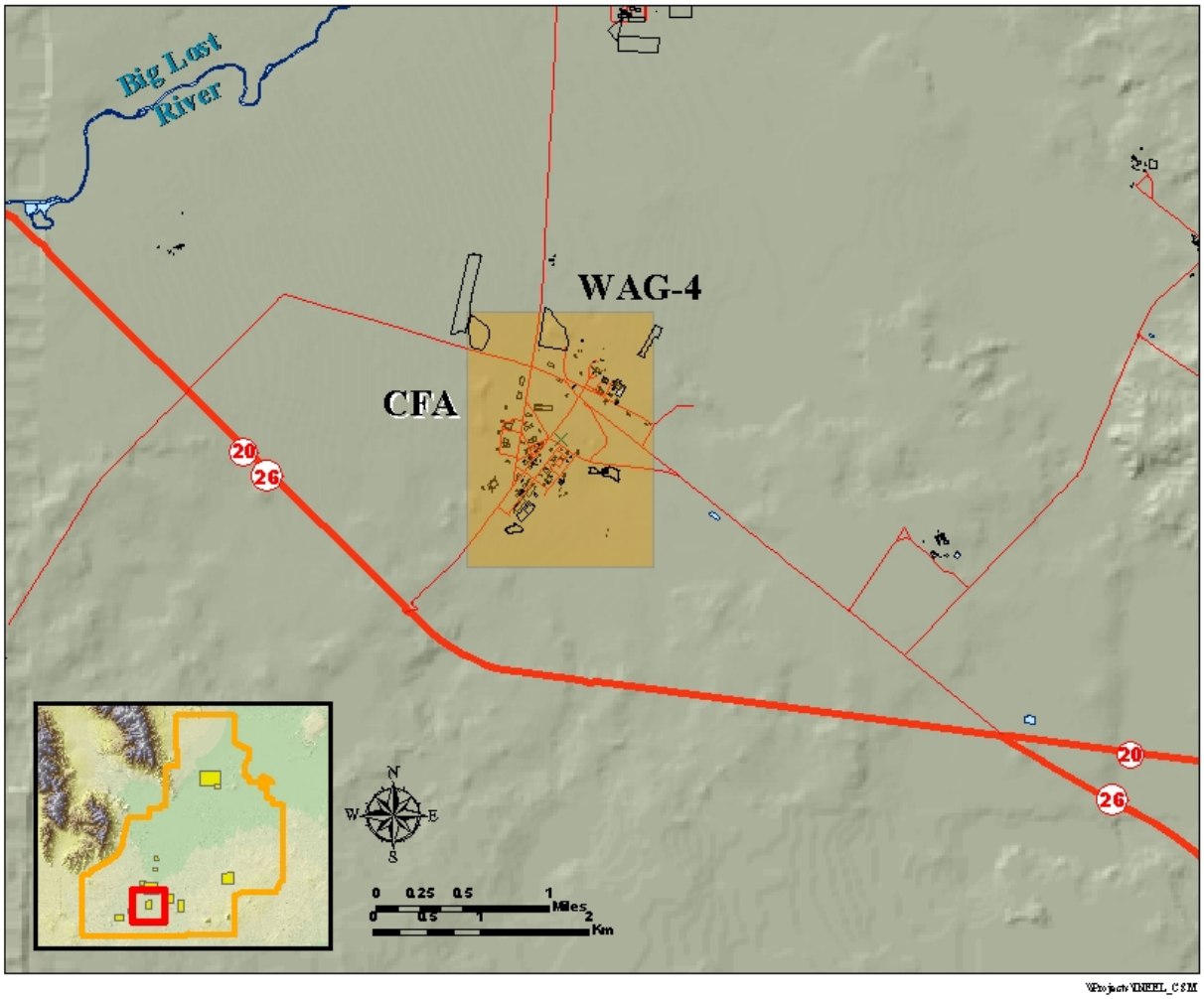


Figure 3-18. WAG 4 is associated with the CFA in the south-central part of the INEEL.

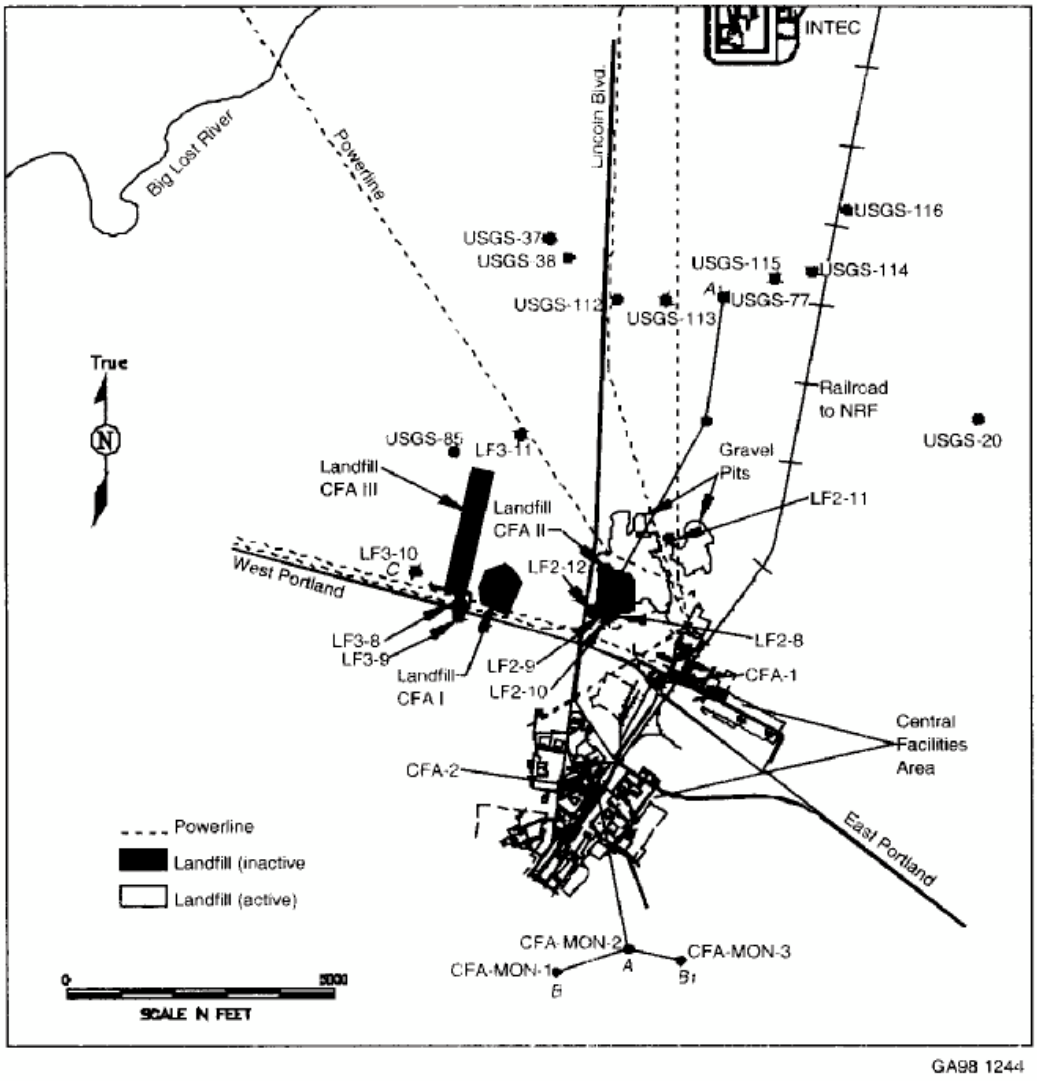


Figure 3-19. Well map for CFA area indicating stratigraphic cross section lines (adapted from Burgess et al. 2000).

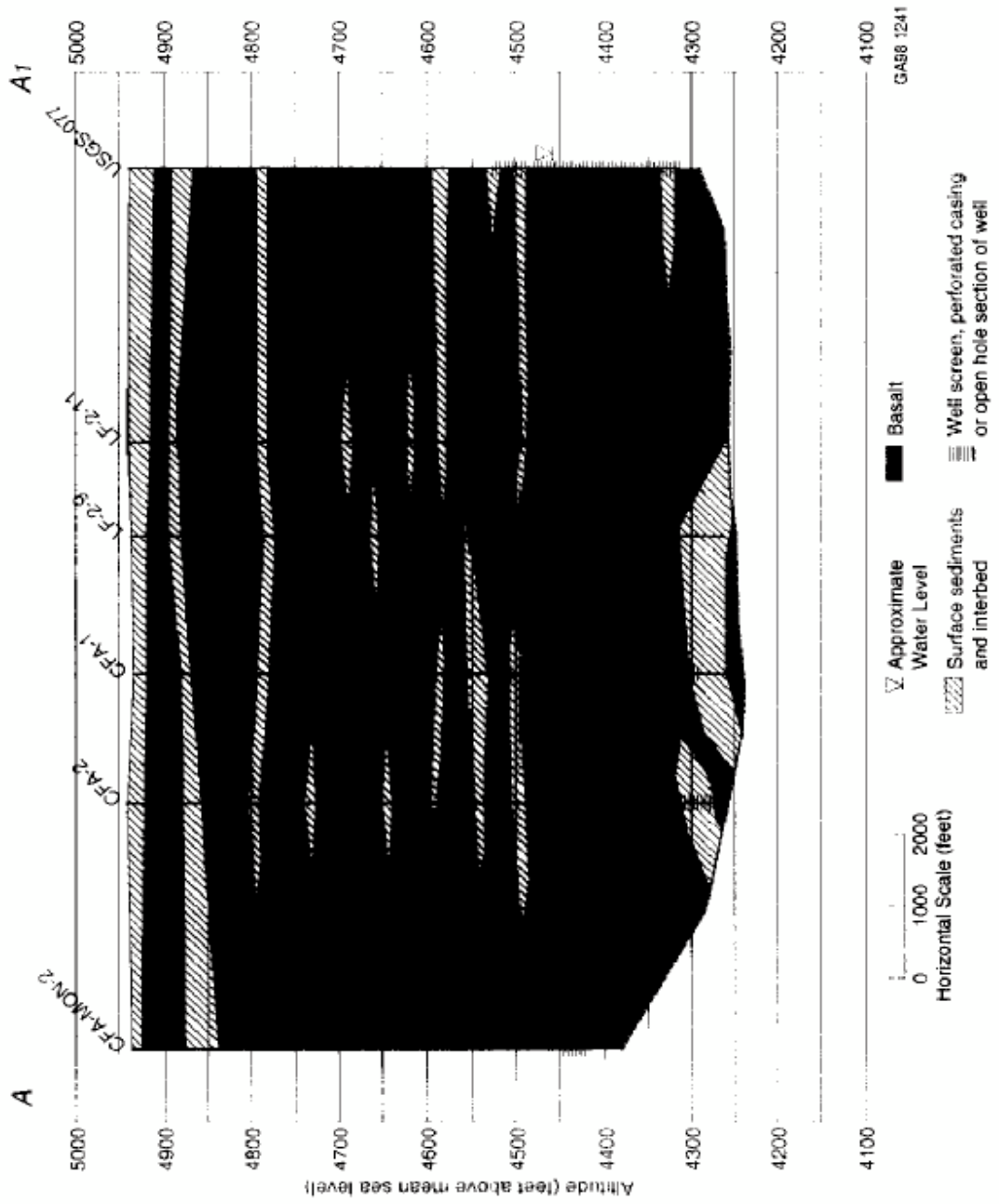


Figure 3-20. Stratigraphic cross sections in the CFA area (adapted from Burgess et al. 2000).

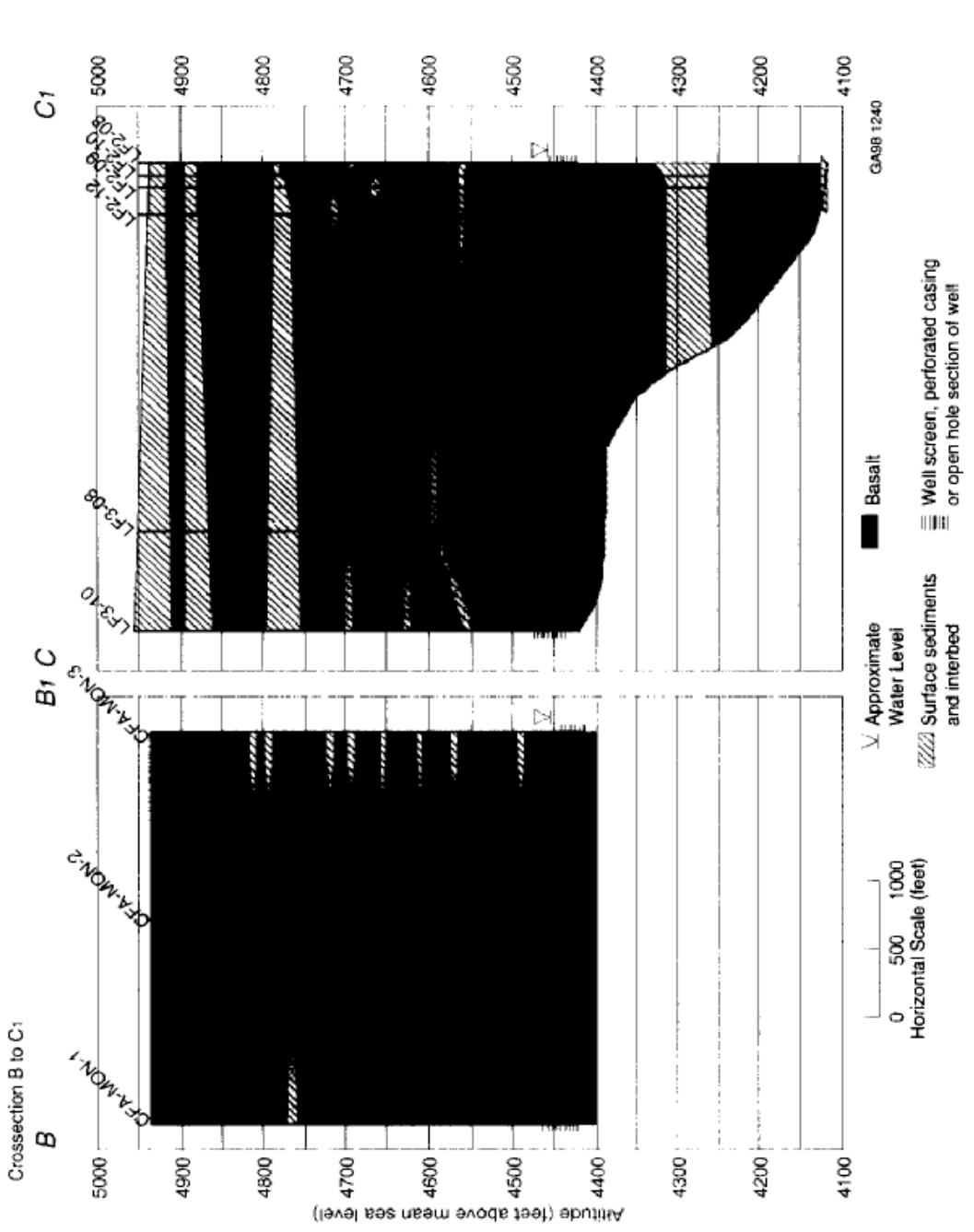


Figure 3-21. Stratigraphic cross sections in the CFA area (adapted from Burgess et al. 2000).

***3.4.2.2 Matrix Characteristics.*** Cation exchange capacities (CECs) were determined for a few interbed samples taken from the CFA landfills area. The average CEC is reported as 6.27 meq/100g in the RI/FS. Additional discussion in the RI/FS defaulted to information obtained from WAG 7 sedimentary cores taken near the RWMC facility, 7 mi further south.

Basalt matrix characteristics were not developed specifically for WAG 4, as the fate and transport modeling used a conservative approach where basalts were ignored (discussed further in subsequent sections). The reader is referred to discussions of basalt properties in Chapter 2 of this document.

### *3.4.2.3 Recharge/Discharge*

***Underflow—***The effects of underflow at WAG 4 have not been investigated.

***Recharge from Precipitation—***Rain and snow precipitation is relatively low in the INEEL region. At WAG 4, there is little runoff or collection of precipitation except during heavy rainstorms or rapid snowmelt. High evapotranspiration rates (greater than 80% of the available water) result in very low infiltration rates (Anderson et al. 1987). In WAG 4 modeling work, a conservative value of 10 cm/yr was used for the infiltration rate.

***Episodic Recharge—***The Big Lost River bed runs nearby the CFA, however, all substantial flows are diverted upstream to the RWMC spreading areas. Very minimal volumes of water are observed in the WAG 4 region. Estimates of recharge were not developed for WAG 4.

***Recharge from Wastewater Disposal—***Two perched water zones had been detected at WAG 4 from 1944 to 1995. These perched aquifers were caused by the CFA sewage treatment drainfield. The sewage treatment plan was deactivated in 1995 and the perched water zones dissipated shortly thereafter.

***Aquifer Discharge to Production Wells—***Two production wells are in use at CFA. These wells provide potable water for offices, cafeterias, the fire department, etc. The effect of the water production on local aquifer flow has not been investigated.

### *3.4.2.4 Hydraulics*

***Vadose Zone—***Infiltration through the WAG-4 landfill covers was investigated (Keck et al. 1994) and the surface soils and vadose zone were found to be relatively dry, with the exception of a few localized drainage areas where snowmelt occasionally collected in small depressions. Hydraulic properties of deeper vadose zone features were not investigated in the 1994 work or in the 2000 RI/FS. Data collected from studies at the RWMC were utilized in the WAG 4 conceptual model.

In general, investigators concluded that the movement of water through the vadose zone can be rapid during periods of saturation but slow during periods of low-water content, as the same features that contribute to rapid flow during saturated conditions (e.g., open fractures and large pores) impede water movement under unsaturated conditions (Keck et al. 1994).

***Snake River Plain Aquifer—***The hydraulic gradient at WAG 4 has been estimated to be 0.2 m/km (1 ft/mi; Lewis and Jensen 1984). Aquifer transmissivity calculated by Ackerman (1991) from nearby wells has ranged from a low of 0.9 $m^2$/day (10 $ft^2$/day) to a high of 68,400 $m^2$/day (760,000 $ft^2$/day). The median value is 5,040 $m^2$/d (56,000 $ft^2$/d). The lower values may be related to problems with well construction as well as heterogeneities in the aquifer system. Interestingly, in 1967 Barraclough et al. used a peak tritium discharge to the ICPP disposal well to calculate groundwater flow rates south of

INTEC. Based on the arrival time of this peak in wells near the CFA, an average groundwater flow rate of 3.4 m/day (11 ft/day) was calculated.

Aquifer storavity was estimated to be 0.0003, based on the barometric efficiency of two wells in the CFA area (Burgess et al. 2000).

***3.4.2.5 Ground-Water Chemistry.*** The water at WAG 4 is described as calcium bicarbonate, thought to be indicative of recharge from northern clastic and carbonate sedimentary rocks (Burgess et al. 2000).

#### *3.4.2.6 Contaminant Transport*

***Source Term—***A variety of waste generating processes contributed to the contamination of WAG 4. In addition to industrial support facilities such as vehicle maintenance, welding, and other crafts, an industrial waste landfill, radiological laboratories, and radiological laundry facilities also operated at the CFA. During the RI/FS, individual sites were evaluated to identify contamination areas that had the potential to pose future human health risk. Thirteen individual contamination areas (contaminated soil sites) were characterized and the nature and extent of contamination was described. Doing this allowed investigators to define source terms for individual sites to support separate modeling efforts for each area. In general, the source terms were comprised of soils contaminated by heavy metals including lead, arsenic, and mercury; radionuclides including Am-241, Ra-226, C-137, Ag-108, and U-235/238; and organic compounds associated with petroleum products.

In support of the RI/FS for WAG 4, the mass of contaminant of interest in the CFA surface soils were estimated primarily by results of soil sampling. Individual source volumes were estimated and the concentration indicated by sampling was distributed evenly across the element volume. Estimated masses or activities for each contaminant of interest are presented in Section 6 of the RI/FS. As the sources of contamination at WAG 4 are contaminated soil sites, the mechanism of release is simply leaching of contaminants by precipitating soil moisture.

As with other WAGs across the INEEL, release rates have not been directly measured at WAG 4. Instead, contaminant flux into the vadose zone is estimated using contaminant specific distribution coefficients and average infiltration rates. Leaching from the source term is assumed to be a first order process where the fraction leached is constant and the contaminant flux is proportional to the source term for the contaminant (Burgess et al. 2000).

***Vadose Zone Transport—***As described by Burgess et al. (2000), contaminant movement in the vadose zone is controlled by the water infiltration rate, contaminant specific sorption coefficients, and hydraulic properties of the interbeds. In the WAG 4 conceptual model, effects of basalt sequences on contaminant movement are ignored. Each contaminant source area is assigned a combined sedimentary thickness, which was derived from drilling logs of nearby wells. Sedimentary sequences are assumed to retard water and contaminant movement, unit gradient conditions are assumed throughout the unsaturated zone. Lateral flow across and between sedimentary lenses is not considered. Dispersion and diffusion are also not accounted for in the vadose zone.

***Aquifer Transport—***The WAG 4 CSM treats the saturated zone as a homogenous isotropic aquifer of infinite lateral extent and finite thickness (Burgess et al. 2000). Contaminants disperse horizontally and vertically as they move downgradient. As described previously, gradients are shallow in the WAG 4 area, and flow direction(s) is not completely understood. However, for fate and transport estimating purposes, the flow direction is considered to be directly south.

***Extent of Contamination—***Twenty-five contaminants (including VOCs and inorganic and radiological chemicals) have been detected in CFA groundwater monitoring wells. Contaminants such as chromium, nitrate, trichloroethene, tritium, strontium, cesium, plutonium, and americium have impacted groundwater quality in the WAG 4 area (Orr and Cecil 1991). However, the groundwater monitoring network at WAG 4 was determined to be inadequate to determine the nature and extent of contamination, primarily due to the lack of downgradient wells (Burgess et al. 2000). Inconsistencies in monitoring efforts also confound the analysis. In general, the majority of the groundwater contaminants detected at CFA are thought to be derived from waste generating processes at INTEC. A series of wells upgradient of the CFA indicate that contaminants such as chromium, I-129, and H-3 are migrating from INTEC. Several contaminants (i.e., TCE and zinc) may be derived from local CFA sources. Interestingly, the elevated concentrations of zinc are thought to be attributable to the use of galvanized components in the monitoring wells (Burgess et al. 2000).

### 3.4.3 Numerical Analyses

Investigators developed a transport model for WAG 4 using GWSCREEN (Rood 1994) to estimate future contaminant concentrations for purposes of evaluating human health risk for the groundwater pathway. Two separate modeling efforts were performed, the first effort done by Keck et al. (1994) focused on the CFA landfills, the second effort by Burgess et al. (2000) encompassed the entire WAG 4 area. The modeling approaches were very similar. The latter effort performed in support of the comprehensive RI/FS, is described here. Site characterization data were insufficient to support a complex modeling approach. Additionally, because the CFA operations did not generate significant volumes of hazardous waste (in comparison to other INEEL facilities) and the probability of potential groundwater risk was thought to be low, a conservative and simplistic modeling approach was considered adequate (Burgess et al. 2000).

In the GWSCREEN model, the vadose zone was considered to be a homogeneous, isotropic porous media with constant unidirectional (downward) flow. Unsaturated flow was modeled through sediments only. The unsaturated basalt sequences were excluded from the model as results of the LSIT indicated rapid flow through a dense fracture network. The sedimentary interbeds and surficial sediment thicknesses were summed and assigned conservative sorption coefficients for contaminants of interest. Infiltration was considered to be spatially uniform.

The initial aquifer thickness at the point that contaminants intersect the aquifer was set at 15 m (49 ft). This averaging concentration depth was based on the default Track 2 length of the well screen (DOE-ID 1994). At the downstream receptor locations, contaminants are considered to diffuse across an effective aquifer thickness of 76 m (250 ft).

Saturated zone parameters, including effective porosity, pore velocity, and dispersivity, were obtained from the default INEEL Track 1 and 2 guidance manuals (DOE-ID 1994). For the aquifer model, investigators used a vertical dispersivity value that was 10 times less than the transverse dispersivity to add conservatism to the fate and transport estimates. Table 3-4, adapted from the RI/FS (Burgess et al. 2000) summarizes the parameters used in the contaminant fate and transport modeling.

Table 3-4. GWSCREEN parameters and the values used for transport modeling (adapted from Burgess et al. 2000).

| Parameter Description | Value[a] | Units |
|---|---|---|
| Infiltration rate (Darcy flux) | 0.1 | m/yr |
| Aquifer pore velocity | 570 | m/yr |
| Volumetric water content in source | 0.3 | Unitless |
| Volumetric water content in unsaturated zone | 0.3 | Unitless |
| Bulk density at source | 1.5 | $g/cm^3$ |
| Bulk density in unsaturated zone | 1.5 | $g/cm^3$ |
| Bulk density of aquifer | 1.9 | $g/cm^3$ |
| Sorption coefficient in source[b] | Contaminant-specific | mL/g |
| Sorption coefficient in unsaturated zone[b] | Contaminant-specific | mL/g |
| Sorption coefficient in aquifer[b] | Contaminant-specific | mL/g |
| Porosity of aquifer | 0.1 | Unitless |
| Depth to aquifer below contamination zone[c] | Site-specific | m |
| Dispersivity in the direction of aquifer flow | 9 | m |
| Dispersivity perpendicular to direction of flow | 4 | m |

a. Values are default Track 2 numbers (unless otherwise noted).

b. Sorption coefficients are, in this analysis, identical for source, unsaturated, and saturated zones.

c. Depth to aquifer is the cumulative vadose zone interbed thickness of each site.

Results of the fate and transport modeling indicated that peak groundwater concentrations would be low and that the time of peak concentration would be thousands of years in the future for most contaminants. The subsequent risk analysis determined that groundwater exposure routes would not pose an unacceptable risk for any contaminant. The model predictions are thought to overestimate the actual concentrations due to the conservative assumptions made during the modeling effort. Although no model calibration was performed, these results are not inconsistent with the observed near-background concentrations of CFA contaminants observed in the WAG 4 monitoring wells.

### 3.4.4 Summary of Competing Hypotheses and Additional Data Requirements

Because WAG 4 does not pose significant groundwater problems, a detailed conceptual model for this site has not been developed. The contaminant fate and transport work performed in support of the RI/FS utilized generalized model parameters from guidance documents. A comprehensive set of site-specific characterization data was not needed and therefore, not compiled. DOE elected to use a simplistic and conservative approach to estimate leaching of contaminants into the aquifer.

### 3.4.5 References Cited


Ackerman, D. J., 1991, *Transmissivity of the Snake River Plain Aquifer at the Idaho National Engineering Laboratory*, U.S. Geological Survey Water-Resources Investigations Report 91-4058, U.S. Geological Survey.

Barraclough, J. T., W. E. Teasdale, J. B. Robertson, and R. G. Jensen, 1967, "Hydrology of the National Reactor Testing Station, Idaho, 1966," U.S. Geological Survey Open File Report TID-4500, U.S. Geological Survey.

Burgess, J., S. Flynn, P. Jessmore, J. Keck, S. McCormick, M. Rohe, I. Stepan, R. VanHorn, S. Fu, L. Trozollo, July 2000, *Comprehensive Remedial Investigation/Feasibility Study for the Central Facilities Area Operable Unit 4-13 at the Idaho National Engineering and Environmental Laboratory*, DOE/ID-10680, Rev 1., Idaho National Engineering and Environmental Laboratory, Prepared for the Department of Energy Idaho Operations Office, Idaho Falls, Idaho.

DOE-ID, January 1994, *Track 2 Sites: Guidance for Assessing Low Probability Hazard Sites at the INEL*, DOE/ID-10389, Department of Energy Idaho Operations Office, Idaho Falls, Idaho.

Keck, K. N., I. Porro, A. J. Sondrup, S. H. McCormick, S. M. Lewis, 1994, *Remedial Investigation/Feasibility Study Report for Operable Unit 4-12: Central Facilities Area Landfills, I, II and III at the Idaho National Engineering Laboratory*, INEL-94/0124, Idaho National Engineering and Environmental Laboratory, Idaho Falls, Idaho.

Lewis, B. D. and R. G. Jensen, 1984, *Hydrologic Conditions at the Idaho National Engineering Laboratory, Idaho, 1979-1981 Update*, U.S. Geological Survey Open-File Report 84-230, IDO-2066, U.S. Geological Survey.

Orr, B. R. and L. D. Cecil 1991, *Hydrologic Conditions and Distribution of Selected Chemical Constituents in Water, Snake River Plain Aquifer, Idaho National Engineering Laboratory, Idaho, 1986 to 1988*, U.S. Geological Survey Water-Resources Investigations Report 91-4047 (DOE/ID 22096), U.S. Geological Survey.

Rood, A. S., 1994, "GWSCREEN: A Semi-Analytical Model for the Assessment of the Groundwater Pathway from Surface Or Buried Contamination: Version 2.0," Theory and User's Manual, EGG-GEO-10797, Idaho National Engineering and Environmental Laboratory, EG&G Idaho, Idaho Falls, Idaho.

# 3.5 Waste Area Group 5

## 3.5.1 Background

Waste Area Group 5 is the designation for the collection of CERCLA OUs associated with the Auxiliary Reactor Area (ARA) and the Power Burst Facility (PBF). Both operational areas are co-located in the south-central portion of the INEEL, north of Highway 20 (Figure 3-22).

The ARA, formerly referred to as the Army Reactor Area, historically consisted of four separate operational areas: 1) ARA-I; 2) ARA-II; 3) ARA-III; and 4) ARA-IV. These facilities, which were constructed in 1957, have been decontaminated, decommissioned, and dismantled. The PBF, once known as the Special Power Excursion Reactor Test (SPERT) facilities, initially consisted of four reactors (SPERT I through IV) that began operation between 1956 and 1961. A fifth reactor, the PBF reactor, was constructed to the north of SPERT I in 1972. Since the mid-1980s, the PBF reactor was placed on stand-by status and several of the facilities at the PBF area have been decontaminated, decommissioned, and dismantled. In 1998, the PBF reactor was placed in shutdown status and is currently preparing for defueling. Other PBF facilities have been modified to support waste management activities at the INEEL. Further information regarding the ARA and PBF facilities, including their operational history and potential sources of contamination, can be found in the OU 5-12 ROD (DOE-ID 2000).

## 3.5.2 Summary of the Present WAG-4 Conceptual Site Model

A detailed conceptual model has not been developed for WAG 5. Because the potential groundwater risks associated with past WAG 5 activities were considered relatively low, there has not been a large effort to characterize the hydrologic system or to monitor potential contaminant transport pathways. What site-specific information is available was developed in support of the WAG 5 Comprehensive RI/FS (Holdren et al. 1999), as summarized in this chapter. This section does not present any original hydrogeologic work, but simply summarizes technical elements that contribute to the conceptual model.

### *3.5.2.1 Geologic Framework*

***System Geometry—***The WAG 5 area encompasses 55 individual contamination sites spread across two operational areas. The contamination sites are relatively small in size, but are located across an area of roughly 16 $mi^2$. Groundwater (SRPA) is approximately 189 m (620 ft) bls at the ARA site and 139 m (455 ft) at PBF.

***Geology—***As with other INEEL sites, WAG 5 geology is comprised of a complex layering of basalt flows and thin sedimentary deposits. Each basalt flow group is comprised of numerous basalt lava flows that erupted from nearby vents. As described in previous chapters, basalt flows are typically described as slabby pahoehoe with vesicular cooling rinds and diktytaxitic flow centers. In the WAG 5 area, basalt flows are the dominant surface features and surface sediments are generally sparse and thin. Interbed sediments consist primarily of fine-grained clays, silts, and sands. Although a range of grain size has been described, WAG 5 is generally considered to be an area of eolian deposition (Holdren et al. 1997).

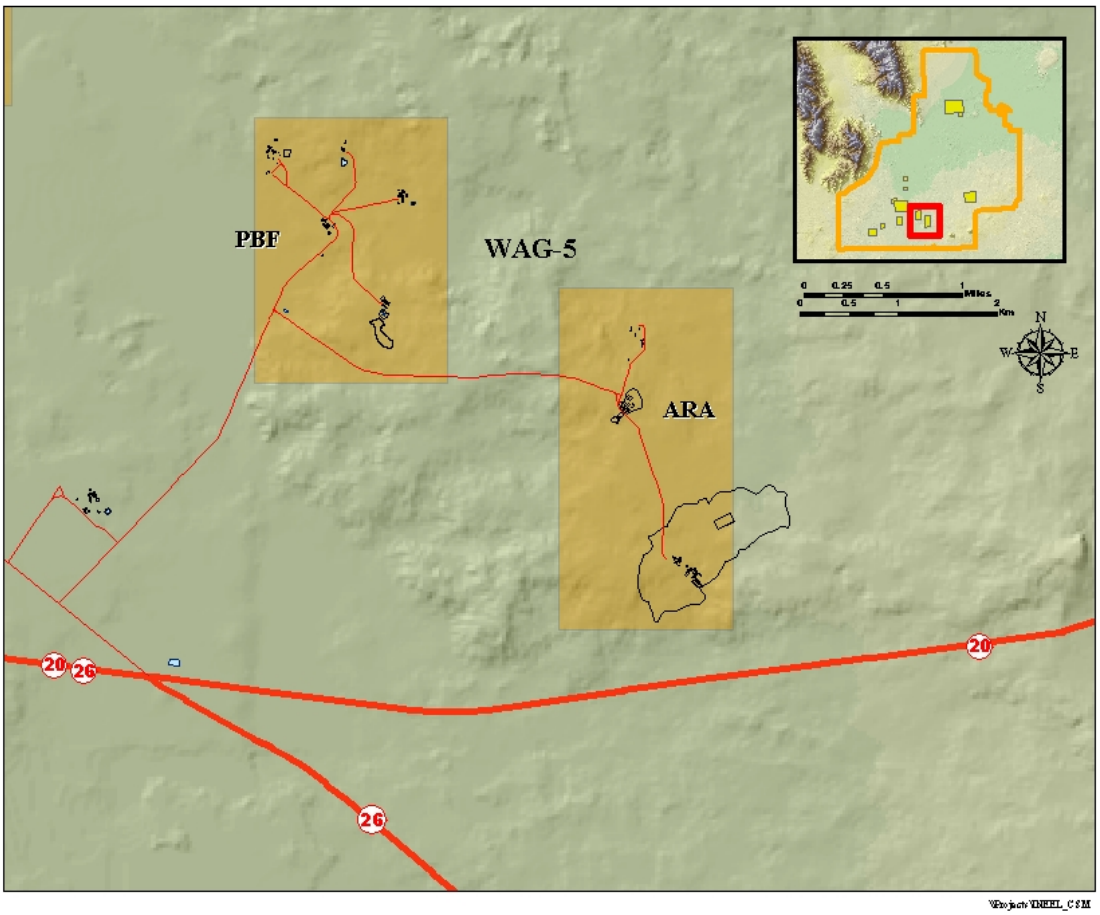


Figure 3-22. WAG 5 is associated with the ARA and the PBF in the south-central part of the INEEL.

***Stratigraphy/Lithology—***Lithologic information is available from 10 groundwater monitoring wells in the WAG 5 area. Similar to other INEEL sites, numerous sedimentary deposits were encountered, but a complete stratigraphic correlation has not been developed. In general, the interbeds are thin and discontinuous and described as sand, silt, and clay. Well logs presented in the RI/FS (Holdren et al. 1999) are included here for convenience (see Figures 3-23, 3-24, and 3-25).

***3.5.2.2 Matrix Characteristics.*** Surface soils at WAG 5 are relatively thin. Data from well logs indicate that the average surface sediment thicknesses are 0.4 m (1.5 ft) at ARA and 3 m (10 ft) at PBF (Holdren et al. 1997).

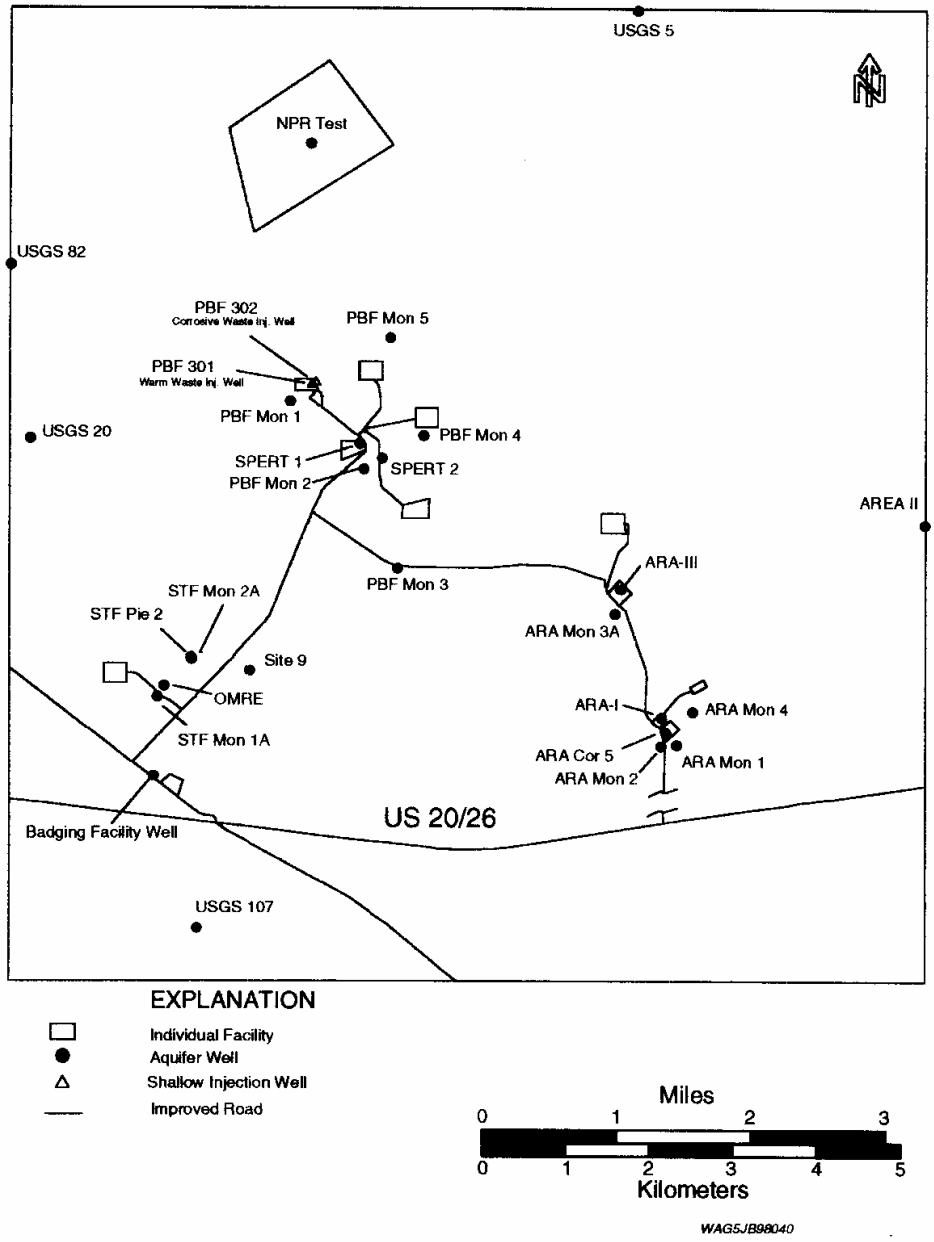


Figure 3-23. Well locations in the WAG 5 area (adapted from Holdren et al. 1999).

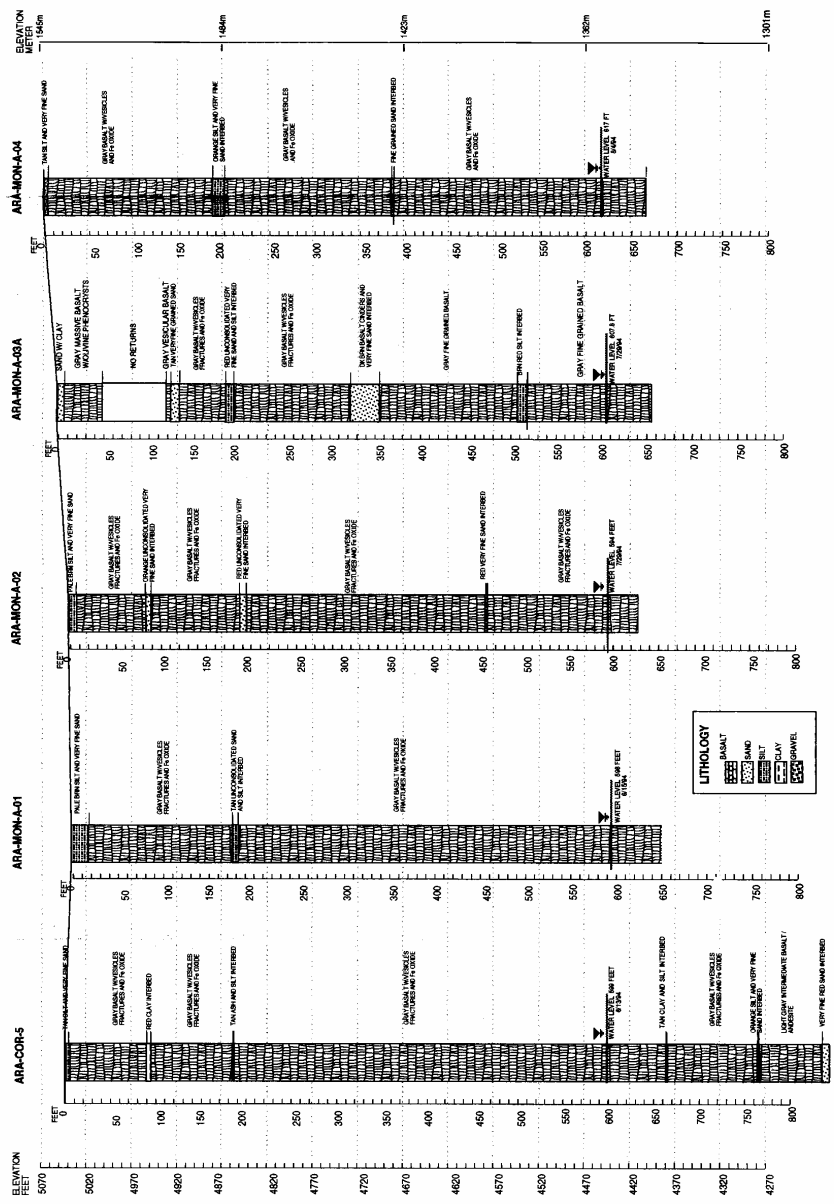


Figure 3-24. Well logs in the WAG 5 area (adapted from Holdren et al. 1999).

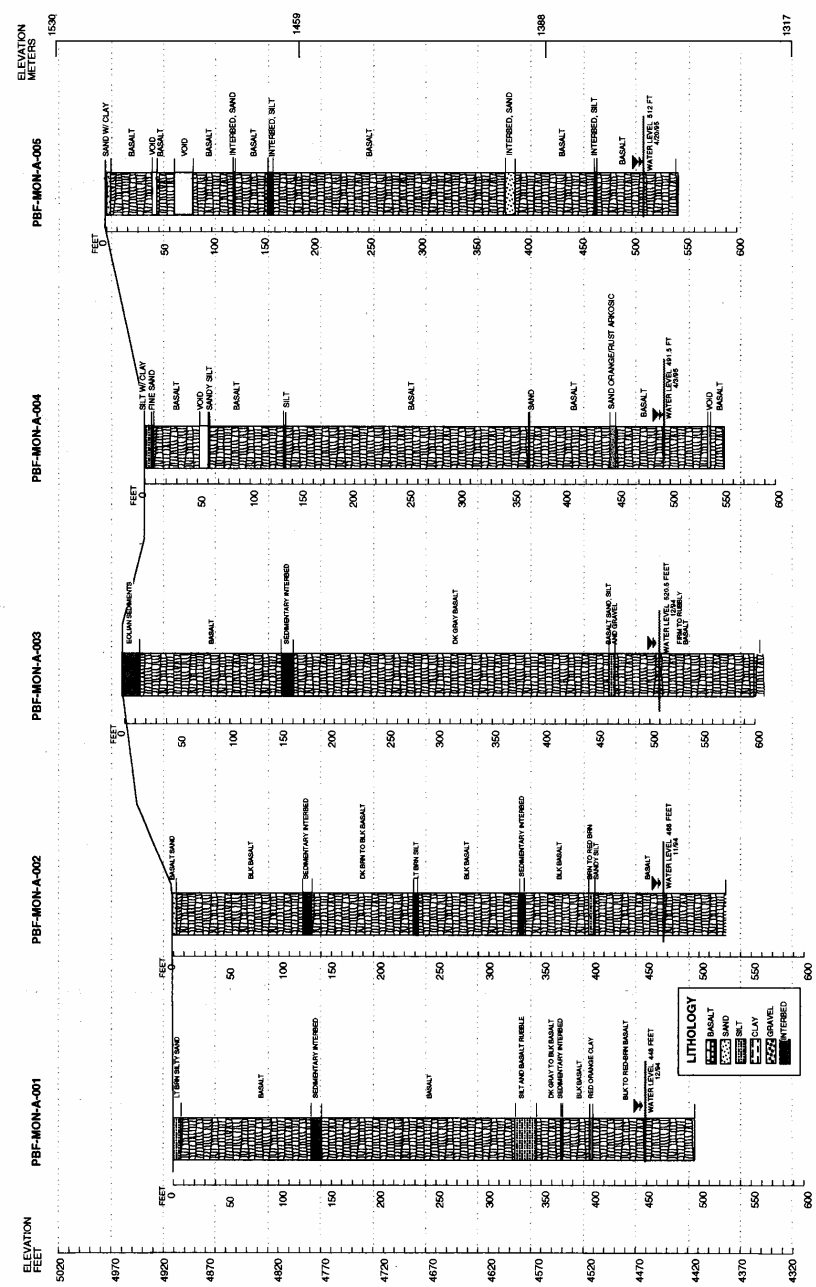


Figure 3-25. Well logs in the WAG 5 area (adapted from Holdren et al. 1999).

Cumulative sedimentary interbed thicknesses are reported as 5.4 to 17.6 m (18 to 58 ft) beneath ARA and 3 to 13 m (10 to 42 ft) under PBF (Holdren et al. 1997). Although not fully characterized, the interbeds at WAG 5 are thought to be discontinuous and limited in areal extent.

Basalt matrix characteristics were not developed specifically for WAG 5 as the fate and transport modeling used a conservative approach where basalts were ignored (discussed further in subsequent sections). Refer to discussions of basalt properties in Chapter 2 of this document.

#### *3.5.2.3 Recharge/Discharge*

***Underflow—***The effects of underflow at WAG 5 have not been investigated.

***Recharge from Precipitation—***Rain and snow precipitation is relatively low in the INEEL region. At WAG 5, there is little runoff or collection of precipitation except during heavy rainstorms or rapid snowmelt. High evapotranspiration rates (> 80% of the available water) result in very low infiltration rates (Anderson et al. 1987). In WAG 5 modeling work, the Track 2 default value of 10 cm/yr (4 in./yr) was used for the infiltration rate. This value is considered to be conservative, as infiltration rates derived from soil moisture monitoring at other INEEL facilities (Magnuson and McElroy 1993; Miller et al. 1990) were lower (Holdren et al. 1999).

***Episodic Recharge—***There are no significant surface water features at WAG 5. The Big Lost River channel turns to the north and runs approximately 7 mi to the west of WAG 5. Surface water flow may occur at ARA and PBF under certain conditions, but is usually rare. Generally, such flow is most likely in the spring when rare, heavy rains combined with warm temperatures, melting snow, and frozen ground may result in overland flow and ponding of water in depressions. There is no consistent local source of natural recharge to the aquifer at ARA or PBF (DOE-ID 2000b). PBF areas are influenced solely by variations in regional sources of recharge to the north, northeast, and northwest.

***Recharge from Wastewater Disposal—***Wastewater discharges from the various PBF-area facilities have largely ceased, and disposal to the two PBF injection wells ended in the late 1970s. Regular use of the percolation ponds associated with the several SPERT facilities ended with the SPERT program. Because no significant local sources of recharge exist and production-well withdrawals are small, water levels in the ARA and PBF region are basically unaffected by anthropogenic recharge/discharge.

***Aquifer Discharge to Production Wells—***The effects of production wells on local aquifer gradients were investigated during the Comprehensive RI/FS. Investigators concluded that the production wells did not affect groundwater gradients (Holdren et al. 1999).

#### *3.5.2.4 Hydraulics*

***Vadose Zone—***Hydraulic characteristics of the unsaturated zone have not been developed specifically for WAG 5. Fate and transport modeling conducted in support of the RI/FS utilized generic INEEL parameters, as discussed further in subsequent sections. Perched water has not been observed at the WAG 5 site.

***Snake River Plain Aquifer—***The hydraulic gradient at WAG 5 varies widely. As reported by Holdren et al. (1999), the general gradient is approximately 0.8 m/km (4 ft/mi) to the south and southwest. At PBF, however, a localized gradient of 4 m/km (23 ft/mi) to the southeast has been observed. An evaluation of elevation data, well construction details, barometric data, and production well pumping data concluded that the variability in gradient was attributable to structural heterogeneities in the aquifer. The

WAG 5 water table contour map developed by Holdren et al. (1999) is presented here for convenience (see Figure 3-26).

The detailed water level evaluations also identified a potentially confined (or semi-confined) portion of the aquifer at depth in the WAG 5 area. The Site 9 well, located roughly 1 mi north of Highway 20, shows an elevated hydraulic head (3.7 m higher than expected based on elevations in nearby wells). The Site 9 well is screened at a depth of 160 m (525 ft) below the water level. It is suggested by Holdren et al. (1999) that the elevated head is indicative of a confined or semi-confined conditions at depth, possibly caused by two substantial sedimentary layers observed at depth.

The transmissivity in the region varies from 130 to 110,000 $ft^2/d$ at ARA-II (DOE-ID 2000).

***3.5.2.5 Ground-Water Chemistry.*** Groundwater at WAG 5 has not specifically been characterized. However, water from the SRPA in the southern half of the INEEL typically is enriched in calcium, magnesium, and bicarbonate (Knobel et al. 1997). Aquifer water underlying WAG 5 would be similar in composition. The background concentrations of sodium, chloride, sulfate, and nitrate are 10, 15, 10 to 40, and 5 mg/L, respectively (Robertson et al. 1974).

***3.5.2.6 Contaminant Transport.*** No regional contaminant plumes are believed to be present beneath ARA and PBF, and fate and transport modeling does not indicate that future contamination in excess of risk-based concentrations from sources at the ARA and PBF will occur.

***Source Term—***Fifty-five individual contamination sites were originally identified at WAG 5. The sites consisted primarily of localized surface and subsurface soils that were contaminated by a range of past practices, such as small unlined impoundments used to dispose of research wastewater, septic leach fields, reactor coolant water blowdown pits, and windblown contaminated soils resulting from the 1961 SL-1 reactor accident. Based on the results of the RI/FS site characterization and screening process, 14 of the 55 sites were retained for risk analysis. The primary contaminants identified were heavy metals and fission products from the reactor operations.

Detailed information regarding the contamination sources at ARA and PBF, including the volumes of the contaminants, is found in the ROD (DOE-ID 2000ARA I Chemical/Evaporation Pond

In support of the RI/FS for WAG 5, the mass of contaminant of interest in the surface soils was estimated primarily by results of soil sampling. Individual source volumes were estimated and the concentration indicated by sampling was distributed evenly across the element volume. Estimated masses or activities for each contaminant of interest are presented in the RI/FS (Holdren et al. 1999). As the sources of contamination at WAG 5 are contaminated soil sites, the mechanism of release is simply leaching of contaminants by precipitating soil moisture. As with other WAGs across the INEEL, release rates have not been directly measured at WAG 5. Instead, contaminant flux into the vadose zone is estimated using contaminant specific distribution coefficients and average infiltration rates.

***Vadose Zone Transport—***As described by Holdren et al. (1999), contaminant movement in the vadose zone is controlled by the water infiltration rate, contaminant-specific sorption coefficients, and hydraulic properties of the interbeds. In the WAG 5 conceptual model, effects of basalt sequences on contaminant movement are ignored. Each contaminant source area is assigned a combined sedimentary thickness, which was derived from drilling logs of nearby wells. Sedimentary sequences are assumed to retard water and contaminant movement, unit gradient conditions are assumed throughout the unsaturated zone. Lateral flow across and between sedimentary lenses is not considered. Dispersion and diffusion are also not accounted for in the vadose zone.

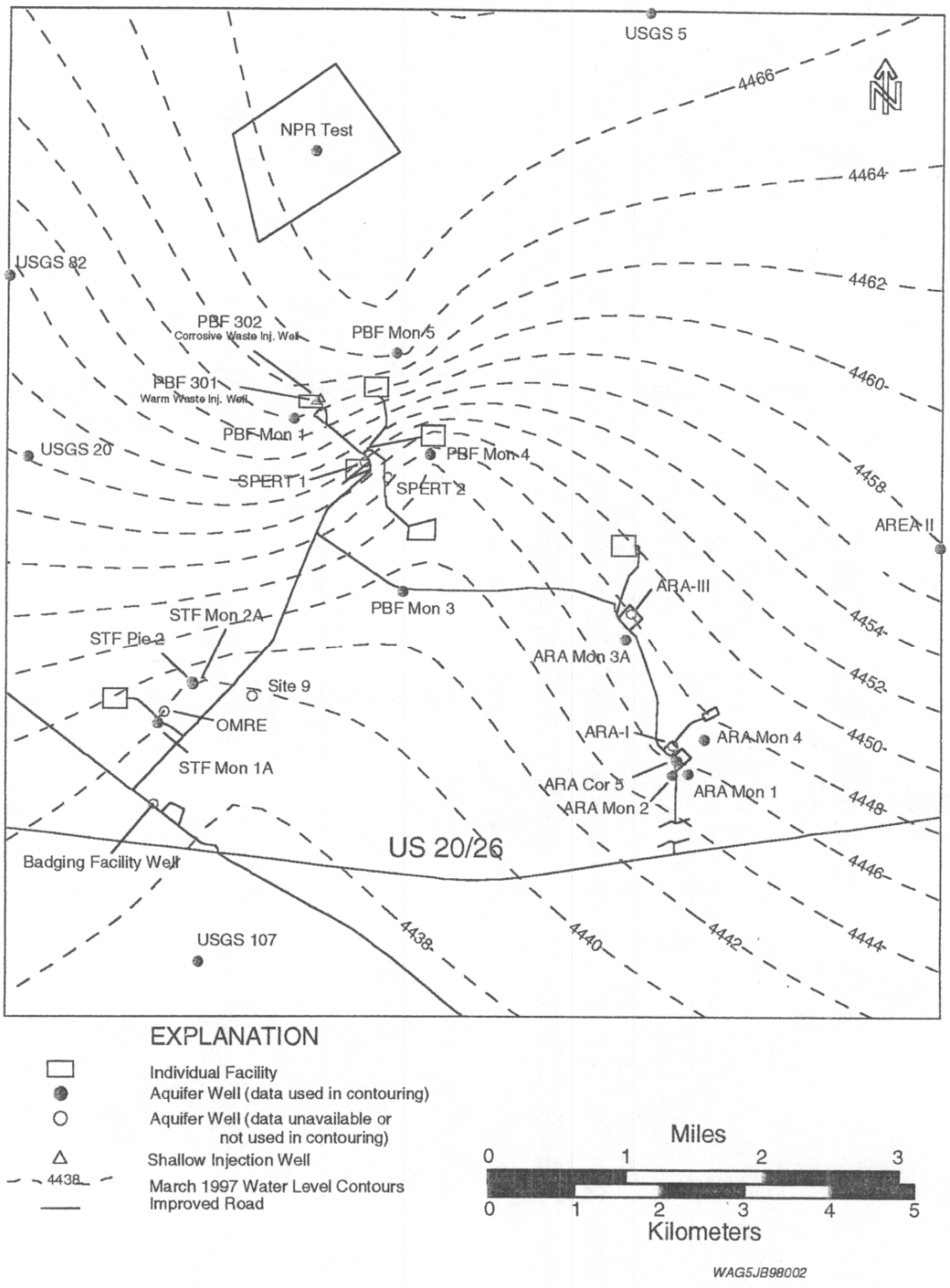


Figure 3-26. WAG 5 aquifer gradient and well locations (adapted from Holdren et al. 1999).

***Aquifer Transport—***The WAG 5 conceptual model treats the saturated zone as a homogenous isotropic aquifer of infinite lateral extent and finite thickness. Contaminants disperse horizontally and vertically as they move downgradient.

***Extent of Contamination of Groundwater at ARA and PBF—***The nature and extent of SRPA contamination at ARA and PBF were evaluated during the RI/FS through analysis of samples collected from eight groundwater monitoring wells and the SPERT-I production well. Beryllium, iron, arsenic, and lead were detected in at least one groundwater sample at concentrations exceeding either the risk-based concentration or MCL. As discussed in the RI/FS; however, concentrations of these contaminants were not attributed to sources at ARA or PBF and beryllium, iron, and arsenic were deemed not to pose an unacceptable risk. Five wells in WAG 5 had at least one groundwater sample with detected lead concentrations exceeding the 15 μg/L standard. These elevated lead concentrations were likely attributable to galvanic corrosion from the original well construction materials, which are now being replaced. Nitrate had also been detected in the past at elevated concentrations in samples drawn from the aquifer at PBF. Organic compounds had been detected infrequently and generally at low concentrations. Radionuclide concentrations were essentially at background levels in the PBF production wells.

### 3.5.3 Numerical Analyses

To estimate future contaminant concentrations for purposes of evaluating human health risk for the groundwater pathway, investigators developed a transport model for WAG 5 using GWSCREEN (Rood 1994). Site characterization data were insufficient to support a complex modeling approach. Additionally, because the probability of potential groundwater risk was thought to be low, a conservative and simplistic modeling approach was considered adequate (DOE-ID 2000).

In the GWSCREEN model, the vadose zone was considered to be a homogeneous, isotropic porous media with constant unidirectional (downward) flow. Unsaturated flow was modeled through sediments only. The unsaturated basalt sequences were excluded from the model as results of the LSIT indicated rapid flow through a dense fracture network. The sedimentary interbeds and surficial sediment thicknesses were summed and assigned conservative sorption coefficients for contaminants of interest. Infiltration was considered to be spatially uniform.

The initial aquifer thickness at the point that contaminants intersect the aquifer was set at 15 m (49 ft). This averaging concentration depth was based on the default Track 2 length of well screen (DOE-ID 1994). At the downstream receptor locations, contaminants are considered to diffuse across an effective aquifer thickness of 76m (250 ft).

Saturated zone parameters including effective porosity, pore velocity, and dispersivity were obtained from the default INEEL Track 2 guidance manuals (DOE-ID 1994). For the aquifer model, investigators used a vertical dispersivity value that was 10 times less than the transverse dispersivity to add conservatism to the fate and transport estimates. Table 3-5, adapted from the RI/FS (Holdren et al. 1999), summarizes the parameters used in the contaminant fate and transport modeling.

Solubility limits were ignored in the release and transport modeling. Solubility limits were conservatively assumed to be essentially infinite; assigning a value of 1.0 E+6 mg/L allowed leachate concentrations to exceed the solubility limit (Holdren et al. 1999). Contaminant specific distribution coefficients were obtained from Track 2 guidance and Dicke (1997).

Table 3-5. Parameters used in WAG 5 numerical modeling (adapted from Holdren et al. 1999).

| Parameter | Value |
|---|---|
| Net Infiltration Rate | 0.10 m/year |
| Moisture Content (source) | 0.3 $m^3/m^3$ |
| Moisture Content (unsaturated) | 0.3 $m^3/m^3$ |
| Solubility limit | 1.0 E +6 mg/L |
| Porosity (saturated) | 0.1 $m^3/m^3$ |
| Aquifer pore velocity | 570 m/year |
| Longitudinal dispersivity (saturated) | 9 m |
| Transverse dispersivity (saturated) | 4 m |
| Vertical dispersivity (saturated) | 0.4 m |

Results of the fate and transport modeling indicated that peak groundwater concentrations would be low and that the time of peak concentration would be thousands of years in the future for most contaminants. The subsequent risk analysis determined that groundwater exposure routes would not pose an unacceptable risk for any contaminant. The model predictions are thought to overestimate the actual concentrations due to the conservative assumptions made during the modeling effort. Although no model calibration was performed, these results are not inconsistent with the observed near-background concentrations of WAG 5 contaminants.

### 3.5.4 Summary of Competing Hypotheses and Additional Data Requirements

Because WAG 5 does not pose significant groundwater problems, a detailed conceptual model for this site has not been developed. The contaminant fate and transport work performed in support of the RI/FS utilized generalized model parameters from guidance documents. A comprehensive set of site-specific characterization data was not needed and not compiled. DOE elected to use a very simplistic, and conservative approach to estimate leaching of contaminants into the aquifer.

### 3.5.5 References Cited

Dicke, C. A., 1997, *Distribution Coefficients and Contaminant Solubilities for the Waste Area Group 7 Baseline Risk Assessment*, INEL/EXT-97-00201, Idaho National Engineering and Environmental Laboratory, Lockheed Martin Idaho Technologies Company, Idaho Falls, Idaho.

DOE-ID, January 1994, *Track 2 Sites: Guidance for Assessing Low Probability Hazard Sites at the INEL*, DOE/ID-10389, Revision 6, U.S. Department of Energy Idaho Operations Office, Idaho Falls, Idaho.

DOE-ID, 1997, *Final Work Plan for Waste Area Group 5 Operable Unit 5-12 Comprehensive Remedial Investigation/Feasibility Study*, DOE/ID-10555, Rev. 0, U.S. Department of Energy Idaho Operations Office, Idaho Falls, Idaho.

DOE-ID, January 2000, *Record of Decision for the Power Burst Facility and Auxiliary Reactor Area*, DOE/ID-10700, U.S. Department of Energy Idaho Operations Office, Idaho Falls, Idaho.

Holdren, K. J., C. M. Hiaring, D. E. Burns, N. L Hampton, B. J. Broomfield, E. R. Neher, R. L VanHorn, I.E. Stepan, R. P. Wells, R. L Chambers, L. Schmeising, R. Henry, January 1999, *Waste Area Group 5 Operable Unit 5-12 Comprehensive Remedial Investigation/Feasibility Study*, DOE/ID-10607, U.S. Department of Energy Idaho Operations Office, Idaho Falls, Idaho.

Holdren, K. J., J. D. Burgess, K. N. Keck, D. L. Lowrey, M. J. Rohe, R. P. Smith, C. S. Staley, and J. Banaee, 1997, *Preliminary Evaluation of Potential Locations on the Idaho National Engineering and Environmental Laboratory of a High-Level Waste Treatment and Interim Storage Facility and a Low-Level Waste Landfill*, INEEL/EXT-97-01324, Idaho National Engineering and Environmental Laboratory, Lockheed Martin Idaho Technologies Company, Idaho Falls, Idaho.

Knobel, L.L., Bartholomay, R.C., and Orr, B.R., 1997, *Preliminary Delineation of Natural Geochemical Reactions, Snake River Plain Aquifer System, Idaho National Engineering Laboratory and vicinity, Idaho*, U.S. Geological Survey Water-Resources Investigations Report 97–4093 (DOE/ID–22139), U.S. Geological Survey.

Magnuson, S. O. and D. L. McElroy, 1993, *Estimation of Infiltration from In Situ Moisture Contents and Representative Moisture Characteristic Curves for the 30', 110', and 240' Interbeds*, EG&G Engineering Design File #RWM-93-001.1, Idaho National Engineering and Environmental Laboratory, EG&G Idaho, Inc., Idaho Falls, Idaho.

Miller, S. M., J. E. Hammel, and L. F. Hall, 1990, *Characterization of Soil Cover and Estimation of Water Infiltration of Central Facilities Area Landfill II, Idaho National Engineering Laboratory (INEL), Research Technical Completion Report*, Idaho Water Resources Research Institute, University of Idaho, Moscow, Idaho.

Robertson, J.B., Schoen, R., and Barraclough, J.T., 1974, *The Influence of Liquid Waste Disposal on the Geochemistry of Water at the National Reactor Testing Station, Idaho*, U.S. Geological Survey Open- File Report, IDO–22053, U.S. Geological Survey.

Rood, A. S., 1994, "GWSCREEN: A Semi-Analytical Model for the Assessment of the Groundwater Pathway from Surface or Buried Contamination," Version 2.0, *Theory And User's Manual*, EGG-GEO-10797, Idaho National Engineering and Environmental Laboratory, EG&G Idaho Inc., Idaho Falls, Idaho.

# 3.6 Waste Area Group 6

## 3.6.1 Background

Waste Area Group 6 is the designation for the collection of CERCLA OUs associated with the Boiling Water Reactor Experiment (BORAX). The BORAX site was located in the south-western portion of the INEEL, south of Highway 20 approximately 1 mi northeast of the RWMC (Figure 3-27).

WAG 6 is the site of the historic BORAX-I reactor. This reactor was constructed in 1953 as a small, simple, and inexpensive light-water reactor. As described by DOE-ID (2001), this type of reactor had a uranium core that was water cooled in an open "swimming pool" type tank and could only be operated in the summer months. The reactor was used to test extreme excursions where the control rod would be ejected suddenly causing the reactor power to spike within milliseconds and vaporize the water in the surrounding tank. The tests reportedly ejected water to a height of 30 ft above the reactor.

As described by Holdren et al. (1995), the reactor was deliberately destroyed in the final excursion in July 1954. The test was designed to melt down the fuel rods with 80 megawatts of energy. However, within a few seconds of the ejection of the fuel rod, the reactor peaked at an estimated 135 megawatts. The resulting explosion displaced the entire reactor superstructure and disintegrated the reactor vessel. Debris was scattered over 84,000 $ft^2$ of ground. During subsequent cleanup activities, the remaining aboveground structures were removed, and the reactor was buried in place. Fragments found in the area had activities as high as 50 R/hr. The area contaminated from the excursion was covered with gravel.

In December 1995, DOE signed a ROD, which called for containment by capping with an engineered, long-term barrier (DOE-ID 1996). The remedial action began in July 1996. Contaminated soil was excavated and a human intrusion barrier was constructed over the consolidated soils consisting of basalt riprap. A chain link fence was installed around the burial ground with "Keep Out" and CERCLA identification signs. Two granite monuments were also installed to warn potential future intruders.

In addition to the original BORAX-I reactor, other reactors were located and tested at the WAG 6 site. For example, the BORAX V experiment (the Argonne Experimental Facility [AEF]-601) resulted in a variety of below ground artifacts including concrete foundations, two reactor vessels, a water storage pit (now dry), an equipment pit, a subreactor room, a utility pipe trench, a stream pipe trench, and a dry storage pit. A leach pond and drainage ditch associated with the BORAX II through V reactor experiments are also located at WAG 6. All of the WAG 6 facilities were remediated, the subsurface structures were entombed with soil and concrete, and the surface structures were excavated and covered.

## 3.6.2 Summary of the Present WAG-6 Conceptual Site Model

A detailed conceptual model has not been developed for WAG 6. Because the potential groundwater risks associated with past WAG 6 activities were considered relatively low, there has not been a large effort to characterize the hydrologic system or to monitor potential contaminant transport pathways. What site-specific information is available was developed in support of the Comprehensive RI/FS for WAGs 6 and 10 (DOE-ID 2001) and the RI/FS for OU 5-05 and 6-01 SL-1 and BORAX I Burial Grounds (Holdren et al. 1995) as summarized in this chapter. This section does not present any original hydrogeologic work, but simply summarizes technical elements that contribute to the conceptual model.

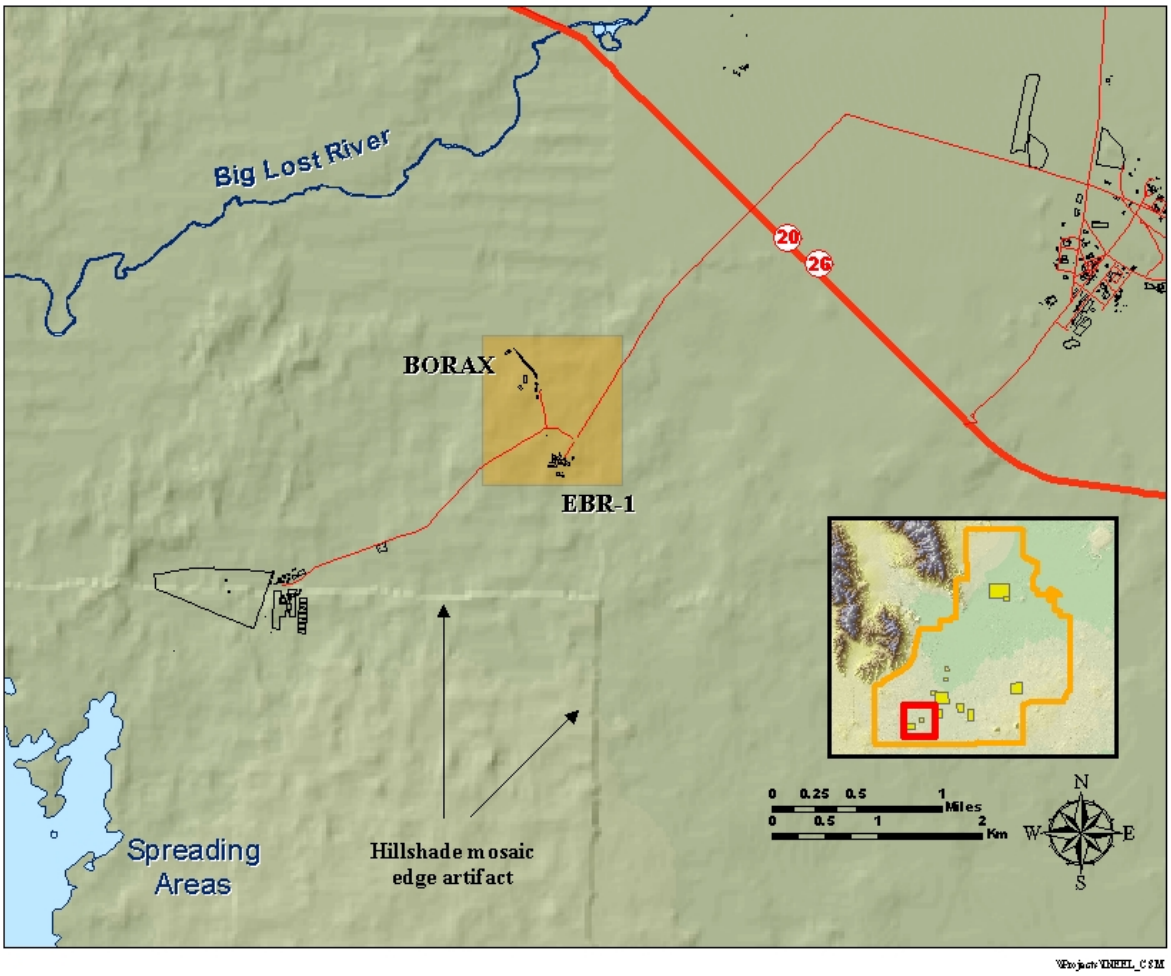


Figure 3-27. WAG 6 is associated with the BORAX in the southwest part of the INEEL.

### 3.6.2.1 Geologic Framework

***System Geometry—***Groundwater (SRPA) depth is reported as 177 m (580 ft) below land surface as measured at the nearby EBR-1 well in the BORAX-I RI/FS (Holdren et al. 1995), but is reported as approximately 196 m (640 ft) bls in the WAG 6 and 10 RI/FS (DOE-ID 2001).

***Geology—***As with other INEEL sites, WAG 6 geology is comprised of a complex layering of basalt flows and thin sedimentary deposits. Each basalt flow group is comprised of numerous basalt lava flows that erupted from nearby vents. Interbed sediments in the area consist primarily of fine grained clays, silts, and sands considered to be of eolian deposition. Site-specific geologic data have not been collected for WAG 6.

***Stratigraphy/Lithology—***Lithologic information is available from one well located at the nearby EBR-I site. Similar to other INEEL sites, numerous sedimentary deposits were encountered, but a stratigraphic description has not been developed specifically for WAG 6. Combined sediment thickness for all interbeds in the vadose zone is reported as 19.5 m (64 ft) based on lithologic information from the nearby EBR-1 well (Holdren et al. 1995).

***3.6.2.2 Matrix Characteristics.*** Matrix characteristics have not been described specifically for WAG 6 basalts and sedimentary units. The fate and transport modeling utilized default values from INEEL Track 2 guidance (DOE-ID 1994).

### 3.6.2.3 Recharge/Discharge

***Underflow—***The effects of underflow at WAG 6 have not been investigated.

***Recharge from Precipitation—***Rain and snow precipitation is relatively low in the INEEL region. WAG 6 is located on a topographic high where there is little runoff or collection of precipitation except during heavy rainstorms or rapid snow melt. High evapotranspiration rates (greater than 80% of the available water) result in very low infiltration rates (Anderson et al. 1987). In WAG 6 fate and transport modeling work, the Track 2 (DOE-ID 1994) default value of 10 cm/yr (4 in./yr) was used for the infiltration rate. This value is considered to be conservative based on actual infiltration rates derived from interbed moisture monitoring at the nearby RWMC facility (Magnuson and McElroy 1993).

***Episodic Recharge—***There are no significant surface water features at WAG 6. The Big Lost River channel turns to the north and runs approximately 1 mi to the West of WAG 6. Any potential effects of the river on aquifer recharge have not been investigated at this site.

***Recharge from Wastewater Disposal—***Wastewater discharges from the various BORAX reactors ended in 1964 (DOE-ID 2001). Because no significant local sources of recharge exist and there are no production wells, water levels in the WAG 6 area are unaffected by anthropogenic recharge or discharge.

### 3.6.2.4 Hydraulics

***Vadose Zone—***Hydraulic characteristics of the unsaturated zone have not been developed specifically for WAG 6. Fate and transport modeling conducted in support of the RI/FS utilized generic INEEL parameters, as discussed further in subsequent sections. Sondrup, Magnuson, and Smith and Rood supported the WAG 6-01 RI/FS by treating unsaturated zone flow as a constant, steady-state process through the sedimentary layers under unit gradient conditions. They concluded, “an adequate, physically based hydrologic description of water movement through the fractured basalt portion of the vadose zone under background or normal infiltration conditions is lacking. Theoretical descriptions are available, but

the applicability to water movement under background infiltration conditions at the INEL has not been demonstrated" (Holdren et al. 1995, Appendix C).

***Snake River Plain Aquifer—***The hydraulic gradient at WAG 6 has not been measured. In the RI/FS, aquifer velocity was estimated to be 570 m/yr (Holdren et al. 1995). Effective thickness of the aquifer was estimated to be 76 m based on Robertson's (1974) work using tritium tracers. Water flow through the aquifer was assumed to exhibit constant and uniform linear velocities and dispersivities for purposes of the fate and transport modeling. The basalts were treated as homogeneous porous media with infinite lateral extent.

#### *3.6.2.5 Groundwater Chemistry—*

Groundwater at WAG 6 has not specifically been characterized. However, water from the SRPA in the southern half of the INEEL typically is enriched in calcium, magnesium, and bicarbonate (Knobel et al. 1997). Aquifer water underlying WAG 6 would be expected to be similar in composition. The background concentrations of sodium, chloride, sulfate, and nitrate are 10, 15, 10 to 40, and 5 milligrams per liter, respectively (Robertson et al. 1974).

#### *3.6.2.6 Contaminant Transport—*

No regional contaminant plumes are believed to be present beneath WAG 6. Fate and transport modeling performed in support of the RI/FS indicated that future contamination would not exceed risk-based concentrations.

The BORAX source term consists of soils and buried debris contaminated primarily by heavy metals and fission products from the reactor operations. Detailed radiological inventories were estimated by Holdren et al. (1995) based on the reactor operating history. For release modeling purposes, the inventory was assumed to be uniformly distributed across the source region. Uranium isotopes comprise a significant fraction of the inventory. Contaminants are leached by infiltrating water; the rate of release is considered to be governed by a first order leach rate constant, which is a function of infiltration rate and contaminant specific partition coefficients.

As described by Holdren et al. (1995), contaminant movement in the vadose zone is controlled by the water infiltration rate, contaminant-specific sorption coefficients, and hydraulic properties of the interbeds. In the WAG 6 conceptual model, effects of basalt sequences on contaminant movement are ignored. The contaminant source area is assigned a combined sedimentary thickness, which was derived from drilling logs of nearby wells. The sedimentary sequences retard contaminant movement as described by linear equilibrium partitioning coefficients. Water is assumed to flow through the unsaturated sediments in a constant, vertical direction under unit gradient conditions. Lateral flow across and between sedimentary lenses is not considered. Dispersion and diffusion are also not accounted for in the vadose zone.

For the purposes of conservatively estimating potential groundwater risk, the WAG 6 conceptual model treats the saturated zone as a homogenous isotropic aquifer of infinite lateral extent and finite thickness. Flow is considered to be uniform and unidirectional with no recharge or discharge sources. Contaminants disperse horizontally and vertically as they move downgradient and are uniformly mixed in the upper portion of the aquifer. Longitudinal and transverse dispersion is assumed to be constant. Sorption in the aquifer is described by linear equilibrium partitioning using distribution coefficients reported in the literature for basalts.

### 3.6.3 Numerical Analyses

To estimate future contaminant concentrations, for purposes of evaluating human health risk for the groundwater pathway, Holdren et al. (1995) utilized GWSCREEN (Rood 1994). Investigators decided that site characterization data were insufficient to support a more complex modeling approach.

Additionally, because the probability of potential groundwater risk was thought to be low, a conservative and simplistic modeling approach was considered adequate.

In the GWSCREEN model, the vadose zone was considered to be a homogeneous, isotropic porous media with constant unidirectional (downward) flow. Unsaturated flow was modeled through sediments only. The unsaturated basalt sequences were excluded from the model, as theoretical descriptions of fracture network flow were not considered defensible at that time. The sedimentary interbeds and surficial sediment thicknesses were summed and assigned conservative sorption coefficients for contaminants of interest using values from the Track 2 guidance (DOE-ID 1994) and other literature. Infiltration was considered to be spatially uniform.

Saturated zone parameters including effective porosity, pore velocity, and dispersivity were obtained from the default INEEL Track 2 guidance manuals (DOE/ID 1994). Table 3-6, adapted from the RI/FS (Holdren et al. 1995) summarizes the parameters used in the contaminant fate and transport modeling.

Solubility limits were not incorporated into the release and transport modeling. Solubility limits were conservatively assumed to be essentially infinite; assigning a value of 1.0 E+6 mg/L allowed leachate concentrations to exceed the solubility limit (Holdren et al. 1995).

Results of the fate and transport modeling indicated that peak groundwater concentrations would be low and that the time of peak concentration would be thousands of years in the future for most contaminants. The subsequent risk analysis determined that only uranium isotopes and progenies reached potential receptor locations at any significant concentration. The estimated risk contributed by the groundwater pathway fell below regulatory thresholds for concern (Holdren et al. 1995).

Table 3-6. Parameters used in WAG 6 numerical modeling (adapted from Holdren et al. 1995).

| Parameter | Value | Unit |
|---|---|---|
| Net Infiltration Rate | 0.10 | m/year |
| Moisture Content (source) | 0.34 | $m^3/m^3$ |
| Moisture Content (unsaturated) | 0.34 | $m^3/m^3$ |
| Solubility limit | 1.0 E +6 | mg/L |
| Porosity (saturated) | 0.1 | $m^3/m^3$ |
| Aquifer pore velocity | 570 | m/year |
| Longitudinal dispersivity (saturated) | 9 | m |
| Transverse dispersivity (saturated) | 4 | m |
| Vadose zone sediment thickness | 19.5 | m |

### 3.6.4 Summary of Competing Hypotheses and Additional Data Requirements

Because WAG 6 does not pose significant groundwater problems, a detailed conceptual model for this site has not been developed. The contaminant fate and transport work performed in support of the RI/FS utilized generalized model parameters from guidance documents. A comprehensive set of site-specific characterization data was not compiled. DOE elected to use a simplistic and conservative approach to estimate leaching of contaminants into the aquifer. Sondrup, Magnuson, Smith and Rood did however, in their characteristic veracity, analyze model sensitivity, concluding that the range in distribution coefficient values overshadowed uncertainties in other parameters (Holdren et al. 1995).

### 3.6.5 References Cited


DOE-ID and IDHW, 1996, *Record of Decision (ROD) for Stationary Low Power Reactor 1 (SL-1) OU 5-05 & BORAX I Burial Grounds OU 6-01 & 10 (Ten) No Action Sites (OU 5-01, 5-03, 5-04, and 5-11)*, INEL-95/0282, U.S. Department of Energy Idaho Operations Office, Idaho Department of Health and Welfare, Idaho National Engineering and Environmental Laboratory, Idaho Falls, Idaho.

DOE-ID, 2001, Comprehensive Remedial Investigation/Feasibility Study for Waste Area Groups 6 and 10 Operable Unit 10-04, DOE/ID-10807, August. Rev 0.

DOE-ID, January 1994, *Track 2 Sites: Guidance for Assessing Low Probability Hazard Sites at the INEL*, DOE/ID-10389, Rev 6, U.S. Department of Energy Idaho Operations Office, Idaho Falls, Idaho.

Holdren, K. J., R. G. Filemyr, D. W. Vetter, March 1995, *Remedial Investigation Feasibility Study (RI/FS) Report For OU 5-05 and 6-01 SL-1 and BORAX I Burial Grounds*, INEL-95/0027 Revision 0, Idaho National Engineering and Environmental Laboratory, Idaho Falls, Idaho.

Knobel, L.L., Bartholomay, R.C., and Orr, B.R., 1997, *Preliminary Delineation of Natural Geochemical Reactions, Snake River Plain Aquifer System, Idaho National Engineering Laboratory and Vicinity, Idaho*: U.S. Geological Survey Water-Resources Investigations Report 97-4093 (DOE/ID-22139), U.S. Geological Survey.

Magnuson, S. O. and D. L. McElroy, 1993, *Estimation of Infiltration from In Situ Moisture Contents and Representative Moisture Characteristic Curves for the 30', 110', and 240' Interbeds*, EG&G Engineering Design File #RWM-93-001.1, Idaho National Engineering and Environmental Laboratory, EG&G Idaho, Inc., Idaho Falls, Idaho.

Robertson, J.B., Schoen, R., and Barraclough, J.T., 1974, *The Influence of Liquid Waste Disposal on the Geochemistry of Water at the National Reactor Testing Station, Idaho*, U.S. Geological Survey Open-File Report, IDO-22053, U.S. Geological Survey.

Rood, A. S., 1994, "GWSCREEN: A Semi-Analytical Model for the Assessment of the Groundwater Pathway from Surface or Buried Contamination," *Version 2.0, Theory and User's Manual*, EGG-GEO-10797, Idaho National Engineering and Environmental Laboratory, EG&G Idaho Inc., Idaho Falls, Idaho.

# 3.7 Waste Area Group 7

WAG 7 is the designation for the collection of CERCLA OUs associated with the RWMC. The RWMC is located in the southwestern quadrant of the INEEL (see Figure 3-28). The WAG 7 site encompasses one of the largest radioactive and hazardous waste landfills in the world, referred to as the Subsurface Disposal Area (SDA). Wastes from government, military, and commercial operations from around the country were placed in shallow excavations at the SDA between 1952 and 1970. The potential risk posed by the waste disposal has been a subject of considerable study since that time.

This chapter summarizes the current conceptual model for WAG 7. It also serves as an index, or researcher's guide, to previous investigations and sources of WAG 7 hydrologic information. This section does not present any original hydrogeologic work, but simply summarizes technical elements that contribute to the conceptual model. The conceptual model is discussed in general terms in Section 3.7.2, followed by detailed discussions of hydrologic information in subsequent sections. Factors affecting contaminant transport are presented in Section 3.7.2.5, which although it is not an exhaustive discussion of contaminant transport, presents several of the key factors currently under investigation. A history and comparison of the numerical models developed for WAG 7 is presented in Section 3.7.3. Finally, a brief discussion of ongoing conceptual model controversy is found in Section 3.7.4.

## 3.7.1 Background

The volume of scientific material related to WAG 7 is very large. The DOE (and its predecessor, the AEC) has funded some level of study at this site for over five decades. Although formal CERCLA requirements for investigation and possible remediation of this site were not imposed until 1991, geohydrologic investigations have been conducted since waste disposal activities began. In addition to the DOE, the USGS also conducted research at the site starting as early as 1952. In 1988, the USGS began a formal study of the stratigraphy of volcanic and sedimentary units underlying the INEEL to identify features that might affect movement of wastes in the subsurface. This work continues today.

In 1960, the AEC concluded that solid radioactive wastes could be disposed at the RWMC without undue risk, but that a potential for aquifer contamination did exist. They recommended that the site be used in an interim period until another site without an underlying aquifer could be identified (as reported in Barraclough et al. 1976). In the same year, the U.S. National Academy of Sciences stated that the "movement of fluids through the vadose zone and the consequent movement of the radioisotopes are not sufficiently understood to ensure safety." An important study conducted by the USGS between 1971 and 1974 (Barraclough et al. 1976) began to describe some of the physical and chemical features controlling contaminant transport. Through the construction of the first 10 wells, the USGS established a lithologic framework and reported detection of trace amounts of radionuclides at depth in the vadose zone.

In December 1991, the DOE entered into a FFA/CO (DOE-ID 1991) with the EPA and the State of Idaho to implement the remediation of the INEEL. The goals of the agreement were to ensure that potential or actual releases of hazardous substances to the environment were thoroughly investigated and that appropriate response actions be taken to protect human health and the environment. To implement the agreement, the INEEL embarked on a decade-long, multi-million-dollar effort to collect environmental data to assess the nature and extent of contamination that had resulted from past activities.

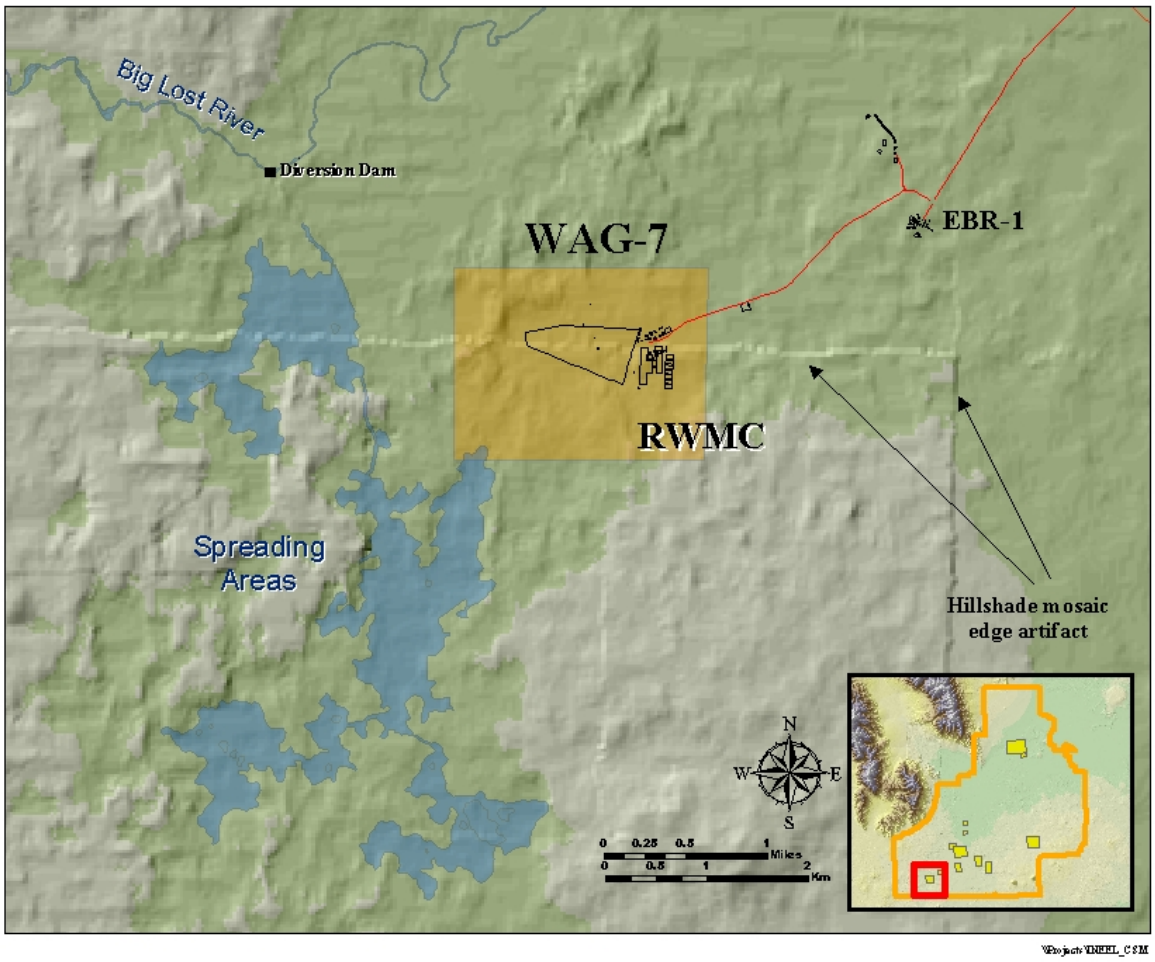


Figure 3-28. WAG 7 is associated with the RWMC in the southwestern quadrant of the INEEL.

Since that time, the WAG 7 geohydrologic work has been conducted in support of a CERCLA comprehensive RI/FS and is the last scheduled investigation under the FFA/CO. This investigation is ongoing and will be a comprehensive evaluation of the potential risk posed by WAG 7.

The investigations conducted at this site have had a strong regulatory focus. That is, the primary objective of the studies was to estimate future risk to support remedial decisions. The majority of the scientific investigations have been performed to this end; data that would not directly influence the decision process were not typically acquired. As a result, data necessary to construct a predictive simulator have been pursued, but a thorough conceptual model has not been explicitly developed.

When taken as a whole, a large number of the investigations were conducted independently of each other and were not part of a cohesive plan to develop and test the conceptual model. Data collection efforts were often discontinuous and frequent changes in experimental designs limited comparability between studies. In general, investigators have worked in succession, building upon previous work, but changing program priorities and funding levels often resulted in discontinuous and inconclusive efforts. More recent work conducted under the RI/FS work plan (Becker et al. 1996) has been well coordinated, but other events have interrupted elements of the technical work (e.g., a recent run of dry weather has confounded tracer studies and perched water monitoring efforts.

Two important reports, the Interim Risk Assessment (Becker et al. 1998) and the Comprehensive Evaluation (Holdren et al. 2002), present a sophisticated contaminant fate and transport simulation and predict long-term risk posed by this site. The authors of these documents are acknowledged for their exceptional work, as well as the assistance they have provided to the Water Integration Project supporting the development of this document. The Holdren et al. (2002) work is relied on heavily for information presented in this section. Additionally, in 1999, the USGS performed an intensive technical review of the Interim Risk Assessment document and subsequently drafted an administrative report to the DOE that discusses many of the uncertainties associated with the current conceptual model. This USGS work, yet unpublished, is likewise referenced frequently as USGS (1999).

### 3.7.2 Summary of the Present WAG-7 Conceptual Model

WAG 7 is nearing the end of a relatively long remedial investigation process. Although a detailed conceptual model has not been explicitly developed, a large body of geologic and hydrologic information has been compiled to support the remedial action decision at this site. The next few pages describe the current WAG 7 conceptual model. This description is a compilation of conceptual model discussions presented in a variety of work ranging from Barraclough et al. 1976 to Holdren et al. 2002. The specific elements of the conceptual model and sources of information are discussed in detail in subsequent sections.

Similar to the regional INEEL geology, the subsurface at WAG 7 is underlain by thick sequences of basalt flows and a number of relatively thin lenses of sedimentary materials, deposited during periods of volcanic quiescence. Contaminants may become mobilized by infiltrating precipitation, ambient soil moisture, or in the case of VOCs, by gaseous diffusion. Largely under the influence of gravity, the water with its associated contaminants percolates through the interlayered network of basalts and sedimentary interbeds. A number of chemical and physical processes are thought to affect the concentration of contaminants in the water as it moves through the vadose zone. When contaminants reach the saturated zone, the material is thought to move slowly in the horizontal plane under a small gradient, slowly diluting with the large body of aquifer water.

Prior to the LSIT test, it had been assumed that the horizontal permeability significantly exceeded vertical permeability due to the highly fractured or rubbleized zones at flow interfaces. Because of the macro scale anisotropy, extensive lateral spreading was expected (Faybishenko et al. 2000); although other researchers (Bishop 1991) found vertical and horizontal hydraulic conductivity to be virtually identical for a number of core samples. Results from the infiltration test indicated that vertical permeability was significantly greater than previously assumed and that lateral spreading appeared to occur at the sedimentary interbeds and not in rubble zones between flows. However, more recent tracer tests of spreading area water give evidence that significant lateral flow, at least during flood conditions, may be occurring in the rubbleized interflow zones.

As a result, some researchers maintain that fracture features, connectivity, and relationship to other geological features are critical to the understanding of contaminant movement at the RWMC. It has been

suggested that a single porosity model may not be sufficient to represent flow in fractured basalt (Faybishenko et al. 2000). Other researchers have stated that "various processes are not well enough understood with respect to unsaturated-zone flow behavior to predict on a theoretical basis the effect on the spread of contamination" (USGS 1999).

However, because the risk assessment work evaluates contaminant concentrations at relatively great distances and time periods, it is generally concluded that the flow through basalt strata can be reasonably simulated by considering all flow to be through fractures, emulating an anisotropic medium with low effective porosity and high permeability, as described in Holdren et al (2002). Although the current conceptual model is acknowledged as a simplification of the actual system, it is generally considered an adequate and conservative approach for assessing risk.

The sedimentary interbeds are likewise spatially variable in terms of elevation, thickness, composition, and hydraulic properties. Three substantial sedimentary layers, found at depths of approximately 30, 110, and 240 ft, are considered to be extensive enough to significantly affect water and contaminant movement. Earlier characterization of the interbeds, based on a few core samples, maintained that they were largely composed of clay-sized materials. Additional coring work was performed in 1999, which revealed that the interbeds were heterogeneous and ranged in composition from silt to gravel, with little clay. In the most recent simulation work (Holdren et al. 2002), the interbeds are represented as spatially variable in thickness, elevation, and hydraulic properties based on core data. Darcian flow is believed to describe water movement through the sedimentary interbeds. The interbeds are also thought to have some water storage capacity that may dampen transient recharge events (Wood et al. 2002).

An extensive moisture monitoring network has allowed researchers to develop spatially-variable and, to a lesser extent, time-dependent infiltration rates. Generally, when conceptualizing the movement of contaminants over long time periods, infiltration is conceptualized as a steady state input. Thin, perched water lenses have been found above some interbeds, which is generally attributed to lower hydraulic conductivity of the sedimentary material.

Although some recharge apparently is contributed by episodic floods of the Big Lost River and its man-made diversions, annual precipitation is thought to contribute the majority of the moisture. The basin and range systems stretching to the northwest of the INEEL are thought to be too distant to affect flow on a local (WAG 7) scale. Although the SRPA thickness is uncertain, the current WAG 7 conceptual model only considers the top 250 ft in regards to contaminant interaction.

Because flow through the basalts is considered to be primarily through the fracture network, there is thought to be relatively little reaction between dissolved contaminants and the basalt matrix. There has been some evidence of sedimentary infilling and precipitated minerals inside of some of the basalt fractures, which in theory would help retard contaminant movement, but this hypothesis has not been developed. In fact, as discussed in subsequent sections, current simulations do not account for any sorption in the fractured basalt.

The sedimentary deposits, although they are known to be spatially variable in thickness and hydrologic properties, are in general considered to be retarding features for contaminant movement. Surficial and interbed sediment sorption has been assumed to follow linear reversible isotherms, which are described by partition coefficients. A set of partition coefficients has been assembled for the WAG 7 contaminants and sediments using a combination of literature values and site-specific data. Due the complexity of the geochemical factors affecting the concentration of contaminants in solution, as well as the limited site-specific data, the sorption process is an uncertainty in the current conceptual model. In addition to difficulties obtaining representative sorption data, non-dissolved transport is also a possibility.

Transport of contaminants in non-dissolved states (particulate forms) has been investigated in laboratory tests and by sensitivity studies, but the concept has not been developed and incorporated into the conceptual model.

The release of contaminant mass from the waste zone is conceptualized as occurring primarily by three processes: surface wash off, diffusion, and/or dissolution. Estimates of flux of contaminants from the waste zone have been made by considering the form of the contaminants and rate of precipitation over a given area. This estimation is considered one of the greatest sources of uncertainty in the conceptual model since little data exist to substantiate the rate of past, present, or future releases.

Contaminant transport simulations based on the current conceptual model indicate that low levels of contamination will impact the aquifer in the future; however, risk to humans and the environment is relatively low (Holdren et al. 2002). However, monitoring data for many contaminants, particularly actinide species, are inconclusive for substantiating the conceptual model and simulation efforts. Holdren et al. (2002) summarizes, "Contaminants of particular interest for model calibration, such as C-14, uranium, and other actinides, are detected sporadically and at very low concentrations that do not describe migration trends. The low concentrations coupled with lack of trends cannot be emulated with any confidence."

#### *3.7.2.1 Geologic Framework*

***System Geometry—***WAG 7 is located in the southwest portion of the INEEL, approximately 1 mi north of the southern INEEL boundary. The RWMC facility encompasses 174 acres, including the SDA, operational, and administrative areas. The site is in a topographic low, surrounded by basaltic ridges. The Big Lost River channel runs north-easterly, roughly 1 ½ mi north of the RWMC. A diversion dam is used periodically to control flood waters on the Big Lost River, diverting water to a series of four playas (referred to as the spreading areas) approximately 1 mi southwest of the RWMC. The RWMC facility itself is protected by large dikes constructed to minimize ponding of snowmelt inside of the facility.

Generally, the WAG 7 area of investigation is defined by the extent of wells that were constructed around the facility at a roughly 2-mi radius. The depth to the top of the aquifer ranges from 180 to 186 m (590 to 610 ft; Holdren et al. 2002). For modeling work in the interim remedial action (IRA) and in the Comprehensive Evaluation, the horizontal simulation domain was defined as a rectangle approximately 27,000 × 34,000 ft, which encompassed the RWMC, spreading areas, and a portion of the Big Lost River, as well as several new wells north of the RWMC. The thickness of the aquifer simulation domain in both the IRA and the Comprehensive Evaluation was set at 250 ft (saturated zone only, not including any of the vadose zone). The assumed aquifer thickness is consistent with that used in the WAG 3 and WAG 10 modeling studies (Becker et al. 1998).

***Stratigraphy/Lithology—***Investigators have installed over 100 wells in the RWMC area since 1976, resulting in a representative stratigraphic description. Data resulting from well cuttings, cores, geophysical logs, potassium-argon ages, and geomagnetic properties were collected from many of the wells. Stratigraphic control was provided by four sequential basalt flows that have reversed geomagnetic polarity and high gamma emissions (Anderson and Lewis 1989). From these data, a reasonably comprehensive picture of subsurface geology could be drawn. Figures 3-29 and 3-30, from Holdren et al. (2002), present cross-sections through the SDA area.

As described in Section 2, the subsurface geology of this area is characterized by interlayered basalt flows and sedimentary deposits of Quaternary age. In the WAG 7 region, there are at least 10 sedimentary interbeds and 11 basalt flow groups between the surface and top 200 ft of the SRPA (Anderson and Lewis 1989; Anderson and Bartholomay 1995; Anderson et al. 1996). The numbers and ages of basalt flows in the saturated zone is uncertain due to the limited number of cores available (USGS 1999).

11 × 17 figure to be inserted separately

Figure 3-29. Stratigraphy beneath WAG 7 (adapted from Holdren et al. 2002).

11 × 17 figure to be inserted separately

Figure 3-30. Stratigraphy beneath WAG 7 (adapted from Holdren et al. 2002).

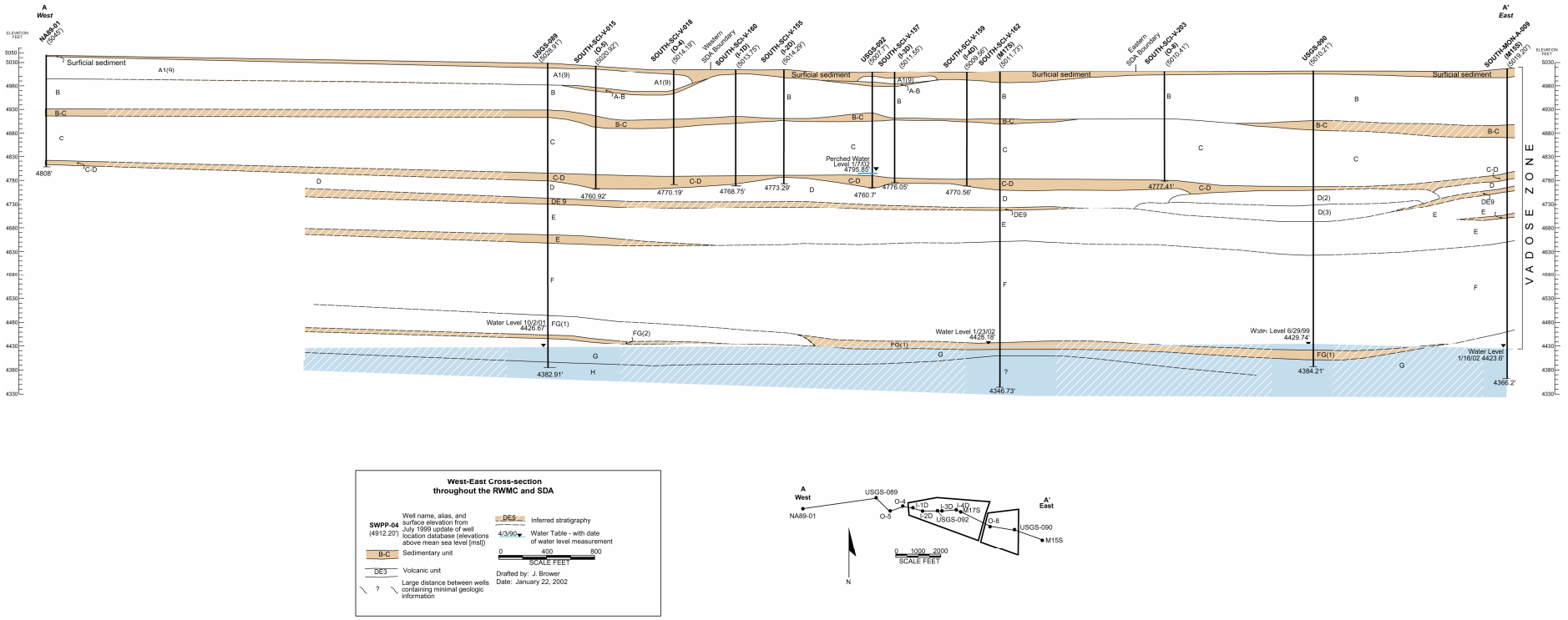


**West-East Cross-section throughout the RWMC and SDA**

SWPP-04 (4912.20') — Well name, alias, and surface elevation from July 1999 update of well location database (elevations above mean sea level [msl])

B-C — Sedimentary unit

DE3 — Volcanic unit

? — Large distance between wells containing minimal geologic information

DE5 — Inferred stratigraphy

4/3/90 — Water Table - with date of water level measurement

0 400 800 SCALE FEET

Drafted by: J. Brower

Date: January 22, 2002




Figure 3-29. Stratigraphy beneath WAG 7 (adapted from Holdren et al. 2002).

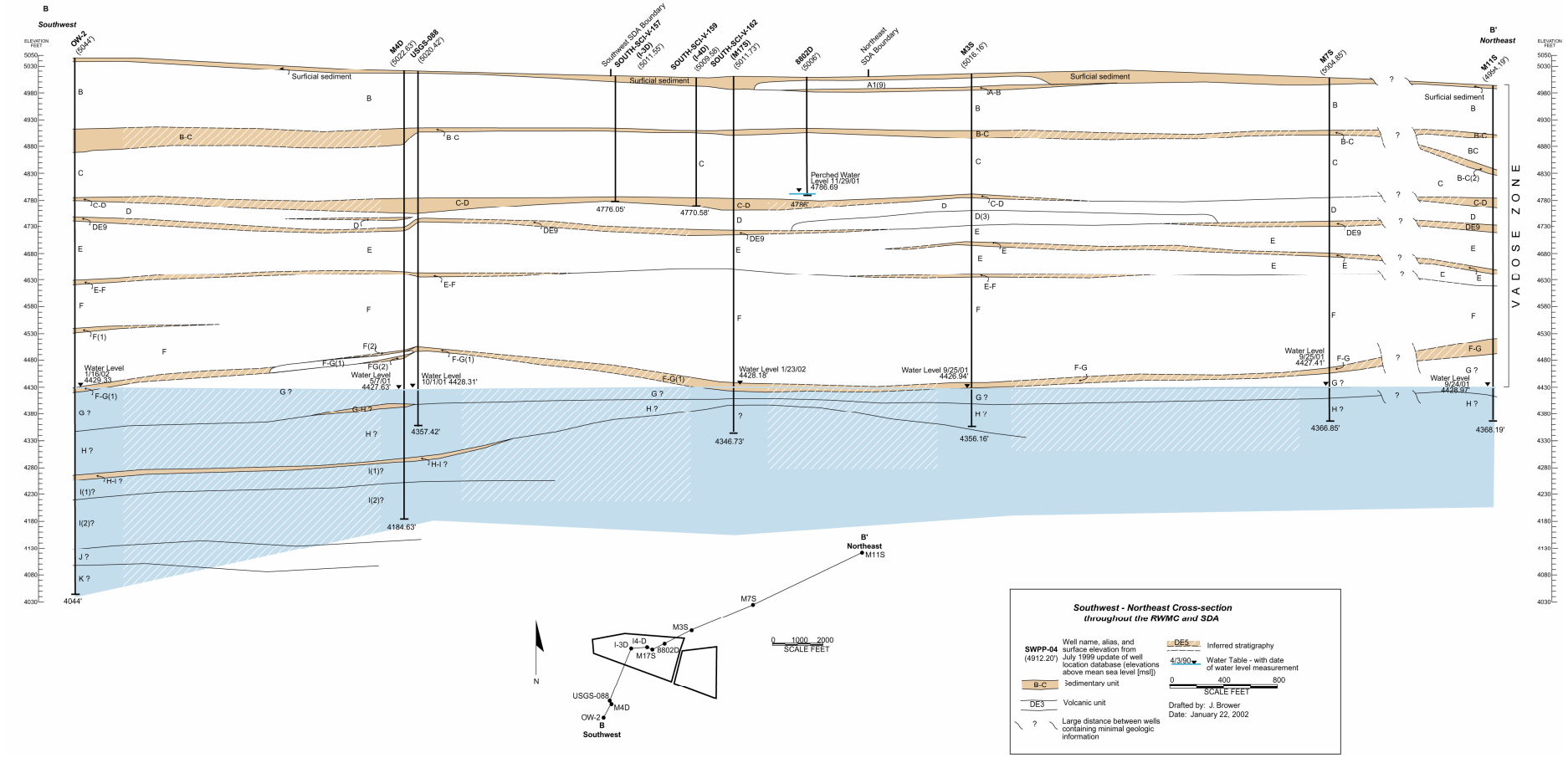


Figure 3-30. Stratigraphy beneath WAG 7 (adapted from Holdren et al. 2002).

Sedimentary deposits consist of fluvial, lacustrine, and eolian deposits of clay, silt, sand, and gravel. Basalt accounts for 90% of the volume of this stratigraphic section (Anderson et al. 1996). Average thicknesses for the flow groups ranges from 22 to 167 ft. Average thicknesses for interbeds range from zero (where flow groups intersect) to over 30 ft for the deeper C-D interbed (Anderson and Lewis 1989; Holdren et al. 2002). Due to the irregular topography of the basalt flows, the interbeds can exhibit abrupt changes in thickness.

The lithologic data presented in the cross-sections were derived primarily from the data compilation done by Anderson et al. (1996), with additions from wells drilled at 13 new locations by DOE in 1999. Leecaster (2002) performed a spatial variability assessment on this data set. The results of the statistical analysis were then used to predict the upper elevations and thickness of the surficial sediments, A-B, B-C, and C-D interbeds. The results of several different kriging methods were compared to actual data, and the most accurate approach was used to assemble the final lithology. (Note that the data below the D layer were too sparse to support modeling [Leecaster 2002]).

As can be seen, the A-B interbed has been found to be discontinuous across the RWMC area. The B-C and C-D interbeds, although not fully characterized, are considered present at most locations in the domain. There are several locations where well borings indicate the B-C and C-D interbeds have zero thickness (that is, they are pinched out by basalt interfaces). Figure 31 from Holdren et al. (2002) illustrates variability in interbed thickness. The lower plot indicates the results of the kriging. As noted in the Comprehensive Evaluation, the locations of zero thickness in the B-C and C-D interbeds were not statistically significant and do not carry over into the kriging results. As discussed further in subsequent sections, the hydraulic properties are also considered to be spatially variable.

***Matrix Characteristics.*** Characterization of numerous core samples has demonstrated that the vadose zone and aquifer basalts are highly anisotropic and heterogeneous units, characterized by a dense network of fractures with high permeability. As described in Section 2, variable cooling patterns and structural stresses of the lava flows resulted in heterogeneous fracture patterns. Generally, the upper surfaces of individual flows are intersected by larger and more frequent fractures than flow centers and bottoms due to more rapid cooling. The basalt sequences are generally represented as a homogenous fracture flow network. Results of the LSIT, as discussed in Section 2, contributed significantly to the treatment of flow through the basalt.

The inverse modeling done by Magnuson (1995), using the LSIT data, is used to describe the field scale hydraulic properties for the basalts. In this study it was demonstrated that flow in the fractured porous basalts could be adequately represented as a high-permeability, low-porosity equivalent porous continuum using a Darcian description. The current numerical representation of water and contaminant movement was originally presented by Magnuson and Sondrup (1998). This representation served as the basis for both the Interim Risk Assessment (Becker et al. 1998) and the Comprehensive Evaluation (Holdren et al. 2002). As described in Section 3.7.3, a number of improvements were made in the most recent work. Table 3-7, adapted from Holdren et al. (2002) summarizes the vadose zone matrix properties used in the Comprehensive Evaluation simulation.

***Surficial Sediments—***Surficial sediment deposits in the RWMC area originated primarily from glaciation and flood plains of the Big Lost River (Dechert et al. 1994; Rightmire and Lewis 1987b). Thickness ranges from 2 to 23 ft and is governed by the undulations of the topmost basalt flow (Anderson, Liszewski, and Ackerman 1996). Clay content in the RWMC surficial soils ranges from 36 to 50% (Chatwin et al. 1992; Lee et al. 1991). Quartz (37.5%), calcite (10%), iron oxy-hydroxide, and other minerals (2.55%) comprise the remainder (Lee et al. 1991). However, Chatwin et al. (1992) also reported high silt content (56%) in some areas.

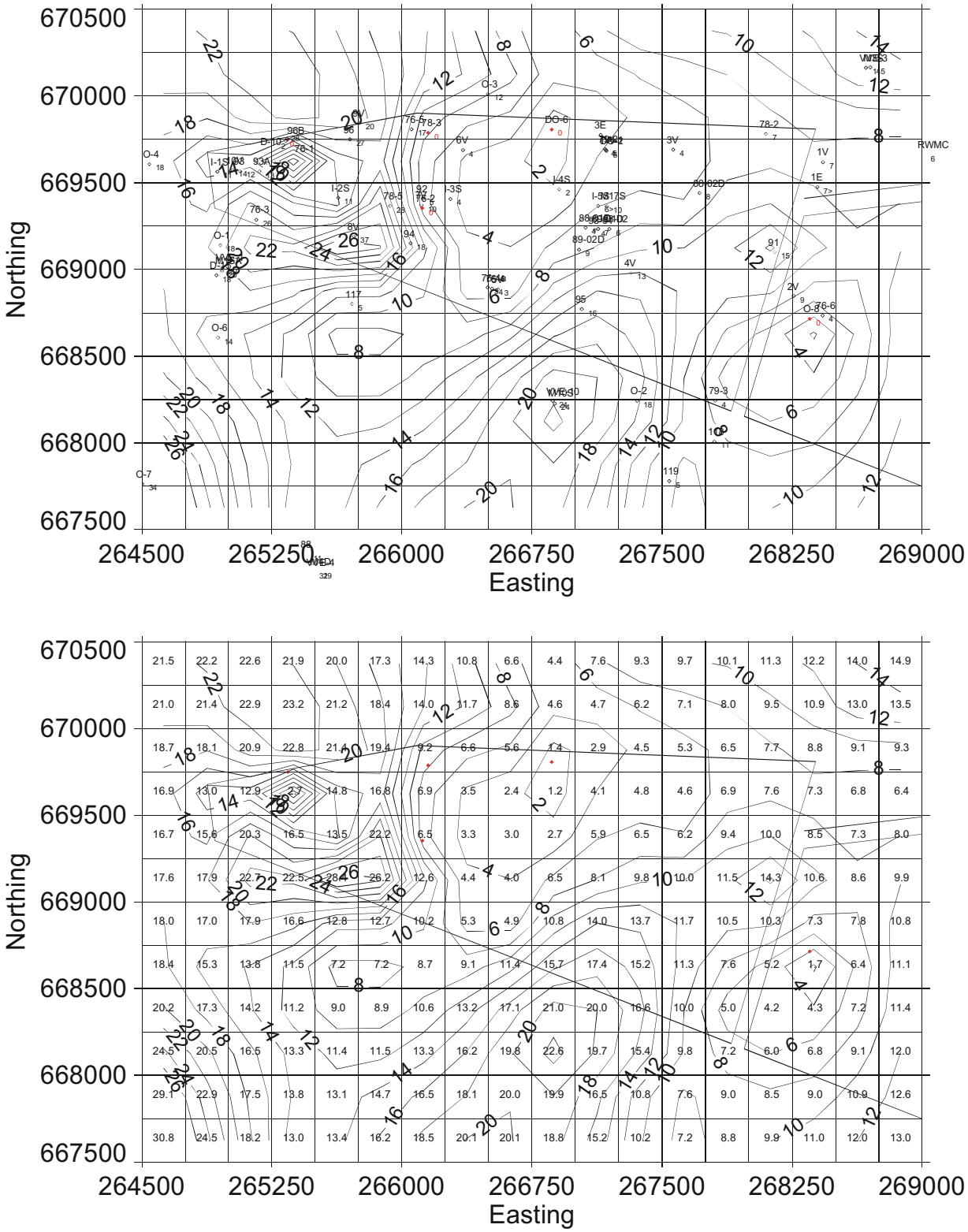


Figure 3-31. Kriged thickness results for the B-C interbed (adapted from Holdren et al. 2002). Interbed thickness is considered to be spatially variable. The lower plot includes the matrix of recent kriging results.

Table 3-7. Parameterization of hydrologic properties and source of parameters for surficial sediments, A-B interbed, and fractured basalt.

| Parameter | Permeability | Porosity |
|---|---|---|
| Surficial sediments | 680 mD, isotropic.<br>Average of calibrated properties in Martian (1995). | 0.50 $cm^3/cm^3$ (Martian 1995) |
| A-B interbed | 4 mD<br>Waste Area Group 3 modeling. | 0.57 $cm^3/cm^3$ (Magnuson and McElroy 1993) |
| Fractured basalt | 300 mD vertical and 9,000 mD horizontal in Magnuson (1995a). | 0.05 $cm^3/cm^3$ (Magnuson 1995a) |

mD = milliDarcy

Detailed descriptions of surficial soils can be found in Voegeli and Deutsch (1953), Nace et al. (1956), Barraclough et al. (1976), Koslow and Van Haaften (1986), Rightmire and Lewis, (1987a,b), McDaniel (1991), Hughes (1993), and Dechert et al. (1994).

Discussions of surficial sediment hydraulic properties can be found in Borghese (1988), Pudney (1994), Shakofsy (1995), Kaminsky (1991), and Bowman et al. (1984).

***Interbed Sediments—***The uppermost interbed, referred to as the A-B interbed, with an average depth of 30 ft., was derived from eolian deposits of fine-grained silt and sand (McElroy et al. 1989) and floodplain deposits of very fine sand and silt (Hughes 1993). The deeper B-C and C-D interbeds, at average depths of 110 and 240 ft respectively, were deposited by low energy fluvial channel systems and consist of sand, silt and some gravels (Hughes 1993). Deeper interbeds have not been characterized, but are thought to be relatively thin and discontinuous and are not considered to have a significant affect on the fate and transport of contaminants (Holdren et al. 2002).

Early work to characterize interbed sediments was done by Rightmire and Lewis (1987b), Hughes (1993), and Barraclough et al. (1976). Bulk mineralogy shows an abundance of quartz and plagioclase feldspar, pyroxene, and clay minerals (primarily illite). Carbonate, primarily in the form of calcite, is also present at various locations ranging in concentration to over 50% (USGS 1999). Bartholomay (1990) provides bulk mineralogy by interbed depth.

Saturated hydraulic conductivities were measured for a set of archived sediment core samples, as presented in McElroy and Hubbell (1990). Values ranged from 7e-03 to 1e-08 cm/sec, falling within literature values for sand, silty sand, silt and clay. In the same study, unsaturated hydraulic conductivity parameters were also calculated and presented. Reported unsaturated zone hydraulic conductivities vary by orders of magnitude for surface and interbed sediments (Barraclough et al. 1976; McCarthy and McElroy 1995).

Interbed lithologic variations, mineralogy, and hydraulic properties have not been fully characterized. Originally, sediments of the B-C and C-D interbeds were considered to consist of fine-grained silt and clays and were thought to have been deposited in a shallow lake or playa (Anderson and Lewis 1989). Subsequent coring revealed a variety in material properties and depositional

environment. It was clear from early work that the interbeds were heterogeneous. The paucity of cores and problems with intact core recovery also limited investigations. At the recommendation of the USGS (1999), DOE installed 22 additional wells at 13 locations and analyzed sedimentary cores for the B-C and C-D interbeds. In addition to stratigraphic data, porosity and permeability measurements were made on 112 core samples. The raw porosity and permeability measurements were found to vary significantly by location. These data have not been published yet, but were incorporated into the Comprehensive Evaluation (Holdren et al. 2002).

To support the development of the Comprehensive Evaluation simulation, Leecaster (2001) developed a set of hydraulic characteristic data for the B-C and C-D interbeds. Using 112 samples from 32 locations in both the B-C and C-D interbeds, porosity and permeability were kriged onto the simulation grid. Hydraulic data from Barraclough et al. (1976), McElroy and Hubbell (1990), and Perkins and Nimmo (2000), as well as unpublished data from the new wells, were compiled to support this analysis. An analysis of kriging error is also presented in Leecaster (2001).

The kriged porosity and permeability for the B-C and C-D interbeds ranged from 0.22 to 0.42 mD and 200 to 3,000 mD respectively. Porosity and permeability maps are presented in Holdren et al. (2002), although a discussion relating kriged data to potential geologic features has not been developed.

As first described by Magnuson (1995), modelers have assigned very low porosity and permeability values (0.05 and 1 mD, respectively) to the top surface of both the B-C and C-D interbeds in order to generate near saturation conditions and lateral movement in the simulation. This technique is thought to represent either a low permeability sedimentary feature at the top of the interbeds or a low permeability feature caused by fine sediments infilling fractures in the basalts immediately above the interbed.

Additional discussion regarding properties of the sedimentary interbeds can be found in Rightmire and Lewis 1987a,b; Bartholomay et al. 1989; Liszewski et al. 1997; Liszewski et al. 1999; Barraclough et al. 1976; Rightmire 1984; Bartholomay et al. 1989; Burgess et al. 1994; and Reed and Bartholomay 1994.

***Basalt Flows—***The RWMC basalt flows consist of medium to dark gray vesicular to dense olivine basalt. Average thicknesses of flow groups range from 22 ft for group A to 167 ft for group F (Anderson and Lewis 1989). The surface of the flows is highly undulating, characterized by ridges and depressions. As described in Chapter 2, the flows generally exhibit dense interiors and rubbly, vesicular surfaces cut by horizontal and vertical cooling fractures (Rightmire and Lewis 1987). Flows are thought to have originated from volcanic vents to the south of the present day RWMC (Kuntz et al. 1994).

A significant amount of work has been done on the geology of the regional basalts. Depositional relations for individual flow groups were developed in Kuntz (1979) and Kuntz et al. (1980; 1984). Kuntz et al. (1980) also provides petrographic and paleomagnetic properties. Ages of flow groups were presented in multiple reports during the 1980s and 1990s and are summarized in Anderson and Liszewski (1997).

Studies of geohydrologic properties of regional basalts are documented in Bishop (1991); Kuntz et al. (1980); Anderson and Liszwenski (1989); Anderson et al. (1996); Rightmire (1984); Rightmire and Lewis (1987); Hughes (1993); and Knutson et al. (1990), among others.

Hydraulic conductivity for regional basalts is highly variable, depending on the structure of the flows (Rightmire and Lewis 1987). In addition, vertical conductivity is enhanced by fractures that penetrate each flow and horizontal conductivity is enhanced by vesicular and rubbly layers near the flow surfaces, as discussed previously.

Faybishenko et al. (2000) reported hydraulic conductivity ranges from 0.003 to 0.9 m/d from work conducted at the nearby Box Canyon study site. The lowest values are thought to be associated with vesicular basalt and the larger values resulting from fractures.

Bishop (1991) conducted a series of studies on 29 vertically-drilled and 17 horizontally-drilled basalt cores. Saturated hydraulic conductivity was measured for each. The mean hydraulic conductivity was 8.42e-8 m/s for horizontal cores and 9.81e-7 m/s for vertical cores. However, the apparent anisotropy was contributed by three samples, which when removed from the set, resulted in virtually indistinguishable properties in both directions. Bishop (1991) did not expect the apparent vertical anisotropy to persist in field scale.

***3.7.2.2 Recharge/Discharge Sources.*** Barraclough et al. (1976) identified four recharge sources affecting RWMC groundwater. These sources include regional underflow in the SRPA from the northeast, infiltration from local precipitation, infiltration from the Big Lost River, and infiltration of streamflow diversions to the spreading areas. Recharge from streamflow and spreading area diversions occurs episodically in response to melting of annual snowpack accumulations in the mountainous drainages of the Big Lost River. Deeper aquifer flow characteristics have not been characterized for the RWMC. The current conceptual model does not include potential recharge from underflow.

***Recharge from Precipitation—***Infiltration of precipitation through the surficial sediments is a key parameter in the conceptual model. Although permanent surface water features do not complicate the hydrology, infiltration is spatially and temporally variable. Keck (1995) shows that Big Lost River is not a potential contaminant transport pathway for surface transport. However, the Big Lost River and associated spreading areas may contribute to subsurface hydrologic conditions, as discussed later in this report. Average annual precipitation is 22.1 cm (8.7 in). The rates of precipitation are highest during May and June, although springtime snowmelt provides another large flux.

The RWMC is in a natural topographic depression, which holds precipitation and collects runoff. Three significant floods resulted from rapid snowmelt and precipitation events in the years 1962, 1969, and 1982. These flooding events caused substantial fluxes of water through the waste and vadose zones. Subsequently, a system of dikes and drainage channels were constructed for storm water control. Local topography across the RWMC facility and the SDA also contributes to the spatial variability in infiltration. Roads, ditches, and small depressions channel runoff and snowmelt to localized ponds within the SDA.

In 1988, the USGS completed construction of a simulated waste trench several hundred yards north of the SDA. The test trench was designed to investigate infiltration in natural, undisturbed sediments; disturbed (excavated and backfilled) sediments; and simulated waste zones. Through the use of tracers and extensive instrumentation (i.e., thermocouple psychrometers, lysimeters, tensiometers, and neutron moisture probes), the USGS quantified soil moisture and variability with depth, time, and temperature and estimated soil hydraulic conductivity, soil-moisture flux, and evapotranspiration rates (Pittman 1995).

The USGS also conducted 24 hr infiltration tests with small, 8-cm deep ponds. The objective of these infiltration tests was to quantitatively compare field scale measured hydraulic properties to the lab scale measurements. Despite the thoroughness of the soil property measurements, the data proved inadequate for predictive one-dimensional modeling. The USGS found that “even with a detailed characterization of a natural soil profile, undetected features may dominate the hydrologic behavior” (Nimmo 1999). It is thought that layering and preferential paths influence flow in undisturbed soil. In disturbed, waste trench soil, initial infiltration is slower but lack of significant layering is thought to permit water to move freely to depth (Nimmo et al. 1999). USGS test trench conclusions, as summarized

by Perkins (2000), were that moisture content is variable in shallow depths but relatively constant at depths below 3 m, even under flood conditions.

The USGS test trench work is further documented in Pittman (1989) and Davis and Pittman (1990). Additional infiltration studies were conducted by Cecil et al. (1992) using Chlorine-36 as a surface water tracer.

A network of neutron-probe access tubes (NATs), with associated tensiometers, was installed across the SDA during the mid 1980s to measure soil moisture and estimate infiltration rates (Bishop 1996a). Monitoring started in 1986 and was performed in a number of discontinuous events across a variably sized network. McElroy (1993) and Bishop (1994; 1996) demonstrated that net infiltration is spatially and temporally variable. Net infiltration was found to range from 49 cm/yr (19.4 in/yr) to less than 0.3 cm/yr (0.1 in /yr) depending on available precipitation (snow depth) and variations in runoff and ponding (Bishop 1996). The greatest infiltration occurs in the spring, since snowmelt is a significant contributor (Holdren et al. 2002). Local topography and soil characteristics also control infiltration.

Martian (1995) analyzed the moisture data obtained from the NATs between 1986 and 1996 to estimate variable infiltration rates across the SDA. These estimated infiltration rates were used in the IRA and the Comprehensive Evaluation. The background infiltration rate outside of the SDA was 1 cm/yr. Infiltration rates within the SDA ranged from 0.64 to 24.1 cm/yr (Martian 1995), with a spatial average of 8.5 cm/yr. The cumulative volume of modeled infiltration at the SDA is approximately 27.8 acre-ft per year (Magnuson and Sondrup 1998).

Despite the thoroughness of the Martian (1995) study, uncertainties remain because a limited number of NATs were located in the disturbed disposal areas, and the moisture monitoring had been limited to the years 1994 and 1996 (Magnuson and Sondrup 1998). Some researchers have concluded that the infiltration estimates used in fate and transport modeling may be too uncertain to reliably predict contaminant movement (USGS 1999).

***Episodic Recharge—***The only significant surface water features at the RWMC are the Big Lost River and associated flood-control spreading areas. To control downstream flooding, excess water is diverted to a series of four playas southwest of the RWMC (see Figure 3-32). During 1981 through 1985, over 800,000 acre-ft of water was diverted into the spreading areas. Because the flows of water in the river and occasional diversions to the spreading areas are episodic, annual infiltration rates are difficult to estimate.

For years, infiltration from the spreading area was considered to be primarily in the vertical direction, locally impacting the SRPA. Pittman et al. (1988) observed water level rises as great as 16 ft in RWMC wells. Apparently, a transitory groundwater mound existed in the aquifer beneath the spreading areas in response to vertical recharge during the 1982 through 1985 timeframe (Pittman et al. 1988). This and similar observations were corroborated during the LSIT, where rapid, vertical flow with little spreading was observed. Hubbell (1990), and Bennett (1990) also examined water level data and noticed apparent correlations to spreading area diversions.

Figure 3-32. Big Lost River water is periodically diverted to the Spreading Areas southwest of the RWMC.

More recently, however, researchers have observed evidence of rapid, lateral flow of spreading area water through the vadose zone (Nimmo et al. 2002; discussed further in a subsequent section). As a result of this work, recharge from the spreading areas was simulated in the Comprehensive Evaluation as a steady state influx (due to the extremely long time frame of the simulation). To support the Comprehensive Evaluation simulations, historic flow data from the Big Lost River (beginning in 1965) were analyzed and an additional 1 acre-ft (1,233 $m^3$) per day was applied to the western boundary (Holdren et al. 2002). The length of time and amounts of water were derived from Nimmo et al. (2002). The volume of water in the simulation was adjusted to an average of 1 acre-ft per day, which was enough to affect the western portion of the C-D interbed beneath the SDA (Holdren et al. 2002). Sensitivity studies were conducted to explore the effect of transient influences from spreading areas. When additional water representing recharge from the spreading areas was input into the aquifer, the southeasterly groundwater flow velocities increased under the eastern portion of the SDA, but the directions did not significantly change (Holdren et al. 2002). A simplifying assumption was also made that recharge from the Big Lost River spreading areas does not influence flow in the aquifer in the immediate vicinity of the RWMC.

The three large-scale floods that occurred in the SDA in 1962, 1969, and 1982 were caused by heavy precipitation and rapid snow melt. Estimates of floodwater volumes were made by Vigil (1988b). Although the estimates are highly uncertain they were used in both the IRA and the Comprehensive

Evaluation (Becker et al. 1998; Holdren et al. 2002). Due to the construction of flood-control dikes around the facility, large-scale floods are not considered to have a significant, permanent affect on flow in the aquifer (Holdren et al. 2002).

***Discharge from Wells—***The RWMC production well provides water for administrative and facility maintenance requirements. The water use; however, is relatively minor and has not been an important factor in the WAG 7 conceptual model.

#### *3.7.2.3 Hydraulics*

***Snake River Plain Aquifer—***As discussed in Section 2, the regional SRPA is an unconfined aquifer; however, at local scales, the saturated basalt can behave as a leaky, confined aquifer. Permeability is spatially variable within the aquifer, as indicated in pump test results and as implied by a non-uniform hydraulic gradient in the southern section of the INEEL (although other factors, including enhanced recharge from the Big Lost River Spreading Areas, could also contribute to the heterogeneity of the gradient; Whitmire 2001).

Transitory, perched water bodies have been regularly observed at the RWMC. Changes in hydraulic conductivity between lava flows, between fractured basalts and sediments, or due to sedimentary and chemical filling of fractures creates intermittent occurrences of perched water lenses. Sources of perched water include excessive infiltration, surface flooding events, and the Big Lost River and the associated diversion areas (Cecil et al. 1991). Interestingly, Rightmire and Lewis (1987b) noted light isotopic content in perched water, which suggested a high altitude source (i.e., flood water from the Big Lost River). Perched water has been identified in a number of RWMC wells at depths corresponding to the B-C and C-D interbeds (Holdren et al. 2002). Thickness of perched water at both locations is approximately 1 ft. The buildup of water is intermittent, and at most locations is often of insufficient volume to collect samples for analysis; however, well USGS-92 (located inside the SDA) has yielded a perched water sample every year since 1976.

The aquifer gradient near the RWMC is relatively small. Bartholomay et al. (1997) reports an average of 2 ft/mi (3.52e-4 ft/ft). The most current water maps used in the Comprehensive Evaluation display a range of 4.9e-4 ft/ft to 3.7e-4 ft/ft (Holdren et al. 2002).

There is also evidence of anomalous water level behavior in the RWMC region. In addition to variability associated with episodic spreading area recharge, pump tests from well USGS 88, located directly south of the RWMC, indicate that this region may be isolated from the main body of the SRPA (Burgess, Higgs and Wood 1994). Additionally, Barraclough (1976) suggested that local reversals were possibly influenced by episodic recharge.

The heterogeneity of subsurface volcanic formations in the RWMC area results in complex anisotropy in the hydrologic system. Aquifer flow is thought to be controlled by fractures and inter-flow zones rather than by matrix porosity. Heterogeneity in these and other features contribute to spatial variability in aquifer flow. Although the regional flow direction is northeast to southwest, estimating direction and velocities of water movement on the smaller scale of the WAG 7 facility is complicated by anisotropic behavior and paucity of measurement points on that scale. Additionally, the low-gradient and apparent low-permeability region to the south-southwest of the SDA precludes accurate determination of groundwater flow directions (Holdren et al. 2002).

Velocities in the RWMC region are significantly less than average SRPA velocities discussed in Section 2. Pump tests conducted by Wylie and Hubbell (1994) and Wylie (1996) indicate a region of low permeability near the southern and southwestern border of the SDA. Whether this low permeability

region exists, its lateral extent and continuity is uncertain (Becker et al. 1998). The IRA presented the hypothesis that flow velocities under the SDA are relatively slow based on the results of a number of aquifer tests including Ackerman (1991), Wylie et al. (1995), Bishop (1991; 1996), and Welhan and Wylie (1997). Roback et al. (2001) hypothesized that the RWMC is in a low permeability region that extends southerly from the Big Lost River Range onto the INEEL. Determination of the direction and timing of aquifer flow velocities in the SDA is ongoing.

During the development of the Comprehensive Evaluation, SRPA permeability was based on transmissivity data from pumping tests and specific capacity information for 21 wells located inside the model domain (Ackerman 1991; Wylie and Hubbell 1994; Wylie 1996). Permeability data range from 4 mD to 1508700 mD. Using this data, in addition to data from recently installed wells, Whitmire (2001) averaged the data into three permeability classes: (1) low, 153 mD representing wells immediately south of the SDA, (2) middle, 9,300 mD representing wells located north and northwest of the SDA, and (3) high, 712,000 mD representing wells south and east of the SDA.

***Vadose Zone—***The vadose zone is believed to be a particularly important component of the subsurface flow system beneath the RWMC, functioning as the principal pathway for RWMC-derived contaminants to the SRPA. The vadose zone is conceptualized as a filtering system that prevents or restricts movement of contaminants to the aquifer. The migration of contaminants generally is believed to be extremely slow under normally small, local recharge conditions. The notable exception is $CCl_4$, with concentrations exceeding regulatory levels in some RWMC aquifer wells.

Researchers first noted the presence of moist zones above the water table in five wells at the RWMC during 1976-77 (EG&G Idaho 1988). These zones generally were associated with sedimentary interbeds. Since that time, perched groundwater at the RWMC has been monitored using wells, tensiometers, and lysimeters. Perched groundwater bodies have been associated with the B-C and C-D interbeds at depths of 80 to 90 ft and 200 to 220 ft, respectively. Monitoring data indicate that perched groundwater beneath the RWMC typically is transitory (Holdren et al. 2000). Much of the time, monitoring wells are dry or contain insufficient water for routine sample collection.

Perched groundwater bodies at the RWMC form in response to movement of recharge water through a vertical basalt/sediment sequence that is characterized by contrasting hydraulic conductivities. Cecil et al (1991) suggested that these contrasting hydraulic conductivities may occur between basalt flows and sedimentary interbeds, in interflow baked zones, in transition zones from fractured to unfractured basalt, and in zones of sedimentary and chemical filling of fractures.

One source of perched groundwater at the RWMC is from infiltration of local precipitation. Net water infiltration rates through soils from local precipitation near the RWMC have been estimated using environmental tracer data and neutron logging data to range from 0.36 to 1.1 cm/year (Cecil et al.1992). This range is equivalent to 2 to 5% of the annual precipitation. Researchers in part have attributed the presence of moist zones to focused recharge from spring snowmelt and local flooding of the RWMC during the 1960's and 1970's.

Researchers (Rightmire and Lewis 1987; Hubbell 1990) have noted from perched groundwater fluctuations and isotopic chemical data that lateral vadose-zone flow from the INEEL spreading areas to the south and west may provide a substantial source of recharge to perched groundwater beneath the RWMC. A tracer test conducted by the USGS in the INEEL spreading areas during 1999 (Nimmo et al 2002) provided compelling evidence that significant amounts of water from the spreading areas have moved rapidly through the vadose zone to the RWMC. In this test, a chemical tracer introduced in the spreading areas during a period of large diversions from the Big Lost River were detected in one perched zone well completed above the C-D interbed at the RWMC. The estimated arrival time indicated that

water had moved from the spreading areas to the RWMC in less than 90 days. This test demonstrated that rapid, lateral flow can occur along preferential pathways associated with the basalt/sediment stratigraphy. Researchers concluded that the sporadic and randomly distributed detections of radionuclides in the vadose zone and the vertical and lateral migration of $CCL_4$ may be attributed to these episodic events (USGS 1999).

#### *3.7.2.4 Groundwater Chemistry*

***Pore Water (Vadose Zone)—***A key parameter for estimating future fate and transport of contaminants is chemistry of the infiltrating water and subsequent leaching of contaminant from the waste. In the surficial soils, precipitation can be altered by soil minerals and in some cases by the presence of the waste itself. Groundwater geochemistry has been investigated repeatedly, as reported in Olmstead 1962; Robertson et al. 1974; Rightmire and Lewis 1987; Rawson and Hubbell 1989; Rawson et al. 1991; Cleveland and Mullin 1993; and Knobel et al. 1997.

In the RWMC area, hydrogen potential is about $8 \pm 0.5$, buffered by calcite-water-$CO_2$ interactions. Caliche, an impermeable, concrete-like soil naturally cemented by calcite, is common in the area. The oxidation-reduction potential is oxidizing and equivalent to air. The soil moisture is saturated with respect to calcite and super-saturated with dolomite (Wood and Norell 1996).

As described previously, a network of lysimeters was installed in the SDA to monitor water chemistry near the waste zone. As identified by Hull and Pace (2000), however, certain lysimeter results were apparently affected by a magnesium chloride solution that was used as a dust suppressant on roads; additionally bromide tracer installed with some lysimeters may have also contaminated some samples. After eliminating suspect samples, Hull and Pace (2000) compiled water chemistry results from 90 samples taken from 13 lysimeters in the SDA. They found little variation with time, but significant spatial variability with no apparent correlation to specific areas within the SDA.

The most "representative" water chemistry for the SDA is defined in Hull and Pace (2000). Oxidized conditions persist, with dissolved oxygen in the range of 4.8 to 7.8 mg/L. Soil zone $CO_2$ levels are very high (up to 10%) in the SDA waste area. The pH of soil moisture is found to be only slightly alkaline (ranging from 7.2 to 8.2), possibly due to high concentrations of $CO_2$ in soil gas resulting from organic decomposition of waste materials. Pore water is saturated with respect to calcite.

***Perched and SRPA Water.*** As summarized by the USGS (1999), perched water samples have been shown to be oversaturated with zeolite minerals and clay minerals. Perched water has been described as either sodium chloride or sodium bicarbonate (Rawson and Hubbell 1989). Perched water chemistry for the RWMC has also been presented in Barraclough et al. (1976), Rightmire and Lewis (1987), Knobel et al. (1992), Knobel et al. (1997), Rawson et al. (1991), Tucker and Orr (1998), Bartholomay (1998), and Rawson et al. (1991).

The SRPA water samples from near the RWMC are typically calcium-magnesium bicarbonate in character, and supersaturated with respect to aragonite, calcite, and dolomite and undersaturated with respect to fluorite, sulfate minerals, and silicate minerals (Knobel et al. 1997). Aquifer water chemistry in the WAG 7 region is also presented in Mann and Knobel (1988), Liszewski and Mann (1993), and Burgess et al. (1994).

Chemical characteristics that affect transport of actinides are summarized by the USGS (1999) as (1) a pH ranging from 7.8 to 8.4; (2) dissolved oxygen concentrations nearly saturated to slightly supersaturated with respect to air; (3) slightly saturated with respect to calcite; and (4) dissolved organic carbon near or below 1 mg/L.

### 3.7.2.5 Contaminant Transport

***Source Term—***The inventory of waste disposed of at the SDA is unique in its variety, concentration, and mass of contaminants. In 1995, a comprehensive effort was made to catalog all of the wastes known to have been disposed between 1952 and 1983 (LMITCO 1995a). The project, referred to as the Historical Data Task (HDT), resulted in a database of inventory information. The information was derived from facility operations records, technical reports, shipping records, generator interviews, and nuclear physics calculations. The information was organized by waste stream and by generator. Quantities of each contaminant were presented with best-estimate, upper-bound, and lower-bound estimates. The inventory of low-level waste disposals between 1984 and 1993 was similarly developed in a second volume (LMITCO 1995b).

The inventory of the primary VOC contaminants (carbon tetrachloride [$CCl_4$], tetrachloroethylene, and methylene chloride) was subsequently revised. These VOCs originate primarily from a single waste stream generated between 1966 and 1970 at the Rocky Flats Plant (RFP). Although previous estimates were considerably lower, current analysis indicates that 8.2 E+05 kg of $CCl_4$, 9.8 E +04 kg of tetrachloroethylene, and 1.41e+04 kg of methylene chloride were originally disposed of in the SDA (Varvel 2001; Miller and Varvel 2001). Although the remaining mass of $CCl_4$ in the waste zone has been investigated using gamma-chlorine reactions in probehole logging, the estimates of remaining mass are considered highly uncertain (Holdren et al. 2002).

There is also considerable uncertainty associated with the inventory of radiological contaminants. In particular, estimates of C-14, Tc-99, and U isotopes from INEEL and U.S. Navy generators are under review and may be revised in the future. Tables in Section 5 of Holdren et al. (2002) provide an excellent summary of inventory estimates and waste types for COCs at WAG 7.

***Extent of Contamination—***The extent of contamination in the WAG 7 area has been investigated intermittently since the early 1960's, and more thoroughly during the late 1990s. The AEC collected perched water samples from shallow wells in 1962, 1965, and 1969, finding some cesium and strontium contamination (Schmalz 1972). The USGS analyzed water and sediment samples from a number of vadose zone wells during the 1970s and 1980s. Although some researchers concluded that actinides had migrated to the B-C interbed and not the C-D interbed (Laney et al. 1988), sporadic detections and concerns with sample contamination resulted in inconclusive results (Barraclough 1976; Burgus and Maestas 1976; Humphrey and Tingey 1978; Humphrey 1980). Soil sampling at interbeds and near waste showed very limited migration of adsorbed transuranic elements (Humphrey et al. 1980, Bargelt, et al. 1992).

Soil water and perched water have been sampled quarterly since 1996 in support of the WAG 7 RI/FS. $CCl_4$ and nitrates are regularly detected in aquifer wells near the SDA. In addition, C-14, Tc-99, Am-241, uranium, and plutonium have been detected at low concentrations in the vadose zone. Detections are most frequent above the B-C interbed, although some contaminants have been detected in the C-D interbed.

Describing the extent of actinide contamination continues to be problematic. As illustrated in the Comprehensive Evaluation, plutonium and americium have been detected in only 1% of the thousands of aquifer samples taken from the RWMC area. The detections have been sporadic in frequency, with typically low concentrations and variable locations. Recent work utilizing Thermal Ionization Mass Spectrometry (TIMS) indicates that elevated uranium concentrations in aquifer samples are non-anthropogenic (Roback et al. 2000).

As described in detail by Holdren et al. (2002), numerous detections of Tc-99 in the vadose zone suggest migration. Elevated concentrations of U (multiple isotopes) at several locations in the vadose zone suggest migration. However, there are no identifiable trends observed in the vadose zone (with exception of $CCl_4$), and only sporadic detections of radionuclides in the aquifer.

All three VOCs ($CCl_4$, tetrachloroethylene, and methylene chloride), especially $CCl_4$, are prevalent in SDA soil gas, perched water, and aquifer water. $CCl_4$ detections have been highest in the 50 ft above the B-C interbed and decrease sharply between B-C and C-D. However, extensive monitoring for $CCl_4$ below the C-D has not been conducted. $CCl_4$ is routinely detected in aquifer samples. As reported in Holdren et al. (2002), $CCl_4$ has been detected in 16 of the aquifer wells near the RWMC, 5 of which have concentrations near or exceeding the maximum contaminant level (MCL). However, the distribution of aquifer concentrations does not correlate with proximity of the well to the source areas. Some of the wells with highest concentrations of $CCl_4$ are located a significant distance from the SDA or to the North (upgradient) from the source areas. It is hypothesized that the wells near the southern border of the SDA are located in a low permeability formation, which limits the $CCl_4$ concentrations (Sondrup 1998). Furthermore, trends in concentrations over the last few years are also erratic, rising, dropping, or remaining constant depending on time period and well location. Detections of tetrachloroethylene and methylene chloride have been infrequent and at considerably lower levels than $CCl_4$ (Holdren et al. 2002).

In summary, continued migration of both VOC and radionuclide contamination is expected, but the impact on aquifer quality is uncertain given current data. Holdren et al. (2002) presents the most detailed analysis of the nature and extent of contamination developed to date, including illustrations of detection locations for selected contaminants. Figure 3-33 provides a graphic example of the distribution of contaminant detections as presented in Holdren et al. (2002).

***Release Mechanisms—***The source and availability of contaminants for transport is a complex and poorly understood issue at WAG 7. As discussed previously, the contaminant source is encompassed in a variety of waste streams, most of which were disposed in relatively immobile forms. With the exception of VOCs, virtually no data exist that would provide empirical estimates of release rates. Therefore, to support the estimation of future risk at this site, researchers have relied on relatively simple mathematical simulations to estimate the flux of contaminants from the waste forms. Release of contaminants from the original waste stream is conceptualized by three processes: wash off, diffusion, or dissolution (Becker et al. 1998). The only work done to date to estimate contaminant release has been done by the WAG 7 program using a computer simulator developed by Sullivan (1992). The source release model provides mass (or activity) estimates for total yearly releases from all source areas on a contaminant basis using equations as described in Sullivan (1992; 1993). A number of key equation parameters, including inventory, container failure rates, corrosion rates, infiltration rates, and release coefficients, control the rates of release.

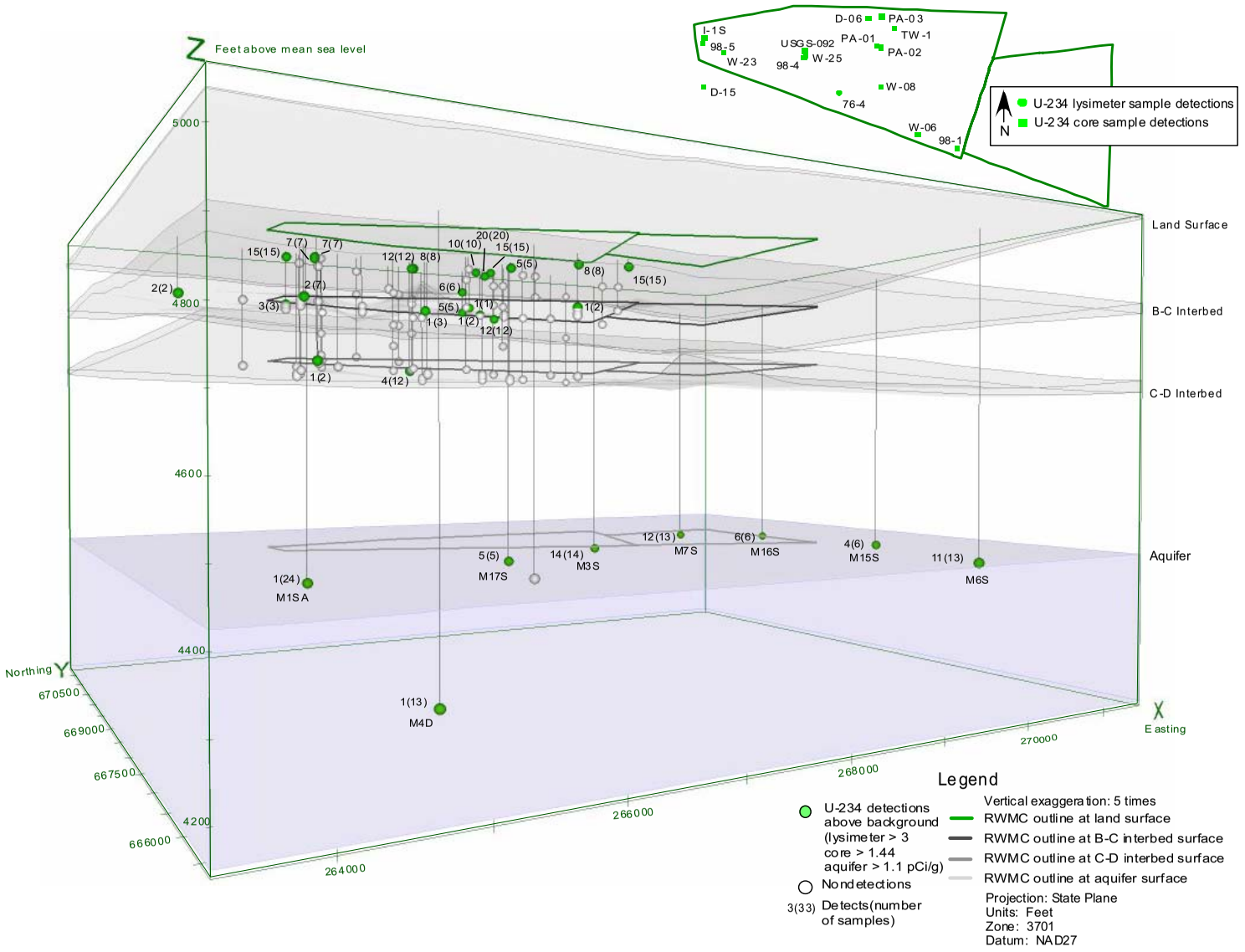


Figure 3-33. Detection of contaminants in the WAG 7 subsurface is sporadic and spatially variable. An illustration of U-234 detections as presented in Holdren et al. (2002) is presented as an example of the distribution of contaminants. Illustrations for other contaminants are provided in Holdren et al. (2002).

As discussed previously, inventory and waste stream descriptions were developed in LMITCO (1997a, b). In the IRA (Becker et al. 1998), the high (bounding) inventory estimates were used for purposes of contaminant screening. In the Comprehensive Evaluation, the best estimates were used to estimate future risk. As described previously, best estimates of total inventory (mass or activity) of each COC, its waste stream, and assumed release mechanism, is provided in Holdren (2002). Many contaminants are associated with multiple waste streams, each of which is modeled using differing mechanisms of release. To estimate contaminant specific flux, the total yearly disposal mass of each contaminant was proportioned between the three available release mechanisms based on an analysis of the waste type (actinides associated with metal waste streams were modeled as surface wash off; activation products associated with metal waste streams were modeled as dissolution of the base metal; etc.) (Becker et al. 1998; Holdren et al. 2002).

Container failure rates were developed to represent the timing of the release of contaminants from the variety of waste containers (drums, boxes, etc.) associated with each waste stream. Failure rates for each type of container were developed by Becker et al. (1996) and Becker (1997). For example, a randomly dumped drum was estimated to have a mean failure time of 11.7 years with a standard deviation of 5 years. To support the IRA, Becker et al. (1998) proportioned the waste inventory by container type and assigned the year of release based on the disposal date and estimated container failure time. This information was also used in the Comprehensive Evaluation. (Note that with organic contaminants and contaminants encased in concrete casks, diffusion through the containers was used in lieu of container failure times.)

The release of activation products is based on the rate of corrosion of the base metal as well as the geometry of the waste object. Corrosion rates for stainless steel and beryllium were estimated by Adler Flitton et al. (2001) and by Nagata and Banaee (1996) for carbon steel. This work was based primarily on a series of experiments with samples of different metal types buried in a test area near the SDA. In addition, in the Comprehensive Evaluation, the metal corrosion rates were increased to account for the presence of magnesium chloride, which was used as a dust suppressant on roads at the RWMC. Additional work regarding corrosion rates is documented in Mizia et al. (1999).

Infiltration rates used in the release modeling are based on those developed for the transport model, as discussed in previous sections. Because the release rate simulator is a one dimensional model, Holdren et al. (2002) divided the inventory into 13 source areas based on the distribution of contaminants across the SDA. Spatially variable infiltration rates were averaged for each of the 13 simulation areas. Simulating release from each area separately provided spatially variable, as well as time variable, release rates for input into the transport simulator.

Release coefficients were derived from a number of sources and vary according to the type of release being considered. Partition coefficients and contaminant solubility data are presented in Dicke (1997). Metal corrosion rates are developed in Nagata and Banaee (1996) and Adler Flitton et al. (2001). VOC diffusion was estimated in Kudera and Brown (1996).

Clearly, the release coefficients have a high degree of uncertainty. Metal corrosion is influenced by available moisture, which, as described in previous sections, is spatially variable. Problems with developing and using partition coefficients are discussed in subsequent sections of this report. Although VOC diffusion is relatively well described, there are uncertainties with the inventory remaining in the waste zone. During the development of the IRA and the Comprehensive Evaluation, modelers attempted to select conservative estimates whenever possible to ensure future risk was not underestimated. However, because site-specific release data have been unavailable to calibrate the release model, the estimate of contaminant release remains uncertain. It should be noted that technical reviews of the WAG 7 modeling work have consistently excluded the release portion of the conceptual model. It is expected

that continued monitoring of waste zone probes (Anderson 2001a, b) will provide critical data to validate the release rate modeling.

***Transport Mechanisms—***Contaminant transport is largely affected by the geochemical environment. Due in part to unavailability of geochemical data, and in part to the risk assessment approach of using simplifying (bounding) assumptions, geochemical factors in the WAG 7 conceptual model have not been developed in detail.

The current INEEL conceptual models use an equilibrium, reversible distribution coefficient to emulate the various geochemical factors affecting retardation the transport codes. Distribution coefficients (i.e., Kds) are commonly used in computer modeling as a mathematically simple representation of sorption. Kd values encompass all processes that remove a contaminant from solution. They are a bulk term representing the ratio of adsorbed to dissolved concentrations, typically given in units of mL/g. Typically, the value is obtained by fitting a linear isotherm to results of batch or column experiments, neglecting the actual mechanisms responsible for contaminant removal (Dicke 1997). Kds are incorporated into a constant retardation factor in the advection-dispersion equation enabling modelers to simulate a reduction in contaminant concentration as the solution passes through the various vadose zone structures.

Use of distribution coefficients, or Kds, is widely accepted as a defensible method to simplify transport calculations. However, where there exists significant temporal and spatial heterogeneities in the geochemical environment, the use of Kds becomes problematic. For example, Hull (2001) comments that multiple water types have been identified in the WAG 7 subsurface, indicating that geochemical conditions are not uniform.

To date, WAG-specific simulations have relied on the linear isotherm approach using a limited set of site-specific data. Although the results are generally considered conservative for purposes of risk assessment, a number of investigators have suggested that long-term evaluations be conducted to provide a basis for more representative geochemical modeling.

There are a number of limitations with using the Kd approach. For example, spatial or temporal variability in chemical conditions and solubility potentials cannot be addressed with singular partition coefficients. Additionally, it is difficult to accurately represent actual field conditions in batch sorption experiments (Hull and Pace 2000). Or as stated by the USGS (1999), the measured Kd values are applicable only to the specific conditions under which the experiments were conducted. Other problems with the use of Kd values include poor design of batch experiments, competition between species for sorption sites, and non-linear response to increasing aqueous concentration.

The literature regarding the use of Kd values is extensive. As a starting point, the reader is referred to the discussions developed by Landa, Glynn, Stollenwerk, and Curtis (USGS 1999). USGS (1999) reviewed the use of Kds at WAG 7 for four specific contaminants (Am, Np, Pu and U) and concluded that "the experimental conditions used to measure Kds for the IRA model do not adequately represent the aqueous and solid phase variability at WAG 7." The reviewers proposed the use of a surface complexation model, as specific surface-complexation and ion-exchange constants are important parameters to utilizing Kd measurements.

In order to support the simulation work for the IRA, Dicke (1997) developed a set of Kds and solubility limits for WAG 7 COCs. This compilation utilized literature values and results of batch tests on RWMC cores where available. The paucity of site-specific data prompted testing on additional samples in the 1999 timeframe.

In the Comprehensive Evaluation, analyses were conducted on approximately 60 interbed core samples for sorption isotherms for uranium and neptunium, particle size distributions, surface area, exchangeable cations and anions, clay mineralogy, and extractable silica, iron, manganese, and aluminum. Comparison of partition coefficients from the sorption isotherms to the values from Dicke (1997) supported the conclusion that the partition coefficients elected for the uranium and neptunium are physically plausible and conservative because they are on the lower end of the measured partition coefficient distribution. The sorption isotherms measured from the core samples were nonlinear, but for risk assessment purposes, the more conservative linear values were preferred (Holdren et al. 2002).

A key parameter controlling the sorption reactions is the oxidation state of the contaminant of interest. It has been shown that the transport and adsorptive characteristics of contaminants, particularly actinides, are strongly affected by their initial oxidation state and by oxidation/reduction reactions within the vadose zone (Hull and Pace 2000; USGS 1999). Oxidation states and associated potential for organic and inorganic complexation controls, in part, the fraction of contaminant entering and remaining in solution. Speciation of contaminants (i.e., their form as disposed and as altered by waste zone characteristics), as well as redox state of the water, is not well known and thought to be highly variable.

The WAG 7 contaminants display a wide range of geochemical properties. Chemical interactions with pore water, sediments, and basalt matrices are complex and supported by a small set of empirical data. Solubility calculations on a contaminant-by-contaminant basis indicate that the effect of oxidation/reduction potential and hydrogen potential on the solubility of these contaminants varies. However, for many contaminants (particularly actinides) the ambient SDA conditions, with moderately reduced environment and approximately neutral pH, may minimize solubility (Hull and Pace 2000).

Researchers have concluded that inadequate characterization of contaminant oxidation/reduction states contributes significantly to the uncertainty in predicting transport of contaminants, especially for actinides (USGS 1999). The reader is referred to the work done by Curtis, Glynn, Stollenwerk and Bartholomay in USGS (1999) as a starting point for discussion of oxidation/reduction and speciation reactions at WAG 7.

Although dissolved phase transport is generally considered the predominant transport mechanism, transport may be facilitated by movement of suspended particulate forms of contaminants. As summarized by the USGS (1999), colloidal particles originating from mineral fragments, precipitates, and other mechanisms exist in RWMC basalt fractures and groundwater. Their mobility is controlled by the stability of colloids in groundwater, chemical interactions between colloids and matrix surfaces, and other hydrological and physical factors. In the SDA vadose zone, filtration of colloids by interbed sediments is hypothesized as a mechanism of removing colloids from solution.

Experiments have given evidence that actinides elute from interbed sediment columns at a greater rate than those attributable to equilibrium sorption of aqueous species. This enhanced mobility fraction has been attributed to colloidal transport (Fjeld et al. 2000). Further evidence for particulate transport facilitated by colloids comes from the detection of actinides in the interbeds (USGS 1999).

The hypothesis regarding facilitated transport has not yet been developed and incorporated into modeling efforts. However, a series of sensitivity studies was performed (as part of the Comprehensive Evaluation) to explore the impact of a small fraction of highly mobile, particulate forms of Pu-238 and Pu-239 on groundwater risk. The results of the sensitivity studies appeared to greatly over-predict aquifer concentrations (Holdren et al. 2002).

### 3.7.3 Numerical Analyses Performed to Date.

Several numerical unsaturated and saturated flow and transport models have been developed that have incorporated elements of the site conceptual model. In some cases, predictive modeling has contributed to the understanding of site hydrologic processes. A summary of several important modeling investigations is presented below.

***Baca et al., 1992—***Baca et al. (1992) used several analytical hydrological models to simulate infiltration rates, evaluate the effects of past flooding events on pit 10, and estimate water travel times in the vadose zone. Input parameters to the models included climatic data (specifically for the infiltration calculations), unsaturated hydraulic properties (including representative characteristic curves and hydraulic conductivity curves), and saturated hydraulic parameters such as hydraulic conductivity and effective porosity.

Infiltration rates were determined assuming two specific cases: infiltration in undisturbed sediments and infiltration in disturbed sediments (i.e., pit and trench covers). Using a water balance approach and assuming that infiltration is an areally diffuse process, infiltration was simulated for each case. The primary conclusions were:

1. The dynamic moisture movement occurred in the upper meter of sediments

2. The maximum moisture flux at the land surface was estimated to be 7 cm/yr (roughly 30% of annual precipitation)

3. The net infiltration for the disturbed and undisturbed cases were very similar

4. Conservative analyses can be performed by assuming net infiltration rates of 10 cm/yr or greater.

Pit 10 flooding evaluations were performed under two scenarios. The first represented fractures as an equivalent porous medium. The second was similar but included a large vertical, cross-cutting fracture. The primary conclusions were that the wetting front created by pit 10 flooding could have reached the vicinity of the 110 ft interbed in about 1 month's time and vertical, cross-cutting, unfilled fractures can serve as high permeability conduits that can transmit water rapidly through the vadose zone. The results further suggest that the flooding events may have been a major factor causing the migration of nonsorbing, dissolved contaminants in the vadose zone.

Water travel times were estimated using a Monte Carlo simulation approach because single-valued representation of hydraulic properties were considered inappropriate given the complexities of the flow system at the RWMC. Results included the observation of log-normally distributed soil water travel times and a geometric mean average linear velocity of about 0.3 m/yr.

This study suggested that additional hydraulic data, including characteristic curves, saturated hydraulic conductivities, and effective porosity, be collected in order to further characterize the site and provide valuable information for future modeling efforts. In addition, geostatistical interpretation of the hydraulic properties of the major hydrostratigraphic units was advised.

***Magnuson 1995.*** Magnuson (1995) conducted an inverse modeling study to obtain a representative description of flow and transport through vadose-zone fractured basalts for use in field-scale modeling studies. An equivalent porous media approach, assuming both a single porosity and a dual porosity

system, was used for the simulations. Data were calibrated to observed hydrographs and conservative tracer breakthrough curves. The primary observations suggested by the simulations were:

1. The dual porosity model improved the match to calibration targets but is likely not worth the additional computational burden unless a need is demonstrated

2. It was necessary to add a low permeability layer above the interbed to reproduce observed perched water behavior

3. The effective porosity of the calibrated model was low (0.01 to 0.05)

4. While the elevation of the surface of the sedimentary interbed likely controlled the spread of perched water that developed during the test, the available information used to discretize the interbed was insufficient to assure an accurate representation.

In addition, it was observed that that the presence of rubble zones was an insignificant controlling factor in the migration of water in the vadose zone.

***Martian 1995.*** Martian (1995) simulated historic infiltration rates at the SDA using the computer code UNSAT-H (Fayer and Jones 1990). Simulated soil moisture profiles were calibrated to soil moisture data collected in NATs.

To facilitate using the infiltration rates obtained from this study in the WAG 7 baseline risk assessment SDA subsurface flow model (Magnuson and Sondrup 1998), the daily infiltration record from the final simulations were interpolated and assigned to different areas across the SDA. Infiltration rates were spatially categorized into low, medium, and high zones so that a minimal number of infiltration rates could be applied to the SDA subsurface flow model. Because site topography was determined to be a major influencing factor on infiltration rates during this work, the infiltration rates were categorized based on observations of standing water in 1995, the annual average infiltration rates obtained during this study, and current site topography.

The daily, simulated infiltration rates were grouped temporally such that data inputs to the subsurface flow model could be minimized while still capturing the transient effects of infiltration at the site. The end result of the spatial categorization and temporal grouping of the daily infiltration data was a data set that contained the minimum amount of grid cells and time steps required to adequately simulate transient infiltration at the SDA.

***Magnuson and Sondrup 1998—***Magnuson and Sondrup (1998) used the petroleum/geothermal code (Tetrad) to simulate water and contaminant movement through the vadose zone and the eastern SRPA using an equivalent porous medium approach. This modeling effort was unique in that both the flow and transport aspects of the simulator were at least partially calibrated to existing field methods. In addition, the effort was unique at the RWMC because it coupled flow and transport in the vadose zone and the eastern SRPA.

The vadose zone flow model incorporated the observation of Magnuson (1995) realizing that it was necessary to add a low permeability layer to the top of the interbeds in order to recreate observed perched water behavior. In addition, the infiltration description provided by Martian (1995) was used to describe the flux of water at the surface in this effort.

The modeling effort was a success for several reasons:

- Outstanding agreement between simulated and observed VOC concentrations in the aquifer and vadose zone was achieved

- With few notable exceptions, the model overall can be considered representative of VOC behavior

- The model provided predictions of contaminant concentrations that could be validated through future site characterization efforts.

The simulator was able to represent the occurrence of perched water bodies in most cases; however, the existence of perched water in the vicinity of well 92 could not be replicated.

While this effort used an extensive data set in an effort to discretize and parameterize the model domain, several recommendations were provided for revising the simulations, including:

1. Separation of the vadose zone and aquifer simulation domains for the contaminants that exist only in the dissolved phase. The change is intended to allow for more computationally-efficient simulations.

2. Once the vadose zone and aquifer models are decoupled, adjust the grid refinement on the more computationally-efficient vadose zone model in order to more closely match observed perched water behavior in the vicinity of well 92.

3. Consider continuing calibration efforts in order to more closely match observed chromium distribution and to include the vapor vacuum extraction (VVE) remediation system.

Overall, this model is the best representation of the flow system at the RWMC to date. An exhaustive data set was used in the development of both the vadose zone and aquifer portions of the simulator. The results of several previous modeling studies were used during the development of this simulator.

***Whitmire 2001—***Using the suggestions of Magnuson and Sondrup (1998), the aquifer and vadose zone portions of the RWMC flow and transport model were decoupled. Whitmire (2001) developed the groundwater flow (i.e., aquifer) portion of the decoupled simulator.

The aquifer model was developed using the assumptions and hydraulic parameter information identified in Magnuson and Sondrup (1998). In addition, the best calibrated simulation from the earlier model was used as a base case in the decoupled aquifer model. An improved match to observed water levels was achieved through a minor refinement of the permeability field used by Magnuson and Sondrup. In addition, a new and improved water level data set was used to establish boundary conditions.

Whitmire attempted to use kriged permeability data to parameterize the aquifer flow simulator. However, the calibration was poor using that geospatial representation. The reason for the poor match was a “bulleted” simulated head field resulting from a relatively short spatial correlation range.

***Holdren et al., 2002—***Holdren et al. (2002) presented a model to describe dissolved-phase transport in the vadose zone and groundwater beneath the SDA. The model was based on the Magnuson and Sondrup (1998) flow model with several notable improvements:

- The vadose zone and aquifer domains were separated

- Conformable gridding was used in the new model, which allowed for more accurate representation of interbeds

- Improved linkage between the source release model and the Magnuson and Sondrup model was achieved by using an approximation of the Magnuson and Sondrup infiltration rates in the source model

- Additional wells were available after the 1998 work; this allowed more rigorous lithologic interpretation and spatial variability assessment

- Aquifer model calibration was improved, as described in (Whitmire 2001)

- Additional contaminant data allowed better calibration

- Additional hydrologic and transport data were gathered from soil cores collected in 1999 and were used to improve the model

- The influence of the spreading areas was simulated by adding additional water to the western portion of the SDA at a depth just above the B-C interbed.

The model was used to estimate concentrations of the COCs at prescribed locations throughout the domain to support risk analyses.

### 3.7.4 Summary of Competing Hypotheses and Additional Data Requirements

As described in subsequent sections, a substantial amount of characterization work has been completed at WAG 7. Because the process of risk assessment can utilize conservative (if not bounding) descriptions for the individual elements of the conceptual model, the most recently developed transport simulation is considered to be adequate for the regulatory purposes of determining appropriate remedial action. Clearly though, the complexities of the geochemical and hydrological system, coupled with difficulties estimating contaminant chemical forms and rates of release, frustrates the development of a detailed and representative conceptual model.

A fundamental question regarding the conceptual model is on what scale the conceptual model needs to be, and can be, developed. The heterogeneity of the system increases as the scale decreases, quickly reaching a point where the macro level characterization currently available is insufficient. As the scale increases, the characterization requirements are lessened, but the peculiarities of the system are lost and correlation to observational data quickly diminishes. Studies of basalt hydrological properties have been conducted at scales ranging from individual microfractures to the LSIT, each yielding differing results. Similarly, interbed characteristics are scale dependent. Although on a large scale the hydraulic properties may be estimated using the available core data, relatively small areas of high permeability or discontinuous structure could have a significant affect on the fate and transport of contaminants.

The USGS (1999) suggests that preferential flow mechanisms add uncertainty to the transport predictions and may provide a possible explanation for the few sporadic detections of actinides beneath and nearby the RWMC. The detection of Pu-238 and Pu-239/240 at well D15 is referenced as possible evidence of lateral movement of water. Several types of preferential flow, including macropore flow, funnel flow, and fingered flow, may increase vertical and horizontal flow of water, as well as dissolved contaminants. Faybishenko et al. (2000) has questioned whether a Darcian description of vadose-zone flow is adequate in a fractured media.

Perhaps more importantly than hydrological and geochemical properties of the natural vadose zone and aquifer systems is the chemical form of the contaminants and their flux into the transport system. Some unusually strong-sorbing contaminants such as plutonium have migrated to at least the B-C interbed (and quite likely into the C-D interbed) in at least one location. Anthropic uranium has been detected at the B-C and C-D interbeds at selected locations. Although the use of conservative assumptions is generally regarded as adequate for the purposes of risk assessment, the USGS (1999) suggested that given the uncertainty in the conceptual model, resulting predictions of future contaminant concentrations may not be conservative.

As discussed previously, geochemical characteristics also vary significantly between and within geologic structures. Use of single, constant retardation coefficients clearly is not representative of the natural system. Again, the available data demonstrate heterogeneity but the conceptual model utilizes simplified representations. The question of whether to use an isotherm approach (linear or other) or to use surface complexation theory in a geochemical reactive transport code remains unresolved. A number of investigators have suggested that long-term evaluations be conducted to provide a basis for more representative geochemical modeling. Hull (2001) recommended a course of action to incorporate geochemistry in to INEEL fate and transport models with both short term and long term research activities. These types of recommendations need to be further evaluated as part of the INEEL conceptual model development.

In addition to the larger issues of scale, geochemistry researchers have identified a number of specific issues that remain unresolved:

- The spreading area water is poorly characterized in terms of volume of water and point(s) that it enters the WAG 7 domain
- Erratic flow behavior in the aquifer has been attributed to low permeability structures, however the degree of continuity of the low permeability area, as well as directions of flow beneath the SDA, are not well understood
- Potential transient influences of spreading area discharges on flow directions in aquifer are not understood
- It is still unclear whether concentrations of contaminants in aquifer are influenced by upgradient sources
- The amount of infiltration through the waste is uncertain as lateral influence of enhanced infiltration in ditches and low topographic areas on waste may create some degree of focusing and channeling
- Facilitated transport mechanisms are potential contributors, although their contribution is thought to be minor
- The reliability of low level detection in aquifer monitoring is uncertain
- It is unclear to what extent chromium serves as an indicator of dissolved phase transport through the vadose zone beneath the SDA.

### 3.7.5 Selected References


Ackerman, D.J., 1991, Transmissivity of the Snake River Plain aquifer at the Idaho National Engineering Laboratory, Idaho: U.S. Geological Survey Water-Resources Investigations Report 91–4058 (DOE/ ID–22097).

Adler Flitton, M. Kay, Carolyn W. Bishop, Ronald E. Mizia, Lucinda L. Torres, and Robert D. Rogers, 2001, Long Term Corrosion/Degradation Test Third-Year Results, INEEL/EXT-01-00036, Idaho National Engineering and Environmental Laboratory, Bechtel BWXT Idaho, LLC, Idaho Falls, Idaho.

Anderson, Danny L., 2001a, *OU 7-13/14 Integrated Probing Project Soil* Moisture Instrumented Probe, Engineering Design File EDF-ER-234, Idaho National Engineering and Environmental Laboratory, Bechtel BWXT Idaho, LLC, Idaho Falls, Idaho.

Anderson, Danny L., 2001b, Operable Unit (OU) 7-13/14 Integrated Probing Project Tritiated Soil Gas Sampling System for the Soil Vault Rows, Engineering Design File EDF-ER-262, Rev. 0, Idaho National Engineering and Environmental Laboratory, Bechtel BWXT Idaho, LLC, Idaho Falls, Idaho.

Anderson, S. R. and B. D. Lewis, 1989, Stratigraphy of the Unsaturated Zone at the Radioactive Waste Management Complex, Idaho National Engineering Laboratory, Idaho, Water-Resources Investigations Report 89-4065, DOE/ID-22080, U.S. Geological Survey.

Anderson, S. R., D. A. Ackerman, M. J. Liszewski, and R. M. Freiburger, 1996, Stratigraphic Data for Wells at and near the Idaho National Engineering Laboratory, Idaho, DOE/ID-22127, U.S. Geological Survey Open-File Report 96-248, U.S. Geological Survey.

Anderson, S. R., M. J. Liszewski, and D. J. Ackerman, 1996, *Thickness of Surficial Sediment at and near the Idaho National Engineering Laboratory, Idaho*, U.S. Geological Survey Open-File Report 96-330, U.S. Geological Survey.

Anderson, S.R., and Bartholomay, R.C., 1995, Use of natural-gamma logs and cores for determining stratigraphic relations of basalt and sediment at the Radioactive Waste Management Complex, Idaho National Engineering Laboratory, Idaho: Journal of the Idaho Academy of Science, 31:1.

Anderson, S.R., and Liszewski, M.J., 1997, Stratigraphy of the unsaturated zone and the Snake River Plain aquifer at and near the Idaho National Engineering Laboratory, Idaho: U.S. Geological Survey Water-Resources Investigations Report 97–4183 (DOE/ID–22142).

Anderson, S.R., Kuntz, M.A., and Davis, L.C., 1999, Geologic controls of hydraulic conductivity in the Snake River Plain aquifer at and near the Idaho National Engineering and Environmental Laboratory, Idaho: U.S. Geological Survey Water-Resources Investigations Report 99–4033 (DOE/ID–22155).

Baca, R. G., S. O. Magnuson, H. D. Nguyen, and P. Martian, 1992, A Modeling Study of Water Flow in the Vadose Zone Beneath the Radioactive Waste Management Complex, EGG-GEO-10068, EG&G Idaho, Inc., Idaho Falls, ID.

Bargelt, R.J., C. A. Dicke, J. M. Hubbell, M. Paarmann, D. Ryan, R. W. Smith, T. R. Wood, 1992, Summary of RWMC Investigations Report, EGG-WM-9708, Rev 0, January. EG&G Idaho, Inc. Idaho Falls, Idaho.

Bargelt, R.J., C.A. Dicke, J. M. Hubbell, M. Paarmann, D. Ryan, R. W. Smith, and T.R. Wood, 1992, Summary of RWMC Investigations Report, EGG-WM-9708, Rev.0, EG&G Idaho, Inc.

Barraclough, J. T., J. B. Robertson, and V. J. Janzer, 1976, Hydrology of the Solid Waste Burial Ground, as Related to the Potential Migration of Radionuclides, Idaho National Engineering Laboratory, IDO-22056, U. S. Geological Survey, Open File Report 76-471, Idaho Falls, Idaho.

Barraclough, J. T., W. E. Teasdale, and R. G. Jensen, February 1967, Hydrology of the National Reactor Testing Station Area, Idaho: Annual Progress Report 1965, USGS Open File Report, United States Geological Survey, Idaho Falls, Idaho.

Bartholomay, R.C., 1990, Mineralogical correlation of surficial sediment from area drainages with selected sedimentary interbeds at the Idaho National Engineering Laboratory, Idaho: U.S. Geological Survey Water- Resources Investigations Report 90–4147 (DOE/ID–22092).

Bartholomay, R.C., 1998, Distribution of selected radiochemical and chemical constituents in perched ground water, Idaho National Engineering Laboratory, Idaho, 1992–95: U.S. Geological Survey Water-Resources Investigations Report 98–4026 (DOE/ID–22145).

Bartholomay, R.C., Knobel, L.L., and Davis, L.C., 1989, Mineralogy and grain size of surficial sediment from the Big Lost River drainage and vicinity, with chemical and physical characteristics of geologic materials from selected sites at the Idaho National Engineering Laboratory, Idaho: U.S. Geological Survey Open-File Report 89–384 (DOE/ID–22081).

Bartholomay, R.C., Tucker, B.J., Ackerman, D.J., and Liszewski, M.J., 1997, Hydrologic conditions and distribution of selected radiochemical and chemical constituents in water, Snake River Plain aquifer, Idaho National Engineering Laboratory, Idaho, 1992 through 1995: U.S. Geological Survey Water- Resources Investigations Report 97–4086 (DOE/ID–22137).

Becker, B. H., 1997, *Selection and Development of Models Used in the Waste Area Group 7 Baseline Risk Assessment*, INEL-EXT-97-00391, Idaho National Engineering and Environmental Laboratory, Lockheed Martin Idaho Technologies Company, Idaho Falls, Idaho.

Becker, B. H., J. D. Burgess, K. J. Holdren, D. K. Jorgensen, S. O. Magnuson, and A. J. Sondrup, 1998, Interim Risk Assessment and Contaminant Screening for the Waste Area Group 7 Remedial Investigation, DOE/ID-10569, U.S. Department of Energy Idaho Operations Office, Idaho Falls, Idaho.

Becker, B. H., T. A. Bensen, C. S. Blackmore, D. E. Burns, B. N. Burton, N. L. Hampton, R. M. Huntley, R. W. Jones, D. K. Jorgensen, S. O. Magnuson, C. Shapiro, and R. L. VanHorn, 1996, Work Plan for Operable Unit 7-13/14 Waste Area Group 7 Comprehensive Remedial Investigation/Feasibility Study, INEL-95/0343, Idaho National Engineering and Environmental Laboratory, Lockheed Martin Idaho Technologies Company, Idaho Falls, Idaho.

Bennett, C.M., 1990, Streamflow losses and ground-water level changes along the Big Lost River at the Idaho National Engineering Laboratory, Idaho: U.S. Geological Survey Water-Resources Investigations Report 90–4067 (DOE/ID–22091).

Bishoff, J. R., 1979, INEL Transuranic Storage Cell Penetration and Inspection, TREE-1311, Idaho National Engineering and Environmental Laboratory, EG&G Idaho, Idaho Falls, Idaho.

Bishoff, James R., and Robert J. Hudson, 1979, Early Waste Retrieval Final Report, TREE-1321, Idaho National Engineering and Environmental Laboratory, EG&G Idaho, Idaho Falls, Idaho.

Bishop, C. W., 1991, Hydraulic Properties of Vesicular Basalt, Masters Thesis, University of Arizona, Tucson, AZ.

Bishop, C. W., 1994, Expansion of Moisture Monitoring Network at the Subsurface Disposal Area, INEL-94/0144, Idaho National Engineering and Environmental Laboratory, Lockheed Martin Idaho Technologies Company, Idaho Falls, Idaho.

Bishop, C. W., 1996a, LMITCO Internal Report, Soil Moisture Monitoring Results at the Radioactive Waste Management Complex of the Idaho National Engineering Laboratory, FY-96, FY-95, and FY-94, INEL-96/297, Idaho National Engineering and Environmental Laboratory, Lockheed Martin Idaho Technologies Company, Idaho Falls, Idaho.

Bishop, C. W., 1996b, Interdepartmental Communication to D. J. Kuhns, "Pad A Horizontal Hole Neutron Monitoring," Idaho National Engineering and Environmental Laboratory, Lockheed Martin Idaho Technologies Company, Idaho Falls, Idaho, CWB-16-96, December 18, 1996.

Borghese, J.V., 1988, Hydraulic Characteristics of Soil Cover, Subsurface Disposal Area, Idaho National Engineering and Environmental Laboratory, Idaho Falls, ID, Masters Thesis, University of Idaho, Moscow, Idaho.

Bowman, A. L., W. F. Downs, K. S. Moor, and B. F. Russell, 1984, INEL Environmental Characterization Report, Vol. 2, EGG-NPR-6688, Idaho National Engineering and Environmental Laboratory, EG&G Idaho, Idaho Falls, Idaho.

Burgess, J. D., 1995, Results of the Neutron and Natural Gamma Logging, Stratigraphy, and Perched Water Data Collected During a Large-Scale Infiltration Test, ER-WAG7-60, INEL-95/062, Idaho National Engineering and Environmental Laboratory, Lockheed Martin Idaho Technologies Company, Idaho Falls, Idaho.

Burgess, J. D., 1996, Tritium and Nitrate Concentrations at the RWMC, Engineering Design File EDF-ER-024, INEL-96/204, Idaho National Engineering and Environmental Laboratory, Lockheed Martin Idaho Technologies Company, Idaho Falls, Idaho.

Burgess, J. D., B. D. Higgs, and T. R. Wood, 1994, *WAG 7 Groundwater Pathway Track 2 Summary Report,* EGG-ER-10731, Idaho National Engineering and Environmental Laboratory, EG&G Idaho, Idaho Falls, Idaho, June 1994.

Burgus, W. H., and S. E. Maestas, 1976, The 1975 RWMC Core Drilling Program, U.S., Energy Research and Development Administration Office, Office of Waste Management, Idaho Operations Office Publication, IDO-10065.

Burgus, W.H., and Maestas, S.E., 1976, *A further investigation of subsurface radioactivity at the Radioactive Waste Management Complex, Idaho National Engineering Laboratory*, U.S. Energy Research and Development Administration, INEL Report IDO–10065.

Burns, D. E., 1995, Interdepartmental Communication to D. K. Jorgensen, "Estimated Percentages of the OU 7-13/14 COPCs Disposed in Individual SDA Pits and Trenches," Idaho National Engineering and Environmental Laboratory, Lockheed Martin Idaho Technologies Company, Idaho Falls, Idaho, DEB-08-95, October 25, 1995.

Burns, D. E., B. H. Becker, and R. W. Jones, 1994, Preliminary Scoping Track 2 Summary Report for Operable Unit 7-01, INEL-94/0241, Idaho National Engineering and Environmental Laboratory, Lockheed Martin Idaho Technologies Company, Idaho Falls, Idaho.

Burns, D. E., B. H. Becker, R. M. Huntley, C. A. Loehr, S. M. Rood, P. Sinton, and T. H. Smith, 1994, Revised Preliminary Scoping Risk Assessment for Waste Pits, Trenches, and Soil Vaults at the Subsurface Disposal Area, Idaho National Engineering Laboratory, EG&G-ER-11395, Idaho National Engineering and Environmental Laboratory, EG&G Idaho, Idaho Falls, Idaho.

Burns, D. E., C. A. Loehr, and S. M. Waters, 1993, "Draft Final Scoping Track 2 Summary Report for Operable Unit OU 7-05: Surface Water Pathways and Surficial Sediments," EGG-ERD-10449, Rev. 0, Idaho National Engineering and Environmental Laboratory, EG&G Idaho, Idaho Falls, Idaho.

Busenberg, E., Plummer, L.N., Bartholomay, R.C., and Wayland, J.E., 1998, Chlorofluorocarbons, sulfur hexafluoride, and dissolved permanent gases in ground water from selected sites at and near the Idaho National Engineering and Environmental Laboratory, Idaho, 1994 through 1997: U.S. Geological Survey Open-File Report 98–274 (DOE/ID–22151).

Busenberg, E., Weeks, E.P., Plummer, L.N., and Bartholomay, R.C., 1993, Age dating ground water by use of chlorofluorocarbons ($CCl_3F$ and $CCl_2F_2$), and distribution of chlorofluorocarbons in the unsaturated zone, Snake River Plain aquifer, Idaho National Engineering Laboratory, Idaho: U.S. Geological Survey Water-Resources Investigations Report 93–4054 (DOE/ID-–22107).

Card, D. H., 1977, Early Waste Retrieval Interim Reports, TREE-1047, Idaho National Engineering and Environmental Laboratory, EG&G Idaho, Idaho Falls, Idaho.

Card, D. H., and D. K. Wang, 1976, Initial Drum Retrieval Interim Report July 1974 to September 1976, TREE-1079, Idaho National Engineering and Environmental Laboratory, EG&G Idaho, Idaho Falls, Idaho.

Case, Marilyn J., Arthur S. Rood, James M. McCarthy, Swen O. Magnuson, Bruce H. Becker, and Thomas K. Honeycutt, 2000, Technical Revision of the Radioactive Waste Management Complex Low-Level Waste Radiological Performance Assessment for Calendar Year 2000, INEEL/EXT-2000-01089, Idaho National Engineering and Environmental Laboratory, Bechtel BWXT Idaho, LLC, Idaho Falls, Idaho.

Cecil, L. D., B. R. Orr, T. Norton, and S. R. Anderson, 1991, Formation of Perched Ground-Water Zones and Concentrations of Selected Chemical Constituents in Water, Idaho National Engineering Laboratory, Idaho 1986-88, DOE/ID-22100, U.S. Geological Survey Water-Resources

Investigations Report 91-4166, prepared in cooperation with the U.S. Department of Energy, Idaho Falls, ID, November.

Cecil, L. D., J. R. Pittman, T. M. Beasley, R. L. Michel, P. W. Kubik, P. Sharma, U. Fehn, and H. Gove, 1992, "Water Infiltration Rates in the Unsaturated Zone at the Idaho National Engineering Laboratory Estimated from Chlorine-36 and Tritium Profiles, and Neutron Logging," in Proceedings of the 7th International Symposium on Water-Rock Interaction - WRI-7, Y. K. Kharaka and A. S. Meest (eds.), Park City, UT.

Cecil, L.D., 1989, Reporting of radionuclide data of environmental concern, *in* Pedersen, G.L., and Smith, M.M., compilers, U.S. Geological Survey Second National Symposium on Water Quality, Abstracts of the Technical Sessions, Orlando, Florida, November 12–17, 1989: U.S. Geological Survey Open File Report 89–409.

Cecil, L.D., J.R. Pittman, T.M. Beasley, R.L. Michel, P.W. Kubik, P. Sharma, U. Fehn, and H.E. Gove (1992) Water infiltration rates in the unsaturated zone at the Idaho national Engineering Laboratory estimated from chlorine-36 and tritium profiles, and neutron logging, pp 709-714 in: Y.K. Kharaka and A.S. Maest (eds.), Water-Rock Interaction, Proc. of the 7th Intl Symposium on Water-Rock Interaction, A.A. Baldema, Rotterdam.

Cecil, L.D., Orr, B.R., Norton, Teddy, and Anderson, S.R., 1991, Formation of perched ground-water zones and concentrations of selected chemical constituents in water, Idaho National Engineering Laboratory, Idaho 1986–88: U.S. Geological Survey Water-Resources Investigations Report 91– 4166 (DOE/ ID–22100).

Chatwin, T. D., A. D. Coveleski, K. J. Galloway, J. M. Hubbell, R. M. Lugar, G. E. Mathern, O. R. Perry, A. J. Sondrup, and S. N. Stanisich, 1992, Final Work Plan for the Organic Contamination in the Vadose Zone, Operable Unit 7-08, Focused Remedial Investigation/Feasibility Study, EGG-WM-10049, Idaho National Engineering and Environmental Laboratory, EG&G Idaho, Idaho Falls, Idaho.

Choppin, G. R., A. H. Bond, and P. M. Hromadka, 1997, "Redox Speciation of Plutonium," Jour of Radioanalytical and Nuclear Chemistry, 1997, Vol. 219, pp. 203-210.

Clark, D. T., 2001a, "OU 7-13/14 Integrated Probing Project Lysimeter Probe Design (Draft)," Engineering Design File EDF-ER-236, Rev. A, Idaho National Engineering and Environmental Laboratory, Bechtel BWXT Idaho, LLC, Idaho Falls, Idaho.

Clark, Don T., 2001, *Operable Unit 7-13/14 Integrated Probing Project Vapor* Port Instrument Probe, Engineering Design File EDF-ER-235, Rev. 0, Idaho National Engineering and Environmental Laboratory, Bechtel BWXT Idaho, LLC, Idaho Falls, Idaho.

Clemson University, June 2001, The sorption of Selected Radionuclides in Sedimentary interbed soils from the Snake River Plain, INEEL/EXT-01-01106 Rev0, Idaho National Engineering and Environmental Laboratory.

Cleveland J.M., and Mullin, A.H., 1993, Speciation of plutonium and americium in ground waters from the Radioactive Waste Management Complex, Idaho National Engineering Laboratory, Idaho: U.S. Geological Survey Water-Resources Investigations Report 93–4035.

Dames and Moore, 1992, Compilation and summarization of the Subsurface Disposal Area Radionuclide Transport data at the Radioactive Waste Management Complex: U.S. Department of Energy, INEL Report EGG–ER–10546.

Dames and Moore, 1994, Compilation and Summarization of the Subsurface Disposal Area Radionuclide Transport Data at the Radioactive Waste Management Complex, Revision 3, EGG-ER-10546, prepared for EG&G Idaho Inc., Idaho Falls, ID.

Davis, L.C., and Pittman, J.R, 1990, Hydrological, meteorological, and geohydrological data for an unsaturated zone study near the Radioactive Waste Management Complex, Idaho National Engineering Laboratory, Idaho—1987: U.S. Geological Survey Open-File Report 90–114 (DOE/ID– 22086).

Dechert, T. V., P. A. McDaniel, A. L. Falen, 1994, Aggradational and Erosional History of the RWMC at the INEL, EGG-WM-11049, September.

Dicke, C. A., 1997, *Distribution Coefficients and Contaminant Solubilities for the Waste Area Group 7 Baseline Risk Assessment*, INEL/EXT-97-00201, Idaho National Engineering and Environmental Laboratory, Lockheed Martin Idaho Technologies Company, Idaho Falls, Idaho.

Dicke, C. A., 1998, Carbon-14 Distribution Coefficients Measured from Batch Experiments on SDA Sediments, INEEL/INT-98-00068, EDF-RWMC-1011, Lockheed Martin Idaho Technologies Company, May.

DOE, 1999, Operable Unit 7-13/14, In Situ Grouting Treatability Study Work Plan, DOE/ID-10690, September, U.S. Department of Energy, Idaho Operations Office.

DOE-ID, 1983, A Pl*an for Studies of Subsurface Radionuclide Migration at the Radioactive Waste Management Complex of the Idaho* National Engineering Laboratory, Vols. I and II, DOE/ID-10116, U.S. Department of Energy, Idaho Field Office, Idaho Falls, Idaho.

DOE-ID, 1998, Addendum to the Work Plan for the Operable Unit 7-13/14 Waste Area Group 7 Comprehensive Remedial Investigation/Feasibility Study, DOE/ID-10622, U.S. Department of Energy Idaho Operations Office, Idaho Falls, Idaho.

Duncan, F. L., R. E. Troutman, and A. J. Sondrup, 1993, Remedial Investigation/Feasibility Study Report for the Organic Contamination in the Vadose Zone-Operable Unit 7-08 at the Idaho National Engineering Laboratory, Volume I: Remedial Investigation, EGG-ER-10684, Idaho National Engineering and Environmental Laboratory, EG&G Idaho, Idaho Falls, Idaho.

Dunnivant, F. M. and M. E. Newman, 1995, Migration of Radionuclide Tracers Through Fractured Media: Preliminary Modeling Results of Breakthrough Curves Obtained During the Large-Scale Aquifer Pumping and Infiltration Tests, INEL-95/288, Lockheed Martin Idaho Technologies, Idaho Falls, ID.

EG&G, December 1988, RCRA Facility Investigation Work Plan, Vol. 1., EGG-WM-8219, EG&G Idaho, Inc.

EPA, 1999, Understanding Variation in Partition Coefficient, Kd Values, EPA 402-R—99-004A&B, U. S. Environmental Protection Agency, Office of Radiation and Indoor Air.

Fabryka-Martin, Gee, and Flint 1999

Faybishenko B, Doughty C, Steiger M, Long CS, Wood TR, Jacobsen JS, Lore J, Zawislanski PT "Conceptual model of the geometry and physics of water flow in a fractured basalt vadose zone" WRR, 36 (12): 3499-3520 Dec 2000

Fayer, M. J., and T. L. Jones, 1990, UNSAT-H Version 2.0: Unsaturated Soil Water and Heat Flow Model, PNL-6779, Pacific Northwest Laboratory, Richland, WA.

Fjeld, R. A., J. T. Coates, and A. W. Elzerman, 2000, *Column Tests to Study the Transport of Plutonium and other Radionuclides in Sedimentary Interbed at INEEL*, Department of Environmental Engineering and Science, Clemson University, Clemson, South Carolina.

Fjeld, R.A., Coates, J.T., Elzerman, A.W., and Navratil, J.D., 1998, Column studies of plutonium transport in sedimentary interbeds from the Snake River Plain: Proceedings of Waste Management 98 Symposium, Tucson, Arizona.

Fjeld, Robert A, John T. Coates, and Alan W. Elzerman, 2000, Final Report, Column Tests to Study the Transport of Plutonium and Other Radionuclides in Sedimentary Interbed at INEEL, INEEL/EXT-01-00763, Clemson University, Department of Environmental Engineering and Science, Clemson, South Carolina, for the Idaho National Engineering and Environmental Laboratory, Bechtel BWXT Idaho, LLC, Idaho Falls, Idaho, December 21, 2000.

Goff, R.W., 1994, The sorption of select radionuclides on basalt and interbed material of the Snake River Plain in southern Idaho: Clemson University, M.S. Thesis.

Hackett, W. R., J. A. Tullis, R. P. Smith, S. J. Miller, T. V. Dechert, P. A. McDaniel, and A. L. Falen, 1995, Geologic Processes in the RWMC Area, Idaho National Engineering Laboratory: Implications for Long Term Stability and Soil Erosion at the Radioactive Waste Management Complex, INEL-95/0519, Idaho National Engineering and Environmental Laboratory, Lockheed Martin Idaho Technologies Company, Idaho Falls, Idaho.

Holdren, K. J., B. H. Becker, N. L. Hampton, L. D. Koeppen, S. O. Magnuson, T. J. Meyer, G. L. Olson, A. J. Sondrup, 2002, "WAG 7 Operable Unit 7-13/14 Comprehensive Evaluation of the Nature and Extent of Contamination and Potential Risk Associated with the Radioactive Waste Management Complex," Draft document to be released as an INEEL external report by September 2002 (Document title subject to change in final version)

Honeycutt, T. K., 1996, Interdepartmental Communication, "Factors Controlling Radionuclide Release for Ion Exchange Resin," Draft, Idaho National Engineering and Environmental Laboratory, Lockheed Martin Idaho Technologies Company, 1996.

Hubbell, J. M., 1990, Perched Ground Water at the Radioactive Waste Management Complex of the Idaho National Engineering Laboratory, EGG-ER-8779, EG&G Idaho, Inc., Idaho Falls, ID.

Hubbell, J. M., 1992, Perched Water at the Radioactive Waste Management Complex, EDF-VVED-ER-098, EG&G Idaho, Inc., Idaho Falls, ID.

Hubbell, J. M., 1993, Perched Ground Water Monitoring in the Subsurface Disposal Area of the Radioactive Waste Management Complex, FY-1993, EDF-ER&WM-EDF-002293, EG&G Idaho, Inc., Idaho Falls, ID.

Hubbell, J. M., 1995, Perched Groundwater Monitoring in the Subsurface Disposal Area of the Radioactive Waste Management Complex, Engineering Design File EDF-INEl-95/149, Idaho National Engineering and Environmental Laboratory, Lockheed Martin Idaho Technologies Company, Idaho Falls, Idaho, September 1995.

Hubbell, J. M., et al., 1985, Annual Progress Report: FY-1985, Subsurface Investigations Program At the Radioactive Waste Management Complex of the Idaho National Engineering Laboratory, DOE/ID-10136, Idaho National Engineering and Environmental Laboratory, Lockheed Martin Idaho Technologies Company, Idaho Falls, Idaho.

Hubbell, J. M., L. C. Hull, T. G. Humphrey, B. F. Russell, J. R. Pittman, and K. M. Cannon, 1985, Annual Progress Report: FY-1985. Subsurface Investigations Program at the Radioactive Waste Management Complex of the Idaho National Engineering Laboratory. DOE/ID 10136.

Hubbell, J. M., L. C. Hull, T. G. Humphrey, B. F. Russell, J. R. Pittman, and P. R. Fischer, 1987, Annual Progress Report FY-1986, Subsurface Investigation Program at the Radioactive Waste Management Complex of the Idaho National Engineering Laboratory, DOE/ID-10153, U.S. Department of Energy Idaho Operations Office, Idaho Falls, Idaho, January 1987.Hubbell, J. M., et al., 1987, Annual Progress Report: FY-1986, Subsurface Investigations Program at the Radioactive Waste Management Complex of the Idaho National Engineering Laboratory, DOE/ID-101153, January 1987.

Hubbell, J.M., 1990, Perched ground water at the Radioactive Waste Management Complex: U.S. Department of Energy, EDF–VVED–ER–098, EG&G Idaho, Inc.

Hubbell, J.M., Hull, L.C., Humphrey, T.G., Pittman, J.R., and Fischer, P.R., 1987, Subsurface investigations program at the Radioactive Waste Management Complex of the Idaho National Engineering Laboratory, Annual Progress Report FY-1986, U.S. Department of Energy, DOE/ID– 10153.

Hughes, J. D., 1993, Analysis of characteristics of sedimentary interbeds at the Radioactive Waste Management Complex, Idaho national Engineering Laboratory, Idaho: Idaho State University, M.S. thesis.

Hull, L. and M. N. Pace, 2000, Solubility Calculations for Contaminants of Potential Concern at OU 7-13/14, INEEL/EXT-2000-00465, Idaho National Engineering and Environmental Laboratory, Idaho Falls, Idaho.

Hull, Larry, 2001, Interoffice Memorandum to Theodore J. Meyer, Doug Burns, Swen Magnuson, and James McCarthy, “Approach to Simulation of Actinides for the OU 7-13/14 Baseline Risk Assessment,” Idaho National Engineering and Environmental Laboratory, Bechtel BWXT Idaho, LLC, Idaho Falls, Idaho, LCH-04-01, April 4, 2001.

Hull, Laurence, and Mary N. Pace, 2000, *Solubility Calculations for* Contaminants *of Potential Concern, OU 7-13/14*, INEEL/EXT-2000-00465, Idaho National Engineering and Environmental Laboratory, Bechtel BWXT Idaho, LLC, Idaho Falls, Idaho.

Humphrey, T. G., 1980, Subsurface Migration of Radionuclides at the Radioactive Waste Management Complex 1978, EGG-2026, EG&G Idaho, Inc., Idaho Falls, Idaho.

Humphrey, T. G., and F. H. Tingey, 1978, The Subsurface Migration of Radionuclides at the Radioactive Waste Management Complex, 1976-1777, TREE-1171, Idaho National Engineering and Environmental Laboratory, EG&G Idaho, Idaho Falls, Idaho.

Humphrey, T. G., and F. H. Tingey. 1978. The Subsurface Migration of Radionuclides at the Radioactive Waste Management Complex 1976-1977, TREE-1171, EG&G Idaho, Inc., Idaho Falls, Idaho.

Humphrey, T. G., T. H. Smith, and M. C. Pope, 1982. "Projected Subsurface Migration of Radionuclides from Buried Idaho National Engineering Laboratory Transuranic Waste," Nuclear Technology, 58.

Humphrey, T.G., 1980, Subsurface migration of radionuclides at the Radioactive Waste Management Complex, 1978: U.S. Department of Energy, INEL Report EGG–2026, 44.

Humphrey, T.G., and Tingey, F.H., 1978, The subsurface migration of radionuclides at the Radioactive Waste Management Complex, 1976–1977: U.S. Department of Energy, INEL Report TREE–1171.

INEEL, 2000c, Operable Unit 7-13/14 Plan for the Installation, Logging, and Monitoring of Probeholes in the Subsurface Disposal Area, INEEL/EXT-98-00856, Rev 1, Idaho National Engineering and Environmental Laboratory, Bechtel BWXT Idaho, LLC, Idaho Falls, Idaho.

INEEL, 2001b, Geographic Information System Shipping Database, WasteOScope, Idaho National Engineering and Environmental Laboratory, Bechtel BWXT Idaho, LLC, Idaho Falls, Idaho, URL: remus4.inel.gov/wasteoscope.html

Keck, K. N., 1995, SDA Surface Water Description and Data, Engineering Design File ER-WAG7-66, INEL-95/119, Idaho National Engineering and Environmental Laboratory, Lockheed Martin Idaho Technologies Company, Idaho Falls, Idaho, 1995.

Knobel, L. L., B. R., Orr, and L. D. Cecil, June 1992, "Summary of Background Concentrations of Selected Radiochemical and Chemical Constituents in Groundwater from the Snake River Plain Aquifer, Idaho: Estimated from an Analysis of Previously Published Data," Journal of the Idaho Academy of Science, Vol. 28, X10.1.

Knobel, L.L., and Mann, L.J., 1988, Radionuclides in ground water at the Idaho National Engineering Laboratory, Idaho: U.S. Geological Survey Open-File Report 88–731 (DOE/ID– 22077).

Knobel, L.L., Bartholomay, R.C., and Orr, B.R., 1997, Preliminary delineation of natural geochemical reactions, Snake River Plain aquifer system, Idaho National Engineering Laboratory and vicinity, Idaho: U.S. Geological Survey Water-Resources Investigations Report 97–4093 (DOE/ID–22139).

Knobel, L.L., Bartholomay, R.C., Cecil, L.D., Tucker, B.J., and Wegner, S.J., 1992a, Chemical constituents in the dissolved and suspended fractions of ground water from selected sites,

Idaho National Engineering Laboratory and vicinity, Idaho, 1989: U.S. Geological Survey Open-File Report 92–51 (DOE/ID–22101).

Knobel, L.L., Bartholomay, R.C., Wegner, S.J., and Edwards, D.D., 1992b, Chemical constituents in water from wells in the vicinity of the Naval Reactors Facility, Idaho National Engineering Laboratory, Idaho: U.S. Geological Survey, Open File Report 92–156 (DOE/ID–22013).

Knobel, L.L., Cecil, L.D., and Wood, T.R., 1995, Chemical composition of selected core samples, Idaho National Engineering Laboratory, Idaho: U.S. Geological Survey, Open-File Report 95–748 (DOE/ ID–22126).

Knutson, C. F., K. A. McCormick, J. C. Crocker, M. A. Glenn, and M. L. Fishel, 1992, 3D RWMC Vadose Zone Modeling (Including FY-89 to FY-90 Basalt Characterization Results), EGG-ERD-10246, Idaho National Engineering and Environmental Laboratory, EG&G Idaho, Idaho Falls, Idaho.

Knutson, C.F., McCormick, K.A., Smith, R.P., Hackett, W.R., O'Brien, J.P., and Crocker, J.C., 1990, FY-89 Report RWMC vadose zone basalt characterization: EG&G Idaho, Inc., EGG–WM–8949.

Koslow, K.N. and D. H. Van Haaften, 1986, Flood Routing Analysis for a Failure of Mackay Dam, EGG-Ep-7-7184, Idaho National Engineering and Environmental Laboratory, Idaho Falls, ID.

Kudera, D. E., and B. W. Brown, 1996, Volatile Organic Compounds Disposed of from 1952 Through 1983 at the Radioactive Waste Management Complex: Quantities Forms, Release Mechanisms and Rates, ER-WAG7-90, Idaho National Engineering and Environmental Laboratory, Lockheed Martin Idaho Technologies Company, Idaho Falls, Idaho.

Kuntz, M. A., B. Skipp, M.A. Lanphere, W. E. Scott, K. L. Pierce, G. B. Dalrymple, D. E. Champion, G.F. Embree, W. R. Page, L. A. Morgan, R. P. Smith, W. R. Hackett, and D. W. Rodgers, 1994, Geologic Map of the Idaho National Engineering Laboratory and Adjoining Areas, Eastern Idaho, Miscellaneous Investigation Map, I-2330, 1:100,000 scale, U.S. Geological Survey.

Kuntz, M. A., Dalrymple, G.B., Champion, D.E., and Doherty, D.J., 1980, Petrography, age and paleomagnetism of volcanic rocks at the Radioactive Waste Management Complex, Idaho National Engineering Laboratory, Idaho, with an evaluation of potential volcanic hazards: U.S. Geological Survey Open-File Report 80-388.

Kuntz, M.A., and Dalrymple, G.B. 1979, Geology geochronology, and potential volcanic hazards in the Lava Ridge-Hells Half Acre area, eastern Snake River Plain, Idaho: U.S. Geological Survey Open File Report 79-1657.

Laney, P. T., S. C. Minkin, R. G. Baca, D. L. McElroy, J. M Hubbell, L. C. Hull, B. F Russell, G. J. Stromberg, and J. R. Pittman, 1988, Annual Progress Report: FY-1987 - Subsurface Investigations Program at the Radioactive Waste Management Complex of the Idaho National Engineering Laboratory, DOE/ID-10183, EG&G Idaho, Inc., Idaho Falls, ID.

Lee, C. B., 1991, A statistical model of three hydrogeological parameters used in contaminant transport modeling at the Radioactive Waste Management Complex, Idaho National Engineering and Environmental Laboratory. Masters Thesis, Idaho Sate University.

Lee, J., Martins, G. P., Weidner, J. R., 1991, Characterization Studies on: (a) Contaminated Batch of Rocky Flats Soil, and (b) Uncontaminated Batch of INEL Soil, EG&G-WTD-9794, EG&G Idaho, Inc., Idaho Falls, Idaho

Leecaster, M. K., April 2002, Geostatistic Modeling of Subsurface Characteristics in the Radioactive Waste Management Complex Region, Operable Unit 7-13/14, INEEL/EXT-02-00029, Revision 0, Bechtel BWXT Idaho, LLC.

Leenheer, J.A., and Bagby, J.C., 1982, Organic solutes in ground water at the Idaho National Engineering Laboratory: U.S. Geological Survey Water-Resources Investigation 82–15 (IDO–22061).

Lewis, B.D., and Goldstein, F.J., 1982, Evaluation of a predictive ground-water solute-transport model at the Idaho National Engineering Laboratory, Idaho: U.S. Geological Survey Water-Resources Investigation Report 82–25 (DOE/ID–22062).

Liszewski, M.J., and Mann, L.J., 1993, Concentrations of 23 trace elements in ground water and surface water at and near the Idaho National Engineering Laboratory, Idaho, 1988–91: U.S. Geological Survey Open-File Report 93–126 (DOE/ID–22110).

Liszewski, M.J., Rosentreter, J.J., and Miller, K.E., 1997, Strontium distribution coefficients of surficial sediment samples at the Idaho National Engineering Laboratory, Idaho: U.S. Geological Survey Water-Resources Investigations Report 97–4044 (DOE/ID–22140).

Liszewski, M.J., Rosentreter, J.J., Miller, K.E., and Bartholomay, R.C., 1999, Chemical and physical factors affecting strontium distribution coefficients of surficial sediment samples at the Idaho National Engineering and Environmental Laboratory, Idaho: Environmental Geology.

Little, Marianne, Joan K. McDonald, Jon D. Grandy, Michael L. Carboneau, Andrea G. Chambers, Shannon C. Flynn, L. Don Koeppen, and John A. Logan, 2001, A Comprehensive Inventory of Radiological and Nonradiological Contaminants to Be Buried or Projected to Be Buried in the Subsurface Disposal Area of the INEEL RWMC During the Years 1984 to 2003 Supplement, INEL-95/0135 Supplement, Rev. 0, Idaho National Engineering and Environmental Laboratory, Bechtel BWXT Idaho, LLC, Idaho Falls, Idaho, August 2001.

LMITCO, 1995a, A Comprehensive Inventory of Radiological and Nonradiological Contaminants in Waste Buried or Projected to Be Buried in the Subsurface Disposal Area of the INEL RWMC During the Years 1984-2003, INEL-95/0135, Rev. 1, Idaho National Engineering and Environmental Laboratory, Lockheed Martin Idaho Technologies Company, Idaho Falls, Idaho.

LMITCO, 1995a, A Comprehensive Inventory of Radiological and Nonradiological Contaminants in Waste Buried in the Subsurface Disposal Area of the INEL RWMC During the Years 1952–1983, INEL-95/0310 (formerly EGG-WM-10903), Rev. 1, Idaho National Engineering and Environmental Laboratory, Lockheed Martin Idaho Technologies Company, Idaho Falls, Idaho.

LMITCO, 1999, Progress Report: Tritium and Carbon-14 Sampling at the Radioactive Waste Management Complex, INEEL/EXT-98-00669, Idaho National Engineering and Environmental Laboratory, Lockheed Martin Idaho Technologies Company, Idaho Falls, Idaho.

Lodman, D. W., S. Dunstan, W. T. Downs, A. J. Sondrup, D. H. Miyasaki, K. J. Galloway, and K. Izbicki, 1994, Treatability Study Report for the Organic Contamination in the Vadose Zone, OU 7-08, EGG-ER-11121, Idaho National Engineering and Environmental Laboratory, EG&G Idaho, Idaho Falls, Idaho.

Loehr, C. A., B. H. Becker, D. E. Burns, R. M. Huntley, S. M. Rood. P. Sinton, and T. H. Smith, 1994, Preliminary Scoping Risk Assessment for Waste Pits, Trenches, and Soil Vaults at the Subsurface Disposal Area, Idaho National Engineering Laboratory, EGG-WM-11181, Idaho National Engineering and Environmental Laboratory, EG&G Idaho, Idaho Falls, Idaho.

Loehr, C., J. J. Einerson, and D. K. Jorgensen, 1993, SDA Core Analysis Summary for the Radioactive Waste Management Complex Non-TRU Pits and Trenches at the Idaho National Engineering Laboratory 1971 to 1989, ER-WAG7-36, Idaho National Engineering and Environmental Laboratory, EG&G Idaho, Idaho Falls, Idaho.

Magnuson, S.O., and Sondrup, A.J. (1998) Development, Calibration, and Predictive Results of a Simulator for Subsurface Pathway Fate and Transport of Aqueous-and Gaseous-Phase Contaminants in the Subsurface Disposal Area at the Idaho National Engineering and Environmental Laboratory. INEEL/EXT-97-00609.

Magnuson, S. O. and A. J. Sondrup, 1992, A Modeling Study of Contaminant Transport Resulting From Flooding of Pit 9 at the Radioactive Waste Management Complex, Idaho National Engineering Laboratory, EGG-EEL-10498, EG&G Idaho, Inc., Idaho Falls, ID.

Magnuson, S. O. and A. J. Sondrup, 1998, Development, Calibration, and Predictive Results of a Simulator for Subsurface Pathway Fate and Transport of Aqueous- and Gaseous-Phase Contaminants in the Subsurface Disposal Area at the Idaho National Engineering and Environmental Laboratory, INEEL/EXT-97-00609, Lockheed Martin Idaho Technologies Company, Idaho Falls, ID.

Magnuson, S. O. and D. L. McElroy, 1993, Estimation of Infiltration from In Situ Moisture Contents and Representative Moisture Characteristic Curves for the 30', 110', and 240' Interbeds, EG&G Engineering Design File #RWM-93-001.1, EG&G Idaho, Inc., Idaho Falls, ID.

Magnuson, S. O., 1993, A Simulation Study of Moisture Movement in Proposed Barriers for the Subsurface Disposal Area, INEL, EGG-WM-10974, EG&G Idaho, Inc., Idaho Falls, ID.

Magnuson, S. O., 1995, Inverse Modeling for Field-Scale Hydrologic and Transport Parameters of Fractured Basalt, INEL-95/0637, Lockheed Martin Idaho Technologies Company, Idaho Falls, ID.

Magnuson, S. O., 1995b, SDA Soil, Basalt, and Water Concentration Data Compilation: Radionuclides and Inorganics, ER-WAG7-72, INEL-95/216, Idaho National Engineering and Environmental Laboratory, Lockheed Martin Idaho Technologies Company, Idaho Falls, Idaho.

Magnuson, S. O., 1998, Sensitivity of the SDA Flow and Transport Simulator to the Low Permeability Region in the Aquifer, Engineering Design File INEEL/INT-01066, Lockheed Martin Idaho Technologies.

Magnuson, S. O., Interdepartmental Communication to D. K. Jorgensen, "Transmittal of TETRAD Benchmarking Report," Idaho National Engineering and Environmental Laboratory, Lockheed Martin Idaho Technologies Company, Idaho Falls, Idaho, SOM-01-96, January 3, 1996.

Magnuson, S.O. (1995) Inverse Modeling for Field-Scale Hydrologic and Transport Parameters of Fractured Basalt, INEL-95-0637.

Maheras, S. J., A. S. Rood, S. O. Magnuson, M. E. Sussman, and R. N. Bhatt, 1994, Radioactive Waste Management Complex Low-Level Waste Radiological Performance Assessment, EGG-WM-8773, EG&G Idaho, Inc., Idaho Falls, ID.

Maheras, S. J., A. S. Rood, S. O. Magnuson, M. E. Sussman, and R. N. Bhatt, 1997, *Addendum to Radioactive Waste Management Complex* Low-*Level Waste Radiological Performance Assessment (EGG-WM-8773)*, INEEL/EXT-97-00462 (formerly EGG-WM-8773), Idaho National Engineering and Environmental Laboratory, Lockheed Martin Idaho Technologies Company, Idaho Falls, Idaho.

Mann, L.J., 1986, Hydraulic properties of rock units and chemical quality of water for INEL-1—a 10,365- foot deep test hole drilled at the Idaho National Engineering Laboratory, Idaho: U.S. Geological Survey Water-Resources Investigations Report 86–4020 (IDO–22070).

Mann, L.J., and Knobel, L.L., 1988, Concentrations of nine trace metals in ground water at the Idaho National Engineering Laboratory, Idaho: U.S. Geological Survey Open-File Report 88–332 (DOE/ ID–22075).

Markham, O.D., 1978, Activation and fission products in the environment near the Idaho National Engineering Laboratory Radioactive Waste Management Complex: U.S. Department of Energy, IDO–12095.

Martian, P. (1995) UNSAT-H Infiltration Model Calibration at the Subsurface Disposal Area, Idaho National Engineering Laboratory, INEL-95/0596.

Martian, P., 1995, UNSAT-H Infiltration Model Calibration at the Subsurface Disposal Area, Idaho National Engineering Laboratory, INEL-95/0596, Lockheed Idaho Technologies Company, Idaho Falls, ID.

Martian, P., and S. O. Magnuson, 1994, A Simulation Study of Infiltration Into Surficial Sediments at the Subsurface Disposal Area, Idaho National Engineering Laboratory, EGG-WM-11250, Idaho National Engineering and Environmental Laboratory, EG&G Idaho, Idaho Falls, Idaho.

McCarthy, J. M., 1995, Hydraulic Characterization Data Compilation: Basalts, Engineering Design File EDF INEL-95/129, Idaho National Engineering and Environmental Laboratory, Lockheed Martin Idaho Technologies Company, Idaho Falls, Idaho.

McCarthy, J. M., and D. L. McElroy, 1995, SDA Hydraulic Characterization Data Compilation: Surficial Sediments and Interbeds, Engineering Design File EDF ER-WAG7-71, INEL-95/130, Idaho National Engineering and Environmental Laboratory, Lockheed Martin Idaho Technologies Company, Idaho Falls, Idaho.

McCarthy, J. M., B. H. Becker, S. O. Magnuson, K. N. Keck, and T. K. Honeycutt, 2000, Radioactive Waste Management Complex Low-Level Waste Radiological Composite Analysis, INEEL/EXT-97-01113, Idaho National Engineering and Environmental Laboratory, Bechtel BWXT Idaho, LLC, Idaho Falls, Idaho.

McCarthy, J. M., R. C. Arnett, R. M. Neupauer, M. J. Rohe, and C. Smith, 1995, *Development of a Regional Groundwater Flow Model for the Area of the Idaho National Engineering Laboratory,* Eastern *Snake River Plain Aquifer*, INEL-95/0169, Rev. 1, Lockheed Martin Idaho Technologies Company.

McCarthy, J.F., and Degueldre, C., 1993, Sampling and characterization of colloids and particles in groundwater for studying their role in contaminant transport: Environmental Particles, v. 2, p. 247– 315.

McCarthy, J.F., and Zachara, J.M., 1989, Subsurface transport of contaminants: Environmental Science and Technology, v. 23, no. 5, p. 496–502.

McCarthy, J.F., Czerwinski, K.R., Sanford, W.E., Jardine, P.M., and Marsh, J.D., 1998a, Mobilization of transuranic radionuclides from disposal trenches by natural organic matter: Journal of Contaminant Hydrology, v. 30, p. 49–77.

McCarthy, J.F., Sanford, W.E., and Stafford, P.L., 1998b, Lanthanide field tracers demonstrate enhanced transport of transuranic radionuclides by natural organic matter: Environmental Science and Technology, v. 32, p. 3,901–3,906.

McCarthy, J.M., and McElroy, D.L., 1995, SDA hydraulic characterization data compilation—surficial sediments and interbeds: Lockheed Martin Idaho Technologies Company, Engineering Design File ER–WAG7–71, INEL–95/130.

McCarthy, J.M., Arnett, R.C., Neupauer, R.M., Rohe, M.J., and Smith, C., 1995, Development of a regional groundwater flow model for the area of the Idaho National Engineering Laboratory, Eastern Snake River Plain Aquifer: Lockheed Martin Idaho Technologies Company, INEL–95/0169, rev 1.

McClellan, Y., I. del C. Figueroa, and J. J. King, 1991, Preliminary Risk Evaluation for Pit 9, EGG-WM-9938, Rev. 0, Idaho National Engineering and Environmental Laboratory, EG&G Idaho, Idaho Falls, Idaho.

McDaniel, Paul A., 1991, Interpretation of Soil Properties at the RWMC and Spreading Area Sites, INEL, Idaho, Soil Science Division, University of Idaho, Moscow, Idaho.

McElroy, D. L. and J. M. Hubbell, 1990, Hydrologic and Physical Properties of Sediments at the Radioactive Waste Management Complex, EGG-BG-9147, EG&G Idaho, Inc., Idaho Falls, ID.

McElroy, D. L., 1990, Vadose Zone Monitoring at the Radioactive Waste Management Complex at the Idaho National Engineering Laboratory 1985-1989, EGG-WM-9299, EG&G Idaho Falls, Inc., Idaho Falls, ID.

McElroy, D. L., 1993, FY-1993 Soil Moisture Monitoring Results at the Radioactive Waste Management Complex of the Idaho National Engineering Laboratory, EGG-WM-11066, EG&G Idaho, Inc., Idaho Falls, ID.

McElroy, D. L., 1996, Subsurface Disposal Area Perched Water Level Data Compilation, Engineering Design File EDF INEL-96-226, Idaho National Engineering and Environmental Laboratory, Lockheed Martin Idaho Technologies Company, Idaho Falls, Idaho.

McElroy, D. L., and J. M. Hubbell, 1989, Vadose Zone Monitoring at the Radioactive Waste Management Complex of the Idaho National Engineering Laboratory in Focus 89 Nuclear Waste Isolation in the Unsaturated Zone, Las Vegas, September.

McElroy, D. L., and J. M. Hubbell, 2001, *Radioactive Waste Management Complex Tensiometer Status as of November 2000*, INEEL/EXT-01-01624, National Engineering and Environmental Laboratory, Bechtel BWXT Idaho, LLC, Idaho Falls, Idaho.

McElroy, D.L, Rawson, S.A., Hubbell, J.M., Minkin, S.C., Baca, R.G., Vigil, M.J., Bonzon, C.J., Landon, J.L., Laney, P.T., Pittman, J.R., Anderson, S.R., and Davis, L.C., 1989, Site characterization program at the Radioactive Waste Management Complex of the Idaho National Engineering Laboratory: Annual Progress Report, FY-1988 (draft), EG&G Idaho, Inc.

McKinley, K. B, and K. D. McKinney, 1978a, Initial Drum Retrieval Final Report, TREE-1286, August, Idaho National Engineering and Environmental Laboratory, EG&G Idaho, Idaho Falls, Idaho.

McKinley, K. B. and K. D. McKinney, 1978b, Early Waste Retrieval Interim Report, TREE-1265, Idaho National Engineering and Environmental Laboratory, EG&G Idaho, Idaho Falls, Idaho.

Miller, E. C., and J. D. Navratil, 1998, *Estimate of Carbon* Tetrachloride *in 743 Series Sludges Buried in the Subsurface Disposal Area at the Radioactive Waste Management Complex*, INEEL/EXT-98-00112, Rev. 0, Idaho National Engineering and Environmental Laboratory, Lockheed Martin Idaho Technologies Company, Idaho Falls, Idaho.

Miller, Eric C., and Mark D. Varvel, 2001, Reconstructing Past Disposal of 743 Series Waste in the Subsurface Disposal Area for Operable Unit 7-08, Organic Contamination in the Vadose Zone, INEEL/EXT-01-00034, Rev. 0, Idaho National Engineering and Environmental Laboratory, Bechtel BWXT Idaho, LLC, Idaho Falls, Idaho.

Nace, R.L., Deutsch, Morris, and Voegeli, P.T., 1956, Geography, geology, and water resources of the National Reactor Testing Station, Idaho, part 2, geography and geology: U.S. Atomic Energy Commission Publication IDO–22033.

Nagata, P. K., and J. Banaee, 1996, Estimation of the Underground Corrosion Rates for Low-Carbon Steels: Types 304 and 316 Stainless Steels; and Inconel 600, 601, and 718 Alloys at the Radioactive Waste Management Complex, INEL096/098, Idaho National Engineering and Environmental Laboratory, Lockheed Martin Idaho Technologies Company, Idaho Falls, Idaho.

Nagata, P. K., Interdepartmental Communication to T. H. Smith, “Letter Report on Tritium Release from Buried Beryllium Reflectors,” Idaho National Engineering and Environmental Laboratory, EG&G Idaho, Idaho Falls, Idaho, December 22, 1993.

Navratil, J., 1996, Evaluation of plutonium data: interoffice memo of May 24, 1996 to Doug Jorgenson: Lockheed Martin Idaho Technologies Company.

Neupauer, R. M., 1995, SDA Lithology and Perched Water Data Compilation, Engineering Design File ER-WAG7-69, INEL-95/127, Idaho National Engineering and Environmental Laboratory, Lockheed Martin Idaho Technologies Company, Idaho Falls, Idaho.

Newman, M. E. and F. M. Dunnivant, 1995, Results from the Large-Scale Infiltration Test: Transport of Radionuclide Tracers, EDF-ER-WAG7-77, INEL-95/146, Lockheed Martin Idaho Technologies, Idaho Falls, ID.

Newman, M. E. I. Porro, R. Scott, F. M. Dunnivant, R. W. Goff, M. D. Blevins, S. M. Ince, J. D. Leyba, T. A DeVol, A. W. Elzerman, and R. A Fjeld, 1995, *Evaluation of the Mobility of Am, Cs, Co, Pu, Sr, and U through INEL Basalt and Interbed Materials: Summary Report of the INEL/Clemson University Laboratory Studies*, Engineering Deign File, ER-WAG7-82, INEL-95/282.

Newman, M.E., I. Porro, R. Scott, F.M. Dunnivant, R.W. Goff, M.D. Blevins, S.M. Ince, J.D. Leyba, T.A. DeVol, A.W. Elzerman, and R.A. Fjeld (1996). Evaluation of the mobility of Am, Cs, Co, Pu, Sr, and U through INEL basalt and interbed materials: Summary report of the INEL/Clemson University Laboratory Studies, WAG7-82, INEL-95/282, September 19.

Nimmo, J. R., K. S. Perkins, P. A. Rose, J. P. Rousseau, B. R. Orr, B. V. Twining, and S. R. Anderson, 2002, "Rapid Transport of Naphthalene Sulfonate Tracer in the Unsaturated and Saturated Zones near the Big Lost River Flood-Control Areas at the Idaho National Engineering and Environmental Laboratory," Submitted to the *Vadose Zone Journal*.

Nimmo, R.R., K.S. Perkins, P.E. Rose, J.P. Rousseau, B.R. Orr, B.V. Twining, and S.R. Anderson, 2002, "Kilometer-Scale Rapid Transport of Naphthalene Sulfonate Tracer in the Unsaturated Zone at the Idaho National Engineering and Environmental Laboratory," *Vadose Zone Journal 1:59-109.*

Nimmo, J.R., 1999, Laboratory and field hydrologic characterization of the shallow subsurface at an Idaho National Engineering and Environmental Laboratory waste-disposal site.

Nimmo, J.R., Perkins, K.S., Rose, P.A., Rousseau, J.P., Orr, B.R., Twining, B.V., and Anderson, S.R., 2002, Rapid transport of naphthalene sulfonate tracer in the unsaturated and saturated zones near the Big Lost River flood-control areas at the Idaho National Engineering and Environmental Laboratory: submitted to Vadose Zone Journal (approval pending).

Nimmo, J.R., Perkins, K.S., Rose, P.A., Rousseau, J.P., Orr, B.R., Twining, B.V., and Anderson, S.R., 2001, Kilometer-scale rapid flow in a fractured-basalt unsaturated zone at the Idaho National Engineering and Environmental Laboratory, In: Kueper, B.H., Novakowski, K.S., and Reynolds, D.A., eds., Fractured Rock 2001 Conference Proceedings, March 26-28, 2001, Toronto.

Nimmo, J.R., Shakofsky, S.M., Kaminsky, J.F., and Lords, G.S., 1999, Laboratory and field hydrologic characterization of the shallow subsurface at an Idaho National Engineering and Environmental Laboratory waste-disposal site: U.S. Geological Survey Water-Resources

Investigations Report
99–4263 (DOE/ID-22163).

Nimmo, R.R., Shakofsky, S.M., Kaminsky, J.F., Lords, G.S., 2000, Laboratory and field hydrologic characterization of the shallow subsurface at an Idaho National Engineering and Environmental Laboratory waste-disposal site: U.S. Geological Survey Water-Resources Investigations Report 99-4263 (DOE/ID-22163).

Olmsted, F.H., 1962, Chemical and physical character of ground water in the National Reactor Testing Station, Idaho: U.S. Atomic Energy Commission Publication IDO–22043.

Orr, B. R., L. D. Cecil, and L. L. Knobel, 1991, Background Concentrations of Selected Radionuclides, Organic Compounds, and Chemical Constituents in Ground Water in the Vicinity of the Idaho National Engineering laboratory, DOE/ID-22094, U.S. Department of Energy Idaho Operations Office.

Pace, B. Ringe, 1999, Well Drilling and Sampling at the Radioactive Waste Management Complex, INEEL Cultural Resource Management Office Internal Report No. 99-31, Idaho National Engineering and Environmental Laboratory, Lockheed Martin Idaho Technologies Company, Idaho Falls, Idaho.

Pace, M.N., Rosentreter, J.J., and Bartholomay, R.C., 1999, Strontium distribution coefficients of selected core samples from the Idaho National Engineering and Environmental Laboratory, Idaho: U.S. Geological Survey Water-Resources Investigations Report 99–4145.

Payne, T.E., Edis, R., and Seo, T., 1992, Radionuclide transport by groundwater colloids at the Koongarra uranium deposit: Proceedings of Material Resource Society Symposium, v. 257, p. 481–488.

Perkins, K.S., 2000, Hydrological and Meteorological Data for an Unsaturated Zone Study Near the Radioactive Waste Management Complex, Idaho National Engineering Laboratory, Idaho 1997-1999, U.S. Geological Survey Open File Report 00-248, (DOE/ID-22171).

Perkins, K.S., J.R. Nimmo, 2000, Measurement of hydraulic properties of the B-C interbed and their influence on contaminant transport in the unsaturated zone at the Idaho National Engineering and Environmental Laboratory, Idaho: U.S. Geological Survey Water-Resources Investigation Report 00-4073, (DOE/ID-22170), April.

Perkins, K.S., J.R. Nimmo, J.R. Pittman, 1998, Hydrological and Meteorological Data for an Unsaturated Zone Study Near the Radioactive Waste Management Complex, Idaho National Engineering Laboratory, Idaho 1990-1996, U.S. Geological Survey Open File Report 98-9, (DOE/ID-22154).

Pfeifer, M. C. and H. T. Andersen, 1995, Report on the Electrical Resistivity Monitoring During the Aquifer Pumping and Infiltration Test, INEL-95/010, Rev. 0, Lockheed Martin Idaho Technologies, Idaho Falls, ID.

Pittman, J.R., 1989, Hydrological and Meteorological data for an Unsaturated Zone Study near the Radioactive Waste Management Complex of the Idaho National Engineering Laboratory, Idaho 1985-1986, U.S. Geological Survey Open File Report 89-74, (DOE/ID-22079), April.

Pittman, J.R., 1995, Hydrological and Meteorological Data for an Unsaturated Zone Study Near the Radioactive Waste Management Complex, Idaho National Engineering Laboratory, Idaho 1988 and 1989, U.S. Geological Survey Open File Report 95-112, (DOE/ID-22118), January.

Pittman, J.R., Jensen, R.G., and Fischer, P.R., 1988, Hydraulic conditions at the Idaho National Engineering Laboratory, 1982 to 1985: U.S. Geological Survey Water-Resources Investigations Report 89–4003 (DOE/ID–22078).

Porro, I. and C. W. Bishop, 1995, Large Scale Infiltration Test CPN Data Analysis, EDF-WAG7-58, INEL-94/040, Lockheed Martin Idaho Technologies, Idaho Falls, ID.

Porro, Indrek, 2000, Hydrologic Behavior of Two Engineered Barriers Following Extreme Wetting, INEEL/EXT-2000, 2000602, Idaho National Engineering and Environmental Laboratory, Bechtel BWXT Idaho, LLC, Idaho Falls, Idaho.

Ramsay, J.D.F., 1988, The role of colloids in the release of radionuclides from nuclear waste: Radiochemical Acta, v. 44/45, p. 165–170.

Rawson, S. A., 1989, "Preliminary Evaluation of Geochemical Controls on Radionuclide Migration at the Radioactive Waste Management Complex (RWMC)," Unpublished Report, Idaho National Engineering and Environmental Laboratory, EG&G Idaho, Idaho Falls, Idaho.

Rawson, S. A., J. C. Walton, and R. G. Baca, 1991, "Migration of Actinides from a Transuranic Waste Disposal Site in the Vadose Zone," Radiochemical Acta 52/53, pp. 477-486.

Rawson, S.A., and Hubbell, J.M., 1989, Geochemical controls on the composition of soil pore waters beneath a mixed waste disposal site in the unsaturated zone, *in* FOCUS'89, Nuclear waste isolation in the unsaturated zone: American Nuclear Society, Las Vegas, Nev., March 1989, Proceedings, p. 241–247.

Rawson, S.A., Walton, J.C., and Baca, R.G., 1991, Migration of actinides from a transuranic waste disposal site in the vadose zone: Radiochemical Acta, v. 53.

Reed, M. F., and Bartholomay, R.C., 1994, Mineralogy of selected sedimentary interbeds at or near the Idaho National Engineering Laboratory, Idaho: U.S. Geological Survey Open-File Report 94–374 (DOE/ID–22116).

Rightmire, C. T. and B. D. Lewis, 1987, Hydrogeology and Geochemistry of the Unsaturated Zone, Radioactive Waste Management Complex, Idaho National Engineering Laboratory, Idaho, U.S. Geological Survey Water-Resources Investigations Report 87-4198 (DOE/ID-22073), Idaho Falls, ID.

Rightmire, C. T., and Lewis, B. D., 1987a, Geologic Data collected and analytical procedures used during a geochemical investigation of the unsaturated zone, Radioactive Waste Management Complex, Idaho National Engineering Laboratory, Idaho: U.S. Geological Survey Open File Report 87-246 (DOE/ID-22072).

Rightmire, C.T., 1984, Description and hydrogeologic implications of cored sedimentary material from the 1975 drilling program at the Radioactive Waste Management Complex, Idaho: U.S. Geological Survey Water-Resources Investigations Report 84–4071 (IDO–22067).

Rightmire, C.T., and Lewis, B.D., 1987a, Geologic data collected and analytical procedures used during a geochemical investigation of the unsaturated zone, Radioactive Waste Management Complex, Idaho National Engineering Laboratory, Idaho: U.S. Geological Survey Open-File Report 87–246 (DOE/ ID–22072).

Rightmire, C.T., and Lewis, B.D., 1999, Influence of the geochemical environment on radionuclide migration in the unsaturated zone, radioactive waste management complex, Idaho National Engineering Laboratory, Idaho: U.S. Geological Survey, Open-File Report (in preparation).

Ritter, P. D., and D. L. McElroy, 1999, Progress Report: Tritium and Carbon-14 Sampling at the Radioactive Waste Management Complex, INEEL/EXT-98-00669, Idaho National Engineering Laboratory, Lockheed Martin Idaho Technologies Company, Idaho Falls, Idaho.

Roback R. C., Johnson T. M., McLing T. L., Murrell M. T., Luo, S. and Ku, T. L. (2001) Uranium isotopic evidence for groundwater chemical evolution and flow patterns in the eastern Snake River Plain Aquifer, Idaho, Geol. Soc. Amer. Bull., 113, 1133-1141

Roback, R. C., D. W. Efurd, M. T. Murrell, R. E. Steiner, and C. J. Duffy, 2000, Assessment of Uranium and Plutonium in the Saturated and Unsaturated Zones Beneath the Surface Disposal Area, INEEL, LA-UR-00-5471, Los Alamos National Laboratory, Los Alamos, NM.

Roback, R.C., Murrell, M.T., Nunn, A., Luo, S., Ku, T.L., and McLing, T., 1998, Uranium and thorium series isotopes in fresh groundwater at the INEEL: EOS Transactions, American Geophysical Union, v. 79(45), Fall Meeting Supplement, p. F343.

Roback, Robert C., Deward W. Efurd, Michael T. Murrell, Robert E. Steiner, and Clarence J. Duffy, 2000, *Assessment of Uranium and Plutonium in the Saturated and Unsaturated Zones Beneath the Surface Disposal Area, INEEL*, Rev. 0, Los Alamos National Laboratory, Los Alamos, New Mexico.

Robertson, J. B., 1974, Digital Modeling of Radioactive and Chemical Waste Transport in the Snake River Plain Aquifer at the National Reactor Testing Station, Idaho, IDO-22054, U.S. Geological Survey Open File Report, U.S. Geological Survey.

Robertson, J.B., Schoen, R., and Barraclough, J.T., 1974, The influence of liquid waste disposal on the geochemistry of water at the National Reactor Testing Station, Idaho: U.S. Geological Survey Open- File Report, IDO–22053.

Rood, A. S., 1994 GWSCREEN: A Semi-analytical Model for Assessment of the Groundwater Pathway from Surface or Buried Contamination, Rev 2, EGG-GEO-10797, Idaho National Engineering Laboratory, Idaho Falls, Idaho.

Rood, A. S., 1999, GWSCREEN: A Semi-Analytical Model for Assessment of the Groundwater Pathway from Surface or Buried Contamination, Theory and User's Manual Version 2.5, INEEL/EXT-9800750, Idaho National Engineering and Environmental Laboratory, Lockheed Martin Idaho Technology Company, Idaho Falls, Idaho.

Salomon, Hopi, 2001, Field Sampling Plan for Monitoring of Type B-Probes in Support of the Integrated Probing Project Operable Unit 7-13/14, INEEL/EXT-2000-01435, Rev. 0, Idaho National

Engineering and Environmental Laboratory, Bechtel BWXT Idaho, LLC, Idaho Falls, Idaho, June 2001.

Schakofsky, S., March 1995, Changes in Soil Hydraulic Properties Caused by Construction of a Simulated Waste Trench at the Idaho National Engineering Laboratory, Idaho, DOE/ID-22121, U.S. Geological Survey Water-Resources Investigations Report 95-4058, prepared in cooperation with the U.S. Department of Energy, Idaho Falls, Idaho.

Schmalz, B. L. 1972, Radionuclide Distribution in Soil Mantle of the Lithosphere as a Consequence of Waste Disposal at the National Reactor Testing Station, IDO-10049, Idaho Operations Office, U.S. Atomic Energy Commission, Idaho Falls, Idaho.

Schmalz, B. L., 1972, Radionuclide Distribution in Soil Mantle of the Lithosphere as a Consequence of Waste Disposal at the National Reactor Testing Station, IDO-10049, U.S. Atomic Energy Commission, Idaho Falls, Idaho.

Schmidt, C. E., 1993, *Results of Soil Flux Emission Rate Testing During* July 1993 at the RWMC, Operable Unit 7-08, Engineering Design File EDF-ER-VVED-121, Idaho National Engineering and Environmental Laboratory, EG&G Idaho, Idaho Falls, Idaho.

Seitz, Roger R., Karen N. Keck, and James M. McCarthy, 2001, Interim Closure Concept for the Low-Level Waste Disposal Facility at the Radioactive Waste Management Complex, INEEL/EXT-01-00178, Rev. 0, Idaho National Engineering and Environmental Laboratory, Bechtel BWXT Idaho, LLC, Idaho Falls, Idaho1.

Settle, S. R., 2000, "Waste Area Group 7, Operable Unit 7-13/14, Well Drilling Project at Radioactive Waste Management Complex, End of Well Reports," INEEL/EXT-2000-00400, Draft Rev. A, Idaho National Engineering and Environmental Laboratory, Bechtel BWXT Idaho, LLC, Idaho Falls, Idaho, August 2000.

Shakofsky, S. M., 1995, Changes in Soil Hydraulic Properties Caused by Construction of a Simulated Waste Trench at the Idaho National Engineering Laboratory Idaho, U.S. Geological Survey Water Resources Investigation Report 95-4058, DOE/ID-22121, U.S. Department of Energy Idaho Operations Office, Idaho Falls, Idaho.

Shakofsky, S.M., and Nimmo, J.R., 1996, Unsaturated zone properties at a waste disposal site at the Idaho National Engineering Laboratory, *in* Morganwalp, D.W., and Aronson, D.A., eds., U.S. Geological Survey Toxic Substances Hydrology Program—Proceedings of the Technical Meeting, Colorado Springs, Colorado, 1993: U.S. Geological Survey Water-Resources Investigations Report 94–4015.

Shook, G. M., 1995, Development of an Environmental Simulator from Existing Petroleum Technology, INEL-94/0283, Idaho National Engineering and Environmental Laboratory, Lockheed Martin Idaho Technologies Company, Idaho Falls, Idaho.

Sisson, J. B., and B. Faybishenko, 1995, Box Canyon Hot Air Injection Study and Vadose Zone Instrument Development Results, INEL-95/0597, Lockheed Idaho Technologies Company, Idaho Falls, Idaho.

Sisson, J. B., and G. C. Ellis, 1991, Summary Report of Results of the Vapor Vacuum Extraction Test at the RWMC, EGG-WM-9301, Rev. 1., Idaho National Engineering and Environmental Laboratory, EG&G Idaho, Idaho Falls, Idaho.

Sondrup, A. J., 1998, Preliminary Modeling of VOC Transport for Operable Unit 7-08, Evaluation of Increased Carbon Tetrachloride Inventory, INEEL/EXT-2000-00849, Rev. 0, Idaho National Engineering and Environmental Laboratory, Bechtel BWXT Idaho, LLC, Idaho Falls, Idaho.

Sondrup, A. J., W. C. Downs, J. R. Weidner, and T. G. Kaser, 1994, Vertical Air Permeability in the Unsaturated Zone at the Radioactive Waste Management Complex, Engineering Design File EDF ER-VVED-116, Idaho National Engineering and Environmental Laboratory, EG&G Idaho, Idaho Falls, Idaho.

Starr, R. C. and M. J. Rohe, 1995, Large-Scale Aquifer Stress Test and Infiltration Test: Water Management System Operation and Results, INEL-95/059, Lockheed Martin Idaho Technologies, Idaho Falls, ID.

Sullivan, T. M., 1992, Development of DUST: A Computer Code That Calculates Release Rates from LLW Disposal Unit, BNL-NUREG-47118, Brookhaven National Laboratory, U.S. Nuclear Regulatory Commission.

Sullivan, T. M., 1993, DUST Data Input Guide, NUREG/CR-6041, U.S. Nuclear Regulatory Commission.

Thompson, R. J., 1972, Solid Radioactive Waste Retrieval Test, ACI-120, Idaho National Engineering and Environmental Laboratory, Allied Chemical Corporation, Idaho Falls, Idaho, May 1972.

Tucker, B.J., and Orr, B.R., 1998, Distribution of selected radiochemical and chemical constituents in water from perched ground water, Idaho National Engineering Laboratory, Idaho, 1989–91: U.S. Geological Survey Water-Resources Investigations Report 98–4028 (DOE/ID–22144).

U.S. Geological Survey, 1998, Significant issues to be resolved to support and defend the Interim Risk Assessment and additional work required to resolve those issues—Task 5, Independent technical review of the Interim Risk Assessment Radioactive Waste Management Complex WAG 7–13/14 Operable Units: U.S. Geological Survey Letter Report.

U.S. Geological Survey, 1999, Review of the Transport of Selected Radionuclides in the Interim Risk Assessment for the Radioactive Waste Management Complex, Waste Area Group 7 Operable Unit 7-13/14, Idaho National Engineering and Environmental Laboratory, Idaho, Draft U.S. Geological Survey Administrative Report, Prepared for Idaho Operations Office U.S. Department of Energy under IAG DE-A107-97ID13556, Idaho Falls, Idaho.

U.S. National Academy of Science, 1966, Report to the U.S. Atomic Energy Commission by the Committee on Geologic Aspects of Radioactive Waste Disposal of the Division of Earth Sciences, Washington, D.C.

Van Genuchten, M. T., 1980, “A closed-Form Equation for Predicting the Hydraulic Conductivity of Unsaturated Soils,” Solo Science society of America Journal, Vol. 44 pp. 892-898

Varvel, Mark D., 2001, *Mass Estimates of Organic Compounds Buried in the Subsurface Disposal Area for Operable Unit 7-08 and 7-13/14*, INEEL/EXT-01-00277, Engineering Design File EDF-ER-301, Rev. 0, Idaho National Engineering and Environmental Laboratory, Bechtel BWXT Idaho, LLC, Idaho Falls, Idaho.

Vigil, M. J., 1988a, Initial Estimate of Hazardous Waste Constituents in Pit 9, Engineering Design File EDF-BWP-02, Idaho National Engineering and Environmental Laboratory, EG&G Idaho, Idaho Falls, Idaho.

Vigil, M. J., 1988b, Estimate of Water in Pits During Flooding Events, Engineering Design File EDF-BWP-12, Idaho National Engineering and Environmental Laboratory, EG&G Idaho, Idaho Falls, Idaho.

Vigil, M.J., 1989, Subsurface Disposal Area Waste Identification, 1952 –1970 emphasis. EGG-EM-8727, Rev. 1, October.

Voegeli, P.T. and Deutsch, M. 1953, Geology, Water Supply, and Waste Disposal at Sites 11 and 11A, Burial Ground and Vicinity, National Reactor Testing Station, Idaho: IDO-22027-USGS, issued by U.S. Atomic Energy Commission, Idaho Operations Office.

Voegeli, P.T., and D. Morris, 1953, Geology Water Supply, and Waste Disposal at Sites 11 and 11A, Burial Ground D, and Vicinity, National Reactor Testing Station, Idaho: IDO-22027-USGS, U.S. Atomic Energy Commission, Idaho Operations Office.

Weidner, J. R., A. J. Sondrup, T. G. Kaser, and W. C. Downs, 1992, Vapor Port Permeability, Engineering Design File EDF ER-VVED-101, Idaho National Engineering and Environmental Laboratory, EG&G Idaho, Idaho Falls, Idaho.

Welhan, J.A., and Wylie, A., 1997, Stochastic modeling of hydraulic conductivity in the Snake River Plain aquifer—evaluation of lithologic controls at the core and borehole scales: Symposium on Engineering Geology and Geotechnical Engineering, 32d, Boise, Idaho, March 26–28, 1997, Proceedings.

Whitaker, Cheryl A., 2002, "Analysis of Facilities Within the Waste Area Group 7 Cumulative Impact Region (Draft)," INEEL/EXT-01-00027, Rev. A, Idaho National Engineering and Environmental Laboratory, Bechtel BWXT, Idaho Falls, Idaho.

Whitmire, D. L., 2001, Summary Report: Simulation of Groundwater Flow near the Subsurface Disposal Area at the Idaho National Engineering and Environmental Laboratory, INEEL/EXT-01-01643, Rev. 0, North Wind Environmental, Idaho National Engineering and Environmental Laboratory, Bechtel BWXT Idaho, LLC, Idaho Falls, Idaho.

Wood, T. R. and G. T. Norell, 1996, Integrated Large-Scale Aquifer Pumping and Infiltration Tests, INEL-96/0256, Idaho National Engineering Laboratory, Idaho Falls, Idaho.

Wood, T. R., and A. H. Wylie, 1991, Ground Water Characterization Plan for the Subsurface Disposal Area, EGG-WM-9668, Rev. 0, Idaho National Engineering and Environmental Laboratory, EG&G Idaho, Idaho Falls, Idaho.

Wood, T. R., and G. T. Norrell, 1996, Integrated Large-Scale Aquifer Pumping and Infiltration Tests, Groundwater Pathways OU 7-06, Summary Report, INEL-96/0256, Rev. 0, Idaho National Engineering and Environmental Laboratory, Lockheed Martin Idaho Technologies Company, Idaho Falls, Idaho.

Wood, T. R., D. Bates, C. W. Bishop, G. L. Heath, L. C. Hull, R. M. Lehman. S. O. Magnuson, E. D. Mattson, J. M. McCarthy, I. Porro, P. D. Ritter, M. Roddy, J. B. Sisson, R. P. Smith, 2000, Deficiencies in Vadose Zone Understanding at the Idaho National Engineering and Environmental Laboratory, INEEL/ EXT-99-00984, Idaho National Engineering and Environmental Laboratory, Bechtel BWXT Idaho, LLC, Idaho Falls, Idaho.

Wood, T. R., D. Bates, C. W. Bishop, G. L. Heath, L. C. Hull, R. M. Lehman. S. O. Magnuson, E. D. Mattson, J. M. McCarthy, I. Porro, P. D. Ritter, M. Roddy, J. B. Sisson, R. P. Smith, August 2000, *Deficiencies in Vadose Zone Understanding at the Idaho National Engineering and Environmental Laboratory*, INEEL/ EXT-99-00984, Idaho National Engineering and Environmental Laboratory, Bechtel BWXT Idaho, LLC, Idaho Falls, Idaho.

Wood, T. R., December 1989, Preliminary Assessment of the Hydrogeology at the Radioactive Waste Management Complex, EGG-WM-8694, Idaho National Engineering and Environmental Laboratory, EG&G Idaho, Idaho Falls, Idaho.

Wood, T.R., and Norrell, G.T., 1996, Integrated large-scale aquifer pumping and infiltration tests, groundwater pathways: Summary report, INEL–96/0256.

Wood, W.W., and Low, W.H., 1986, Aqueous geochemistry and diagenesis in the Eastern Snake River Plain aquifer system, Idaho: Geologic Society of America Bulletin**,** v. 97.

Wylie, A. H., 1996, Borehole Deviation Survey Results of Radioactive Waste Management Complex Ground Water Wells, DRAFT, Engineering Design File INEL-96/155, Lockheed Idaho Technologies Company, Idaho Falls, ID.

Wylie, A. H., 1996, Pumping Test of Pit 9 Production Well, Engineering Design File INEL-96/171, Lockheed Idaho Technologies Company, Idaho Falls, ID.

Wylie, A. H., and J. M. Hubbell, 1994, Aquifer testing of wells M1S, M3S, M4D, M6S, M7S, and M10S at the Radioactive Waste Management Complex, Engineering Design File ER-WAG7-26, Rev. 1, EG&G Idaho Inc., Idaho Falls, ID.

Wylie, A. H., E. Neher, J. M. McCarthy, and B. D. Higgs, February 1995, Large-Scale Aquifer Pumping Test Results, Engineering Design File EDF ER-WAG7-56, Idaho National Engineering and Environmental Laboratory, Lockheed Martin Idaho Technologies Company, Idaho Falls, Idaho.

# 3.8 Waste Area Group 8

WAG 8 is the designation for the collection of CERCLA OUs associated with the NRF. Section 3.8 does not include new geohydrologic interpretations but summarizes elements of the present WAG-8 conceptual model of groundwater flow and contaminant transport as described in the NRF comprehensive Remedial Investigation (Westinghouse Electric Corporation 1996).

Section 3.8.1 presents the historical background of WAG 8 and includes a summary of previous investigations and sources of WAG 8 hydrologic information. The conceptual model is discussed in general terms in Section 3.8.2, followed by detailed discussions of hydrologic information and factors affecting contaminant transport. A history of the numerical models developed for WAG 8 is presented in Section 3.8.3. Finally, a brief discussion of CSM competing hypotheses and data requirements is presented in Section 3.8.4.

## 3.8.1 Background

The NRF was established in 1949 as a prototype site for the Naval Nuclear Propulsion Program. The NRF is operated by Bechtel Bettis, Inc., under contract with and direct supervision of the Naval Nuclear Propulsion Program. The NRF is located in the west-central part of the INEEL (see Figure 3-34) and covers an area of approximately 80 developed acres of the eastern Snake River Plain. At various times, the NRF has been occupied by up to 3,300 people.

Three operating naval nuclear reactor prototype plants, the Submarine Thermal Reactor Prototype (SlW), Large Ship Reactor Prototype (AlW), and Submarine Reactor Plant Prototype (S5G), were constructed and operated at NRF during 1953 through 1995. S1W began operation in 1953 and continued until 1989 when it was permanently shut down. A1W began operation in 1958 and continued until it was permanently shut down in January 1994. S5G began operation in 1965 and was permanently shut down in May 1995. Additionally, the Expended Core Facility (ECF) was constructed in 1958 (Westinghouse Electric Corporation 1996) to test and inspect expended naval nuclear fuel cores and to perform material examinations.

Six major geotechnical investigations were conducted after 1950, as noted in the 1996 Comprehensive RI/FS (Westinghouse Electric Corporation 1996). These investigations consisted of geotechnical investigations conducted during 1961 through 1963, the 1987 through 1988 Phase I Closure Plan sample collection report, the 1988 Knolls Atomic Power Laboratory (KAPL) Report, the 1991 Well Construction and Hydrogeologic Investigation Project, the 1993 RI/FS of the Industrial Waste Ditch, the 1995 Well Construction Hydrogeologic Investigation Project, and the 1996 Comprehensive RI/FS. Numerous minor studies were also conducted at NRF since 1950 that provided valuable geohydrologic information.

***3.8.1.1 Geotechnical Investigations Conducted During 1961-1963.*** Data collected from drilling and investigative programs during 1961 through 1963 identified two perched groundwater bodies beneath the A1W and S1W leaching beds. This study also defined the configuration of the underlying basalt surface. This information was used to evaluate contaminant migration from the leaching beds.

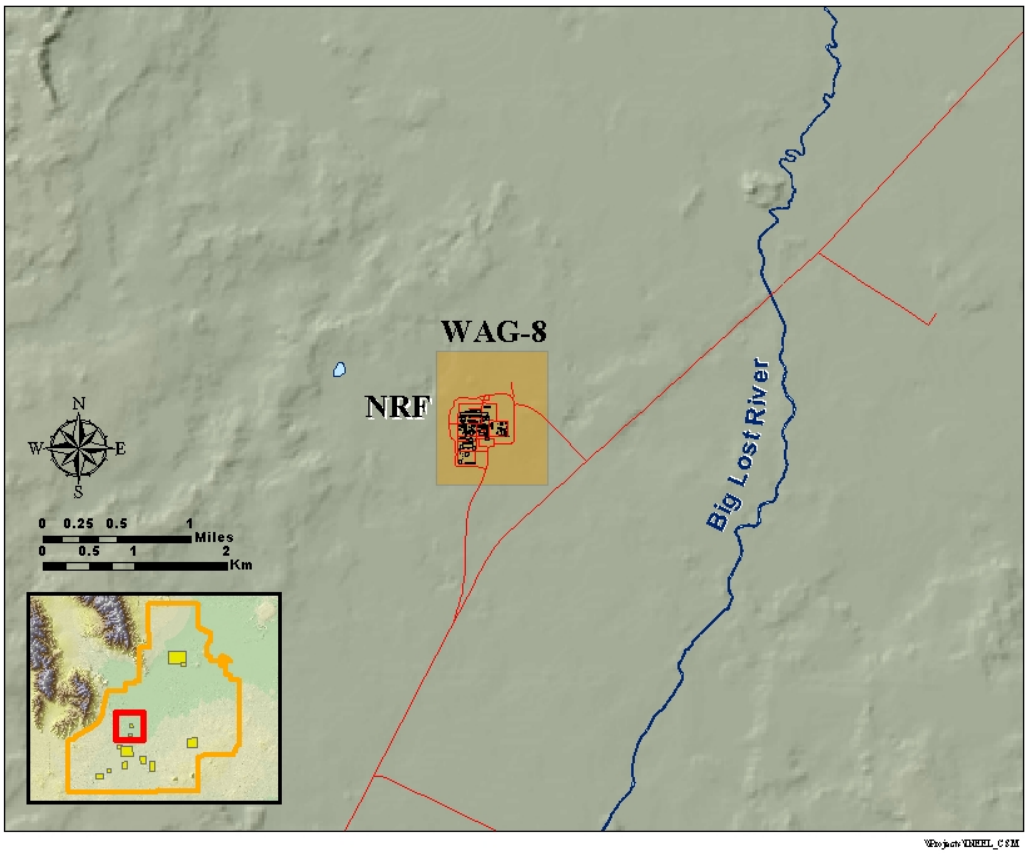


Figure 3-34. The WAG 8 site (NRF) is located in the west central part of the INEEL.

***3.8.1.2 1987-1988 Phase I Closure Plan Sample Collection Report.*** A detailed sampling program was conducted in 1987 to comprehensively evaluate the distribution of contaminants in sediments and rocks adjacent to the industrial waste ditch. Data collected during this investigative program included soil-sample data, contaminant data, and geophysical data.

***3.8.1.3 1988 KAPL Report.*** A 1988 geotechnical investigation was conducted for the KAPL. This investigation characterized engineering and seismic properties of materials near NRF.

***3.8.1.4 1991 Well Construction and Hydrogeologic Investigation Project.*** Hydrologic investigations were conducted in 1991 to collect additional information about stratigraphy, hydraulic properties, occurrence of water, and groundwater chemistry at NRF. This work included drilling of 3 aquifer wells, 15 shallow boreholes, and 7 piezometer wells. Work also included analyses on geologic and water samples, mineral identification, collection of geophysical data, and determination of aquifer properties.

***3.8.1.5 1993 RI/FS of the Industrial Waste Ditch.*** Work performed at the industrial waste ditch included collection of surface and subsurface samples, metal and organic constituent analyses, and other hydrogeologic data. Several boreholes, swells, and piezometers were installed.

***3.8.1.6 1995 Well Construction Hydrogeologic Investigation Project.*** Six wells were drilled and constructed in 1995 as part of the Remedial Design and Remedial Action (RD/RA) work for the NRF landfills. This work provided soil and interbed samples and aquifer test data,

***3.8.1.7 1996 Comprehensive Remedial Investigation/Feasibility Study.*** The NRF Comprehensive RI/FS addresses the 68 potentially contaminated sites at NRF and 13 additional potential release sites. The RI/FS addresses the cumulative risk associated with all 81 of these sites. Fifteen of the 81 sites had not been evaluated prior to the start of the NRF Comprehensive Remedial Investigation. Additionally, one previously evaluated site (Unit 8 03-23, Sewage Lagoons) was determined to require additional evaluation during the NRF Comprehensive Remedial Investigation.

The NRF Comprehensive Remedial Investigation consisted of four primary tasks. The first task required individual site investigations to be conducted for previously unevaluated sites. The investigations are to include the review of existing data, the collection of additional field data, if necessary, and a determination of the potential risk associated with each site. The second task required a hydrogeologic study to be performed to assess the potential of a groundwater pathway from NRF sources. The third task required a cumulative risk assessment to be conducted that provides an assessment of the combined affects to human health. The information obtained from the individual site evaluations and the hydrogeologic study is to be used to help complete the cumulative risk assessment. The fourth task required an ecological risk assessment to be performed to evaluate the overall potential risk to ecological receptors.

## 3.8.2 Summary of the Present WAG-8 Conceptual Site Model

The NRF Comprehensive Remedial Investigation Report (Westinghouse Electric Corporation 1996) describes the geohydrologic conditions in the vicinity of NRF. The basalts and sediments of the vadose zone and SRPA at NRF are capable of transporting locally discharged wastewater and contaminants. In general, groundwater flow in the area probably is slow and contaminants do not move rapidly through the system. Conceptual model elements are described in subsequent sections.

***3.8.2.1 Geologic Framework.*** The geologic framework of the eastern Snake River Plain underlying NRF controls groundwater flow and contaminant transport. The following sections describe the current understanding of the system geometry and geology at NRF.

***System Geometry—***The area within the NRF security fence encompasses about 80 acres. The area extends east to west approximately 2,100 ft along the northern side and north to south approximately 2,000 ft.

The Industrial Waste Ditch extends about 2 mi north-northeast from NRF. Monitoring wells in proximity to NRF enclose an area 1 × 2/3 mi. Upgradient wells are located up to 4 mi north and downgradient wells are located about 2 mi to south. The closest hydrologic feature is the Big Lost River, located about 1-½ mi to the east.

Depth to the top of the aquifer at NRF is approximately 370 ft bls (Westinghouse Electric Corporation 1996). The INEL-1 deep corehole was drilled in 1979 about 3 mi south of NRF (Westinghouse Electric Corporation 1996). This corehole penetrated about 2,200 ft of layered basalt flows overlying a very thick rhyolitic unit. The NRF conceptual model assumes that most flow takes place in the upper 250 ft of the layered basalts (Westinghouse Electric Corporation 1996).

***Geology—***The geology of the NRF area includes geomorphologic, structural, and stratigraphic features. These features define the geologic framework of the SRPA near NRF.

The NRF is located on a fluvial plain attributed to deposition of the Big Lost River (Westinghouse Electric Corporation 1996) approximately 1.5 mi from the river channel. The fluvial plain dips gently to the north and ranges in elevation from 4,870 ft above sea level south of NRF to 4,830 ft above sea level to the north of NRF. The plain is characterized by numerous, abandoned meander channels that range from hardly noticeable depressions to channels that exceed 6 ft in depth.

The relatively flat fluvial plain surrounding NRF is bordered to the east by basalt outcrops. These outcrops rise approximately 30 ft above the plain. An arcuate basalt ridge is located to the northwest of NRF. Low-lying, weathered basalt flows rising as much as 30 ft above the plain are located approximately 0.5 mi west of NRF.

Basalt outcrops to the east infer a possible north-trending vent corridor. An arcuate ridge to northwest of NRF infers the presence of a series of eruptive vents (Westinghouse Electric Corporation 1996). This series may intersect the industrial waste ditch. The northwest-trending Lava Ridge Volcanic Rift Zone lies approximately 7 mi northeast of NRF (Anderson and Bowers 1995). The axial volcanic zone lies approximately 12 mi east of NRF.

Surficial sediments at NRF consist of wind-blown loess and fluvial deposits. Surficial loess ranges in thickness from several inches to 10 ft and consists predominantly of montmorillinite clay. The loess deposits are underlain by sand and gravel deposits of the fluvial meander plain. These deposits include interbedded sand, gravel, silt, and clay that exceed 60 ft in thickness in places (Westinghouse Electric Corporation 1996). The deposits indicate that the climate of deposition was wetter than today. The sand and gravel deposits at NRF are underlain by a thin clay unit over basalt or widespread fluvial/lacustrian clay and silt deposits in places where the altitude of the top of basalt is less than 4,825 ft above sea level (Westinghouse Electric Corporation 1996). These deposits consist largely of silty clay with fine sand and some gravel.

Approximately 1,500 to 2,000 ft of olivine basalts underlies the surficial sediments at NRF. Individual basalt flows typically range in thickness from 5 to more than 70 ft and are fractured to massive. Fractures were derived from cooling processes; some flows are fractured from top to bottom other flows are devoid of fractures. Commonly, fractures are concentrated at the tops of flows.

Basalt flows underlying NRF commonly are separated by sedimentary interbeds (Westinghouse Electric Corporation 1996). Four locally extensive interbeds have been identified. The uppermost interbed has been penetrated at depths from 70 to 120 ft and ranges in thickness from less than 1 ft to more than 14 ft. It is believed that the top of this unit is baked at the top, but the deeper section is unconsolidated. Three other continuous interbeds were penetrated at 205, 267, and 370 ft in well NRF-9.

***3.8.2.2 Matrix Characteristics.*** Aquifer test data from 13 tests in 11 NRF wells were used to estimate transmissivity of the basalt aquifer at NRF (Westinghouse Electric Corporation 1996). Transmissivity estimates from those tests range from 3.1 to 576,000 $ft^2$/day, similar to other estimates at the INEEL. Hydraulic conductivity is estimated to range from 1.34 to about 256,000 ft/day. No estimate of the storage coefficient of the basalt aquifer at NRF is available.

***3.8.2.3 Recharge/Discharge Sources.*** Several sources of water are available for recharge to the SRPA at NRF. These sources include precipitation, episodic recharge from the Big Lost River, and wastewater disposal. Discharge takes place from production well pumpage.

Snowmelt in the spring is considered to be the most significant contributor to recharge from precipitation at NRF. Although runoff sufficient to provide for substantial recharge could occur in response to large rainfall events, these events rarely take place (Westinghouse Electric Corporation 1996)

The NRF is about 1.5 mi west of the Big Lost River. Episodic recharge near NRF has been observed in response to large flows in the River. Recharge to the aquifer from high flows during 1982 through 1985 temporarily modified the local direction of groundwater flows (Westinghouse Electric Corporation 1996).

The Industrial Waste Ditch (IWD) has been used for more than 30 years to dispose of nonradioactive, non-sewage, industrial, and storm-water discharge. The IWD occupies parts of two meander channels. The IWD is about 3.2 mi long, but water presently flows in the first 0.5 to 1.2 mi. Prior to shutdown of the S1W, A1W, and S5G plants, water flowed through the entire reach of the ditch. Present discharges range from 50 to 150 gal per minute for an annual discharge of about 53 million gal (Westinghouse Electric Corporation 1996). An estimated 2.1 million gal of water evaporates annually from the ditch.

Two sewage lagoons are located directly northeast of NRF. These infiltration lagoons have been used to dispose of an estimated 10 to 23 million gal per year (Westinghouse Electric Corporation 1996). Four production wells supply the water needs at NRF. During 1991 to 1996, pumpage ranged from 82,562,000 to 293,511,000 gal per year. Much of this water returns to the aquifer through the IWD and sewage lagoons.

***3.8.2.4 Hydraulics.*** The distribution of water in the vadose zone and in the SRPA is controlled by the integration of hydrologic features at NRF, including geologic framework, matrix characteristics, and inflows and outflows to the area.

***Perched Groundwater—***Perched groundwater bodies at NRF have formed in the vadose zone in response to disposal of wastewater to the subsurface. These bodies are a part of the pathway for water and contaminants to move to the SRPA across the water-table boundary. Perched water has been observed beneath the A1W leaching beds, S1W leaching beds and leaching pit, the sewage lagoons, the S5G Test and S5G Deep wells, and the industrial waste ditch (Westinghouse Electric Corporation 1996).

Perched-water bodies associated with the sewage lagoons and the A1W and S1W leaching beds principally occur at the top of the basalt surface (Westinghouse Electric Corporation 1996). The perching mechanism appears to be fine sediment filling fractures in basalt. These perched-water bodies cease to exist upon cessation of discharge, although deeper perched-water body beneath the leaching beds was observed in one well. The distribution of water in this body is unknown, but the water body is estimated to have a radius of about 500 to 600 ft.

Perched water associated with the industrial waste ditch occurs at a range of depths (i.e., from 20 to 200 ft). Perched-water bodies contained insufficient water to complete wells for long-term monitoring.

In general, the distribution of perched water bodies is transitory and dependent on significant sources of wastewater discharge. Water in these zones may move laterally and some commingling of water from different sources may occur (Westinghouse Electric Corporation 1996). Lateral flow from the industrial waste ditch may be focused into a small area, increasing recharge to the aquifer in that area, and possibly mounding water in the aquifer (Westinghouse Electric Corporation 1996).

***SRPA—***Groundwater underflow at the NRF principally originates from three sources (Westinghouse Electric Corporation 1996). These sources include recharge from the Little Lost River to the north, the

Big Lost River to the east; and regional flow from Birch Creek, the Upper Snake River Plain, and the Yellowstone Plateau. Water-level data from wells near NRF indicate that the local direction of groundwater flow depends on the relative magnitude of recharge from these three different sources. In the early 1980's, when the Big Lost River flowed extensively, the groundwater flow direction was to the southwest. The extended drought during the late 1980's and early 1990's resulted in a local shift to the southeast. Presently, the hydraulic gradient is slightly more than 1 ft/mi at NRF. The small gradient infers that water moves very slowly in the aquifer beneath NRF. Local mounding is believed to occur in response to recharge from the industrial waste ditch and sewage lagoon.

***3.8.2.5 Groundwater Chemistry.*** The background chemistry of groundwater at NRF generally is similar to water chemistry elsewhere on the INEEL. Olmsted (1962) noted that groundwater derived from mountainous carbonate drainages to the west is enriched in calcium, magnesium, and bicarbonate (Busenberg et al. 2001). A second water composition, derived from the area northeast of the INEEL, is characterized by increased occurrence of rhyolitic and andesitic rocks and is enriched in calcium, magnesium, and bicarbonate but with a larger equivalent fraction of sodium, potassium, fluoride, silica, and chloride. Minor changes in groundwater chemistry at NRF may be attributed to the temporal changes in flow direction and water source.

***3.8.2.6 Contaminant Transport.*** The transport of contaminants in the subsurface at NRF is controlled by the source term and transport mechanism. The distribution of contaminants in the vadose zone and SRPA is dependent on transport of these contaminants through the environment.

***Source Term—***Radioactive, inorganic, and organic chemicals were contained in wastewater disposed to the subsurface at NRF. The source term for these contaminants includes a description of the contaminant inventory and the mechanisms for release to the environment.

Contaminants of potential concern at NRF primarily are radionuclides and trace elements (Westinghouse Electric Corporation 1996). A total of 345.41 Ci of radioactivity were released to the NRF leaching beds, industrial waste ditch, and other disposal points during 1953 through 1979 (Westinghouse Electric Corporation 1996). This activity was contained in almost 390 million gal of wastewater. Radioactive constituents with half-lives exceeding 5 years included cesium-137 (23.8 Ci), cobalt-60 (75.2 Ci), tritium (112.3 Ci), and strontium-90 (1.65 Ci; Westinghouse Electric Corporation 1996). Trace elements that were disposed to the subsurface at NRF include chromium, lead, mercury, and silver. Inorganic constituents having elevated concentrations at NRF included sodium, chloride, and nitrate.

***Release Mechanisms—***The prototype facilities at NRF generated wastewater effluent that contained small amounts of radioactivity as a result of normal operations (Westinghouse Electric Corporation 1996). From June 1953 until April 1979, this low-level radioactive effluent was discharged to leaching pits, ponds, lagoons, basins, and drainfields.

In 1968, the total volume of low-level radioactive effluent streams was minimized by removing nonradiological waste streams from discharge to the leaching beds and developing procedures for recycling radioactive liquid (Westinghouse Electric Corporation 1996). By 1972, the ECF was a completely self-contained facility that recycled all radioactive liquids and no-longer-discharged low-level radioactive effluent to the environment. During the 1970's, recycling processes were instituted at all prototypes; the last low-level radioactive discharge was made in April 1979.

- **S1W Wastewater Disposal Facilities**

  Beginning in 1953, low-level radioactive effluent was sent to a drainfield known as the Sl W Tile Drainfield (Unit 8-08-l1). The drainfield became plugged in 1955 (presumably with oil).

In 1955, the SIW Leaching Pit (Unit 8-08-12), constructed to the west and south of the original drainfield, consisted of an open trench 8- to 10- ft deep, 8-ft wide, and 50-ft long excavated at the end of the discharge header to maintain an adequate discharge capacity. Unit 8-08-12A is the piping portion of the leaching field. Unit 8-08-128 is the trench or pit portion of the unit. In 1960, a new leaching bed was constructed for Sl W discharges and the open trench was backfilled.

The new leaching bed was constructed south of Sl W in 1960 (Sl W Industrial Waste Lagoons [Unit 8-08-14]). This leaching bed utilized seepage and evaporation of the water by allowing ponding within the bed. A similar bed was constructed adjacent to this bed in 1963. These discharge facilities (commonly known as the Sl W Leaching Beds) received Sl W effluent from 1960 to 1979.

The SI W Temporary Leaching Pit (Unit 8-08-13) was a basin constructed in 1956 for a one-time discharge of radioactive effluent that contained oil (Westinghouse Electric Corporation 1996). The basin was used to prevent the other leaching beds from being plugged because of the oil content in the liquid. The basin was filled in with the soil excavated immediately after the discharge.

- **A1W/ECF Wastewater Disposal Facilities**

The Al W Leaching Bed (Unit 8-08-19) constructed to the west of NRF to receive the effluent from ECF and Al W, began operation in 1958 (Westinghouse Electric Corporation 1996). The Al W leaching bed was used sporadically after problems were noted in 1964, which were attributed to oil inhibiting the seepage capacity of the bed. Due to inadequate seepage capacity of the Al W leaching bed, the Sl W leaching beds started receiving ECF effluent in 1964 and Al W effluent in 1965. S5G operations began in 1965 and also sent low-level radioactive effluent to the Sl W leaching beds. During 1965 through 1972, the Al W leaching bed was used a few months of the year only for overflow. The last discharge to the Al W leaching bed was in May 1972.

- **Accidental Radiological Discharges**

Accidental radiological discharges have occurred at NRF because of corroded underground piping, leakage from underground basins, and releases from radiological tanks (Westinghouse Electric Corporation 1996). Surface releases generally were cleaned up so that any radioactive material above background levels was retrieved. Underground releases were remediated to the maximum extent practical so that background radiation levels were not affected.

Accidental release sites where contaminants may not have been completely removed include the Sl W Retention Basins, the Sl W Radiography Building Collection Tanks, the Hot Storage Pit, the ECF Water Pit Release, the Al W/S1 W Radioactive Line Near BB19, and the Al W Processing Building Area Soil (Westinghouse Electric Corporation 1996). Other sites include historical cross-contamination associated with the Old Sewage Treatment Plant, Seepage Basin Pump Out Area, and Sewage Lagoons. Other sites include the potentially radiologically-contaminated Old Ditch Surge Pond and S5G Basin Sludge Disposal Bed.

***Transport Mechanisms—***Contaminant transport through sediments and basalts at NRF is affected by chemical processes and conditions that occur in the subsurface. These processes and conditions include sorption, pH, colloid filtration, and oxidation/reduction.

Sorption processes affect the persistence of contaminants released to the subsurface at NRF (Westinghouse Electric Corporation 1996). The distribution coefficient (Kd) provides a measure of these processes. Site-specific values of Kd were determined for different constituents and different soil types at NRF (Westinghouse Electric Corporation 1996). Inorganic constituents included chromium, lead, mercury, and silver. The Kd value for chromium ranged from 0.5 to 4.6, depending on the soil type. The Kd for lead exceeded 388. The Kd for mercury ranged from 110 to 3,049 and the Kd for silver ranged from 78 to 463. Contaminants tend to persist longer with larger Kd values. Radioactive constituents, including cesium-137, are believed to have sorbed to surficial sediments and are not migrating to the aquifer.

Activities of radioactive contaminants released to the subsurface at NRF will be reduced with radioactive decay (Westinghouse Electric Corporation 1996). The persistence of these contaminants is affected by the length of the parent half-life.

The pH of water in the vadose zone and SRPA will affect the persistence of a contaminant in those systems (Westinghouse Electric Corporation 1996). Solubility increases with increased pH.

Colloidal particles may form when contaminated solutions react with groundwater or the soil (Westinghouse Electric Corporation 1996). Colloidal particles, which may contain contaminants, may be filtered out in the surficial loess and other fine-grained sedimentary deposits.

A large percentage of inorganic contaminants released to the subsurface at NRF are believed to have been transformed into more insoluble forms through oxidation and reduction reactions in the soil (Westinghouse Electric Corporation 1996). These contaminants would not migrate to the aquifer but would be retained as oxide, hydroxide, and oxyhydroxide minerals or coatings on minerals.

***Extent of Contamination—***In 1996, tritium activity in water from NRF wells ranged from 15 to 308 pCi per liter (Westinghouse Electric Corporation 1996). Larger concentrations were in wells near the leaching beds and the industrial waste ditch.

Chloride concentrations ranged from 7 to 213 milligrams per liter in 1996 (Westinghouse Electric Corporation 1996). Largest concentrations were associated with the industrial waste ditch. Nitrate concentrations ranged from 0.45 to 2.04 milligrams per liter.

Chromium was used extensively as a rust inhibitor and was discharged with wastewater. Chromium has been detected in water from NRF wells. In 1996, chromium concentrations ranged from 6.79 to 35.20 micrograms per liter in several NRF wells (Westinghouse Electric Corporation 1996). Background concentrations in water from the SRPA are 2 to 3 micrograms per liter.

### 3.8.3 Numerical Analyses Performed to Date

Numerical modeling techniques have been used to test components of the WAG-8 conceptual model of flow and transport. These techniques have included GWSCREEN, MEMO, and MODFLOW model formats.

***3.8.3.1 GWSCREEN Numerical Model.*** GWSCREEN was used to assess the effect on groundwater from release of selected contaminants. The results were used in risk assessment calculations.

GWSCREEN results indicated that small well spacings (approximately 700 ft) would be required assuming conservative dispersivity values that are Track 2 default values used at the INEEL (Westinghouse Electric Corporation 1996). Larger well spacings (1,400 ft) could be achieved with larger dispersivities, as suggested by researchers.

***3.8.3.2 MEMO Numerical Model.*** Contaminant transport modeling was conducted using MEMO, a Golder Associates model that optimizes monitoring well locations. The MEMO model was used to confirm results of the GWSCREEN model. The results of the MEMO and GWSCREEN models were used to locate additional wells for monitoring potential contaminant releases at NRF.

***3.8.3.3 1993-94 Numerical Modeling using MODFLOW.*** Two numerical simulations were conducted at NRF. Initially, subregional (600 $mi^2$) and local (2 $mi^2$) models were constructed. The regional model was constructed to test the hypothesis that groundwater flow direction at NRF changes over time. The local model was constructed to predict the effects that operations at NRF have on the SRPA. The local model was inconclusive in evaluating point source effects on the aquifer.

***3.8.3.4 1996 Numerical Modeling using MODFLOW.*** Another local model was constructed as part of the remedial investigation. This model used additional information collected as part of previous investigations. The purpose of this numerical modeling exercise was to investigate the effect of a water-table mound east of NRF on contaminant transport. Modeling results indicated that water infiltrating from the Industrial Waste Ditch and the Sewage Lagoons could be captured by NRF production wells (Westinghouse Electric Corporation 1996).

### 3.8.4 Summary of Competing Hypotheses and Additional Data Requirements

Groundwater flow velocities in vicinity of NRF are reported to be slow, as evidenced by the small hydraulic gradient. The direction of flow and the source of underflow are dependent on changes in the relative magnitude of recharge components from the Big Lost River, Little Lost River, and the upland Snake River Plain. Additionally, the decrease in discharge of wastewater to the environment is believed to be a major factor in the decrease of contaminant concentrations in the aquifer.

### 3.8.5 References Cited

Anderson, S.R., and Bowers, B., 1995, *Stratigraphy of the Unsaturated Zone and Uppermost Part of the Snake River Plain Aquifer at Test Area North, Idaho National Engineering Laboratory, Idaho*, U.S. Geological Survey Water-Resources Investigations Report 95-4130 (DOE/ID-22122), U.S. Geological Survey.

Busenberg, E., Plummer, L.N., and Bartholomay, R.C., 2001, *Estimated Age and Source of the Young Fraction of Ground Water at the Idaho National Engineering and Environmental Laboratory*, U.S. Geological Survey Water-Resources Investigations Report 01-4265 (DOE/ID-22177), U.S. Geological Survey.

Olmsted, F.H., 1962, *Chemical and Physical Character of Ground Water in the National Reactor Testing Station, Idaho*, IDO-22043-USGS, U.S. Geological Survey.

Westinghouse Electric Corporation, 1996, *Final NRF Comprehensive Remedial Investigation/Feasibility Study, Waste Area Group 8, Naval Reactors Facility, Idaho Falls, Idaho, Part 1 – Remedial Investigation Report: Volumes 1 and 2*, prepared for the U.S. Department of Energy.

# 3.9 WAG-9

WAG 9 is the designation for the collection of CERCLA OUs associated with Argonne National Laboratory West (ANL-W). ANL-W is located near the southeastern corner of the INEEL approximately 16 mi northeast of CFA (see Figure 3-35). ANL-W is the easternmost DOE facility on the INEEL and is operated for the DOE by the University of Chicago (U of C) through the DOE- Chicago Operations Office (DOE-CH).

## 3.9.1 Background

Construction began on Experimental Breeder Reactor (EBR)-II in the mid-1950s. EBR-II began operation in stages from 1959 through the mid-1960s. The EBR-II reactor and associated hot cells, laboratories, and support facilities were constructed for research and development (R&D) of advanced reactor technology. The EBR-II reactor was shut down in 1994 and closure activities on EBR-II have been continuing since that time. ANL-W was redirected to new missions devoted mainly to R&D on nuclear technologies and nuclear environmental management.

## 3.9.2 Summary of the Present WAG-9 Conceptual Site Model

Components of the conceptual model of flow and transport are presented in the Comprehensive RI/FS for ANL-W (Lee et al. 1997), the final ROD (DOE et al. 1998), and the ANL-W Environmental Monitoring Program Plan (Argonne National Laboratory 2002). Subsequent sections discuss the geologic framework at the ANL-W, matrix hydraulic characteristics of geologic materials, local recharge and discharge, a description of the field of flow, and elements of contaminant transport.

***3.9.2.1 Geologic Framework.*** The eastern Snake River Plain near ANL-W is characterized by volcanic terrain similar to the rest of the INEEL. The geologic framework within which ANL-W is situated is described by the system geometry, stratigraphy, and geological structure.

***System Geometry—***ANL-W is located in a closed topographic drainage area in the southeastern corner of the INEEL (DOE et al. 1998). The surface of the facility slopes from south to north and the topographic relief is about 50 ft. ANL-W maintains administrative control over an area of approximately 890 acres of the INEEL. Most of the ANL-W facilities are within a double security fence that is approximately 1,902 ft from west to east and 2,512 ft from north to south. Facilities occupy less than 60 acres.

The top of the SRPA at ANL-W is about 680 ft bls and about 4,480 ft above sea level. The effective base of the aquifer, marked by an extensive sedimentary interbed and a marked change in basalt, has been penetrated at a depth of 1,795 ft bls.

***Stratigraphy—***Most of the area in the vicinity of ANL-W is covered by surficial sediments. These sediments typically range in thickness from 0 to 20 ft (DOE et al. 1998). East of ANL-W, low basalt ridges rise 100 ft above the level of the plain.

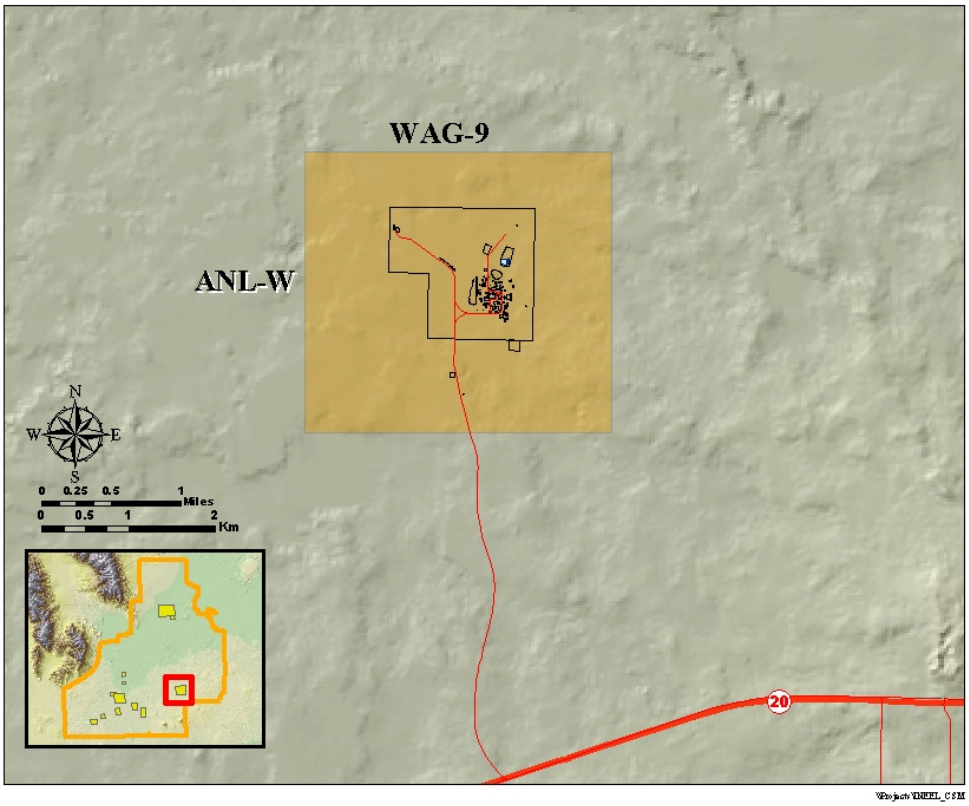


Figure 3-35. WAG 9 is associated with ANL-W in the southeastern part of the INEEL.

The basalt stratigraphic sequence is similar to the rest of the INEEL. Basalt flows range in thickness from 10 to 100 ft (DOE et al. 1998). The upper surfaces of flows typically are irregular, vesicular, and highly fractured. Fractures and joints may be filled with sediment. Interflow rubble zones commonly consist of blocky or loose basalt. Flow interiors of thicker basalt flows contain fewer vesicles and are dominated by vertical cooling fractures.

Unlike other INEEL sites, thick, continuous sedimentary interbeds are not present within the basalt sequence at ANL-W. Sedimentary interbeds generally are discontinuous and range in thickness from less than 1 in. to 15 ft. Interbeds generally are composed of calcareous silt, sand, or cinders. Rubble zones between basalt flows are composed of sand and gravel to boulder-sized material.

A discontinuous, but locally extensive interbed was penetrated at a depth of 40 to 50 ft in boreholes near the industrial waste pond and the main cooling tower blowdown ditch. Other, more extensive interbeds have been observed in the vadose zone at depths of approximately 400, 550, and 600 ft. There is no evidence that these interbeds contain perched water; however, they may affect the vertical movement of water and produce preferential flow in the vadose zone.

The sequence of interbedded basalt and sediments has been observed at ANL-W far below the regional water table. A deep corehole, drilled at ANL-W in 1994 in an attempt to find the effective base of the aquifer, penetrated an extensive interbed approximately 15 ft thick and an underlying low-permeability basalt at a depth of 1,795 ft.

***Structure—***ANL-W is located along the axial volcanic zone of the eastern Snake River Plain. This zone is characterized by increased thicknesses of basalts and decreased occurrence of sedimentary interbeds. The rhyolitic domes of the East and Middle Buttes lie approximately 6 mi to the southwest.

***3.9.2.2 Matrix Characteristics.*** Transmissivity of the SRPA at ANL-W was estimated from two production well aquifer tests to range from 29,000 to 556,000 $ft^2$ per day (Argonne National Laboratory, 2002). The effective porosity of the aquifer is estimated to be 5%.

***3.9.2.3 Recharge/Discharge Sources.*** Sources of local recharge include precipitation and wastewater disposal. ANL-W does not inject any wastewater directly into the SRPA (Argonne National Laboratory 2002). The only source of discharge is from production well pumpage.

***Precipitation—***The annual average precipitation at CFA (8.71 in.) is accepted as the precipitation estimate for ANL-W (Argonne National Laboratory 2002). Precipitation is largest during May and June. Moderate recharge may take place in response to rapid snowmelt during the spring; however, large evapotranspiration losses during the summer and fall probably reduce recharge from precipitation. No estimates of recharge from precipitation at ANL-W are available.

***Recharge from Wastewater Disposal—***The industrial waste pond, located at the northwest corner of ANL-W, has been operational since 1964. The pond is an unlined evaporative seepage pond that is fed by a system of drainage ditches (Argonne National Laboratory 2002). Water disposed to the pond prior to shut down of the EBR-II reactor in 1994 predominantly consisted of blowdown effluent from the main cooling tower. The average discharge to the pond during 1979 through 1994 was 39 million gal/yr; discharge rates ranged from 1.42 to 4.22 million gal/month (Argonne National Laboratory 2002). Since then, discharge to the pond has been reduced greatly. Remaining sources of discharge to the pond have consisted of blowdown effluent from the auxiliary cooling tower and auxiliary boiler, water from air-conditioning systems, and non-contact cooling water from other sources. Reductions in discharge to the pond have resulted in drying of the pond.

Ditches have been used to transport surface water from runoff and facility drains at ANL-W to the industrial waste pond. These unlined ditches, which include the main cooling tower blowdown ditch, ditches A, B, and C, the industrial waste discharge ditch, and the interceptor canal, are described below.

The main cooling tower blowdown ditch runs north to the industrial waste pond. This unlined ditch is approximately 700 ft long. During 1962 through 1996, the ditch was used to convey industrial wastewater from the cooling tower to the industrial waste pond. Contaminants principally consisted of water treatment chemicals derived from regeneration of ion exchange resin beds. During 1962 through 1980, contaminants included a chromate-based corrosion inhibitor.

Ditch A conveys industrial wastewater from the EBR-II power plant auxiliary cooling tower and storm water runoff to the main cooling tower blowdown ditch. Wastewater from this unlined ditch eventually flows to the industrial waste pond (DOE et al. 1998). Ditches B and C have been used to convey storm water runoff and wastewater from the power plant and fire station to the industrial waste pond through the cooling tower blowdown ditch (DOE et al. 1998).

The industrial waste discharge ditch is approximately 500 ft long (DOE et al. 1998). The unlined ditch receives industrial wastewater derived from cooling water, photo processing wastes (containing photo developers, fixers, stabilizers, and acids), and retention tank overflows containing ethanol, sodium hydroxide, and some radionuclides.

The interceptor canal has been used to convey industrial waste to the industrial waste pond (DOE et al. 1998). This unlined canal also is used to divert surface runoff. Industrial wastewater is delivered to this canal through two pipes, one from the cooling tower and the other from the industrial waste lift station. That pipeline also has been used to convey radioactive wastes to the EBR-II leach pit. Discharge of industrial wastes and cooling tower blowdown water was discontinued in 1973 and 1975, respectively.

The sanitary sewage lagoons are located north of ANL-W. These three lagoons were constructed in 1965 and 1974 and cover approximately 2 acres. They receive most of the sanitary wastewater generated at ANL-W. They also have received some photo processing solutions. The bottoms of these lagoons are sealed with bentonite.

The EBR-II leach pit was constructed into basalt and used to dispose of liquid waste containing cooling tower blowdown, sanitary effluent, cooling condensates, and radioactive effluent until 1973 (DOE et al. 1998). Approximately 90,000 gal of wastewater were disposed annually.

***Discharge from Pumping Wells—***During 1979 through 1994, withdrawals for ANL-W water needs averaged 138 million gal of water per year (Argonne National Laboratory 2002). This water was used for plant non-contact cooling water operations, boiler water, and potable water. This supply is provided from two production wells at ANL-W. Approximately 87% of this water was returned to the subsurface through the industrial waste pond, sanitary sewage lagoons, and subsurface septic systems.

***3.9.2.4 Hydraulics.*** Groundwater in the vicinity of ANL-W occurs as unsaturated and saturated flow within the vadose zone and as saturated flow within the SRPA. The distribution of vadose-zone and aquifer water is controlled by hydraulic features as described by components of the conceptual model of flow and transport.

Vadose Zone—At ANL-W, small, localized zones of saturation occur above some interbeds and dense basalt flows. These zones are incapable of producing significant water (DOE et al. 1998). The limited occurrence of perched zones within the vadose zone at ANL-W is controlled, in part, by the small volume of disposal to wastewater facilities and by the discontinuous nature of sedimentary interbeds (Argonne National Laboratory 2002).

The thick, unfractured basalt directly above the water table in one well may locally result in lateral flow of infiltrating wastewater and contaminants in the vadose zone (DOE et al. 1998). Deeper zones of saturation may occur in the vadose zone at ANL-W. Borehole geophysical data indicate that sedimentary interbeds at depths of 400, 550 and 600 ft may contain perched water.

***SRPA—***The flow field within the SRPA at ANL-W is defined by the gradient, direction of flow, and velocity. The hydraulic gradient in the vicinity of ANL-W, determined from altitude of water surfaces in wells, ranges from 2 to 4 ft/mi. The direction of flow is from the northeast to the southwest. Estimated flow velocities range from 0.9 to 16.8 ft/day.

The response of water levels in most wells to changes in barometric pressure indicates that groundwater flow typically is unconfined (DOE et al. 1998). However, the slow response in one well indicates that locally thick, unfractured basalt flows at the water table may partially confine flow.

***3.9.2.5 Groundwater Chemistry.*** Water from the SRPA at ANL-W is enriched in calcium and bicarbonate (Argonne National Laboratory 2002). Wastewater disposed to ditches, ponds, and pits also is enriched in sodium.

***3.9.2.6 Contaminant Transport.*** Potential release sites at ANL-W include wastewater structures and leaching ponds, underground storage tanks, rubble piles, cooling towers, an injection well, French drains, and spills (DOE et al. 1998). Subsequent sections describe the source term, vadose-zone and aquifer transport mechanisms, and distribution of contaminants in the subsurface.

***Source Term—***The main cooling tower blowdown ditch was used to convey wastewater from the cooling tower to the industrial waste pond (DOE et al. 1998). Wastewater contained water-treatment chemicals and hexavalent chromium from a chromate-based corrosion inhibitor. During 1962 through 1980, wastewater also contained concentrations of sulfuric acid and sodium hydroxide. Following a pH measurement of 1.86 in 1986, a neutralization tank was installed to treat water prior to ditch disposal.

The interceptor canal was used to transport industrial waste and cooling tower effluent to the industrial waste pond and to divert local surface runoff for flood control. The pipeline that transported industrial wastes also transported liquid radioactive wastes that were diverted to the leach pit. The presence of cesium-137 in canal sediments indicates that some radioactive wastes were transported with the industrial wastes.

Ditches A, B, and C also conveyed wastewater to the industrial waste pond. Based on contaminant concentrations, these other ditches transported wastewater containing mercury, chromium, and zinc.

The industrial waste pond received wastewater from these different ditches. Contaminants present in pond sediments indicate that wastewater contained concentrations of cesium-137, trivalent chromium, mercury, selenium, and zinc (DOE et al., 1998).

The sewage lagoons are sealed with bentonite clay. Photo processing solutions were discharged to the sewage lagoons. Also, no known radioactive or hazardous substances have been released to the lagoons.

Wastewater disposed to the lined EBR-II leach pit contained 10.4 Ci of radioactivity derived primarily from cesium-137, strontium-90, cobalt-60, and uranium-238.

Other sources of contaminants included the main cooling tower riser pits. The presence of arsenic, trivalent chromium, lead, and mercury in pit sediments indicates that these inorganic contaminants were contained in wastewater disposed to the pits.

***Transport Mechanisms—***Contaminant transport in the subsurface occurs as wastewater, which contains contaminants that infiltrate pond, ditch, and pit bottoms. This transport mechanism requires water volumes sufficient to sustain flow through the vadose zone. Processes of sorption tend to inhibit transport; these processes are evident in subsequent discussion of contaminant distribution in the subsurface at ANL-W.

***Extent of Contamination—***Soil and sediment samples collected from the industrial waste pond as part of four different investigations during 1986 through 1994 contained concentrations of cesium-137, trivalent chromium, mercury, selenium, and zinc (DOE et al. 1998). The area of surficial contamination was estimated to be approximately 200 × 250 ft and contamination was contained in the upper 0.5 ft of pond sediments. Mercury was contained along the entire length of ditch A and in the upper 0.5 ft of sediments. Trivalent chromium and zinc were contained in sediments in ditch B (DOE et al. 1998).

Mercury, which was contained in sludge samples from the sewage lagoons, was contained in sediments along the entire reach of ditch C (DOE et al. 1998). Sediment samples from the entire length of the main cooling tower blowdown ditch contained mercury and chromium. Most of the contaminants have been retained in the top 0.5 ft of sediment.

The interceptor canal sediments contained concentrations of cesium-137. Cesium-137 also is contained in sediments dredged from the canal and disposed to a mound on the canal bank.

The water quality monitoring network at ANL-W consists of four monitoring wells and one production well (Argonne National Laboratory 2002). In addition, the USGS routinely monitors water chemistry in three more local wells near ANL-W (Bartholomay et al. 2000). No contaminants have been detected in water from ANL-W monitoring wells completed in the SRPA.

### 3.9.3 Numerical Analyses

The GWSCREEN model was used to evaluate the fate and transport of groundwater contaminants at ANL-W (DOE et al. 1998; Lee et al. 1997). This numerical analysis determined that arsenic and chromium are the only contaminants at ANL-W that pose a potentially unacceptable groundwater contaminant risk. The chromium risk was less than the 10-6 while the arsenic risk was calculated to be $3 \times 10\text{-}4$ for ingestion of groundwater. Because arsenic was determined to originate from natural sources, it was screened as a COC.

### 3.9.4 Summary of Competing Hypotheses and Additional Data Requirements

A detailed conceptual model of groundwater flow and contaminant transport has not been prepared for ANL-W because ANL-W does not pose significant groundwater problems. Studies describing hydrogeologic conditions at ANL-W do not present competing hypotheses concerning components of the conceptual model of flow and contaminant transport. They do highlight several important features concerning contaminant migration.

***Wastewater Disposal—***The absence of detectable concentrations of contaminants in water from the SRPA at ANL-W is attributed to the relatively small volumes of wastewater discharged to ditches, ponds, and pits and to the relatively small amounts of radioactive and nonradioactive chemical contaminants. Most of the contaminants sorb to surficial sediments, as evidenced by the largest distribution of cesium-137 and trace elements in the upper 0.5 ft of pond and ditch sediments.

***Thick Vadose Zone—***The thick vadose zone is characterized by both fractured and massive, nonfractured basalt flows. The massive flows provide a barrier to vertical flow and migration of contaminants. The vadose zone is characterized by few, areally continuous sedimentary interbeds. The absence of these interbeds limits formation of perched groundwater bodies.

### 3.9.5 References Cited

Argonne National Laboratory, 2002, *ANL-W Environmental Monitoring Program Plan – Chapter 1 – Program Description*.

Bartholomay, R.C., Tucker, B.J., Davis, L.C., and Greene, M.R., 2000, *Hydrologic Conditions and Distribution of Selected Constituents in Water, SRPA, Idaho National Engineering and Environmental Laboratory, Idaho, 1996 through 1998*, U.S. Geological Survey Water-Resources Investigations Report 00-4192 (DOE/ID-22167), U.S. Geological Survey.

Department of Energy, Idaho Department of Health and Welfare (DEQ), and Environmental Protection Agency (Region 10), 1998, Final record of decision, Argonne National Laboratory-West.

Lee, S.D., Rohe, M.J., Rood, A.S., and Stepan, I.E., 1997, "Comprehensive Remedial Investigation/Feasibility Study for Argonne National Laboratory-West Operable Unit 9-04 at the Idaho National Engineering and Environmental Laboratory (Final)," W7500-0000-ES-02, Rev 2, Idaho National Engineering and Environmental Laboratory, Idaho Falls, Idaho.

# 4. IMPLICATIONS FOR AN INTEGRATED CONCEPTUAL SITE MODEL OF THE INEEL SUBREGION

The preceding discussion of subregional and facility-scale conceptual models of flow and transport identifies those features of conceptual-model components that are critical to the subregional migration of INEEL-derived contaminants. The following sections summarize the range and maturity of hypotheses associated with these components.

## 4.1 Geohydrologic Framework

Several components of the geohydrologic framework within the INEEL subregion provide alternative hypotheses that warrant further investigation. These components include the geometry of the SRPA, structural orientation of geohydrologic units, and other structural/volcanic features.

### 4.1.1 Aquifer Geometry

The USGS conceptual model groups the complex basalt stratigraphy of the eastern Snake River Plain into three hydrogeologic units: (1) Unit 1 consists of many younger, thin, fractured basalt flows and interbedded sediments that lie below the water table in the central part of the INEEL subregion and range in thickness from 0 to perhaps as much as 300 ft; (2) Unit 2 underlies unit 1 and consists of younger, thick, dense basalt flows and interbedded sediments. Unit 2 rises above the water table in the southwestern part of the INEEL subregion; and (3) Unit 3, consisting of slightly altered basalts interbedded with sediments of intermediate age, is saturated throughout the INEEL subregion and represents the thickest part of the aquifer. The base of Unit 3 may exceed 2,500 ft bls in the eastern part of the subregion and more than 4,000 ft in the southwestern part, based on electrical resistivity and borehole data.

The WAG-10 conceptual model uses hydrogeologic units similar to those of the USGS. An upper fractured basalt is equivalent to the USGS unit 1. Composite layer 7 is equivalent to USGS unit 2. Composite layer 7 intersects the water table south of the INEEL. The WAG-10 model uses two interpretations of aquifer thickness based on temperature, geophysical, and borehole data. The “thick” aquifer interpretation includes a north-trending zone exceeding 1,300 ft in thickness. The thin aquifer interpretation assumes that the aquifer gradually thickens toward the center of the plain from a thickness of 328 ft or less along the northwest to a maximum of 1,300 ft.

The effective thickness of the aquifer used in individual WAG modeling efforts is 250 ft. This thickness is typical of the upper geohydrologic unit in the two subregional conceptual models.

### 4.1.2 Structural Orientation of Geohydrologic Units

The USGS conceptual model hypothesizes that the intersection of Unit 2 with the water table south of the INEEL forces groundwater flow paths and contaminants to dive. This hypothesis is based on limited data and requires additional information about vertical gradient profiles and head distribution in that area.

The WAG-10 conceptual model agrees concerning the probable intersection of the smaller permeability basalts south of the INEEL; however, this intersection is not hypothesized to force downward flow. Again, this divergence of hypotheses is based on limited data.

The individual WAGs are sufficiently distant from the probable intersection of smaller-permeability basalts with the water table south of the INEEL. This area of interest also does not include anything below the upper geohydrologic unit of the subregional conceptual models.

### 4.1.3 Other Structural/Volcanic Features

The USGS conceptualizes that large-scale fractures in rift zones perpendicular to the axis of the eastern Snake River Plain may result in anisotropy over broad areas. The largest range of hydraulic conductivity occurs in volcanic rift zones with many aligned vents and fissures. Volcanic features related to individual dike systems within these rift zones are approximated in the subsurface by vent corridors. Vent corridors at and near the INEEL generally are perpendicular to groundwater flow and average about 1 to 2 × 5 to 15 mi. Forty-five vent corridors are inferred to be beneath the INEEL and adjacent areas. Features associated with these vent corridors may provide localized, preferential pathways for groundwater flow, or may even impede flow.

The WAG 10 conceptual model observes that northwest-oriented major faults and rift zones are perpendicular to the eastern Snake River Plain axis and may locally influence the direction of groundwater flow, creating local anisotropy. The effect of vent corridors on facility-scale flow and contaminant transport has not been evaluated.

## 4.2 Matrix Hydraulic Properties

The subregional and facility-scale conceptual models of flow and transport agree that the SRPA is characterized by large ranges in hydraulic conductivity. These ranges are attributed to the complex stratigraphic sequence, heterogeneities in distributions of fractures and sedimentary interbeds, and the effect of the many vent corridors across the subregion. These heterogeneities may affect horizontal dispersion of contaminants. The subregional conceptual models all infer a correlation between the increases in the cumulative thickness of sedimentary interbeds associated with the Big Lost Trough and reduced aquifer transmissivity. This correlation may affect the subregional distribution and migration of contaminants.

The USGS conceptual model notes that the hydraulic conductivity of the SRPA at and near the INEEL ranges from about $1.0 \times 10^{-2}$ to $3.2 \times 10^{4}$ ft/day. This six-order of magnitude range of hydraulic conductivity was estimated from single-well tests in 114 wells, and is attributed mainly to the physical characteristics and distribution of basalt flows and dikes. Bulk hydraulic conductivity of the fractured basalt of unit 1 ranges from about 0.01 to 32,000 ft/day. Estimates greater than 100 ft/day are principally associated with interflow zones of thin flows. Smaller estimates probably are associated with localized dikes or dike swarms. Estimates of the bulk hydraulic conductivity for dense basalt of unit 2 at the INEEL range from about 0.01 to 800 ft/day. The average hydraulic conductivity of unit-3 basalts probably is about one order of magnitude smaller than that of younger basalts. The present USGS conceptual model suggests that water in the upper part of the aquifer generally moves horizontally at the INEEL and that vertical flow is impeded by the horizontal and subhorizontal layering of basalt.

WAG-10 researchers use the same data set for aquifer transmissivity as USGS researchers. However, distributions of hydraulic conductivity are not presented in the WAG-10 conceptual model. Average values at the subregional scale have not been estimated because of heterogeneity (even at the large scale) and because of the potential to assign misleading mean property values.

Transmissivities and hydraulic conductivity estimates used by individual WAGs were obtained from the same data sets used by subregional researchers. These estimates are consistent with the six-order range of magnitude of hydraulic conductivity. The WAG-3 vadose zone models assume that the ratio of vertical to horizontal permeability is 1 to 300. Similarly, the WAG-3 aquifer model assumes that horizontal flow dominates because of the layered nature of the basalt aquifer.

In the current USGS subregional conceptual model, the effective porosity of fractured basalt is estimated to range from 5 to 25%. The porosity of dense basalt probably is at the lower end of this range.

The storage coefficient used in numerical analyses for individual WAGs is less than the storage coefficient assumed in subregional conceptual models. Effective porosity of the SRPA beneath TAN was estimated, through model calibration to the tritium plume and through inverse modeling of pumping test results, to be about 3%, approximately half of what has been estimated during a similar, large-scale characterization effort at the INEEL. The effective porosity used by WAG 3 was estimated using inverse modeling techniques and contaminant distribution data as 6%. Wag-7 modelers have used estimates of effective porosity ranging from 1 to 5%.

## 4.3 Sources of Recharge and Discharge

Subregional underflow estimates are consistent, largely because they are indirectly calculated using similar gradient and aquifer property information. Outflow estimates south of the INEEL are based on limited head information.

Flow across the base of the aquifer is acknowledged by subregional researchers to be relatively small. This potential source of recharge/discharge probably does not affect subregional or WAG-specific flow and contaminant transport.

The USGS conceptual model estimates that areal recharge from precipitation is 0.02 to 0.04 ft/year with a maximum recharge contribution of about 70 $ft^3/s$ over the entire subregion. The net effect of recharge from precipitation is probably very small when compared to other sources of inflow and is a less important consideration than more concentrated sources such as streamflow infiltration. The WAG-10 conceptual model uses similar estimates for areal recharge and suggests that direct precipitation on the plain locally recharges the aquifer to a limited degree, particularly when snow melts rapidly in the spring.

Large volumes of water have been recharged historically to the SRPA in response to episodic runoff from the Big Lost River drainage basin. Recharge has occurred along the channel of the Big Lost River and in the INEEL spreading areas near sources of INEEL-derived contaminants. This source of large episodic recharge has locally affected hydrologic conditions in the vadose zone and aquifer. However, the effect of this recharge on contaminant transport is not well understood. The USGS tracer test conducted in the INEEL spreading areas in 1999 demonstrated that rapid, lateral flow can occur in the vadose zone in response to episodic recharge. Subregional and WAG-specific studies (in proximity to episodic effects of streamflow recharge) recognize that more information is required to adequately assess the effects of episodic recharge on flow and contaminant migration.

Wastewater disposal from INEEL facilities does not noticeably impact subregional flow, but does affect the subregional distribution of conservative contaminants. At the facility scale, pumpage withdrawals have locally affected horizontal and vertical distributions of contaminants in the SRPA.

## 4.4 Geochemistry

Geochemical data indicate that preferential flow may occur in the SRPA at the INEEL. These preferential flow paths are not easily identified with existing head information. The vertical distribution of contaminants in the aquifer is dependent on vertical permeability. Conceptual models at all scales presently assume that most of the contaminant inventory in the aquifer remains in the upper, more permeable sections. Additional geochemical data are needed to better characterize preferential flow and deep circulation of flow and contaminants.

## 4.5 Contaminant Characteristics

Although the hydrologic characteristics of the INEEL system will largely control the fate of contaminants in terms of their final location and concentration, the source of contaminants and their entry

into the aqueous system is an area of great uncertainty. The vast majority of work conducted at the INEEL over the last 5 decades has been related to the geology and hydrology of the natural system, as reflected in this report. Relatively little study has been conducted to describe the specific contaminant-water-rock interactions that are known to occur. WAG specific studies, with a few exceptions, rely on generalized knowledge of chemical behavior. Little site-specific data regarding contaminant chemical forms, mechanisms of release, chemical speciation, adsorption, complexation, etc. has been incorporated into INEEL conceptual models.

Recent efforts to collect leachate from the RWMC SDA are of particular interest as, so far, there has been virtually no empirical data regarding the flux of contaminants into the transport system and their chemical makeup. Analysis of leachate, as it becomes available, is expected to make a significant contribution to the understanding of the release of contaminants from buried sources.

Besides governing the flux of contaminants from their original waste forms into the aqueous system, geochemical reactions also control the concentration of contaminants as a solution propagates through the unsaturated and saturated matrices. The current INEEL conceptual models use an equilibrium, reversible distribution coefficient to emulate the various geochemical factors affecting retardation the transport codes. Use of distribution coefficients, or Kds, is widely accepted as a defensible method to simplify transport calculations. However, where significant temporal and spatial heterogeneities in a geochemical environment exist, the use of Kds becomes problematic.

The question of whether to use an isotherm approach (linear or non-linear) or to use a surface complexation theory in a geochemical reactive transport code remains unresolved. To date, WAG-specific simulations have relied on the linear isotherm approach using a limited set of site-specific data. Although the results are generally considered conservative for purposes of risk assessment, a number of investigators have suggested that long-term evaluations be conducted to provide a basis for more representative geochemical modeling. As discussed previously, several researchers recommended a course of action to incorporate geochemistry into INEEL fate and transport models with both short-term and long-term research activities. These types of recommendations need to be further evaluated as part of the INEEL conceptual model development.

## 4.6 Summary

Many of the conceptual model features that are key to understanding groundwater flow and contaminant transport are associated with the geologic framework of the SRPA. These key features include the structural orientation of geohydrologic units, heterogeneities in the distribution of hydraulic properties, stratigraphic and structural controls of vertical/horizontal ratios of permeability, the effective thickness of the SRPA, the distribution of sediments related to the Big Lost Trough, controls over preferential flow, and the vertical distribution of contaminants in the aquifer. Some features are associated with recharge sources and include the effect of episodic recharge on the distribution of contaminants in the aquifer and in the vadose zone. Finally, conceptual model features are associated with the source term and its uncertainties in the availability and release of contaminants to the subsurface. Additional information needed to adequately define key features of the subregional conceptual model of flow and contaminant transport will include carefully designed research activities, deep-drilling programs, and well-posed numerical analyses using existing data.